Cellular Substrate of Eligibility Traces in Cortex

Léa Caya-Bissonnette

Thesis submitted to the
University of Ottawa
in partial fulfillment of the requirements
for the Doctorate in Philosophy in Neuroscience

Department of Cellular & Molecular Medicine

Faculty of Medicine

University of Ottawa

Table of Contents

List of Figures

Manuscript I

Manuscript II

Manuscript IV

List of Appendix Figures

List of Tables

List of Abbreviations

1P	1-photon
2P	2-photon
16p	16p11.2 gene deletion
5-HT	Serotonin
ACC	Anterior Cingulate Cortex
ACh	Acetylcholine
AI	Artificial Intelligence
AMPAR	α-Amino-3-hydroxy-5-Methyl-4-isoxazolePropionic Acid Receptors
AP	Action Potential
APV	2-amino-5-phosphonovaleric acid
ATP	Adenosine triphosphate
bAPs	backpropagating Action Potentials
BAPTA	1,2-bis(o-aminophenoxy)ethane-N,N,N',N'-tetraacetic acid.
BDNF	Brain-Derived Neurotrophic Factor
BTSP	Behavioral Timescale Synaptic Plasticity
CA1/2/3	Cornu Ammonis 1/2/3
CAC	Cholinergic Agonist Carbachol
CaMKII	Calcium-Calmodulin-dependent protein Kinase II
cAMP	cyclic Adenosine MonoPhosphate
CICR	Calcium-Induced Calcium-Release
CNQX	6-Cyano-7-nitroquinoxaline-2,3-dione
CPA	CycloPiazonic Acid
CR	Conditioned Response
CS	Conditioned Stimulus
CV	Coefficient of Variation
D-AP5	5-Phosphono-D-norvaline
DA	Dopamine
DAG	Diacylglycerol

DC	Direct Current
EC3	Entorhinal Cortex Layer 3
EGTA	Ethylene Glycol-Bis(β-aminoethyl Ether)-N,N,N',N'-Tetraacetic Acid
EPSC	Excitatory PostSynaptic Current
EPSP	Excitatory PostSynaptic Potential
ER	Endoplasmic Reticulum
Fig.	Figure
Fluo-4FF	Fluorescein-based Ca^{2+} indicator with enhanced Fluorescence and Fast kinetics
FS	Fast-Spiking
GABA	Gamma-Aminobutyric Acid
GluA2	Glutamate receptor, Subtype A, subunit 2
GLuN1-2-3	Glutamate receptor, NMDA, Subunit 1,2,3
GPCR	G-protein Coupled Receptor
GTP	Guanosine Triphosphate
HEPES	4-(2-Hydroxyethyl)piperazine-1-ethanesulfonic acid
HFS	High Frequency Stimulation
iGluSNFR	intensity-based Glutamate-Sensing Fluorescent Reporter
Ih	hyperpolarization-activated current
IICR	IP_3-Induced Calcium-Release
IL	InfraLimbic
IP_3	Inositol 1,4,5-trisphosphate
IP_3R	IP_3 Receptors
ISI	Inter-Spike-Interval
L2/3, L5	Layer 2/3, Layer 5
LFS	Low Frequency Stimulation
LTD	Long-Term Depression
LTP	Long-Term Potentiation
M1	Primary Motor Cortex

M2	Secondary Motor Cortex
mGluR	metabotropic Glutamate Receptor
MNI-Glu	4-methoxy-7-nitroindolinyl - Glutamate
mPFC	medial PreFrontal Cortex
mRNA	messenger RiboNucleic Acid
MTEP	3-((2-Methyl-4-thiazolyl)ethynyl)pyridine
MWM	Morris Water Maze
n	sample size
NE	Norepinephrine
NMDA	N-methyl-D-aspartate
NMDAR	NMDA Receptor
NR1	NMDAR subunit 1
OGB	Oregon Green 488 BAPTA-1
P	Postnatal days
PFC	PreFrontal Cortex
PIP_2	Phosphatidylinositol 4,5-bisphosphate
PKA	Protein Kinase A
PKC	Protein Kinase C
PLC	Phospholipase C
post	postsynaptic
$post_b$	postsynaptic burst
$post_s$	postsynaptic single
pre_s	presynaptic single
pre_t	presynaptic train
PPR	Paired-Pulse Ratio
pre	presynaptic
PrL	Prelimbic
PSD	Post-Synaptic Density
PTX	Picrotoxin

Rel	Relative
RyR	Ryanodine Receptor
SEM	Standard Error of the Mean
SERCA	Sarco/Endoplasmic Reticulum Ca2+-ATPase
SFA	Spike Frequency Adaptation
STAPCD	Short-Term Associative Plasticity of Calcium Dynamics
STDP	Spike-Timing Dependent Plasticity
TARPs	Transmembrane AMPAR-Regulatory Proteins
TD	Temporal Difference
TrkB	Tyrosine protein kinase
UOJM	University of Ottawa Journal of Medicine
$uPre_t$	uncaging Presynaptic train
VGCC	Voltage-Gated Calcium Channel
Vh	Voltage holding

Acknowledgements

I would like to start by expressing my deepest gratitude and a special thanks to Dr. Jean-Claude Béïque for the extraordinary mentorship and for providing me with countless opportunities to grow. I would also like to thank my co-supervisor Dr. Leonard Maler and my advisory committee members Dr. Richard Naud, Dr. Simon Chen and Dr. André Longtin for their invaluable support and guidance throughout my doctoral journey. I am also immensely grateful to my colleagues and friends. Their support has made the research process more enjoyable and has contributed to my personal and intellectual development. Above all, I would like to thank my parents for providing me with a nurturing and supportive environment that ignited my curiosity and shaped my academic journey. I also extend my heartfelt appreciation to my sister and brother, whose love and guidance have enriched my life and academic aspirations. Lastly, I will be forever grateful to my partner for the countless ways he has supported me. His continuous encouragement and belief in my capabilities have been an endless source of motivation, and I consider myself incredibly fortunate to have him as my companion.

I acknowledge the financial support provided by the University of Ottawa (Excellence Scholarship, Mark and Gail Marcogliese Scholarship & Saroj and Kishori Lal Family Scholarship), the province of Ontario (Ontario Graduate Scholarship) & Québec (Fonds de recherche du Québec Nature et technologies) and the government of Canada (National Sciences and Engineering Research Council) for their financial support and investment in my research and professional development.

Abstract

Contemporary cellular models of learning and memory are articulated around the idea that synapses undergo activity-dependent weight changes. However, conventional forms of Hebbian plasticity do not adequately address certain features inherent to behavioral learning. First, associative learning driven by delayed behavioral outcomes introduces a temporal credit assignment problem, whereby one must remember which action corresponds to which outcome. Yet, current models of associative synaptic plasticity, such as spike-timing-dependent plasticity, require near coincident activation of pre- and postsynaptic neurons (*i.e.*, within ~ 10 ms), a time delay that is orders of magnitude smaller than that required for behavioral associations. For individual neurons to associate two cues, a biological mechanism capable of potentiating synaptic weights must be able to bind events that are separated in time. Theoretical work has suggested that a synaptic eligibility trace, a time-limited process that momentarily renders synapses eligible for weight updates via delayed instructive signals, can solve this problem. However, no material substrate of eligibility traces has been identified in the brain. Second, under certain conditions, neurons need to swiftly update their weights to reflect rapid learning. Current plasticity experiments require the repetition of multiple pairings to induce long-term synaptic plasticity. In this thesis, I addressed these problems using a combination of whole-cell recordings, two-photon uncaging, calcium imaging, and mechanistic modeling. I uncovered a form of synaptic plasticity known as behavioral timescale synaptic plasticity (BTSP) in layer 5 pyramidal neurons in the prefrontal cortex of mice. BTSP induced synaptic potentiation by pairing temporally separated pre- and postsynaptic events (0.5 s - 1 s), regardless of their order. The temporal window for BTSP induction offers a line of solution to the temporal credit assignment problem by highlighting the presence of a synaptic mechanism that expands the time for the induction of activity-dependent long-term synaptic plasticity, spanning hundreds of milliseconds. We further found that BTSP can be induced following a single pairing, enabling rapid weight updates required for one-shot learning. Using two-photon calcium imaging in apical oblique dendrites, I discovered a novel short-term and associative plasticity of calcium dynamics (STAPCD) that exhibited temporal characteristics mirroring the induction rules of BTSP. I identified a core set of molecular components crucial for both STAPCD and BTSP and developed a computational simulation that models the calcium dynamics as a latent memory trace of neural activity (*i.e.,* eligibility traces). Together, we find that calcium handling by the endoplasmic reticulum enables synaptic weight

updates upon receipt of delayed instructive signals, obeys rules of burst-dependent one-shot learning, and thus provides a mechanism that satisfies the requirements anticipated of eligibility traces. Collectively, these findings offer a neural mechanism for the binding of cellular events occurring in single shot and separated by behaviorally relevant temporal delays to induce potentiation at synapses, providing a cellular model of associative learning.

Les modèles cellulaires contemporains de l'apprentissage et de la mémoire sont articulés autour de l'idée que les synapses subissent des changements de poids en conséquence de l'activité neuronale. Cependant, les formes conventionnelles de la plasticité Hebbienne n'abordent pas de manière adéquate certaines caractéristiques inhérentes à l'apprentissage comportemental. Tout d'abord, l'apprentissage associatif induit par des résultats comportementaux retardés introduit un problème d'attribution temporelle du crédit, où l'on doit se souvenir quelle action correspond à quel résultat. Pourtant, les modèles actuels de plasticité synaptique associative, tels que la plasticité dépendante de la synchronisation des décharges (*spike-timing dependent plasticity*), nécessitent une activation quasi-coïncidente des neurones présynaptiques et postsynaptiques (c'est-à-dire, dans un délai d'environ ~ 10 ms), un retard temporel qui est des ordres de grandeur plus petits que celui requis pour les associations comportementales. Pour que les neurones individuels associent deux indices, un mécanisme biologique capable de potentialiser les poids synaptiques doit être en mesure de lier des événements séparés dans le temps. Le travail théorique a suggéré qu'une trace d'éligibilité synaptique, un processus limité dans le temps qui rend momentanément les synapses éligibles aux mises à jour de poids via des signaux instructifs retardés, peut résoudre ce problème. Cependant, aucun substrat matériel des traces d'éligibilité n'a été identifié dans le cerveau. De plus, dans certaines conditions, les neurones doivent rapidement mettre à jour leurs poids pour refléter un apprentissage rapide. Les expériences de plasticité actuelles nécessitent la répétition de multiples appariements pour induire des changements de plasticité à long terme. Dans cette thèse, j'ai abordé ces problèmes en utilisant une combinaison d'enregistrements de cellules entières, de photolyse biphotonique, d'imagerie calcique et de modélisation mécanistique. J'ai découvert une forme de plasticité synaptique appelée plasticité synaptique à l'échelle temporelle comportementale (*Behavioural Timescale Synaptic Plasticity*; BTSP) dans les neurones pyramidaux de la couche 5 dans le cortex préfrontal des souris. La BTSP induit une potentialisation

synaptique en associant des événements présynaptiques et postsynaptiques temporellement séparés (0,5 s - 1 s), indépendamment de leur ordre. La fenêtre temporelle pour l'induction de la BTSP offre une solution au problème d'attribution temporelle du crédit en mettant en évidence la présence d'un mécanisme synaptique qui étend le temps pour l'induction de la plasticité synaptique à long terme, couvrant des centaines de millisecondes. De plus, nous avons constaté que la BTSP peut être induite après un seul appariement, permettant des mises à jour rapides des poids nécessaires pour l'apprentissage en une seule fois. En utilisant l'imagerie calcique biphotonique dans les dendrites obliques apicaux, j'ai découvert une nouvelle plasticité à court terme et associative des dynamiques calciques (*Short-Term and Associative Plasticity of Calcium Dynamics*; STAPCD) qui présentait des caractéristiques temporelles reflétant celles des règles d'induction de la BTSP. J'ai identifié un ensemble central de composants moléculaires cruciaux pour la STAPCD et la BTSP, et j'ai développé une simulation informatique qui modélise les dynamiques calciques comme une trace de mémoire latente de l'activité neuronale (c'est-à-dire, des traces d'éligibilité). Ensemble, nous constatons que la régulation calcique par le réticulum endoplasmique permet des mises à jour de poids synaptiques à la réception de signaux instructifs retardés, obéit aux règles d'apprentissage en une seule fois dépendant des rafales d’activité, et fournit ainsi un mécanisme qui répond aux exigences anticipées des traces d'éligibilité. Dans l'ensemble, ces découvertes offrent un mécanisme neuronal pour la liaison d'événements cellulaires survenant en une seule fois et séparés par des retards temporels pertinents sur le plan comportemental pour induire une potentialisation au niveau des synapses, fournissant ainsi un modèle cellulaire d'apprentissage associatif.

Copyright Authorizations

Manuscript II was published in *Neurophotonics* in 2023.

Caya-Bissonnette L, Béïque JC. Low throughput screening in neuroscience: using light to study central synapses one at a time. Neurophotonics. 2023 Oct;10(4):044407. doi: 10.1117/1.NPh.10.4.044407. Epub 2023 Oct 24. PMID: 37881180; PMCID: PMC10594030.

Manuscript III was published in the *Journal of Neuroscience* in 2020

Caya-Bissonnette, L. (2020). Heterosynaptic Plasticity in Cortical Interneurons. Journal of Neurosciences. 40(9):1793-1794. DOI: https://doi.org/10.1523/JNEUROSCI.2567-19.2020

Manuscript VI was published in the *University of Ottawa Journal of Medicine* in 2021

Caya-Bissonnette L. Le vaccin à ARNm, au-delà du COVID-19. UOJM. Published online August 26, 2021;11(S1). doi:10.18192/uojm.v11iS1.6028

GENERAL INTRODUCTION

American writer, Alvin Toffler, famously wrote "The illiterate of the 21st century will not be those who cannot read and write, but those who cannot learn, unlearn, and relearn." But how do we capture, preserve, and recall what we encounter? We learn at a level unprecedented by any technology, or beings on earth. Yet, the precise neural mechanisms underlying the acquisition of even the simplest skills or piece of knowledge still elude us.

Early psychology studies have laid the foundational work to the study of learning and memory. Notably, Ivan Pavlov's classical conditioning experiments demonstrated that dogs could be conditioned to salivate at the sound of a bell through repeated pairings with food (Pavlov, 1910). In later years, B.F. Skinner developed the building blocks of operant conditioning by examining the effects of rewards and punishments on learning (Skinner, 1963), and, closely thereafter, Albert Bandura's research proposed that children learn by imitating adult models (Bandura, 1977). To accomplish these complex behavioral tasks, the brain processes an innumerable amount of information, but by what means does the brain achieves this feat?

The continual venture towards an all-enlightening answer to the question; *how do we learn?* has brought up some of the most influential and Nobel prize-worthy work in neurosciences, starting by the 1906 Nobel prize awarded to Camillo Golgi and Santiago Ramón y Cajal. Although earlier work, notably by Dutch scientist Jan Swammerdam and Italian scientist Luigi Galvani established the existence of nerve cells, Golgi and Cajal contributed to the first in-depth description of neurons, dendrites, and axons, and hypothesized their role as information hubs.

Connections between neurons are named *synapses*, a termed coined by Sir Charles Sherrington, who, along with Edgar Adrian, won the 1932 Nobel prize for their functional work on neurons and the discovery of synaptic transmission. Sherrington suspected that information transmission occurred at synapses by means of chemical signals due to the comparative time course of electric impulse across the neurons and the one of synaptic transmission (Sherrington, 1906). Almost 30 years later, Hodgkin and Huxley, and Eccles won their Nobel prize for their discoveries of ionic currents underlying membrane excitability and the action potential (AP), and synaptic transmission, respectively. In short, initiation of the AP is prompted by membrane depolarization from synaptic inputs that causes Na^+ channel activation, and is terminated by

membrane repolarization through K^+ conductance (Coombs et al., 1955; Barakan et al., 1949; Hodgkin & Huxley, 1952). The AP is initiated at the axon initiation segment in an all-or-none fashion and propagates along the axon to the axon terminal. There, it activates voltage gated Ca^{2+} channels (VGCCs) that facilitates synaptic transmission by chemical transmitter release (Fatt & Katz, 1952; del Castillo & Katz, 1954; Katz & Miledi, 1967; Kandel et al., 2000). This discovery led to the 1970 Nobel prize being awarded to Sir Bernard Katz, Ulf von Euler, and Julius Axelrod. Although not without debate (Soup *vs* Spark), these notable discoveries paved the way to understand how neurons receive, integrate, and transmit information.

At the turn of the millennium, Eric Kandel, alongside Arvid Carlsson and Paul Greengard, won the Nobel prize for their discoveries regarding the role of neurotransmitters in the nervous system, and the synaptic and molecular mechanisms underlying habituation, a form of associative learning and memory (Kandel, 1976). In the latter discovery, habituation was observed by studying the gill-withdrawal reflex in *Aplysia Californica*. This reflex is reduced by repeated stimulation (*i.e.*, habituation), which can be explained by activity-dependent synaptic depression at sensory-motor synapses (Castellucci & Kandel, 1974; Armitage & Siegelbaum, 1998). Though recent studies suggest a more complex process than initially thought (Glanzman, 2006), it was clear from this point on that synapses should be at the epicenter of research on cellular learning.

In this thesis, I build upon these findings by exploring the intricate strategies employed by neurons to update their synaptic weights by investigating electrical and biochemical dendritic integration, and synaptic transmission. To introduce the discoveries resulting from the original research presented here, I will first provide a comprehensive overview of the topics that have led to their development.

1 LONG-TERM SYNAPTIC PLASTICITY

Pavlov, Skinner & Bandura's research collectively described the idea that we learn from experience (1910, 1963, 1977). The relatable nature of this phenomenon has captivated the curiosity of many neuroscientists before us. Since the inception of neuroscience, notable figures have contended that learning necessitates association and modulation of neural activity (for review, see Markram et al., 2011; Malenka, 2003). However, it wasn't until 1949, that a postulation of a cellular model of learning was presented (Hebb, 1949). It was Canadian neuroscientist Dr. Donald

O. Hebb who famously wrote that: "When an axon of cell A is near enough to excite a cell B and repeatedly or persistently takes part in firing it, some growth process or metabolic change takes place in one or both cells such that A's efficiency, as one of the cells firing B, is increased.", suggesting that information transmission between two neurons can be modulated by their correlated neural activity.

1.1 **Long-term Potentiation and Depression**

Experimental support for the idea that positively correlated activity should be reinforced began to emerge several years after Dr. Hebb's publication. This was first achieved by Timothy Bliss and Terje Lømo (Bliss & Lømo, 1973), who demonstrated that high-frequency stimulation (HFS) of the perforant path in the anesthetized rabbit's hippocampus resulted in a durable enhancement of synaptic transmission, as recorded by field potentials. This enhancement lasted for hours after the initial stimulation, and was thus named Long-Term Potentiation (LTP; Douglas & Goddard, 1975).

Manuscript I reviews the induction and expression mechanisms of LTP (early and late phases), as well as the relationship between LTP, learning and memory. Briefly, at canonical synapses, LTP depends on Ca^{2+} influx from N-methyl-D-aspartate Receptors (NMDARs; Lynch et al., 1983; Collingridge et al., 1983), which are ionotropic glutamate (co-activated with glycine) receptors that conduct Na^{+}, K^{+} and Ca^{2+} ions (MacDermott et al., 1986; Ascher & Nowak, 1988; Stuart et al., 2016). NMDARs possess a highly non-linear voltage dependence due to Mg^{2+} ion that block their pores at resting membrane potential (Nowak et al., 1984; Mayer et al., 1984; Ascher & Nowak, 1988). As such, NMDARs are activated by coincident excitatory synaptic transmission (*i.e.*, glutamate release) and postsynaptic depolarization (~-30 mV). Intriguingly, although Excitatory Postsynaptic Potentials (EPSPs) can induce sufficient depolarization for NMDAR opening (Caya-Bissonnette et al., 2023), it is typically not sufficient to induce LTP. Instead, strong depolarizations such as that induced by backpropagating of APs (bAPs), or even dendritic spikes, are often required (Lisman & Spruston, 2005, 2010; Markram et al., 1997). Accordingly, NMDARs are coincident detectors of pre- and postsynaptic firing that can induce LTP, providing features that parallel well those of associative learning.

Following NMDAR opening, Ca^{2+} rushes into the cell and binds to endogenous buffers, like Ca^{2+}/Calmodulin-dependent protein Kinase II (CaMKII), that engage in biochemical reactions

eventually leading to α-Amino-3-hydroxy-5-methyl-4-isoxazolepropionic acid receptors (AMPAR) insertion (Herring & Nicoll, 2016; Lisman et al., 2002, 2012; Kessels and Malinow, 2009; Anggono and Huganir, 2012; Huganir and Nicoll, 2013). AMPARs are ionotropic glutamate receptors that open upon glutamate binding and conduct cations such as Na^+ and K^+ (for exceptions, see Stuart et al., 2016; Hume et al., 1991; Hollmann et al., 1991; Tóth & McBain, 1998). AMPARs have very fast inactivation kinetics in the order of 0.5 ms – 1 ms and are thus responsible for the fast component of the EPSP (Silver et al., 1992; Traynelis et al., 2010; Stuart et al., 2016). Their insertions in the membrane cause a long-term increase in synaptic response (*i.e.*, LTP; for variations & more see review Manuscript I). NMDAR-dependent LTP follows squarely the hypothesis enunciated by Hebb (*i.e.*, that correlated synaptic activity should be potentiated), and laid the grounds for research on cellular models of learning.

Under certain conditions, LTP can lead to excessive excitability, implying the requirement of a mechanism for synaptic weight normalization (Sejnowski, 1977; Willshaw & Dayan, 1990). Weight stabilization can be achieved through long-term reduction in synaptic weights, known as long-term depression (LTD). LTD can be induced by low-frequency stimulations (LFS), and, as for LTP, many forms exist and the exact molecular mechanism is incompletely understood (Ito et al. 1982; Levy & Steward, 1983; Dudek & Bear, 1992; Mulkey & Malenka, 1992; Kirkwood et al., 1993; Malenka & Bear, 2004). Generally, LTD depends on Ca^{2+} and its downstream signalling targets (Mulkey et al., 1994; Pi et al., 2010; Zeng et al., 2001), as well as receptors such as NMDARs (Dudek and Bear 1992, Mulkey and Malenka, 1992) and metabotropic Glutamate Receptors (mGluRs; Ito, 1989; Ito et al., 1982; Bolshakov & Siegelbaum, 1994; Oliet et al. 1997). Together, LTP and LTD act as complementary mechanisms to modulate synaptic weights, inducing and maintaining long-term synaptic forms of learning and memory.

1.2 Spike-Timing-Dependent Plasticity

Spike-Timing-Dependent Plasticity (STDP) is a process in which the timing of pre- and postsynaptic spiking determines the direction of plasticity (LTP or LTD; Markram et al., 1997; Bi & Poo, 1998; L. I. Zhang et al., 1998; Debanne et al.. 1998). If synaptic activation is immediately and repetitively followed by postsynaptic APs, LTP is observed (pre-before-post). If presynaptic inputs are immediately and consistently occurring before postsynaptic APs, LTD is observed (post-before-pre). The temporal proximity between pre- and postsynaptic firing is a crucial feature of

STDP. Increasing the time delay between pre- and postsynaptic spiking induces a mono-exponential decay of synaptic weight change that results in a complete extinction of plasticity at delays above 50 ms (Bi & Poo, 1998; Markram et al., 1997; L. I. Zhang et al., 1998; Debanne et al.. 1998). This effect of timing on synaptic weights is in direct consequence to NMDARs activation mechanism, which is determined by the time constant for glutamate binding and depolarization (Kampa et al., 2004). However, these timing requirements are not rigid and vary across different brain regions (Bell et al., 1997; Fino et al., 2005; Froemke et al., 2005; Han et al., 2000; Harvey-Girard et al., 2010; Lamsa et al., 2007; Y. T. Wang & Linden, 2000).

STDP encompasses crucial principles of Hebbian associative plasticity by facilitating the strengthening of correlated inputs (pre-post; LTP). Indeed, the strict time constraint for STDP induction suggests that only presynaptic neurons that participate in the firing of the postsynaptic neurons are potentiated. STDP also weakens uncorrelated firing (post-pre; LTD), effectively reducing the weights of non-causal firing patterns. Due to these properties, STDP has been an important part of research of synaptic models of learning (see review in Manuscript I).

1.3 Heterosynaptic Plasticity

Homosynaptic changes induced by activity-dependent synaptic plasticity represent the bulk of research on LTP and LTD. However, long-term synaptic plasticity can also occur at inactivated synapses, by means of heterosynaptic plasticity. Heterosynaptic plasticity was discovered by Lynch et al., 1977 and is a form of synaptic plasticity that lacks input specificity (Lynch et al., 1977; Royer & Paré, 2003; Caya-Bissonnette, 2020; Chistiakova et al., 2019; Levy & Steward, 1979). Heterosynaptic plasticity has been thought of as an important mechanism to normalize network dynamics and prevent runaway excitation or excessive depression (Chistiakova et al., 2014; Field et al., 2020; Royer & Paré, 2003). This is partly because HFS leading to homosynaptic LTP, can in parallel lead to heterosynaptic depression at unstimulated synapses (Levy & Steward, 1979; Lynch et al., 1977). Analogously, heterosynaptic LTP can occur at synapses neighbouring those undergoing homosynaptic LTD (Royer & Paré, 2003). Due to these properties, heterosynaptic plasticity is considered non-Hebbian. The effect of weight normalization have also been implicated in the formation of receptive fields *in vivo* (Dunfield & Haas, 2009; Bakin & Weinberger, 1996; Froemke et al., 2007, 2013; Kilgard & Merzenich, 1998),

highlighting its potential in generating feature selectivity through bidirectional regulation of synaptic weights.

In Manuscript III, I comment on recent findings regarding the induction of heterosynaptic plasticity in interneurons of the visual cortex and elaborate on its role in weight stabilization (Caya-Bissonnette, 2020; Chistiakova et al., 2019).

Together, long-term synaptic changes hold important functional significance in regulating information transmission at synapses, circuit dynamics, and learning. In the next section, I explore with greater granularity the regulation of Ca^{2+}, an important ion in synaptic plasticity.

2 CALCIUM DYNAMICS

Ca^{2+} serves as a pivotal component in synaptic and dendritic integration. Ca^{2+} mediates the transformation of electrical signals (*e.g.,* APs) into chemical signals, facilitating communication between presynaptic and postsynaptic neurons (Kandel et al., 2000; Katz & Miledi, 1967). Ca^{2+} also activates signaling pathways that have profound influence on synaptic modifications underlying learning and memory, such as by shaping short-term plasticity (Dobrunz & Stevens, 1997; Dittman & Regehr, 1998; Dittman et al., 2000; Regehr et al., 1994, Tank et al., 1995; Chamberland et al., 2017), and establishing long-term synaptic plasticity (Lynch et al., 1983; Herring & Nicoll, 2016; Bittner et al., 2017). Understanding the dynamics of Ca^{2+} and its instrumental role in learning is thus critical to neuroscience research on learning.

2.1 Calcium Entry from the Extracellular Space

The relatively large extracellular Ca^{2+} concentration promotes Ca^{2+} flux into the intracellular space (Kandel et al., 2000). Although many receptors and channels conduct Ca^{2+} (*e.g,* GluA2-lacking AMPARs (Hume et al., 1991; Hollmann et al., 1991; Tóth & McBain, 1998), nicotinic acetylcholine receptors (Szabo et al., 2008; Fayuk & Yakel, 2007; J. Shen & Yakel, 2009), *etc.*), two main sources are of significant importance for long-term synaptic plasticity: NMDARs and VGCCs.

NMDARs are typically di-heteromeric receptors formed from two GluN1 and two GluN2 (2A-2D) subunits, though they can be tri-heterometric if they contain different GluN2 subunits or an extra GluN3 (A or B) subunit (Stuart et al., 2016). Subunit composition affects several biophysical features of NMDARs, such as gating, kinetics and Ca^{2+} permeability. For instance,

GluN2A and GluN2B containing NMDARs are blocked more strongly by Mg^{2+} than other subunits (Kuner & Schoepfer, 1996; Qian et al., 2005; Siegler Retchless et al., 2012; Wrighton et al., 2008), which affects their ability to conduct Ca^{2+}. NMDARs are responsible for the slow component of the Excitatory Postsynaptic Currents (EPSCs) due to their long rise time ~ 10 ms – 50 ms (Haas et al., 1998; Zito & Scheuss, 2009) and inactivation kinetics (Bekkers & Stevens, 1989; Silver et al., 1992), which can vary widely between 40 ms (GluN1/GluN2A) and 2 s (GluN1/GluN2D) (Vicini et al., 1998). Although NMDARs are important synaptic components, they are also present at extra-synaptic sites, a differentiation that can lead to the activation of distinct signalling pathways (Bading et al., 1993; Hardingham et al., 2002; Stark and Bazan, 2011).

Activation of a large number of spines in close spatio-temporal proximity increases dendritic depolarization. This cooperation between spines increases the likeliness of NMDAR activation. As such, NMDAR opening can benefit from clustered synaptic inputs. At the extreme case, this can cause NMDA spikes. NMDA spikes delineate a non-linear activation of NMDARs (Schiller et al., 2000; Larkum et al., 2009; Makara & Magee, 2013). NMDA spikes occur when the depolarization surpasses a critical threshold, allowing the relief of Mg^{2+} block on NMDARs that would typically experience insufficient depolarization. These spikes necessitate a high density of receptors, including AMPARs, to sustain the depolarization above threshold (Branco & Häusser, 2011; Larkum et al., 2009; Major et al., 2013; Nevian et al., 2007; Rhodes, 2006). Moreover, NMDA spikes are limited to the synaptically activated region due to their dependence on glutamate binding. Due to the long activation of NMDAR, NMDA spikes can facilitate the spread of passive and active signal, and are thus important aspects of dendritic integration.

Another important source of Ca^{2+} influx is through VGCCs, which elicit slow and prolonged inward currents, that tend to prolong AP and promote burst firing (Dunlap et al., 1995; Huguenard, 1996; Trimmer & Rhodes, 2004). There are a few different subtypes, mainly T-, N-, L-, P/Q-, and R-type VGCCs, which can be identified by their response to different toxins (Carbone & Swandulla, 1989; Tsien et al., 1988; Usowicz et al., 1992; Stuart et al., 2016). All subtypes of VGCCs are observed in L5 neocortical neurons, including distal tuft and spines (Markram et al., 1995; Schiller et al., 1997).

VGCCs are important in mediating Ca^{2+} dendritic spikes (Houchin, 1973; Llinás & Hess, 1976; Schiller et al., 1997; Stafstrom et al., 1985). Ca^{2+} dendritic spikes can facilitate the electric coupling between the remote tuft and the soma of pyramidal neurons (Larkum et al., 1999), and

may be useful correlates of association between proximal and distal inputs (Larkum et al., 1999; Major et al., 2013).

In sum, VGCCs and NMDARs are important point of entry for Ca^{2+}. Ca^{2+} through VGCCs can act with, or as an alternative to, Ca^{2+} entry through NMDARs to induce LTP (Pigott & Garthwaite, 2016; Weisskopf et al., 1999; Youn et al., 2013). Once inside the cell, Ca^{2+} activates signalling pathways and binds to channels and pumps to induce complex interplays between Ca^{2+} amplification and Ca^{2+} removal mechanisms.

2.2 Intracellular Regulation

Intracellular Ca^{2+} is important for a range of molecular pathways, including cascade enacted by CaMKII underlying long-term synaptic plasticity (Herring & Nicoll, 2016; Lisman et al., 2012). Ca^{2+} may also amplify its own signal, or initiate its removal by interacting with intracellular organelles.

Many intracellular organelles can sequester and release Ca^{2+}, such as mitochondria (Giorgi et al., 2018; Hirabayashi et al., 2017), lysosomes (López-Sanjurjo et al., 2013), golgi apparatus (Chandra et al., 1991), *etc*, but the most notable Ca^{2+} stores are those of the Endoplasmic Reticulum (ER). ER stores are important regulators of intracellular Ca^{2+} (Hirabayashi et al., 2017; Nakamura et al., 1999; Power & Sah, 2007; Satoh et al., 2011) and are present in dendrites, and, occasionally, in spines (Cooney et al., 2002; Spacek & Harris, 1997; Lee et al., 2016; Emptage et al., 1999).

ER stores uptake Ca^{2+} via sarco/endoplasmic reticulum Ca^{2+}-ATPase (SERCA) pumps by removing Ca^{2+} from the intracellular space non-linearly based on Ca^{2+} concentration (Satoh et al., 2011). ER stores can also release Ca^{2+} via either ryanodine receptors (RyR), by a process called Ca^{2+}-induced Ca^{2+}-release (CICR), or by Inositol 1,4,5-trisphosphate (IP_3) receptors (IP_3Rs) through IP_3-induced Ca^{2+}-release (IICR; Koch, 1990; Ashby & Tepikin, 2001; Evstratova & Tóth, 2011). IP_3Rs activate upon binding of Ca^{2+} and IP_3 (Verkhratsky, 2005). IP_3 is generated downstream of G-protein coupled receptors (GPCR), can diffuse to dendritic sites (Stuart et al., 2016; where IP_3Rs are localized in the hippocampus; Berridge, 1998; Sharp et al., 1993), and has a lifetime of a few seconds (Allbritton et al., 1992; S. S. Wang et al., 1995). These release mechanisms are important amplification processes involved in a variety of functions (Cavazzini et al., 2005; C. R. Rose & Konnerth, 2001; Segal et al., 2010).

IICR requires IP_3 formation which is facilitated by GPCRs. There are three main GPCR signaling pathways determined by their associated G-proteins. The first are G_q proteins. They activate phospholipase C (PLC) pathway, which cleaves phosphatidylinositol 4,5-bisphosphate (PIP_2) into diacyl glycerol (DAG) and IP_3, which activate Protein Kinase C (PKC) and intracellular release of Ca^{2+} (Duman & Nestler, 1995). The second are $G_{i/o}$ proteins. They reduce intracellular cyclic adenosine monophosphate (cAMP) production by inhibiting adenylyl cyclase. The third are G_s proteins, which increase cAMP signaling by promoting adenylyl cyclase (Duman & Nestler, 1995). mGluRs of the Group 1 (mGluR1 and mGluR5) are G_q-coupled receptors, and are thus important for IICR.

mGluR Group 1 are mainly expressed postsynaptically (Grueter & Winder, 2009; Shigemoto et al., 1993). They are heavily implicated in synaptic plasticity (Cavazzini et al., 2005; C. R. Rose & Konnerth, 2001; Segal et al., 2010), IICR, which generate large and highly localized Ca^{2+} signal, and in the generation of Ca^{2+} waves in apical dendrites of pyramidal cells (Larkum et al., 2003; Nakamura et al., 1999). mGluRs group 1 can also increase NMDAR activity through PKC-mediated effects (Ben-Ari, 1992; Fitzjohn et al., 1996), and have varying effects on cell excitability via their action on Na^+ channels, K^+ channels and VGCCs (Chemin et al., 2003; El-Hassar et al., 2011; Hildebrand et al., 2009; Yu et al., 2018), such as reduction of synaptic depolarization via indirect activation of Ca^{2+}-activated K^+ channels.

Taken together, Ca^{2+} entering through NMDARs and VGCCs can have varying effects, including signal amplification by inducing CICR and IICR *via* interaction with the ER. The complex effects of Ca^{2+} are important for synaptic plasticity, and are investigated in Manuscript IV.

2.3 Computational Models for Plasticity Induction

The pivotal role of Ca^{2+} in LTP has sparked various hypotheses regarding the mechanism it employs to regulate synaptic changes, many of which have been explored through computational models. Ca^{2+} is involved in both LTP and LTD, despite yielding opposing outcomes in these cases. This paradox has posed a significant challenge. One possible explanation lies in the distinctive CaMKII phosphorylation patterns observed during LTP and LTD (Cook et al., 2021; Pi et al., 2010). For instance, protein kinases are recruited during LTP, while protein phosphatase like

calcineurin are recruited during LTD (Mulkey et al., 1994; Pi et al., 2010; Zeng et al., 2001). Nevertheless, the precise mechanism by which this divergence is accomplished remains unclear.

The first hypothesis to emerge as an explanation for the dual role of Ca^{2+} in long-term synaptic plasticity proposes that the amplitude of Ca^{2+} determines the sign of plasticity (for review see Evans & Blackwell, 2015). This hypothesis, also known as the two-threshold hypothesis, has received some experimental support. Correlational findings provide support for an amplitude-based model, such as evidence that HFS leads to high Ca^{2+} influx, preferentially activates CaMKII, and induces LTP, and LFS leads to low Ca^{2+} influx, preferentially activates phosphatases like calcineurin, and induces LTD (Hansel et al., 1996; L. Li et al., 2012; Mulkey et al., 1994). Further studies demonstrated that reducing Ca^{2+} concentration directly (Mulkey & Malenka, 1992), or by NMDAR antagonist (Cummings et al., 1996) and Ca^{2+} buffers (Cho et al., 2001; Hansel et al., 1996) during LTP-inducing protocols resulted in a switch from LTP to LTD. Using the two-threshold hypothesis, computational simulations successfully replicated STDP curves, as well as the frequency-dependence of long-term synaptic plasticity induction (Bush & Jin, 2012; Inglebert et al., 2020; Shouval et al., 2002). However, a consequence of the two-threshold model is that during large Ca^{2+} influx, such as those induced by LTP pairings, the Ca^{2+} inevitably returns to baseline, creating a period during which Ca^{2+} level can trigger LTD. During pre-before-post STDP pairings, this effect manifests itself at extended timescales (70 ms - 120 ms), resulting in a second LTD window that is not supported by experimental results (Bi & Poo, 1998; Markram et al., 1997). To address this issue, the hypothesis has been refined to consider the duration of Ca^{2+} events (S. N. Yang et al., 1999).

By considering both duration and amplitude, hypotheses regarding the dual role of Ca^{2+} propose that short and high Ca^{2+} influx contribute to LTP, whereas long and low Ca^{2+} influx contribute to LTD. This notion finds support from various induction protocols. HFS, characterized by high Ca^{2+} amplitude and short durations, induces LTP (L. Li et al., 2012; Mulkey et al., 1994). In contrast, LFS induces low Ca^{2+} amplitudes of long durations and LTD (L. Li et al., 2012; Mulkey et al., 1994). In addition, Ca^{2+} release from internal stores, which occurs on slower timescales than ionotropic Ca^{2+} influx, has been implicated in the induction of LTD (Jo et al., 2008; Nishiyama et al., 2000). This hypothesis also aligns well with computational models (Graupner & Brunel, 2012; Rubin et al., 2005). Though, these hypotheses neglect to account for the subcellular localization of Ca^{2+} currents.

The spatial distribution of Ca^{2+} influx and endogenous buffers can redirect activation of signalling pathways (Isaacson & Murphy, 2001; Liang et al., 2003; Naraghi & Neher, 1997). The sources of Ca^{2+} influx are different during LTP and LTD induction (Fino et al., 2005; Nabavi et al., 2013). For instance, the activation of NMDARs in synaptic *versus* extra-synaptic domains have been found to be relevant in determining the sign of plasticity (Liu et al., 2013). The importance of location in determining the sign of plasticity has seen a beginning of computational support (Keller et al., 2008). Yet, it remains unclear how exactly Ca^{2+} can lead to opposite outcomes, understanding its role could provide insights into the complex dynamics and molecular interplay between LTP and LTD. Consequently, we explore this in Manuscript IV, where we modeled Ca^{2+} dynamics within the context of a new form of synaptic plasticity in the hope to shed light on these issues.

3 TEMPORAL CREDIT ASSIGNMENT PROBLEM

Long-term synaptic plasticity provides an interesting correlate of learning and memory at the neuronal level. However, notable disparities between synaptic and behavioral models of learning create obstacles in providing a satisfying model of associative memory. An illustrative instance of a basic associative learning task is exemplified by a baby acquiring the motor skills necessary to grasp and drink from a milk bottle. In this scenario, the gratifying outcome of drinking the milk occurs after the initial cues or motor actions, with a time delay ranging from 200 ms to 2 s (Gerstner et al., 2018). It is ambiguous how the brain retrospectively assigns proper credit to cues (or actions) as being causally related to the delayed rewarding outcome. This is referred to as the temporal credit assignment problem (also known as distal reward problem; Hull, 1943), and highlights the challenge of understanding the neural mechanisms underlying delayed association between cues and rewards.

3.1 The Beginning of a Solution: Behavioral Timescale Synaptic Plasticity

Mounting evidence proposes a strong link between LTP, learning and memory storage (see review Manuscript I). Along these lines, exciting recent results present a compelling argument regarding a form of synaptic plasticity underlying the emergence of place cells in the hippocampus. Place cells are neurons that fire when an animal is in specific locations (O'Keefe & Dostrovsky, 1971; O'Keefe, 1976; Wilson & McNaughton, 1993, O'Keefe & Nadel, 1978). The sequential

order of place cell firing present a spatial map that appear exclusive to that environment, though it can be altered by motivation or other behavioral states (Grienberger & Magee, 2022; Moser et al., 2015; Markus et al. 1995; Frank et al. 2000; Wood et al. 2000; Moita et al. 2004). As such, place cells provide an intriguing mechanism for flexible representation of spatial and contextual cues, a discovery that was instrumental in understanding hippocampal function and spatial navigation; and led to the 2014 Nobel prize in Physiology or Medicine (Fyhn et al., 2004; Hafting et al., 2005; O'Keefe & Dostrovsky, 1971).

Research groups have been interested in understanding the induction of place cells in CA1 neurons. For instance, Jeffrey Magee lab found, as per preceding accounts (Epsztein et al., 2011; Harvey et al., 2009), that CA1 neurons of mice running on a linear thread mill track saw an increase in membrane voltage that ramped up for a couple of seconds before and after place cells firing (Bittner et al., 2015, 2017). This second-long ramp up appeared with place cells firing after their induction by a plateau potential (Bittner et al., 2015, 2017). This second-long ramp up hinted at a non-Hebbian plasticity rule, one in which inputs that are not directly related to the firing of the place cells were potentiated. Bittner et al., (2017) tested this hypothesis *in vitro*, and, remarkably, found that five pairings of subthreshold presynaptic inputs and postsynaptic plateau potentials at seconds delay induced robust potentiation, matching their *in vivo* observations. This plasticity was called Behavioral Timescale Synaptic Plasticity (BTSP), and was defined by the plateau-driven abrupt appearance (one- to few-shots) of place cells, and its asymmetric, seconds-long induction time course. This synaptic plasticity stands in peculiar contradiction to STDP; it can be induced by delayed pre- and postsynaptic spiking (seconds), and in only a few repetitions; yet it is dependent on NMDARs and VGCCs (Bittner et al., 2017; Grienberger & Magee, 2022). This non-Hebbian form of plasticity provides an interesting solution to the temporal credit assignment problem; where inputs can arrive at second delay and undergo LTP, a hallmark of synaptic learning and memory.

In 2022, the Magee group published a paper in which a reward was added at a specific location on the linear treadmill track experimental set up. The reward caused a rearrangement of place cells to over represent reward location (Grienberger & Magee, 2022). This over representation was induced by BTSP as implied by its *in vivo* electrophysiological and pharmacological signature (Grienberger & Magee, 2022). Since BTSP is induced by plateau potentials, and the duration and probability of inducing plateaus in CA1 neurons involve inputs

from entorhinal cortex layer 3 (EC3) (Grienberger et al., 2015; Takahashi & Magee, 2009), Grienberger and Magee (2022), hypothesized that EC3 inputs were crucial for reorganizing place cells. Consistently, the authors found that optogenetic inhibition of EC3 abolished reward over representation, suggesting that EC3 inputs are related to learning the spatial task. Curiously, the activity of EC3 neurons remained constant throughout learning, and represented the target activity pattern that CA1 neurons reached with learning. Together, these results suggest that EC3 neurons convey an instructive signal for place cells induction, and BTSP.

As a development to this work, Karl Deisseroth's lab used all optical methods to reproduce the *in vivo* results (Fan et al., 2023). They used genetically encoded voltage indicators, and ruled out the possibility that BTSP was induced by increased cellular excitability, and also showed that BTSP was prevented when CA2/3 inputs were silenced, suggesting that BTSP underlying place cell formation in the hippocampus is induced at CA2/3 to CA1 synapses. In agreement with the Magee group, inhibition of CA2/3 inputs did not prevent induction of plateau potentials, together implying that plateau potentials are instead induced as error signals to update CA2/3 inputs (Bittner et al., 2015, 2017; Grienberger & Magee, 2022).

To summarize, place cells are cells that fire within a specific location and become stable with training (Vaidya et al., 2023). They can represent multiple environments, including contextual variables, by remapping their activation patterns (Frank et al., 2000; Grienberger & Magee, 2022; Markus et al., 1995; Moita et al., 2004; Wood et al., 2000). Place cells are induced rapidly (one to few shots) by BTSP as a result of distal EC3 input-driven plateau potentials and second-long proximal subthreshold CA2/3 inputs (Bittner et al., 2015; 2017; Grienberger & Magee, 2022; Fan et al., 2023). These findings elaborate on a mechanism for the induction of place cells that relies on synaptic plasticity to induce a strong potentiation at second-long timescales. This discovery caused significant ripples in the field, as it provides a solution to the temporal credit assignment problem by offering a synaptic plasticity mechanism for the association of temporally discontiguous cues.

3.2 The Prefrontal Cortex

BTSP has been discovered in the hippocampus, a region that forms flexible representation of the environment for spatial navigation. We hypothesized that BTSP may be present in other brain region where flexible representation are used to evaluate dynamic environmental and internal

factors, such as in the medial prefrontal cortex (mPFC; Igarashi et al., 2022; Reinert et al., 2021; Samborska et al., 2022).

The PFC is the most rostral part of the neocortex. Although its definitive boundaries are subject to unresolved controversies (see Laubach et al., 2018), Rose and Woolsey (1948) proposed that the PFC be anatomically defined as the recipient of inputs from the mediodorsal nucleus of the thalamus, a feature that is shared between primate and non-primate mammals. The medial part of the PFC, the mPFC, is subdivided in a ventral-dorsal gradient into the infralimbic (IL), prelimbic (PrL), anterior cingulate cortices (ACC) and, sometimes including the secondary motor area (M2; see Laubach et al., 2018). The PFC sustains higher order cognition and has garnered significant attention as an association area that is important for associative learning (Fuster, 1973; J. N. Kim & Shadlen, 1999; Schall & Hanes, 1993; Goldman-Rakic, 1995; Anastasiades & Carter, 2021; Peters et al., 2022). This makes it an excellent candidate for investigating the cellular mechanisms underlying associative learning.

The role of PFC in higher order cognition saw an increased interest in the late 20th century for its role in working memory (Fuster, 1973, 1985; Fuster & Alexander, 1971; Kubota & Niki 1971;34:337–347.). The term *working memory* was first coined by Baddeley & Hitch (1974), and defines the short-term memory responsible for maintaining information in absence of sensory inputs. The work of Goldman-Rakic in the 1990s significantly expanded our understanding of working memory in the PFC (Kritzer & Goldman-Rakic, 1995; Goldman-Rakic, 1995; Constantinidis et al., 2001; Constantinidis & Goldman-Rakic, 2002). Using the delayed-response task, Goldman-Rakic (1995) revealed that monkey's frontal cortex exhibits sustained activity while preserving the memory of a visual stimulus's spatial location prior to motor response. In some cases, working memory can resist distractors (See Appendix E). Working memory has been observed in rodent's PFC (S.-T. Yang et al., 2014), together, suggesting a functional role of PFC, that is conserved across species, in the association of sensory cues and delayed motor output. In recent years, the overarching function of the PFC and its sustained firing activity has been expanded to include broader computations related to flexible behaviors, as its activity reflects rules and categorizations (Reinert et al., 2021; Wallis et al., 2001), and evaluation of decision and motivational factors (Diehl & Redish, 2023; J. N. Kim & Shadlen, 1999; Schall & Hanes, 1993).

Task-related activity in the mPFC appears with learning. Using widefield imaging and neuropixel probes during the learning of a visuomotor association task in mice, Peters et al. (2022)

observed that PFC neurons responded to both stimulus and movement, sometimes within the same neurons, in a ventral-dorsal gradient (from IL region to M2). Interestingly, these responses, which appeared to be occurring in deep layers, were absent in naive mice, suggesting that sensory-motor activity emerges in the PFC during associative learning. How can the PFC learn to make sensory-motor associations when visual inputs and motor commands are separated by hundreds of milliseconds (Peters et al., 2022; Steinmetz et al., 2019; Zatka-Haas et al., 2021)? In other words, how can the PFC solve the temporal credit assignment problem? While previous models of synaptic plasticity have been unable to explain these timescales effectively (see review Manuscript I), recent evidence of BTSP may provide a solution to this issue (see Manuscript IV-V; Bittner et al., 2017).

Persistent firing that binds delayed cues in the mPFC is believed to be encoded by the strong recurrent connectivity in L5 neurons, and constrained by local inhibition (Baker et al., 2018; Collins et al., 2018; E. Kim et al., 2021; Rao et al., 2000; X. J. Wang, 2001). This strong recurrent connectivity is enabled by the significant portion (50 %) of monosynaptic inputs targeting L5 neurons, often proximally, that originates from within the PFC (Collins et al., 2018; DeNardo et al., 2015). Intriguingly, inputs to L5 neurons trigger reward-predictive subthreshold activity during second-long association tasks (Collins et al., 2018; E. Kim et al., 2021; X. J. Wang, 2001). These subthreshold dynamics cause a ramp up in membrane voltage in L5 neurons ahead of firing (E. Kim et al., 2021). This activity thus reflects important task-relevant information that drives L5 neurons on a timescale relevant to BTSP, and may be relevant in the induction of persistent firing.

The ability of the PFC to integrate across a range of behaviorally relevant modalities and exert top-down control over goal-directed behaviors (Miller & Cohen, 2001) is reflected by its wide connectivity. For instance, L5 pyramidal neurons possess large dendritic arbors, long axons, and extensive connectivity with subcortical regions (Anastasiades & Carter, 2021). Areas that receive projections from L5 PFC neurons include sensory areas such as auditory (Bedwell & Tinsley, 2018) and somatosensory cortices (Bedwell et al., 2014), motor areas such as motor cortices (Bedwell et al., 2014), and striatum (Gabbott et al., 2005), as well as limbic structures involved in emotions and motivations such as amygdala, hypothalamus (Gabbott et al., 2005) and dorsal raphe (Geddes et al., 2016). Projection of L5 pyramidal neurons vary by cell types, which can be identified by location, and morphological and electrophysiological features (Anastasiades & Carter, 2021; Baker et al., 2018; Galakhova et al., 2022; Ramaswamy & Markram, 2015).

Together, this connectivity may facilitate the encoding of a wide range of information before appropriate motor output is initiated (Miller & Cohen, 2001).

In manuscript IV, we established the presence of BTSP in the PFC *in vitro*, the first evidence of such plasticity outside of the hippocampus. We tested proximal inputs incoming onto L5 neurons, since a large portion of proximal synapses springs from locally recurrent connections that are important to maintain representation over long periods of time (Bari et al., 2019; N. C. Dembrow et al., 2015; DeNardo et al., 2015; X. J. Wang, 2001). We further investigated the contingencies of BTSP, such as its burst- and repetition-dependency, in Manuscript V (See Appendix A).

3.3 Eligibility traces

Evidence of BTSP provides an interesting line of research to the temporal credit assignment problem; however, the mechanism employed by neurons to achieve the binding of temporally discontiguous cues is unknown. The most relevant theory that attempts to answer this question relates to eligibility traces (Klopf, 1972). Inspired by biological theories of synaptic plasticity, the concept of eligibility traces was first coined in the field of reinforcement learning (Barto, Sutton & Anderson, 1983; Lin, 1992; Tesauro, 1992; Peng & Williams, 1994). Eligibility traces refer to the process of maintaining a record of "synaptic" states, such that future event could update the appropriate connections. This concept became the fundamental theory underlying temporal difference (TD) learning and more (Sutton & Barto, 2014). In TD learning, eligibility traces are updated by backpropagation through time, which is inefficient and biologically implausible, limiting the application of eligibility traces to artificial systems. Nevertheless, some have argued that eligibility traces may exist in biological systems, acting as an elemental structure for associative plasticity at extended timescales (Gerstner et al., 2018).

In 2018, Gerstner et al., delineated a few experimental evidence pointing to the existence of eligibility traces in biological systems. First, Yagishita et al. (2014) induced STDP pairings in medium spiny striatal neurons in the nucleus accumbens using glutamate uncaging. This induction protocol did not lead to plasticity. However, optical release of dopamine (DA) up to 1 s after the end of STDP pairings retrieved potentiation. This suggest that the conjunctive activity of pre- and postsynaptic neurons induced by STDP pairings elicited a silent eligibility trace that could be transformed into LTP by DA. The timescale (1 s) is much longer than that of typical NMDARs

binding and unbinding kinetics (Kampa et al., 2004), and thus reveals the presence of a second-long eligibility trace that binds temporally separated cues. Second, He et al. (2015) showed that visual and PFC neurons could undergo similar eligibility trace-induced potentiation. Here, silent STDP pairings developed into potentiation upon optogenetically released norepinephrine (NE) (and DA in PFC), if the release occurred within 5 s of STDP pairings (pre-before-post). Depression could also be induced by silent post-before-pre pairings if serotonin (5-HT) was released within 2.5 s. They observed no change by acetylcholine (ACh) administration. In another study, Fuchsberger et al. (2022), found that hippocampal synapses undergoing LTD by post-before-pre STDP pairings could transition into LTP up to 10 minutes later by co-occurrence of a burst of postsynaptic APs and DA administration. In these examples, STDP pairings extend the functionality of conjunctive pre- and postsynaptic activity by inducing a memory trace that lasts for seconds. This memory can be transformed into appropriate synaptic weight change by neuromodulators. This framework bears resemblance to associative learning at the behavioral level. For instance, ordinary events may not inherently trigger memory or learning, but none-trivial events, such as those prompting DA or NE release, can. This functional extension implies the presence of biological eligibility traces; synaptic or cellular substrates permissive to the maintenance of a memory for seconds after their inductions.

Another line of evidence supporting the existence of eligibility traces in biological systems is provided by BTSP. BTSP presents a novel synaptic plasticity mechanism that results from the association of pre- and postsynaptic neurons, albeit not within timescales directly relevant for immediate causal influence (*i.e.*, presynaptic inputs do not lead to postsynaptic neuron firing; non-Hebbian). This distinctive characteristic of BTSP is of great significance as it suggests that neurons can link events that are temporally separated, and, in other words, require a synaptic or cellular substrate to bind pre- and postsynaptic events arriving at second-long delays (*i.e.*, eligibility traces). Together, these experimental evidence provide a relevant solution to the temporal credit assignment problem; but if eligibility traces exist, what are their material nature?

In Manuscript IV, we address this question and pursue evidence of eligibility trace manifestations during the binding of temporally discontiguous cues elicited by BTSP induction. We test and validate the role of Ca^{2+}, which is at the crux of LTP, in mediating eligibility traces *via* the recruitment of Ca^{2+} stores.

4 ONE SHOT LEARNING.

Humans demonstrate remarkable ability to learn quickly and efficiently. For instance, upon meeting a new person, our brain can rapidly encode their unique facial features and remember them for subsequent encounters. We can often recognize someone we have only met once, even after a significant period of time has passed. The process by which we can learn in only one or a few exposures has seen some experimental evidence in humans (Thorpe et al., 1996) and in mice (W. B. Kim & Cho, 2020; Radulovic et al., 1998), and may require the PFC (S. W. Lee et al., 2015). Understanding the cellular model of one-shot learning is important as it provides valuable insights into how our brains process and retain information in a rapid and efficient manner.

Computational models have used one-shot learning in algorithms to model learning behaviors (Boucher-Routhier et al., 2021; S. W. Lee et al., 2015; Lehmann et al., 2019; Weaver, 2015; Fei-Fei et al., 2006), but evidence of one-shot learning in synaptic models is largely unexplored. For over 25 years, the standard for studying associative synaptic plasticity has been STDP. However, STDP requires a few dozen pairings to induce potentiation. BTSP, on the other hand, is induced in a few pairings *in vitro*, while place cells induced by BTSP appeared in a single shot *in vivo*. Thus, we ask whether BTSP provide a viable solution to explain one shot, or few shot learning at the synaptic level. In other words, we ask; how can neurons perform such rapid updating of weights? We explore this in Manuscript V, in which we find that bursting, within the context of BTSP induction, is tightly related to the ability of synapses to undergo potentiation in one shot.

Preface to manuscripts

Here, I present five manuscripts that were written during the course of my doctoral studies. The manuscripts were formatted based on the standards of the journals that they were submitted for, and therefore may exhibit small differences in structure.

Manuscripts I provide a review of LTP from past to present and its relationship to learning processes. This review manuscript has been submitted for an invited submission at *Current Biology*.

Manuscript II and III are perspective articles. Manuscript II is an opinion piece of two-photon microscopy techniques and glutamate uncaging and its relevance to studying cellular and dendritic mechanisms, including those related to synaptic plasticity. It has been published in *Neurophotonics* (2023). Manuscript III regards novel findings on heterosynaptic plasticity at cortical interneurons and was published in the *Journal of Neuroscience* (2020).

Manuscripts IV and V are original research studies on BTSP, eligibility traces and one-shot learning. Manuscript IV is undergoing review, while Manuscripts V is still in its early stage of preparation.

Manuscript VI has been published in the *University of Ottawa Journal of Medicine* in the context of a contest on current medical issues. I won 3rd place in the contest.

MANUSCRIPTS

MANUSCRIPT I

Half a Century Legacy of Long-Term Potentiation.

Léa Caya-Bissonnette[1,2,3] Jean-Claude Béïque[2,3]*

This manuscript is submitted for an invited review to *Current Biology*.

Author contribution: L.C.B. and J-C.B. wrote the manuscript and designed the figures.

***Corresponding authors.**

[1] Graduate Program in Neuroscience, University of Ottawa

[2] Brain and Mind Research Institute's Centre for Neural Dynamics and Artificial Intelligence

[3] Department of Cellular and Molecular Medicine

451 ch. Smyth Rd. (3501N), Ottawa ON Canada K1H 8M5

Faculty of Medicine, University of Ottawa

ABSTRACT

In 1973, two papers published back-to-back (Bliss and Lømo; Bliss and Gardner-Medwin) reported the activity-dependent long-term potentiation (LTP) of synaptic transmission in the dentate gyrus of both anesthetized and unanesthetized rabbits. 50 years of hindsight emphatically highlights the colossal research effort that was directly motivated by these landmark contributions. In this brief historical piece, we detail some of the resulting milestones that shape our current mechanistic understanding of the molecular and cellular underpinnings of LTP, from its induction and expression to its potential role in learning and memory processes. We briefly explore some ramifications on network stability, consider current limitations of LTP as a model of associative memory and entertain future research orientations.

MAIN TEXT

A brave young girl blithely decides to climb a towering tree in her backyard. With each upward step, her steadfast resolve does not falter, her eyes locked on the treetop. Reaching the highest branch provides her with an entirely stunning and unanticipated perspective, making her heart race and palms sweaty. Overwhelmed by fear, realizing the perilous descent that awaits her, she vows to never climb that tree again. That single salient experience updated her model of the world in a way that would influence her decision-making process ever so slightly, but potentially for the rest of her life. This simple real world example highlights an intuitively explicit evolutionary grounded role for learning and memory, wherein learning encodes a catalog of memories to guide behavioral policies for survival principles.

This deeply fascinating phenomenon has driven the curiosity of so many before us to understand how the brain ultimately realizes this feat. By the late 19th century, scientists like Ramon y Cajal and Ernesto Lugaro had already suggested the idea that high '*mental activity*' could lead to the formation of new nerve collaterals, or reinforce pre-existing connections, in a clairvoyant foreshadowing of what is now commonly referred to as activity-dependent synaptic plasticity. Fifty years later, Canadian neuroscientist Donald O. Hebb proposed in *The Organization of Behavior*[1]a cellular learning mechanism for a recurrent neural network, famously written as: "*When an axon of cell A is near enough to excite a cell B and repeatedly or persistently takes part in firing it, some growth process or metabolic change takes place in one or both cells such that A's efficiency, as one of the cells firing B, is increased* ". Hebb's postulates thus suggest that 'activities' (loosely defined) that are causally related should be reinforced, ultimately leading to the emergence of stable Hebbian cell assemblies. Despite the apparent simplicity of this idea, it was unclear whether a broadly analogous form of plasticity existed in the brain.

In 1973, Terje Lømo and Timothy Bliss published a study revealing that high-frequency electrical stimulation (so-called tetanic bursting) of the perforant path in the hippocampus of an anesthetized rabbit, led to a long-lasting enhancement in the strength of synaptic transmission as measured by recordings of field potentials (Figure 1)[2]. In the same issue of *The Journal of Physiology*, Bliss and Tony Gardner-Medwin[3] reported analogous findings but from recordings in freely behaving, chronically implanted rabbits. Collectively, these papers outlined a form of

synaptic potentiation that was activity-dependent and could last up to 3 days after the plasticity-inducing stimulation protocol. The now famed appellation of Long-Term Potentiation (LTP; as opposed to long-lasting potentiation as initially described) was coined soon thereafter by Douglas and Goddard[4] in reporting that repeated bursts of inputs were more effective to induce synaptic potentiation. It is difficult to exaggerate the magnitude and extent of the interest, scrutiny, and wonderment that this conceptually relatively simple phenomenon would generate in the decades to come, and this from both experimental and theoretical neuroscience fields alike. LTP has been observed in several brain regions, such as cortex[5-8], striatum[9,10], monoaminergic nuclei and several others[11-14]. Bliss, Lømo, and Gardner-Medwin's findings manifestly marked year 1 of a fascinating, and resolutely still marching, journey that seeks to understand how neurons, and ultimately how *we*, learn. While outstanding reviews of LTP have been written over the years by investigators that have profoundly contributed to LTP research from its inception[14-22], we here provide a summary of important milestones of this journey.

Basic features of LTP at canonical synapses

Early LTP experiments revealed key sets of fundamental properties of LTP. First, Bliss Lømo, and Gardner-Medwin demonstrated that synaptic connections between neurons could be strengthened for a prolonged period of time, exposing the characteristic *persistence* of LTP, fulfilling perhaps one of the most defining features expected of a cellular model of learning and long-term memory (Figue 2A). Second, LTP is *input specific*, in that it is only observed in the tetanized pathway, a property that is likely singularly important for optimal information storage[14] (Fig. 2B) Third, LTP induction is highly constrained, being generated only when sufficiently strong stimulations occur. Such a thresholding operation can be attained through a number of ways, including through *cooperation* between activated synapses (Fig. 2C;[23,24]). Fourth, LTP is *associative* (Fig. 2D). Associativity refers to the idea that weak stimulation of one pathway, which does not induce plasticity, paired with strong stimulation of another pathway, which induces LTP, induce potentiation at both pathways[16,25,26]. It is associative in the sense that LTP can occur following the contribution of two distinct set of inputs. These and other related experiments thus identified four cardinal properties of LTP: it is persistent over hours; input specific; and under some circumstances exhibits synaptic cooperativity and associativity features.

The induction mechanism of LTP

The accepted vernacular defines two mechanistically distinct phases of LTP: the induction and the expression phase. A widely accepted model was first reached for the induction phase of LTP. In 1983, Collingridge et al. reported that while the ionotropic glutamate receptor of the N-methyl-D-aspartate receptors (NMDARs) subtype does not substantially contribute to basal synaptic transmission, it is however necessary for LTP induction[27]. A year later, Nowak et al.,[28] and Mayer et al.[29,30] accounted for this peculiarity by demonstrating that the gating of NMDARs shows a strong voltage dependence, due to a magnesium block of their pore such that the receptors are largely blocked close to resting membrane potential. As such, these results show that NMDAR activation requires both synaptic inputs (*i.e.,* glutamate release) and postsynaptic depolarization, and thus act as a molecular coincident detector of pre- and postsynaptic activity. It is again difficult to overemphasize how this relatively simple concept of coincidence detection permeated into modern thinking of how LTP provides an attractive cellular model of learning and memory.

NMDARs are permeable to calcium ions (Ca^{2+}) [31-33] and that LTP itself is contingent upon Ca^{2+} entry[34], leading to the widely accepted view that it is the Ca^{2+} conductance of NMDARs that is responsible for triggering the molecular cascade ultimately leading to synaptic potentiation. While glutamate release triggers some Ca^{2+} influx through NMDARs even at rest[35-37], synaptically-induced depolarization is typically insufficient to induce LTP unless high frequency trains of presynaptic release are provided. In these cases of high frequency stimulation, α-amino-3-hydroxy-5-methyl-4-isoxazolepropionic acid receptor (AMPAR)-driven synaptic depolarization summates to gradually relieve the Mg^{2+} block from NMDARs to conditionally allow Ca^{2+} influx. A number of important biochemical, electrical and dynamical features derive from the localisation of glutamatergic synapse onto *espinosas*, or dendritic spines, that act as small subcellular compartments, exhibiting varying degrees of biochemical and electrical isolation from the parent dendrites (for *e.g.*, see[38-41]).

Spike-timing dependent plasticity (STDP) as a Hebbian induction rule

The induction mechanism outlined above provided the field with a conceptually crisp and satisfying mechanism that explained well the dependence of LTP induction on high frequency

stimulation that was common to most induction protocols at the time. This mechanism rapidly became textbook knowledge. Yet, it remained somewhat ambiguous whether the obligatory requirement on high frequency burst wholly adhered to Hebb's postulate. Indeed, a strict interpretation of Hebb's rule not only conjectures the conjunctive nature of LTP induction in requiring both presynaptic release and postsynaptic spiking, it also explicitly affirms their causal relationship (" *When .. cell A takes part in firing [Cell B]").* While high frequency presynaptic bursts can lead to sufficient depolarizations and concurrent NMDAR activation to induce LTP, it in principle could do so without inducing post-synaptic spiking. Even in the cases where high frequency bursting was shown to lead to spiking, it was still unclear how this activity (*i.e.*, the postsynaptic spikes) would be mechanistically read out at the level of individual synapses as a conjunctive element to induce LTP.

Two highly related and highly influential discoveries in the 90's answered these fundamental questions. Hebb hypothesized the causal relationship between synaptic drive and postsynaptic spiking as a determining requirement for potentiation, yet plasticity is synapse specific. Are individual synapses informed of the spiking behavior of their parent neuron? Studies in the late 70's-early 80's[42,43] had already suggested that action potentials generated at the soma of neurons could be recorded in dendrites. Yet, the definitive demonstration was provided by Greg Stuart and Bert Sakmann when they performed dual (simultaneous) whole-cell recordings from the soma and the dendrites of the same cortical neuron[44] and showed that somatically triggered action potentials actively propagated into the dendritic tree. This finding is significant for a Hebbian plasticity framework since the dendritic (and spine) invasion of action potentials provides a precise timing cue (with millisecond resolution) of the spiking of a neuron to potentially all of its synapses.

This discovery was soon followed by the direct demonstration of its importance for plasticity. Recordings from synaptically connected cortical neurons by Markram et al.[45] showed that when a synaptic potential onto a postsynaptic neuron is repeatedly paired with a spiking of this postsynaptic neuron, potentiation of the synaptic potential occur. The relative timing of the synaptic activation and postsynaptic firing is exquisitely important. If presynaptic inputs consistently arrive slightly before postsynaptic action potential generation, potentiation ensues. In striking opposition, of the presynaptic inputs arrive slightly *after* the postsynaptic action potentials

(in which case, having no causal role in their generation) , synaptic depression rather rather develops. The immediacy between pre- and postsynaptic firing is crucially important. Indeed, the magnitude of LTP progressively diminishes as the time between glutamate release and postsynaptic spiking is increased, with an effective temporal window of ~5-70 ms[46]. While the timing between pre- and postsynaptic events has been entertained since the late 70's from experimental and theoretical neuroscientists alike as a critical parameter for LTP induction (eg.,[23,47,48]), the ignorance of backpropagating action potentials hindered correct mechanistic conceptualization of these early experiments. The discovery of this Spike-Timing-Dependent Plasticity (STDP; Figure. 3), provides the most direct, and intuitively tangible, experimental realization of Hebb's rule. STDP can be conceptualized as an induction mechanism for plasticity, wherein the timing of pre- and postsynaptic spiking becomes a critical factor. This timing window further reflects well the relatively slow rate of glutamate unbinding from the high affinity NMDARs. It is hard not to conclude that this experimental scheme reflects a causal relationship between the synaptic input(s) from Hebb's neuron A with the firing of the postsynaptic neuron (Hebb's neuron B).

STDP plasticity rules are not invariant across regions and synapses. For instance, in the electric lobe of weakly electric fish pre-post spiking can lead to LTD and post-pre to LTP[49,50], and delays of up to 100 ms can lead to long-term synaptic plasticity[51]. Variations are also observed at inhibitory synapses in L2/3 neocortex[52], some hippocampal interneurons[53], excitatory corticostriatal synapses[54], and in the cerebellum[55] and others.

Expression of LTP

LTP expression refers to the mechanism that underlies the manifestation and realization of synaptic potentiation. In other words, what makes synaptic transmission stronger? In principle, the expression of LTP can occur either at the presynaptic terminal or the postsynaptic membrane. These two possibilities have long been entertained and contrasted. For instance, Hebb favored a presynaptic locus of expression for Hebbian plasticity, while it was argued in the 70's and 80's[56,57] that alterations in postsynaptic receptors might be involved. What is seemingly a relatively straightforward question turned out to be a particularly contentious and at times vexing problem to experimentally address. By the late 1980's, we understood enough about transmission at central

synapses to correctly frame the problem, and the advent of whole-cell electrophysiological recordings approach in brain slices (allowing low-resistance intracellular access in a preparation amenable to study synaptic plasticity) provided tractable means to experimentally follow through. More specifically, the site of LTP expression in principle can be accounted by alterations in any of these 3 parameters: 1) the number of activated synapses (*N*); 2) the probability that glutamate is released following action potential invasion (*p*); or; 3) the size of the postsynaptic response induced by the release of a single synaptic vesicle (*q*). In principle, any enduring modification of these parameters (*N ,p, or q*) can lead to a lasting modification in synaptic weights.

Although new synapses (*N*) can be formed following LTP induction protocols, the process is typically far slower than the fast synaptic potentiation observed during LTP induction protocols[58-60]. The operational definition of release probability is such that any alterations in *p* following LTP would indicate a presynaptic mechanism in the expression of plasticity. In principle, alterations in *q* may reflect changes in either neurotransmitter content within a single vesicle (presynaptic locus) or changes in the function and/or number postsynaptic receptors (postsynaptic locus[59]). However, it is agreed that a change in *q* largely reflects a postsynaptic locus, as the vesicle size and content are generally assumed to be fixed.

A significant research effort has been deployed to measure changes in these quantal parameters as means to identify the locus of expression of LTP, i.e., whether it is pre- or postsynaptic. One approach is based on the intuitive idea that a widespread change in the release probability of a population of stimulated axons will alter the variability statistics of its underlying stochastic synaptic response, an effect that can be detected by analysis of their coefficient of variation (CV; see informative review on this approach[61]). Early studies using this formalism reported that the statistics of synaptic release were altered in a way that suggested a change in release probability occurred following LTP induction[62], pointing towards a presynaptic locus of expression. Moreover, minimal stimulation experiments (monitoring the release of glutamate from a small number of axons - in principle, as little as one), showed that the rate of release failures decreased following LTP induction, again suggesting an increase in release probability as a dominant contributing factor to synaptic potentiation during LTP. Yet, these findings were difficult to reconcile with several basic features of LTP that were generally agreed upon. For instance, LTP leads to an increase in AMPAR-, but not NMDAR-mediated synaptic transmission (when

experimentally allowed to contribute to synaptic transmission). As such, it was difficult (although not impossible, see[63]) to envision how a general enhancement of glutamate release would selectively increase the function of one, but not the other, subtype of glutamate receptors when both are expressed at the postsynaptic membrane. The field was stuck in a delicate position since (generally), it was not the core experimental results that were problematic and contested (several were replicated in independent labs), but their interpretations were fundamentally contradictory and mutually exclusive.

A simple solution to this vexing problem was however provided by the demonstration that a subset of synapses only contains NMDARs, and not AMPARs[64-66]. Because NMDARs are largely non-conducting at resting membrane potential, the term 'silent synapses' was coined, and thereby challenged the core and widely held assumption that most central synapses harbor both these receptor subtypes. Importantly, these silent synapses were also shown to be remarkably plastic, wherein the activation of NMDARs triggered the insertion of new AMPARs into a previously 'silent' synapses (Figure 4). Collectively, these experiments forced a re-interpretation of several prior findings, notably that a reduction of failure rate is solely indicative of a change in release probability. Indeed, the postsynaptic insertion of AMPARs after LTP at a previously silent synapses is precisely expected to lead to a reduction in the rate of failures detected by typical experiments. These results dovetailed with the general lack of alterations of release probability determined by alternative experimental approach (*e.g.*, rate of MK-801 blockade of NMDAR-dependent transmission, and paired-pulse ratio, an index of release probability, during LTP[67,68].

The discovery of silent synapses was highly influential, in part because it forced fundamental reconceptualization of some critical assumptions that severely blurred an entire field for several years[63,66]. Beyond this point, the proportion of silent synapses is believed to be directly related to the plasticity potential of the network they are embedded in. As such, there has been sustained interest in their regulation throughout the years. They have been detected using a variety of approaches, from immunocytochemical detection approaches in neuronal cultures to electrophysiology in slices[69]. Minimal stimulation approaches, that have been key in their discovery, likely still provide the qualitative gold standard to establish their existence, although they do not lend themselves with ease to relatively the relatively high throughput functional sampling required to study them quantitatively. Statistical approaches relying on failure rate

analysis have been used over the years in several brain regions and conditions to provide an estimate of their occurrence using more traditional synaptic physiology experiments. However, these methods are fundamentally underpowered and biased, and their inference validity has recently been questioned[70,71].

Two-photon uncaging of glutamate has provided a useful and flexible means to study several aspects of glutamatergic synapse function and plasticity[72,73], including silent synapse regulation; uncaging onto a subset of synapses has been shown to elicit solely NMDAR-mediated responses[26,74-77]. Importantly, this approach is uniquely characterized by high statistical power and low bias[70,71]. The relative ease in controlling light in space for instance has allowed to map the spatial distribution of silent synapses in developing neuron's dendritic arbor[26]. Cooperative plasticity mechanisms operating over small spatial scales (~10-40 micrometers) was further shown to underlie their spatial clustering of silent synapses in emerging networks[26]. Importantly, several studies have showed a dramatic reduction in the occurrence of silent synapses with increasing postnatal age. While this reduction has been interpreted as a likely correlate of the generally agreed upon reduction of the plasticity potential with increasing age, there remained doubt on whether they existed at all in adult. A recent study showed a higher than anticipated presence of filopodia-like dendritic protrusion in adult cortex that were convincingly shown to be the structural correlate of plastic, silent synapses in adult[78].

The molecular era of AMPAR trafficking as a substrate of LTP

Several electrophysiological strategies were developed in the 90's to provide a faithful estimate of *q* during plasticity, and several of these provided strong evidence supporting the idea that an increase in the function and/or number of AMPARs in the postsynaptic membrane is the dominant factor for LTP expression[67,68,79-81]. Yet, by providing a compelling alternative interpretation for many of the evidence pointing towards a presynaptic mechanism, it is likely fair to say that the demonstration of silent synapses, along with the de *novo* appearance of AMPAR-mediated synaptic currents following an LTP protocol, contributed to sway the field toward a postsynaptic view of LTP expression. The robust LTP induced by repetitive two-photon glutamate uncaging experiments, by circumventing the need for presynaptic release, provided some years later a set of cogent confirmations that synapses are endowed with the machinery to rapidly, and

with synapse-specificity, deliver AMPARs to individual synapses following NMDAR activation, all through a solely postsynaptic mechanism. Indeed, the repetitive delivery of glutamate onto visually identified spines has been shown to lead to robust enlargement of spine volume [26,76,82,83], delivery of fluorescently-tagged AMPARs to stimulated, but not, neighbouring spines [76,82,84], and to increase AMPAR-mediated synaptic currents[78], notably in experiments where the amount of uncaged glutamate reaching the spine of interest remained constant, as monitored using an optical sensor of glutamate release[76].

A natural line of question arising from these findings pertains to the molecular mechanisms driving the insertion - or trafficking, using the established vernacular - of AMPARs to and from synapses during plasticity. Roughly at the turn of the century, a series of technological and technical implementation allowed the merger of molecular biological approach with the electrophysiological study of synaptic plasticity. The generation of knock-out and knock-in mice, along with behavioral, biochemical and electrophysiological characterization of synapse function and plasticity provided a powerful approach to establish, with varying degrees of confidence, correlational relationships between molecular targets, plasticity mechanism and ultimately behaviors (*e.g.*,[85-87]). Moreover, a number of technological implementations allowed to investigate the role of several molecules in shaping synaptic function and plasticity. Such approaches relied initially in acute transfection of dissociated neurons maintained in cultures that were extremely well suited for immunocytochemical detections of protein expression at synapses in response to various molecular interventions. Chemical means were also developed to mimic NMDAR activation and effective LTP-like synaptic strengthening in cultures, thereby allowing the deployment of a collection of varied and clever experimental approaches and strategies relying primarily on electrophysiology, live-cell imaging, immunocytochemistry and biochemical approaches.

Notwithstanding the spectacular progress that was allowed by the versatility of neuronal cultures, these showed limitations related to the study of LTP *per se*. Indeed, the chemical means commonly used to induce LTP in cultures did not capture several of the main features of plasticity that had been so extensively studied in acute slices. The development of organotypic slices, in parallel with the ability to alter the molecular makeup of constituent individual neurons using either viral- or biolistic-based transfection approaches, provided a uniquely powerful and

accessible platform to study molecular details of LTP[82,88]. Contrary to neuronal cultures, organotypic slices: 1) were readily amenable to classic synaptic physiology experimental architecture (specifically, electrical stimulation of axons to trigger glutamate release and ease in activating synaptically located NMDARs) and; 2) expressed robust LTP in response to commonly used stimulation protocols that had been developed in acute slices. This approach opened molecular interrogation of LTP. The field was interested in understanding the role of several proteins known to be located in spines, but for which no clear function was ascribed. For instance, traditional gain- and loss-of function approaches were deployed to understand the role of proteins of the MAGUK class (PSD-95, PSD-93, SAP 102) that were initially believed to regulate synaptic targeting of NMDARS, but that were demonstrated to play key roles in regulating AMPARs, and to regulate plasticity rules[74,89-94].

More closely related to the targeting of AMPAs *per se* during plasticity, a series of pioneering and clever experimental strategies were developed in Roberto Malinow's lab to provide an electrophysiological signature of newly inserted AMPAR and NMDARs to synapses[95-99]. This overall strategy led to an influential model of subunit-dependent rules governing AMPAR trafficking to synapses. For instance, it has been suggested that long tailed AMPARs (*i.e.*, primarily containing the GluA1 subunit) are primarily targeted to synapses during LTP, while short-tailed receptors (primarily containing GluA2) are constitutively targeted to synapses with high turnover[97]. The existence of such subunit-dependent rules has been the subject of research scrutiny over the years using several different molecular strategies, each with their own limitations. For instance, by investigating the ability of several GluA tail mutants to traffic to synapses in neurons devoid of AMPARs, a follow-up study failed to outline strict subunit-dependent rules for AMPAR delivery, and rather reported a promiscuous insertion of AMPARs of different subunits during LTP[100]. However, it has been argued that this molecular replacement approach fundamentally disrupted the competitive molecular landscape found at synapses *in situ*.

Despite the largely consensual findings that an increase in postsynaptic AMPAR function/and or number contributes to LTP at canonical CA1, it still remains somewhat unclear what unfolds between NMDAR-dependent Ca^{2+} entry and AMPAR insertion. The critical and essential role of Ca^{2+}/calmodulin-dependent protein kinase II (CaMKII) for LTP has repeatedly been demonstrated using a variety of pharmacological and molecular approaches[101-105]. Following

high and localized NMDAR-dependent Ca^{2+} influx, Ca^{2+} ions bind to the four cooperative binding sites of calmodulin, each possessing different affinities. Activated calmodulin then proceed to activate CaMKII, and from this point on, it takes approximately 10 s to rapidly increase the number of AMPARs at the synapse[84] through a mechanism that remains largely enigmatic. For instance, CaMKII phosphorylates the ser831 site on the C-tail of GluA1 subunits of AMPARs[103,104], a site that is also know to be phosphorylated during LTP induction[106]. Preventing the phosphorylation of this site reduces the magnitude of LTP, but does not abolish it. Likewise, preventing the phosphorylation of transmembrane AMPAR-regulatory proteins TARPGamma8 by CaMKII reduces LTP, but also does not abolish it[107]. The molecular replacement strategy covered above[100], emphasizes the promiscuous ability of glutamate receptors of different subtypes to be targeted to synapses in the absence of tightly regulated phosphorylation events. An intriguing twist to this conundrum came into light recently with a study that suggests that the ability of CaMKII to trigger LTP reflects a structural, rather than an enzymatic, function of CaMKII[108]. Manifestly, despite the formidable advances seen in the last 30 years or so, the core molecular mechanisms of the highly regulated trafficking of AMPARs to and from synapses during plasticity is still not fully understood.

Synaptic heterogeneity of LTP induction and expression

The quest to understand the expression mechanism of LTP at CA1 synapses was an important but tumultuous journey that is now an integral part of synaptic physiology folklore. While there is little doubt that the highly regulated trafficking of AMPARs to and from synapses contributes to LTP at many synapses, we now know that this plasticity mechanism is not universal in the brain. While presynaptic forms of LTP have been described for several synapses, that occurring at synapses between mossy fibers and CA3 neurons in the hippocampus is perhaps the best characterized[22,109-111]. At least under some conditions and induction protocols, LTP at these synapses is not dependent on NMDAR activation and the collective deployment of a comprehensive set of well-validated metrics of presynaptic function (*i.e.*, paired-pulse ratio, coefficient of variation, failure rate, MK-801 use-dependent blockade) nicely converge in indicating a clear presynaptic locus of expression[22,112-114]. At these synapses, LTP is dependent on PKA activation[109,112,114,115]. Yet, debates have brewed regarding whether the locus of induction of this form of LTP is of pre- or postsynaptic locus since both scenarios have received experimental

support. For instance, it has been argued that the induction occurs postsynaptically in response to postsynaptic Ca^{2+} transients mediated by a mixture of L-type VGCCs and mGluR-mediated Ca^{2+} release from internal stores, that leads to a PKA-dependent retrograde signalling[116-118]. In contrast, several experimental manipulations aimed at inhibiting postsynaptic contributions to plasticity did not abolish LTP[119], and contributed to the idea that repetitive presynaptic Ca^{2+} entry in mossy fiber terminals lead to an increase of presynaptic cAMP levels and PKA activation[114,120,121]. Altogether, while there is a consensus that the expression of LTP at MF-CA3 synapses is presynaptic, there is lingering debate on whether the postsynaptic neurons are involved at all in the induction of this form of plasticity. This distinction bears broader implications in that a pure presynaptic locus of induction squarely confers non-Hebbian properties to this form of plasticity.

Late phase LTP

In 1974, a year after Bliss and Lømo seminal paper, Hansjuergen Matthies (Matthies, 1974) proposed that neuronal mechanisms of memory occurred in different phases reflecting short-term, intermediate, and long-term memory, through different time courses and decay times, different biological correlates, and cellular properties at the synaptic, synaptosomal, and nuclear levels[122]. Most studies focus on the first 1 h – 3 h after LTP induction (early phase LTP), but in the mid-80's it was shown that LTP expression could be maintained beyond 3 h – 6 h (late phase LTP) and that, and in sharp contrast to the early phase, was blocked by Anisomycin, a reversible protein translation inhibitor[123]. These results suggest the existence of at least two types of LTP differentiated by their time course of maintenance, and their need for protein synthesis. The increase in protein synthesis is believed to occur within 1 h of late phase LTP induction in hippocampal CA1 neurons through an increase in protein translation of existing mRNA, while a second increase in protein synthesis, driven by an increase in mRNA synthesis, occurs several hours later[124-126]. These findings suggest that pre-existing mRNAs are necessary and sufficient in the first several hours of LTP; while gene expression is required to maintain LTP for much longer[16]. It has been suggested that NMDAR and resulting calmodulin activation of protein kinases are important for both early- and late-phase LTP[127,128], except for PKC, whose inhibition exclusively disrupts late phase LTP through downstream effects of mGluR activation[129-133]. The requirement for PKC and mGluR in late phase LTP suggests that more receptors and second

messengers are required for its induction compared to its early phase. This offers an interesting paradigm to long-term memory, which, in comparison to short-term memory, requires more contextual associations[134] .

A key question that arises from late phase LTP is how information about synapse specificity is kept for several hours after induction, such that newly synthesized protein can appropriately be delivered to the correct synapse for long-term stabilization. This is believed to be achieved by a synaptic tagging mechanism, where plasticity related proteins bind to recently potentiated synapses, to keep a memory of previous synaptic activity. In a nutshell, late phase LTP is induced by strong stimulations, persists for several hours or days and requires synaptic tagging, translation of proteins and transcription of mRNAs, providing an interesting model for long-term memory storage[134].

Homeostatic balancing of Hebbian plasticity weight updates

One defining feature of the mammalian cortex is that it is organized in highly recurrent networks. One can get the relatively simple intuition that any synaptic potentiation that would develop following Hebb's rule in such a network would gradually increase the excitability of the entire network, leading to an increased probability that synaptic inputs would cause postsynaptic firing, and resulting in even further potentiation. This intuition was formalized in computational simulations of neuronal network that showed that Hebbian-type LTP (and LTD) processes carry an inherent stability problem for network function[135-138]. The concept of weight normalization has been forwarded as one solution. In essence, it assumes that the total synaptic weight onto any given neuron is somehow constant, and that potentiation at some synapses is accompanied by depression at other synapses (*i.e.*, the weights are normalized). However, despite notable exception for some neuronal types, there is little evidence that such normalization occurs in neurons in the cortex or hippocampus.

The discovery of homeostatic synaptic plasticity (also called synaptic scaling) has been received with great interest, in part because it provides a computationally plausible means to address this stability issue[136,139,140]. With features closely resembling the well described denervation supersensitivity[141], this phenomenon refers to ability of neurons to undergo bi-

directional changes in synaptic strength to actively compensate for changes in overall excitability levels[136,142,143].

The experimental paradigms used to outline and study this plasticity mechanim is relatively simple. Intitially, experiments wre carried out in neuronal cultures of dissociated neurons, but later from organotypic slices, where neurons were exposed to pharmacological interventions that chronically (~24-48 hours) decreased or increased overall excitability. Thus, in response to prolonged network activity blockade, individual neurons attempt to restore their excitability level by, amongst other processes, increasing synaptic strength (Figure 5). Conversely, in response to prolonged enhancement of synaptic activity, neurons adapt by reducing synaptic strength. At least in part, these bi-directional homeostatic adjustments are carried out by changes in the number and/or function of excitatory synaptic glutamate receptor of the AMPA subtype (AMPARs)[136,142-145] and NMDA subtype (NMDARs)[145,146]. This plasticity mechanism has received considerable attention such that we gained an increasingly sophisticated mechanistic and molecular understanding of its key features[136,137,143,144,147-161].

A dominant model of homeostatic plasticity posits that all synapses of a neuron engaged in a homeostatic scaling process 'scale' up (or down) by a common, unique, factor[136,143,162]. There is clear computational appeal to this model in the sense that the relative strengths within a population of synapses (presumably reflecting the past history of these synapses sculpted by ongoing Hebbian plasticity) would be maintained by the scaling process that would therefore bear limited information cost. However, and importantly, such uniformity of changes in synaptic strength across all synapses during synaptic scaling has not been universally observed[163-165] and intriguing synapse-specific features have been reported to occur during global homeostatic synaptic scaling[157]. This raises the possibility that, at least in certain conditions, some mechanisms are providing local, synapse-specific, homeostatic control of synaptic strength that locally sculpts, or gates, the global synaptic changes triggered by synaptic scaling[156,157,163,164].

Extending on this idea, studies have shown that prolonged (~48 hours) manipulations of the presynaptic release of individual synapses leads to synapse-specific regulation in their strength with a polarity that is homeostatic in nature (Figure 5D). In some cases, this strengthening is also accompanied by a change in the subunit composition of AMPARs with different biophysical

features[166]. As such, these studies show that individual synapses, like neurons, are also subjected to homeostatic control of their strength, and are thus autonomous homeostatic units. However, if such mechanisms were continuously online, one would expect that they would tend to gradually degrade the encoding of synaptic strength through the accumulation of Hebbian plasticity outlined above. This intuitive information cost is however apparent only within a model where synaptic memory is solely stored through stable modification of synaptic strength, metaphorically termed switches[167]. Despite its intuitive appeal and popularity, this switch-based model is likely too simplistic, since it bears highly limited storage capacity and fails to capture several dynamical features of synapse function and plasticity[168-170]. More modern models argue, for instance, that multiple 'transitions' between synaptic states (and metaplastic states) are much more powerful and relevant[168]. By providing additional 'transition' states, with specific gain, timing, and upper and lower bounds, homeostatic plasticity may thus regulate Hebbian plasticity rules[76,149,171-173]. One can thus ask whether plasticity rules are dependent on prior activity, or 'history'[174], in a process sometimes referred to as metaplasticity[164,175-177]. For instance, one study found that, intriguingly, Hebbian and homeostatic regulation of synaptic strength do not appear to share common upper and lower bounds (dynamic range of synaptic strength). Indeed, a prior homeostatic strengthening did not negatively impact the ability of an LTP protocol administered through two-photon uncaging (*i.e.,* a purely postsynaptic process) to induce the insertion of AMPARs[76]. Worded differently, the homeostatic and Hebbian plasticity did not occlude one another. Yet, the homeostatic process strongly regulated Hebbian plasticity rules at CA1 synapse, but by influencing the short-term dynamics of glutamate release. Altogether, these studies show that Hebbian plasticity rules are not fixed, but rather are modulated by the history of the synapses. However, we still have a very incomplete computational understanding of the functional consequences of these dynamic plasticity rules on network function.

Learning, memory and LTP

Bliss and Lømo immediately considered their findings of LTP through the lens of an attractive cellular model for learning and memory, presciently writing '*Our experiments show that there exists at least one group of synapses in the hippocampus whose efficiency is influenced by activity which may have occurred several hours previously a time scale long enough to be potentially useful for information storage*. This overall idea quickly got traction int the field where

it was soon argued that several key features of activity-dependent forms of plasticity are consistent with the idea that it enacts a memory trace in neural network[178-182], - a synaptic engram. For instance, both learned skills and declarative memory can persist, or decay through time, much like LTP. Additionally, LTP is induced by strict temporal association between pre- and postsynaptic neurons, and thus provides an interesting parallel to associative learning, which can be conceptualized as binding two initially unrelated cues that are presented with some temporal constraints. These associations are specific to the learned cues, following the input specificity of Hebbian LTP. Finally, synapses that are to be potentiated are often insufficient on their own to induce spiking, and thus relies on some level of cooperativity between synaptic inputs (or neuromodulator actions). This has led to several forms of spatial cooperativity between synapses that have been described over the years, such as the clustered wiring of inputs that are closely related in terms of information content[26,183-189], and contribute to computational power by forming compartmentalizing dendrites[190-194]). This cooperativity bears resemblance to behavioural associations which are facilitated by multi-sensory or rewarding-like stimuli. As such, the four properties of LTP previously addressed; persistence, input specificity, associativity, and cooperativity, are reminiscent of behavioral learning[195]

The parallels between LTP and associative learning are intriguing, yet do not provide a sufficiently convincing ground to establish their causal link. Again, this limitation was understood by Bliss and Lømo who candidly closed their paper by writing: '*Whether or not the intact animal makes use in real life of a property which has been revealed by synchronous, repetitive volleys to a population of fibres the normal rate and pattern of activity along which are unknown, is another matter*". According to Martin et al., 2000 and Martin and Morris, 2002, four criteria are necessary to infer a causal association between LTP, learning and memory. We consider them below.

The first criterion follows the idea that if LTP is causally related to behavioral learning and memory, then LTP *per se* should correlate with learning. Early correlation studies were pioneered by Carol Barnes. After developing the Barnes maze in which rodents are prompted to find a hidden escape box from an elevated platform, Barnes found that older animals, which tend to undergo less potentiation (*i.e.*, reduced amplitude and shorter maintenance of LTP), were generally slower at learning, and faster at forgetting the task than younger animals[196]. However, there are examples of animals who exhibit enhanced LTP, yet have impaired learning[74,197]. Using a different approach,

Rogan et al., 1997, recorded field-evoked responses to an auditory cue (*i.e.*, conditioned stimulus (CS)), in the amygdala *in vivo* while it was paired with a foot shock[198]. The authors recorded increase in field potentials as the conditioned response (CR) to the foot shock appeared, suggesting that LTP occurred with learning. Importantly, extinction of the CR by repetitive presentation of the CS without its reinforcement decreased the potentials, hinting at the extinction of learning-induced LTP. Although some confounding variables occur with field potential recordings[182]); the correlational evidence is further supported by *in vitro* recordings in the amygdala of fear-conditioned animals showing an LTP-like increased in AMPAR-mediated transmission[199]. In 2006, Whitlock et al., recorded CA1 field potentials *in vivo* with multi electrode arrays during an inhibitory avoidance task and found potentiation in a subset of neurons for at least 2 h post-training, through a mechanism that closely resemble that of LTP induction[200]. Compellingly, the same subset of neurons showed a reduced ability to exhibit LTP after training (*i.e.*, occlusion, referring to the saturation of synaptic weights that occurs following extensive LTP). Together, these and conceptually related results[201-203] suggest that behavioral learning and memory occurs in parallel to, or is even induced by, LTP mechanism.

The second criterion for a causal relationship between LTP and learning suggest that preventing LTP should impair learning (*i.e.*, blockade). The problem is that it is difficult to identify a strategy that only blocks the induction of LTP, without having any off-target effects. Early pharmacological strategies were aimed at inhibiting NMDARs in behaving animals. For instance, the administration of an NMDAR antagonist in the cerebral ventricles impairs spatial performance at similar concentration at which it impairs plasticity[204,205]. Somewhat intuitively, the application of APV had little effect on recall performance[206,207], suggesting that LTP may be specifically important for task acquisition (induction) rather than maintenance of learned information (expression). However, NMDARs in the brain are significant charge carriers and blocking their activity, irrespective of cell types and circuits, is likely to influence behaviors in ways that are not necessarily related to LTP induction *per se*. Determining the effects of LTP blockade has also been attempted by genetic approaches. While exhibiting normal synaptic transmission, mutant mice lacking alpha-CaMKII showed greatly diminished LTP together with impaired spatial learning[85,86,208,209]. Similar impairment in both LTP and spatial performance were observed when NMDAR subunit NR1 was deleted[181,210]. While consistent with the idea that LTP is involved in

memory formation/recall, this approach suffers from the evident limitations of correlational findings, where a causal relationship between CaMKII and LTP, on the one hand, and that between CaMKII and learning, on the other hand, falls short of showing causality between LTP and learning. To overcome these limitations, an alternative approach involves the preventing of putative behaviorally induced LTP by a prior LTP strengthening. Such an occlusion strategy is pathway-specific and does not carry the side effects associated by genetic manipulation or drug application. Saturation of weights in the perforant path of the dentate gyrus caused impairment in the Barnes maze and Morris water maze on the same timeframe of LTP maintenance[211] Intriguingly, if tested after LTP had sufficient time to decay, acquisition to the task was retrieved[212]. Together, these results suggest that prevention of LTP can impair learning, and does so at timescale consistent with an involvement of LTP.

The third criterion addresses the idea that reversing LTP should delete the associated memory. In support of this argument, mice that were conditioned to associate an optogenetic activation of their auditory to amygdala pathway to a foot shock showed an increase in AMPAR-mediated response at these synapses, suggesting LTP[213]. Strikingly the induction of an LTD protocol by low frequency activation of the auditory to amygdala pathway prevented the CR on subsequent testing days. When the authors induced high frequency stimulation as an LTP-inducing protocol, the CR was reinstated. In a similar study, Kim and Cho (2017) found pathway-specific LTP expression in the auditory to amygdala pathway associated with an auditory tone (CS) that was associated with an aversive stimulus, and also found that depotentiation of the pathway suppressed the CR to the CS[214]. Potentiation and depotentiation of the auditory to amygdala pathway were also found to be involved in memory recall[215] (Abdou et al., 2018). Together, these studies suggest that LTP induction and reversal can cause impairments in recall memory and that learning, and memory instilled by LTP is dynamic, closely matching learning at the behavioral level.

The fourth criterion establishes that LTP induction must directly contribute to the formation of a new memory. In a notable study by Vetere et al., 2019, optogenetic stimulation of a single olfactory glomerulus was induced while an aversive or rewarding stimulation was evoked in the midbrain, causing the creation of a CR[216]. The same CR was later observed in the mice upon presentation of the real odor, associated with the stimulated olfactory glomerulus, which had not

been previously encountered by the mice, supporting the idea that stimulation can generate memories.

Collectively, these behavioral investigations indicate that while learning may not always require LTP, it is expressed during acquired behaviors, and its disruption can hinder learning and memory. This suggests that LTP may be a preferred mechanism for learning. Additionally, it is plausible that LTP collaborates with other processes such as structural plasticity, neurogenesis, alterations in neural excitability (beyond synaptic changes), and so on, working to initiate and maintain the demands of learning and memory.

Limitations of LTP as a cellular model of associative learning.

Understanding the mechanisms that underlie learning and memory has been an historical focus of psychology and neuroscience alike. Decades of research now renders axiomatic the idea that stable and prolonged changes in synaptic weights through synaptic plasticity is an elemental means by which the brain encodes information for later retrieval. It is difficult to identify a single, relatively simple, cellular phenomenon in neuroscience that has triggered as much research interest and dedication than the study of LTP. For one, the phenomenon is remarkably robust, and any competent electrophysiology lab can see it unfold. Moreover, one quickly develops the intuitive perception that studying LTP is peering into the very mechanism by which the brain learns. Despite the formidable progress obtained, it is likely fair to say that the field got ensnarled in complexities that were largely unforeseen and has likely only partially addressed the elemental questions that were posed over 50 years ago. While this piece favorably presented several of the features of LTP as being consistent with those expected of cellular model of learning and memory, one is nonetheless forced to candidly consider nagging limitations. We outline a few here.

Repetition requirement and the role of a molecular integrator*:* Canonical induction protocols require tens of repetitions for effective induction of LTP. This reliance is observed for most induction protocols, largely independently of parameter details (*e.g.,* structure and frequency of burst delivery) or experimental preparation (*e.g.,* in vivo *vs* slice recordings). Tellingly, a high number of repetitions is required even in experimental conditions where near-maximal NMDAR activation is achieved for each repetition (*e.g.,* when the postsynaptic neuron is artificially

depolarized to maximize NMDAR-dependent Ca^{2+} entry, or during optimal STDP protocols), and when each of these repetitions are separated by somewhat lengthy periods of time (in some cases, up to ~ 15-20 seconds). While the mechanisms leading to the coincidence-detection abilities of NMDARS are well understood, it is still somewhat unclear why several NMDAR-dependent Ca^{2+} transients are required to induce plasticity. This reliance on repetition suggests the existence of a molecular integrator that cumulatively counts synaptically-induced Ca^{2+} transients over a protracted timescale and that triggers the realization of LTP after reaching some threshold. Mounting evidence indicates that the autophosphorylation of CaMKII (at Thr286/287) entails CaMKII with a leaky integrator property that may provide such a cumulative counting function during LTP induction[217]. This obligatory reliance on high number of repetitions nonetheless poses a problem for a cellular model of learning, as it is difficult to imagine how LTP, within our current understanding of its induction contingencies, can implement one-, or few-, shot learning that, by definition, does not rely on repetitive presentations. Altogether, it is still unclear how the activity of CaMKII, or more generally the reliance on multiple pairing repetitions for LTP induction, can be appropriately scaled by a biologically relevant learning rate mechanism to allow for fast associative learning[218].

Temporal credit assignment problem*:* A second nagging limitation concerns timing. LTP induced by canonical STDP protocols presents the most cogent realization of the essence of Hebbian plasticity: the synaptic weight increase is restricted to those synapses that *repeatedly and persistently takes part in firing* [*the postsynaptic neuron*]. As such, Hebbian plasticity explicitly holds that it is those synapses that are causally related to postsynaptic spiking that should be potentiated. As covered above, STDP acts as a coincidence detector of pre- and postsynaptic events occurring within a very narrow temporal window (a few tens of milliseconds at most) that is consistent with the synaptic potentials bearing a causal relationship with postsynaptic spiking. Such a timescale is however fundamentally inconsistent with that occurring during many forms of behaviorally-relevant learning. Associative learning reflects the *binding* of distinct, unrelated events or entities. Pavlov's classic experiments showcases an intuitive example of this idea where the dog needs to meaningfully associate a bell sound with a food reward. Somehow, the brain must therefore retrospectively assign proper credit to the prior cues (or actions) as being causally related to the rewarding outcome. This is often referred to as the *temporal credit assignment problem,* and

it's unclear how the brain solves it. The temporal features of Hebbian plasticity induction such as those operant during STDP are fundamentally restrained by neuronal time constants and the rate of glutamate unbinding from NMDARs and, as such, makes it difficult to articulate STDP, and more generally Hebbian forms of LTP, as model of associate learning that provide a readily obvious solution to the temporal credit assignment problem.

Machine learning has conceptualized a partial solution to the temporal credit assignment problem through so-called 'eligibility traces', a time decaying mnemonic process that enables learning and updating between temporally separated stimuli. While eligibility traces are primarily a theoretical construct, they have been the subject of renewed interest in fields outside of machine learning because of recent evidence suggesting that they may have a biological correlate[35,219-221]. A recently described form of synaptic plasticity, termed Behavioral Timescale Synaptic Plasticity[222-224] (BTSP), has triggered significant interest in the field, in part because strong evidence suggesting that it is intimately involved in the formation of place cells[222,225]. Moreover, the temporal features of BTSP induction, while being behaviorally relevant, resolutely cannot not be explained by current model of NMDAR-dependent Hebbian plasticity (Figure 6A). Indeed, the induction rule of BTSP are such that they can bind events that are separated by periods spanning several hundreds of milliseconds (up to ~ one second) and requiring very few repetitions. These temporal features of BTSP have been interpreted as providing support for the existence of eligibility traces in biological systems[220,223], although their material nature remains unclear. However, recent evidence showed that BTSP is observed in the cortex[35], and highlighted a mechanism wherein intracellular Ca^{2+} stores can hold a locally- and synaptically- generated memory to lead to the realization of LTP following a in response to an instructive signal that is delayed by several hundreds of milliseconds (Figure 6B). First, its peculiar timescale provides a line of solution to the temporal credit assignment problem proper to associative learning with behaviorally relevant timescale. Second, despite having been discovered only recently, BTSP has been linked with a complex behavioral role (or, a defined objective function *i.e.*, formation of place field in CA1 neuron), arguably more explicitly than any other form of plasticity. Thus, these salient features of BTSP renders it an extremely attractive cellular model for associative learning.

The next 50 years?

Predicting the trajectories of a field of research is a risky and likely doomed endeavour, but one can try. We entertain 3 broad research orientations that are likely to receive sustained research attention with varying temporal horizons.

1-Complementing connectivity maps with plasticity rules: Fifty years of research have identified at least some core features of LTP that are likely to stand the test of time. Different types of synapses are drawing from this mechanistic catalog (*e.g.,* changes in release probability- vs postsynaptic insertion of AMPARs) to fulfill their plasticity role within the constraints of the circuit that are embedded in. It is likely not realistic, nor required, that we study and understand every major synapse types in the brain with the same level of scrutiny and depth that the few 'canonical' synapses (*e.g.,* CA3, CA1, cerebellar synapses) have benefited from. However, much like the description of the short-term synaptic dynamics of the constituent synapses of any network motif, across scales (*e.g.,* a canonical feed-forward inhibition *vs* the hippocampal formation), is required to identify the computation it may support[226] , an understanding of the plasticity rules of these same synapses are also required to understand how these computations are shaped by experience[168,169]. Even for long-studied, highly stereotyped, and experimentally accessible structures such as the hippocampus, we still have an incomplete (but expanding) characterization of the plasticity rules of several important circuit motifs and subnetworks with still largely cryptic roles (*e.g.,* hilar subnetwork[227-230]). This need obviously applies to still poorly characterized circuit motifs cryptically embedded in less stereotyped networks such as cortex, long-range loops with subcortical structures[231,232] *et cetera*. While the remaining work to fully reach this end is obviously expansive, in principle at least, the current technologies and conceptual framework are largely apt to fulfill this overall research goal given enough time. Here, it is likely the computational frameworks that are likely to gain in sophistication in the coming years to link short and long-term plasticity rules with connectivity features to infer computational meaning[233].

***2-Molecular mechanisms*:** Since *circa* the turn of the century, LTP has squarely entered the molecular era. The merging of traditional molecular biology approaches with classic synaptic physiology and modern imaging approaches has allowed the field to obtain ever deeper insights into the molecular mechanisms regulating LTP. In part, such granularity of understanding is critical for therapeutic targeting strategies. Indeed, disruptions in LTP-like processes have been proposed to be implicated in the pathophysiology of a broad array of neurological and psychiatric

diseases, from major depression, addiction, epilepsy, intellectual disability and autism to stroke recovery and many others[234-238]. The field here has been blessed with a somewhat bittersweet embarrassment of riches. As a natural starting point to study the molecular mechanisms of plasticity, early biochemical efforts (*e.g.*, yeast two-hybrid screening) initially set out to identify the set of proteins present in the postsynaptic density that, for instance, could be involved in the molecular trafficking of AMPARs. While it was expected that a handful of proteins would likely be involved in a relatively simple trafficking phenomenon, significantly more than 1000 proteins have now been identified to reside in the postsynaptic density[239]. While the actual proportion of these proteins that are involved in LTP is currently unknown, it is certainly not insignificant and gives an estimation of the dauting task that remains. In principles, elucidating in mechanistic details these molecular pathways provides opportunities for directed regulation of plasticity and, by extension, of cognitive and memory performance (e.g., the AMPAkines[240-242] or psychedelic or non-psychedelic psychoplastogens[243-245], although these efforts have not yet matched their promises. In turn, efforts in understanding the roles of individual molecules provide a useful framework to link identified mutations in patient populations with their functional consequences (*e.g.*, gain- or loss-of-function mutation; structural *vs* enzymatic roles) and thus to be permissive for developing informed therapeutic strategies. Recent studies on the role played in LTP of the synaptic RasGAP (GTPase-activating protein) SynGAP provides an illuminating case in point. SynGAP has been known for decades to regulate plasticity[246,247], yet it was only recently shown that its role in regulating LTP is independent of its GAP activity, and rather involves its regulated dispersal from the synapses and concurrent increase in the availability of 'slots' for AMPAR retention at synapses[248,249]. This finding is critical for translational purposes since it provides a rationale explaining: 1) the general clinical failure of several existing therapeutics targeting downstream signalling of SynGAP and; 2) that individuals carrying mutations impairing the GAP of activity of SynGAP do not appear to be at increased risks of mental or psychiatric illnesses. These studies highlight a general formalism with broad generability, where one can easily contemplate that deeper understanding of the structure-function relationships of the various molecules involved in plasticity resolutely orients and informs therapeutic strategies, that may, in time, even lead to therapies akin to personalized medicine, for instance for non-monogenic diseases.

***3-Credit assignment problem*:** While the broad research orientations outlined above will undoubtedly benefit from several technological development in the coming years, the general conceptual framework is already well in place. The field has gained collective experience. One fundamental aspect of LTP that however has conspicuously evaded attention is what could be referred to as an algorithmic understanding of LTP. While we have identified with some degree of certainty *how* synaptic plasticity occurs, we have very little information of *when* and *where* LTP-like plasticity occurs in a way that causally supports learning. To illustrate this point, consider a young baby clumsily learning to reach a milk bottle. The baby generates motor commands in motor circuits that lead to sequences of small movements that can be represented as a succession of vectors that favorably, or not, contribute to the intended trajectory. Loosely borrowing from machine learning and the songbird literature, the brain of the baby here acts both as an *actor* (*i.e.,* implementing the motor actions) and as a *critic* (*i.e.,* evaluating the performance of these actions in attaining the intended target). The actor thus generates the movement sequence, and the critic computes errors signals, with the overall goal that, through repetitions, these errors need to be minimized. The (very) many synapses that are participating in the motor sequences must therefore receive the proper credit, or blame, to be iteratively updated to allow the motor commands to evolve towards the intended target movement. How does this occur? This is the credit assignment problem: it is currently unknown how the brain has solved it.

It is here interesting to consider the field of machine learning and artificial intelligence (AI) that, with varying degrees of inspiration from neuroscience, is engineering means to supervise learning in artificial neural networks (ANNs) to carry out complex tasks[250]. In doing so, the field of AI has conceptualized several core principles that in turn may prove useful for neuroscience's attempts to reverse engineer the brain that manifestly has solved the credit assignment problem through evolution. The design of ANNs rests on principles that should intuitively resonate with experimental synaptic physiologists: 1) the architecture of the network; 2) the learning rules of its constituent connections and; 3) the objective function to be carried out (or optimized). One means that ANNs can solve the credit assignment problem is by the so-called backpropagation of error signals. While a strict implementation of the backprop algorithm in the brain is doubtful, it nonetheless rests on synapse-specific weight updates in networks with feedback connections[251], features that dovetail with biological features of LTP. Moreover, emerging computational and

experimental work is beginning to identify how different features such as compartmentalized and active dendrites and burst dependency of LTP can be used by the brain to implement backpropagating-like algorithm to solve the credit assignment problem[250,252-254]

The credit assignment problem emphatically lies at the crossroads between experimental neuroscience and machine learning. The explosion of implementations of ANNs, with increasing inspirations from neuronal function and connectivity, provides a fabulous opportunity as they generate increasingly deep and sophisticated insights into means by which the brain may have solved aspects of the credit assignment problem to be tested experimentally. But this is an extraordinarily tall order, and the field simply has not yet fully developed the technological, conceptual, and analytical framework to fully tackle it. This will undoubtedly require an even broader and more concerted merger of complementary disciplines such experimental neurobiology, genetics, psychology, physics of dynamical systems, applied mathematics, computer science, engineering, machine learning and ethics. As such, coming on almost 75 years since Hebb formulated his learning model, and a whopping 50 years since Bliss, Lømo and Gardner-Medwin experiments demonstrating LTP at synapses, it seems that the quest to understand how synapses and neurons contribute to learning may after all still be at its beginning.

Figures

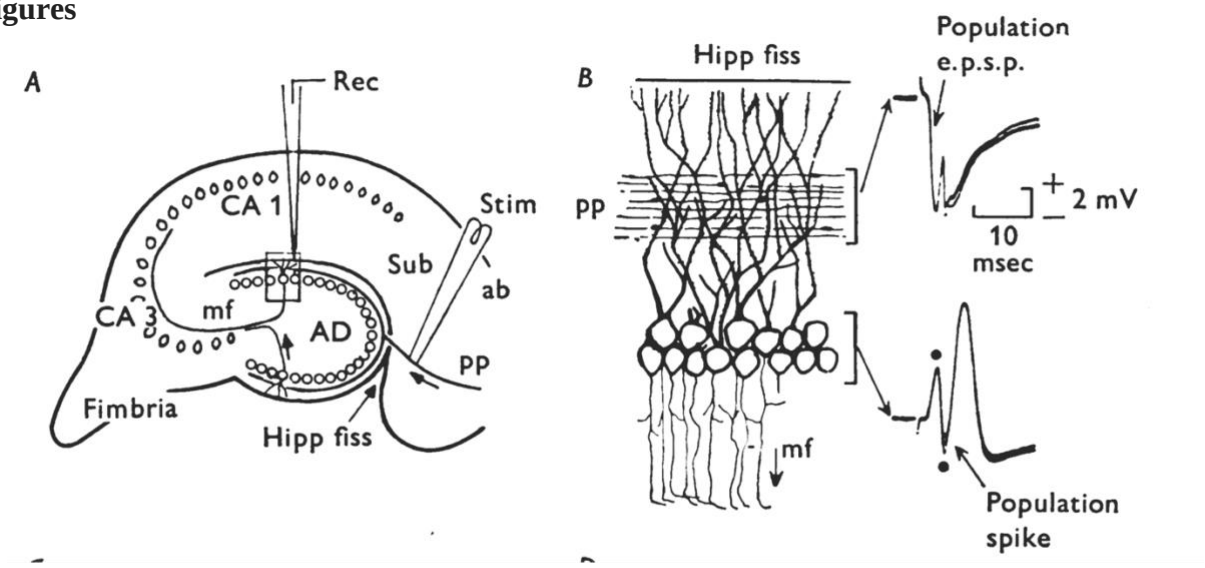

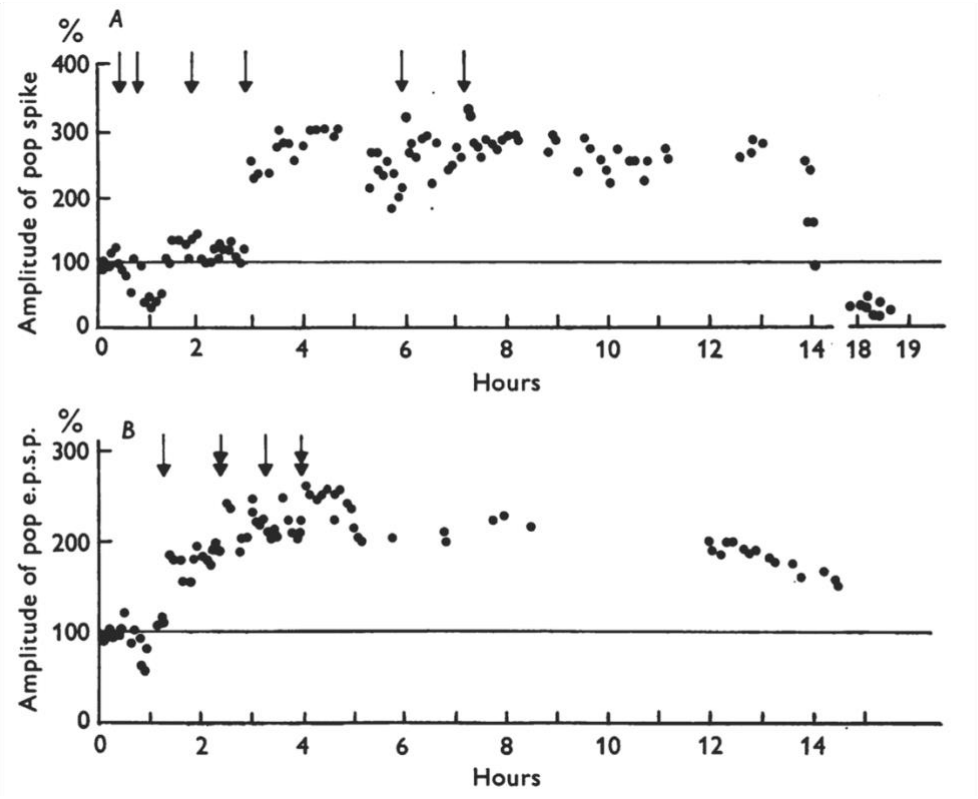

Figure 1. Long-term potentiation, as first reported. The top panel reproduces the diagrammatic parasagittal section through the hippocampal formation as well as an enlargement of the dendate area (AD) showing population responses. This figure (Figure 1)was included in the Methods section. The bottom panel reproduces Figure 12 that showed potentiation that lasted many hours.

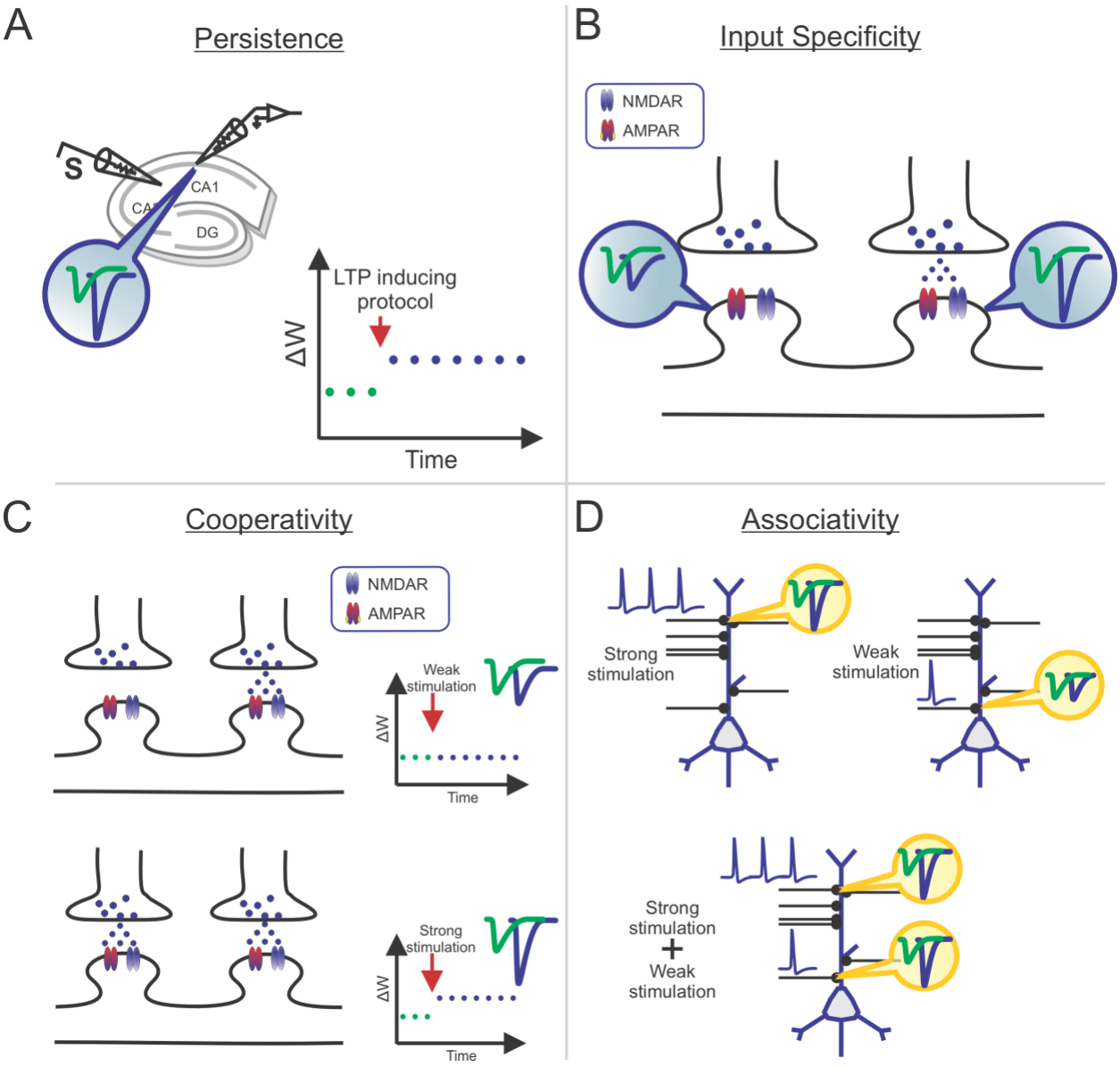

Figure 2. Salient features of LTP as a cellular model of learning.

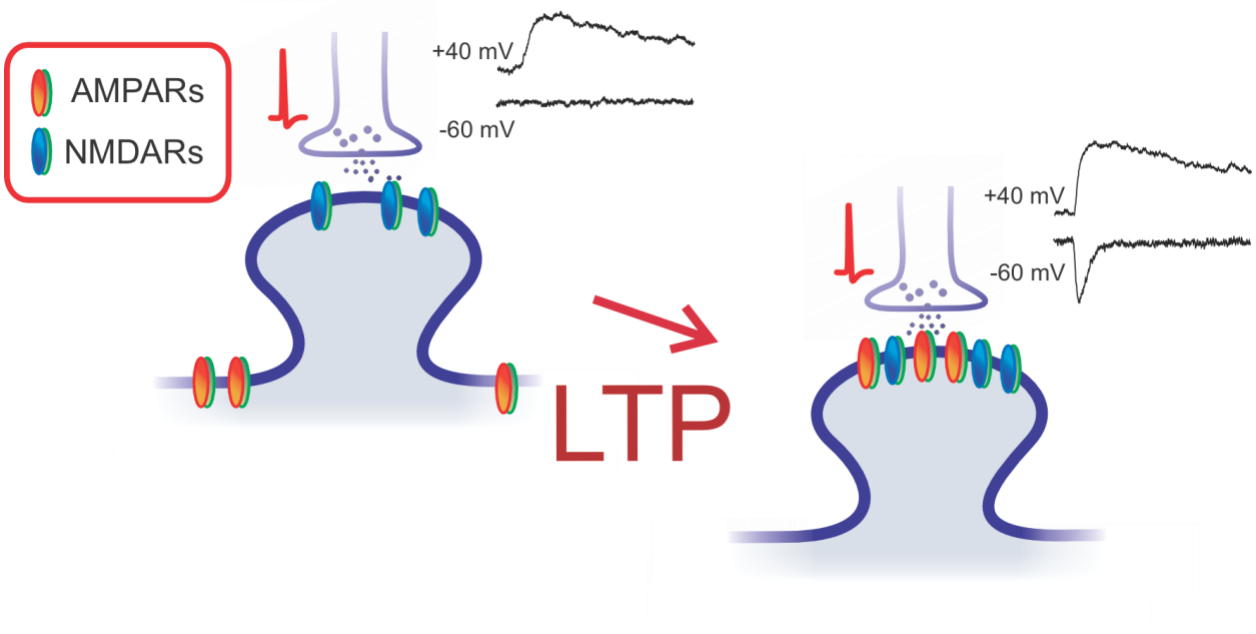

Figure 3. Schematic representation of silent synapses, along with the corresponding Glutamate-induced effects during typical voltage clamp electrophysiological experiments. Traces at -60 mV shows the absence of AMPAR-mediated current in a subset of synapse showing positive deflection at +40 m, indicative of NMDARs. Following LTP, AMPAR-mediated currents are recorded, indicative of direct postsynaptic insertion. See text for details.

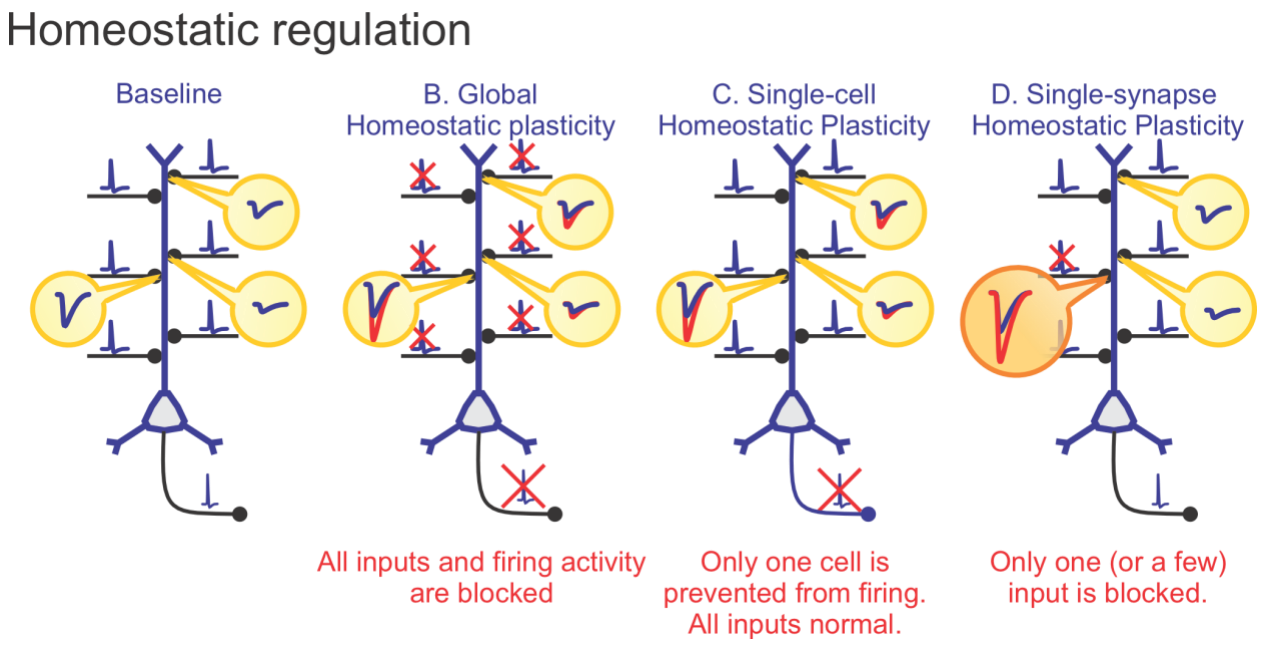

Figure 4. Homeostatic regulation of synaptic weight. The cartoon depicted in B, C, and D depicts experimental paradigms used to induce homeostatic plasticity, and the downward deflection schematizes synaptic currents recorded in voltage clamp experiments. In B, the sodium channel blocker TTX is applied in the media for ~48 hours. In C, only the postsynaptic neuron is prevented from spiking by overexpressing the potassium channel Kir2.1. In this case, the neuron is prevented from spiking, yet it receives normal synaptic inputs. Homeostatic upregulation of synaptic strength ensues, indicating the neurons integrate their own spiking activity over time. In D, the release of single inputs onto a postsynaptic neuron is reduced. The firing of the neuron *per se* is unaltered, yet homeostatic upregulation occurs selectively at the synapses that have been altered.

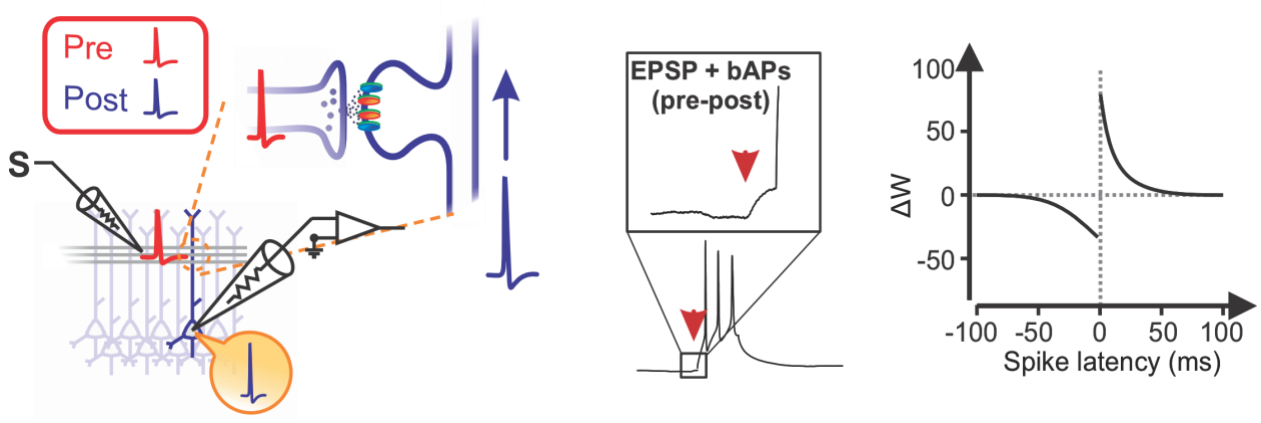

Figure 5. Schematic representation of Spike-Timing-Dependent-Plasticity. The cartoon emphasizes the quasi-simultaneous requirement for synaptic potentials (triggered by presynaptic action potential firing; red) and postsynaptic back-propagating action potentials (bAPs; blue) to trigger synaptic potentiation.

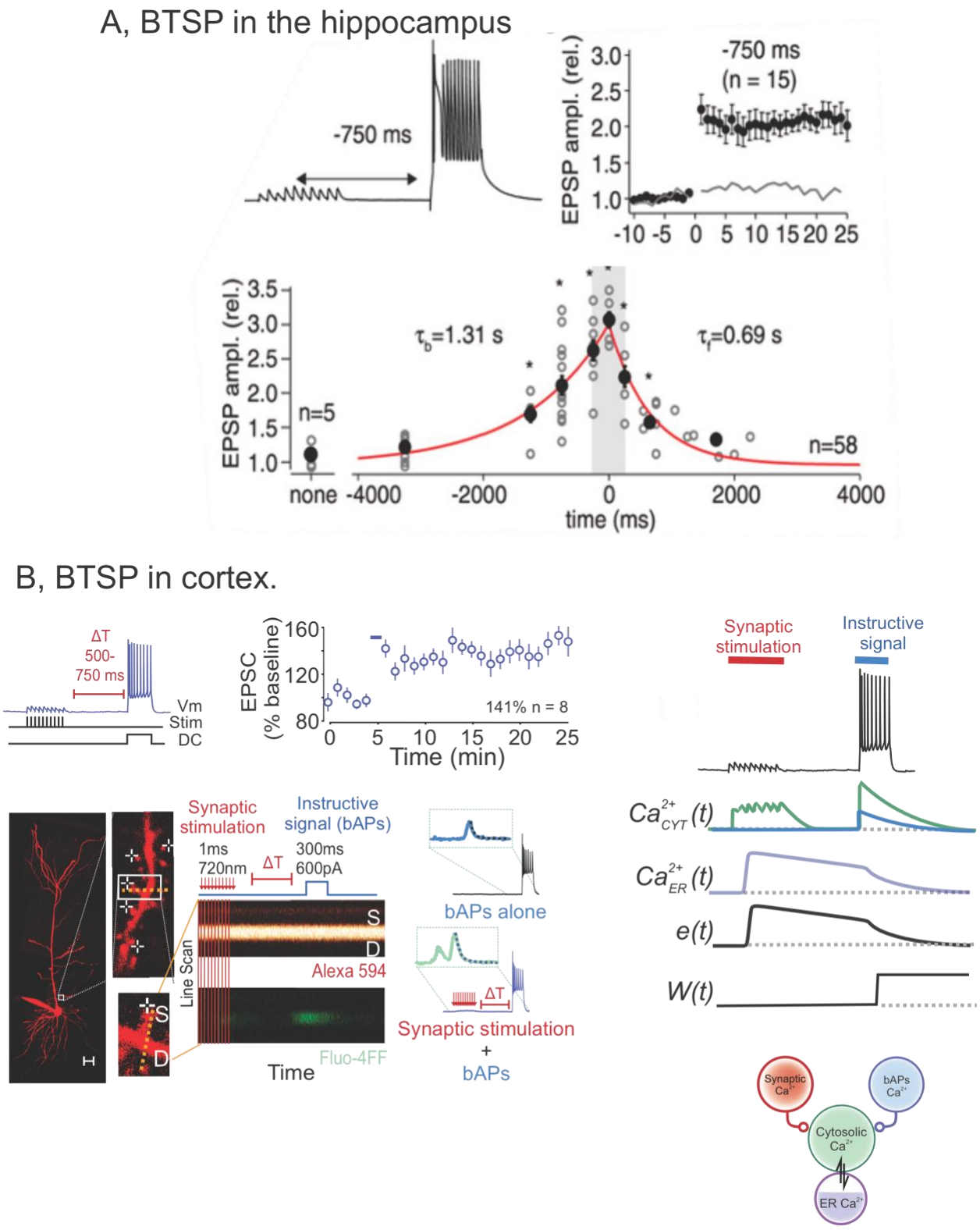

Figure 6. Behavioral Time Scale Plasticity. A, First report of BTSP in the hippocampus[222]. The top panel shows the time interval between synaptic burst inputs and the delayed spiking (mimicking plateau potentials) of the induction protocols. A few repetitions of this protocol is

sufficient to induce robust potentiation. Potentiation ensues irrespective of the order of the synaptic stimulation versus postsynaptic neuron spiking (bottom panel). B, Top left panel shows a highly analogous stimulation paradigm inducing BTSP in recordings from layer V pyramidal neurons of the prefrontal cortex[35]. The bottom left panel summarises two-photon uncaging and calcium imaging experiments that shows that the dendritic Ca^{2+} transients induced by bAPs are larger when a train of clustered synaptic inputs immediately preceded them, with a time scale consistent with that of BTSP.A series of pharmacological and modeling experiments supported the model showed on the bottom right. When occurring alone, a burst of bAPs induce a small Ca^{2+} entry the cytosol (***$Ca^{2+}cyt(t)$***; blue trace). Synaptic stimulation (red) induces NMDAR-dependent Ca^{2+}entry into the cytosol (***$Ca^{2+}cyt(t);$*** green trace). Some of this Ca^{2+} is taken up by intracellular endoplasmic reticulum Ca^{2+} stores (***$Ca^{2+}_{E}(t)$***) that however gradually empties their content. This period dictates a period of eligibility *i.e.,* a decaying eligibility trace (***e(t)***). If a delayed instructive signal (here in the form of a burst of bAPs) invades the dendritic region of activated synapses within that eligibility period, it causes a ryanodine- and IP3 receptor-dependent emptying of Ca^{2+} from internal store, leasing to a significant boost of cytosolic Ca^{2+}, that itself triggers an increase in synaptic weight (***W(t)***). This model is derived from data reported in a preprint[35].

REFERENCES

1. Hebb, D.O. (1949). The organization of behavior; a neuropsychological theory (Wiley).
2. Bliss, T.V., and Lomo, T. (1973). Long-lasting potentiation of synaptic transmission in the dentate area of the anaesthetized rabbit following stimulation of the perforant path. J Physiol *232*, 331-356. 10.1113/jphysiol.1973.sp010273.
3. Bliss, T.V., and Gardner-Medwin, A.R. (1973). Long-lasting potentiation of synaptic transmission in the dentate area of the unanaestetized rabbit following stimulation of the perforant path. J Physiol *232*, 357-374. 10.1113/jphysiol.1973.sp010274.
4. Douglas, R.M., and Goddard, G.V. (1975). Long-term potentiation of the perforant path-granule cell synapse in the rat hippocampus. Brain Res *86*, 205-215. 10.1016/0006-8993(75)90697-6.
5. Feldman, D.E., Nicoll, R.A., and Malenka, R.C. (1999). Synaptic plasticity at thalamocortical synapses in developing rat somatosensory cortex: LTP, LTD, and silent synapses. J Neurobiol *41*, 92-101.
6. Feldman, D.E. (2000). Timing-based LTP and LTD at vertical inputs to layer II/III pyramidal cells in rat barrel cortex. Neuron *27*, 45-56.
7. Sah, P., and Nicoll, R.A. (1991). Mechanisms underlying potentiation of synaptic transmission in rat anterior cingulate cortex in vitro. J Physiol *433*, 615-630. 10.1113/jphysiol.1991.sp018446.
8. Castro-Alamancos, M.A., and Calcagnotto, M.E. (1999). Presynaptic long-term potentiation in corticothalamic synapses. J Neurosci *19*, 9090-9097. 10.1523/JNEUROSCI.19-20-09090.1999.
9. Uno, M., and Ozawa, N. (1991). Long-term potentiation of the amygdalo-striatal synaptic transmission in the course of development of amygdaloid kindling in cats. Neurosci Res *12*, 251-262. 10.1016/0168-0102(91)90115-f.
10. Spencer, J.P., and Murphy, K.P. (2000). Bi-directional changes in synaptic plasticity induced at corticostriatal synapses in vitro. Experimental brain research *135*, 497-503. 10.1007/s002210000523.
11. Ungless, M.A., Whistler, J.L., Malenka, R.C., and Bonci, A. (2001). Single cocaine exposure in vivo induces long-term potentiation in dopamine neurons. Nature *411*, 583-587.
12. Bonci, A., and Malenka, R.C. (1999). Properties and plasticity of excitatory synapses on dopaminergic and GABAergic cells in the ventral tegmental area. J Neurosci *19*, 3723-3730. 10.1523/JNEUROSCI.19-10-03723.1999.
13. Haj-Dahmane, S., Beique, J.C., and Shen, R.Y. (2017). GluA2-Lacking AMPA Receptors and Nitric Oxide Signaling Gate Spike-Timing-Dependent Potentiation of Glutamate Synapses in the Dorsal Raphe Nucleus. eNeuro *4*. 10.1523/ENEURO.0116-17.2017.
14. Malenka, R.C., and Nicoll, R.A. (1999). Long-term potentiation--a decade of progress? Science *285*, 1870-1874. 10.1126/science.285.5435.1870.
15. Malinow, R., and Malenka, R.C. (2002). AMPA receptor trafficking and synaptic plasticity. Annu Rev Neurosci *25*, 103-126.
16. Bliss, T.V., and Collingridge, G.L. (1993). A synaptic model of memory: long-term potentiation in the hippocampus. Nature *361*, 31-39. 10.1038/361031a0.

17. Diering, G.H., and Huganir, R.L. (2018). The AMPA Receptor Code of Synaptic Plasticity. Neuron *100*, 314-329. 10.1016/j.neuron.2018.10.018.
18. Huganir, R.L., and Nicoll, R.A. (2013). AMPARs and synaptic plasticity: the last 25 years. Neuron *80*, 704-717. 10.1016/j.neuron.2013.10.025.
19. Nicoll, R.A. (2017). A Brief History of Long-Term Potentiation. Neuron *93*, 281-290. 10.1016/j.neuron.2016.12.015.
20. Kessels, H.W., and Malinow, R. (2009). Synaptic AMPA receptor plasticity and behavior. Neuron *61*, 340-350.
21. Nicoll, R.A. (2003). Expression mechanisms underlying long-term potentiation: a postsynaptic view. Philos Trans R Soc Lond B Biol Sci *358*, 721-726.
22. Nicoll, R.A., and Schmitz, D. (2005). Synaptic plasticity at hippocampal mossy fibre synapses. Nat Rev Neurosci *6*, 863-876. 10.1038/nrn1786.
23. McNaughton, B.L., Douglas, R.M., and Goddard, G.V. (1978). Synaptic enhancement in fascia dentata: cooperativity among coactive afferents. Brain Res *157*, 277-293. 10.1016/0006-8993(78)90030-6.
24. Levy, W.B., and Steward, O. (1983). Temporal contiguity requirements for long-term associative potentiation/depression in the hippocampus. Neuroscience *8*, 791-797. 10.1016/0306-4522(83)90010-6.
25. Malenka, R.C. (2003). The long-term potential of LTP. Nat Rev Neurosci *4*, 923-926. 10.1038/nrn1258.
26. Lee, K.F., Soares, C., Thivierge, J.P., and Beique, J.C. (2016). Correlated Synaptic Inputs Drive Dendritic Calcium Amplification and Cooperative Plasticity during Clustered Synapse Development. Neuron *89*, 784-799. 10.1016/j.neuron.2016.01.012.
27. Collingridge, G.L., Kehl, S.J., and McLennan, H. (1983). Excitatory amino acids in synaptic transmission in the Schaffer collateral-commissural pathway of the rat hippocampus. J Physiol *334*, 33-46. 10.1113/jphysiol.1983.sp014478.
28. Nowak, L., Bregestovski, P., Ascher, P., Herbet, A., and Prochiantz, A. (1984). Magnesium gates glutamate-activated channels in mouse central neurones. Nature *307*, 462-465. 10.1038/307462a0.
29. Mayer, M.L., and Westbrook, G.L. (1984). Mixed-agonist action of excitatory amino acids on mouse spinal cord neurones under voltage clamp. J Physiol *354*, 29-53. 10.1113/jphysiol.1984.sp015360.
30. Westbrook, G.L., and Mayer, M.L. (1984). Glutamate currents in mammalian spinal neurons: resolution of a paradox. Brain Res *301*, 375-379. 10.1016/0006-8993(84)91107-7.
31. MacDermott, A.B., Mayer, M.L., Westbrook, G.L., Smith, S.J., and Barker, J.L. (1986). NMDA-receptor activation increases cytoplasmic calcium concentration in cultured spinal cord neurones. Nature *321*, 519-522. 10.1038/321519a0.
32. Ascher, P., and Nowak, L. (2009). Early biophysics of the NMDA receptor channel. J Physiol *587*, 4563-4564. 10.1113/jphysiol.2009.178640.
33. Ascher, P., and Nowak, L. (1988). The role of divalent cations in the N-methyl-D-aspartate responses of mouse central neurones in culture. J Physiol *399*, 247-266. 10.1113/jphysiol.1988.sp017078.
34. Lynch, G., Larson, J., Kelso, S., Barrionuevo, G., and Schottler, F. (1983). Intracellular injections of EGTA block induction of hippocampal long-term potentiation. Nature *305*, 719-721. 10.1038/305719a0.

35. Caya-Bissonnette, L.N., R; Beique, JC (2023). Cellular Substrate of Eligibility Traces. BioRxiv.
36. Sabatini, B.L., Oertner, T.G., and Svoboda, K. (2002). The life cycle of Ca(2+) ions in dendritic spines. Neuron *33*, 439-452.
37. Sabatini, B.L., Maravall, M., and Svoboda, K. (2001). Ca(2+) signaling in dendritic spines. Curr Opin Neurobiol *11*, 349-356.
38. Alvarez, V.A., and Sabatini, B.L. (2007). Anatomical and physiological plasticity of dendritic spines. Annu Rev Neurosci *30*, 79-97.
39. Bloodgood, B.L., Giessel, A.J., and Sabatini, B.L. (2009). Biphasic synaptic Ca influx arising from compartmentalized electrical signals in dendritic spines. PLoS Biol *7*, e1000190. 10.1371/journal.pbio.1000190.
40. Lee, K.F., Soares, C., and Beique, J.C. (2012). Examining form and function of dendritic spines. Neural Plast *2012*, 704103. 10.1155/2012/704103.
41. Bloodgood, B.L., and Sabatini, B.L. (2005). Neuronal activity regulates diffusion across the neck of dendritic spines. Science *310*, 866-869. 10.1126/science.1114816.
42. Benardo, L.S., Masukawa, L.M., and Prince, D.A. (1982). Electrophysiology of isolated hippocampal pyramidal dendrites. J Neurosci *2*, 1614-1622. 10.1523/JNEUROSCI.02-11-01614.1982.
43. Wong, R.K., Prince, D.A., and Basbaum, A.I. (1979). Intradendritic recordings from hippocampal neurons. Proc Natl Acad Sci U S A *76*, 986-990. 10.1073/pnas.76.2.986.
44. Stuart, G.J., and Sakmann, B. (1994). Active propagation of somatic action potentials into neocortical pyramidal cell dendrites. Nature *367*, 69-72. 10.1038/367069a0.
45. Markram, H., Lubke, J., Frotscher, M., and Sakmann, B. (1997). Regulation of synaptic efficacy by coincidence of postsynaptic APs and EPSPs. Science *275*, 213-215. 10.1126/science.275.5297.213.
46. Bi, G.Q., and Poo, M.M. (1998). Synaptic modifications in cultured hippocampal neurons: dependence on spike timing, synaptic strength, and postsynaptic cell type. J Neurosci *18*, 10464-10472. 10.1523/JNEUROSCI.18-24-10464.1998.
47. Sejnowski, T.J. (1977). Statistical constraints on synaptic plasticity. J Theor Biol *69*, 385-389. 10.1016/0022-5193(77)90146-1.
48. Sejnowski, T.J. (1977). Storing covariance with nonlinearly interacting neurons. J Math Biol *4*, 303-321. 10.1007/BF00275079.
49. Bell, C., Bodznick, D., Montgomery, J., and Bastian, J. (1997). The generation and subtraction of sensory expectations within cerebellum-like structures. Brain Behav Evol *50 Suppl 1*, 17-31. 10.1159/000113352.
50. Han, V.Z., Grant, K., and Bell, C.C. (2000). Reversible associative depression and nonassociative potentiation at a parallel fiber synapse. Neuron *27*, 611-622. 10.1016/s0896-6273(00)00070-2.
51. Harvey-Girard, E., Lewis, J., and Maler, L. (2010). Burst-induced anti-Hebbian depression acts through short-term synaptic dynamics to cancel redundant sensory signals. J Neurosci *30*, 6152-6169. 10.1523/JNEUROSCI.0303-10.2010.
52. Holmgren, C.D., and Zilberter, Y. (2001). Coincident spiking activity induces long-term changes in inhibition of neocortical pyramidal cells. J Neurosci *21*, 8270-8277. 10.1523/JNEUROSCI.21-20-08270.2001.

53. Lamsa, K.P., Heeroma, J.H., Somogyi, P., Rusakov, D.A., and Kullmann, D.M. (2007). Anti-Hebbian long-term potentiation in the hippocampal feedback inhibitory circuit. Science *315*, 1262-1266. 10.1126/science.1137450.
54. Fino, E., Glowinski, J., and Venance, L. (2005). Bidirectional activity-dependent plasticity at corticostriatal synapses. J Neurosci *25*, 11279-11287. 10.1523/JNEUROSCI.4476-05.2005.
55. Wang, S.S., Khiroug, L., and Augustine, G.J. (2000). Quantification of spread of cerebellar long-term depression with chemical two-photon uncaging of glutamate. Proc Natl Acad Sci U S A *97*, 8635-8640. 10.1073/pnas.130414597.
56. Stent, G.S. (1973). A physiological mechanism for Hebb's postulate of learning. Proc Natl Acad Sci U S A *70*, 997-1001. 10.1073/pnas.70.4.997.
57. Heidmann, T., and Changeux, J.P. (1982). [Molecular model of the regulation of chemical synapse efficiency at the postsynaptic level]. C R Seances Acad Sci III *295*, 665-670.
58. Geinisman, Y., deToledo-Morrell, L., Morrell, F., Heller, R.E., Rossi, M., and Parshall, R.F. (1993). Structural synaptic correlate of long-term potentiation: formation of axospinous synapses with multiple, completely partitioned transmission zones. Hippocampus *3*, 435-445. 10.1002/hipo.450030405.
59. Korn, H., and Faber, D.S. (1998). Quantal analysis and long-term potentiation. C R Acad Sci III *321*, 125-130. 10.1016/s0764-4469(97)89811-3.
60. Loebel, A., Le Be, J.V., Richardson, M.J., Markram, H., and Herz, A.V. (2013). Matched pre- and post-synaptic changes underlie synaptic plasticity over long time scales. J Neurosci *33*, 6257-6266. 10.1523/JNEUROSCI.3740-12.2013.
61. Brock, J.A., Thomazeau, A., Watanabe, A., Li, S.S.Y., and Sjostrom, P.J. (2020). A Practical Guide to Using CV Analysis for Determining the Locus of Synaptic Plasticity. Front Synaptic Neurosci *12*, 11. 10.3389/fnsyn.2020.00011.
62. Malinow, R., and Tsien, R.W. (1990). Presynaptic enhancement shown by whole-cell recordings of long-term potentiation in hippocampal slices. Nature *346*, 177-180.
63. Kerchner, G.A., and Nicoll, R.A. (2008). Silent synapses and the emergence of a postsynaptic mechanism for LTP. Nat Rev Neurosci *9*, 813-825.
64. Isaac, J.T., Nicoll, R.A., and Malenka, R.C. (1995). Evidence for silent synapses: implications for the expression of LTP. Neuron *15*, 427-434.
65. Liao, D., Hessler, N.A., and Malinow, R. (1995). Activation of postsynaptically silent synapses during pairing-induced LTP in CA1 region of hippocampal slice. Nature *375*, 400-404.
66. Vincent-Lamarre, P., Lynn, M., and Beique, J.C. (2018). The Eloquent Silent Synapse. Trends Neurosci *41*, 557-559. 10.1016/j.tins.2018.07.002.
67. Manabe, T., Wyllie, D.J., Perkel, D.J., and Nicoll, R.A. (1993). Modulation of synaptic transmission and long-term potentiation: effects on paired pulse facilitation and EPSC variance in the CA1 region of the hippocampus. J Neurophysiol *70*, 1451-1459. 10.1152/jn.1993.70.4.1451.
68. Manabe, T., and Nicoll, R.A. (1994). Long-term potentiation: evidence against an increase in transmitter release probability in the CA1 region of the hippocampus. Science *265*, 1888-1892. 10.1126/science.7916483.

69. Liao, D., Zhang, X., O'Brien, R., Ehlers, M.D., and Huganir, R.L. (1999). Regulation of morphological postsynaptic silent synapses in developing hippocampal neurons. Nat Neurosci *2*, 37-43.
70. Lynn, M., Naud, R., and Beique, J.C. (2020). Accurate Silent Synapse Estimation from Simulator-Corrected Electrophysiological Data Using the SilentMLE Python Package. STAR Protoc *1*, 100176. 10.1016/j.xpro.2020.100176.
71. Lynn, M.B., Lee, K.F.H., Soares, C., Naud, R., and Beique, J.C. (2020). A Synthetic Likelihood Solution to the Silent Synapse Estimation Problem. Cell Rep *32*, 107916. 10.1016/j.celrep.2020.107916.
72. Heine, M., Groc, L., Frischknecht, R., Beique, J.C., Lounis, B., Rumbaugh, G., Huganir, R.L., Cognet, L., and Choquet, D. (2008). Surface mobility of postsynaptic AMPARs tunes synaptic transmission. Science *320*, 201-205.
73. Caya-Bissonnette, L., and Beique, J.C. (2023). Low throughput screening in neuroscience: using light to study central synapses one at a time. Neurophotonics *10*, 044407. 10.1117/1.NPh.10.4.044407.
74. Beique, J.C., Lin, D.T., Kang, M.G., Aizawa, H., Takamiya, K., and Huganir, R.L. (2006). Synapse-specific regulation of AMPA receptor function by PSD-95. Proc Natl Acad Sci U S A *103*, 19535-19540.
75. Busetto, G., Higley, M.J., and Sabatini, B.L. (2008). Developmental presence and disappearance of postsynaptically silent synapses on dendritic spines of rat layer 2/3 pyramidal neurons. J Physiol *586*, 1519-1527.
76. Soares, C., Lee, K.F.H., and Beique, J.C. (2017). Metaplasticity at CA1 Synapses by Homeostatic Control of Presynaptic Release Dynamics. Cell reports *21*, 1293-1303. 10.1016/j.celrep.2017.10.025.
77. Ashby, M.C., and Isaac, J.T. (2011). Maturation of a recurrent excitatory neocortical circuit by experience-dependent unsilencing of newly formed dendritic spines. Neuron *70*, 510-521. 10.1016/j.neuron.2011.02.057.
78. Vardalaki, D., Chung, K., and Harnett, M.T. (2022). Filopodia are a structural substrate for silent synapses in adult neocortex. Nature *612*, 323-327. 10.1038/s41586-022-05483-6.
79. Manabe, T., Renner, P., and Nicoll, R.A. (1992). Postsynaptic contribution to long-term potentiation revealed by the analysis of miniature synaptic currents. Nature *355*, 50-55. 10.1038/355050a0.
80. Isaac, J.T., Oliet, S.H., Hjelmstad, G.O., Nicoll, R.A., and Malenka, R.C. (1996). Expression mechanisms of long-term potentiation in the hippocampus. J Physiol Paris *90*, 299-303.
81. Oliet, S.H., Malenka, R.C., and Nicoll, R.A. (1996). Bidirectional control of quantal size by synaptic activity in the hippocampus. Science *271*, 1294-1297. 10.1126/science.271.5253.1294.
82. George, J., Soares, C., Montersino, A., Beique, J.C., and Thomas, G.M. (2015). Palmitoylation of LIM Kinase-1 ensures spine-specific actin polymerization and morphological plasticity. eLife *4*, e06327. 10.7554/eLife.06327.
83. Matsuzaki, M., Honkura, N., Ellis-Davies, G.C., and Kasai, H. (2004). Structural basis of long-term potentiation in single dendritic spines. Nature *429*, 761-766.
84. Patterson, M.A., Szatmari, E.M., and Yasuda, R. (2010). AMPA receptors are exocytosed in stimulated spines and adjacent dendrites in a Ras-ERK-dependent manner during long-

term potentiation. Proc Natl Acad Sci U S A *107*, 15951-15956. 10.1073/pnas.0913875107.
85. Silva, A.J., Stevens, C.F., Tonegawa, S., and Wang, Y. (1992). Deficient hippocampal long-term potentiation in alpha-calcium-calmodulin kinase II mutant mice. Science *257*, 201-206. 10.1126/science.1378648.
86. Silva, A.J., Paylor, R., Wehner, J.M., and Tonegawa, S. (1992). Impaired spatial learning in alpha-calcium-calmodulin kinase II mutant mice. Science *257*, 206-211. 10.1126/science.1321493.
87. Lee, H.K., Barbarosie, M., Kameyama, K., Bear, M.F., and Huganir, R.L. (2000). Regulation of distinct AMPA receptor phosphorylation sites during bidirectional synaptic plasticity. Nature *405*, 955-959.
88. Soares, C., Lee, K.F., Cook, D., and Beique, J.C. (2014). A cost-effective method for preparing, maintaining, and transfecting neurons in organotypic slices. Methods Mol Biol *1183*, 205-219. 10.1007/978-1-4939-1096-0_13.
89. Schnell, E., Sizemore, M., Karimzadegan, S., Chen, L., Bredt, D.S., and Nicoll, R.A. (2002). Direct interactions between PSD-95 and stargazin control synaptic AMPA receptor number. Proc Natl Acad Sci U S A *99*, 13902-13907. 10.1073/pnas.172511199.
90. Beique, J.C., and Andrade, R. (2003). PSD-95 regulates synaptic transmission and plasticity in rat cerebral cortex. J Physiol *546*, 859-867.
91. El-Husseini, A.E., Schnell, E., Chetkovich, D.M., Nicoll, R.A., and Bredt, D.S. (2000). PSD-95 involvement in maturation of excitatory synapses. Science *290*, 1364-1368.
92. Elias, G.M., Elias, L.A., Apostolides, P.F., Kriegstein, A.R., and Nicoll, R.A. (2008). Differential trafficking of AMPA and NMDA receptors by SAP102 and PSD-95 underlies synapse development. Proc Natl Acad Sci U S A *105*, 20953-20958.
93. Ehrlich, I., and Malinow, R. (2004). Postsynaptic density 95 controls AMPA receptor incorporation during long-term potentiation and experience-driven synaptic plasticity. J Neurosci *24*, 916-927.
94. Stein, V., House, D.R., Bredt, D.S., and Nicoll, R.A. (2003). Postsynaptic density-95 mimics and occludes hippocampal long-term potentiation and enhances long-term depression. J Neurosci *23*, 5503-5506. 10.1523/JNEUROSCI.23-13-05503.2003.
95. Barria, A., and Malinow, R. (2002). Subunit-specific NMDA receptor trafficking to synapses. Neuron *35*, 345-353.
96. Barria, A., and Malinow, R. (2005). NMDA receptor subunit composition controls synaptic plasticity by regulating binding to CaMKII. Neuron *48*, 289-301.
97. Shi, S., Hayashi, Y., Esteban, J.A., and Malinow, R. (2001). Subunit-specific rules governing AMPA receptor trafficking to synapses in hippocampal pyramidal neurons. Cell *105*, 331-343.
98. Hayashi, Y., Shi, S.H., Esteban, J.A., Piccini, A., Poncer, J.C., and Malinow, R. (2000). Driving AMPA receptors into synapses by LTP and CaMKII: requirement for GluR1 and PDZ domain interaction. Science *287*, 2262-2267.
99. Esteban, J.A., Shi, S.H., Wilson, C., Nuriya, M., Huganir, R.L., and Malinow, R. (2003). PKA phosphorylation of AMPA receptor subunits controls synaptic trafficking underlying plasticity. Nat Neurosci *6*, 136-143. 10.1038/nn997.
100. Granger, A.J., Shi, Y., Lu, W., Cerpas, M., and Nicoll, R.A. (2013). LTP requires a reserve pool of glutamate receptors independent of subunit type. Nature *493*, 495-500. 10.1038/nature11775.

101. Yasuda, R., Hayashi, Y., and Hell, J.W. (2022). CaMKII: a central molecular organizer of synaptic plasticity, learning and memory. Nat Rev Neurosci *23*, 666-682. 10.1038/s41583-022-00624-2.
102. Lisman, J., Yasuda, R., and Raghavachari, S. (2012). Mechanisms of CaMKII action in long-term potentiation. Nat Rev Neurosci *13*, 169-182. 10.1038/nrn3192.
103. Barria, A., Muller, D., Derkach, V., Griffith, L.C., and Soderling, T.R. (1997). Regulatory phosphorylation of AMPA-type glutamate receptors by CaM-KII during long-term potentiation. Science *276*, 2042-2045. 10.1126/science.276.5321.2042.
104. Barria, A., Derkach, V., and Soderling, T. (1997). Identification of the Ca2+/calmodulin-dependent protein kinase II regulatory phosphorylation site in the alpha-amino-3-hydroxyl-5-methyl-4-isoxazole-propionate-type glutamate receptor. J Biol Chem *272*, 32727-32730.
105. Lisman, J., Malenka, R.C., Nicoll, R.A., and Malinow, R. (1997). Learning mechanisms: the case for CaM-KII. Science *276*, 2001-2002. 10.1126/science.276.5321.2001.
106. Lee, H.K., Takamiya, K., Han, J.S., Man, H., Kim, C.H., Rumbaugh, G., Yu, S., Ding, L., He, C., Petralia, R.S., et al. (2003). Phosphorylation of the AMPA receptor GluR1 subunit is required for synaptic plasticity and retention of spatial memory. Cell *112*, 631-643. 10.1016/s0092-8674(03)00122-3.
107. Park, J., Chavez, A.E., Mineur, Y.S., Morimoto-Tomita, M., Lutzu, S., Kim, K.S., Picciotto, M.R., Castillo, P.E., and Tomita, S. (2016). CaMKII Phosphorylation of TARPgamma-8 Is a Mediator of LTP and Learning and Memory. Neuron *92*, 75-83. 10.1016/j.neuron.2016.09.002.
108. Tullis, J.E., Larsen, M.E., Rumian, N.L., Freund, R.K., Boxer, E.E., Brown, C.N., Coultrap, S.J., Schulman, H., Aoto, J., Dell'Acqua, M.L., and Bayer, K.U. (2023). LTP induction by structural rather than enzymatic functions of CaMKII. Nature *621*, 146-153. 10.1038/s41586-023-06465-y.
109. Castillo, P.E., Schoch, S., Schmitz, F., Sudhof, T.C., and Malenka, R.C. (2002). RIM1alpha is required for presynaptic long-term potentiation. Nature *415*, 327-330. 10.1038/415327a.
110. Schmitz, D., Mellor, J., Breustedt, J., and Nicoll, R.A. (2003). Presynaptic kainate receptors impart an associative property to hippocampal mossy fiber long-term potentiation. Nat Neurosci *6*, 1058-1063. 10.1038/nn1116.
111. Castillo, P.E. (2012). Presynaptic LTP and LTD of excitatory and inhibitory synapses. Cold Spring Harb Perspect Biol *4*. 10.1101/cshperspect.a005728.
112. Maccaferri, G., Toth, K., and McBain, C.J. (1998). Target-specific expression of presynaptic mossy fiber plasticity. Science *279*, 1368-1370. 10.1126/science.279.5355.1368.
113. Weisskopf, M.G., and Nicoll, R.A. (1995). Presynaptic changes during mossy fibre LTP revealed by NMDA receptor-mediated synaptic responses. Nature *376*, 256-259. 10.1038/376256a0.
114. Weisskopf, M.G., Castillo, P.E., Zalutsky, R.A., and Nicoll, R.A. (1994). Mediation of hippocampal mossy fiber long-term potentiation by cyclic AMP. Science *265*, 1878-1882. 10.1126/science.7916482.
115. Castillo, P.E., Janz, R., Sudhof, T.C., Tzounopoulos, T., Malenka, R.C., and Nicoll, R.A. (1997). Rab3A is essential for mossy fibre long-term potentiation in the hippocampus. Nature *388*, 590-593. 10.1038/41574.

116. Yeckel, M.F., Kapur, A., and Johnston, D. (1999). Multiple forms of LTP in hippocampal CA3 neurons use a common postsynaptic mechanism. Nat Neurosci *2*, 625-633. 10.1038/10180.
117. Kapur, A., Yeckel, M.F., Gray, R., and Johnston, D. (1998). L-Type calcium channels are required for one form of hippocampal mossy fiber LTP. J Neurophysiol *79*, 2181-2190. 10.1152/jn.1998.79.4.2181.
118. Jaffe, D., and Johnston, D. (1990). Induction of long-term potentiation at hippocampal mossy-fiber synapses follows a Hebbian rule. J Neurophysiol *64*, 948-960. 10.1152/jn.1990.64.3.948.
119. Mellor, J., and Nicoll, R.A. (2001). Hippocampal mossy fiber LTP is independent of postsynaptic calcium. Nat Neurosci *4*, 125-126. 10.1038/83941.
120. Wang, H., Pineda, V.V., Chan, G.C., Wong, S.T., Muglia, L.J., and Storm, D.R. (2003). Type 8 adenylyl cyclase is targeted to excitatory synapses and required for mossy fiber long-term potentiation. J Neurosci *23*, 9710-9718. 10.1523/JNEUROSCI.23-30-09710.2003.
121. Villacres, E.C., Wong, S.T., Chavkin, C., and Storm, D.R. (1998). Type I adenylyl cyclase mutant mice have impaired mossy fiber long-term potentiation. J Neurosci *18*, 3186-3194. 10.1523/JNEUROSCI.18-09-03186.1998.
122. Matthies, H. (1974). The biochemical basis of learning and memory. Life Sci *15*, 2017-2031. 10.1016/0024-3205(74)90019-8.
123. Krug, M., Lossner, B., and Ott, T. (1984). Anisomycin blocks the late phase of long-term potentiation in the dentate gyrus of freely moving rats. Brain Res Bull *13*, 39-42. 10.1016/0361-9230(84)90005-4.
124. Frey, S., Schwiegert, C., Krug, M., and Lossner, B. (1991). Long-term potentiation induced changes in protein synthesis of hippocampal subfields of freely moving rats: time-course. Biomed Biochim Acta *50*, 1231-1240.
125. Sajikumar, S., Navakkode, S., and Frey, J.U. (2005). Protein synthesis-dependent long-term functional plasticity: methods and techniques. Curr Opin Neurobiol *15*, 607-613. 10.1016/j.conb.2005.08.009.
126. Vickers, C.A., Dickson, K.S., and Wyllie, D.J. (2005). Induction and maintenance of late-phase long-term potentiation in isolated dendrites of rat hippocampal CA1 pyramidal neurones. J Physiol *568*, 803-813. 10.1113/jphysiol.2005.092924.
127. Reymann, K.G., Frey, U., Jork, R., and Matthies, H. (1988). Polymyxin B, an inhibitor of protein kinase C, prevents the maintenance of synaptic long-term potentiation in hippocampal CA1 neurons. Brain Res *440*, 305-314. 10.1016/0006-8993(88)91000-1.
128. Reymann, K.G., Schulzeck, K., Kase, H., and Matthies, H. (1988). Phorbol ester-induced hippocampal long-term potentiation is counteracted by inhibitors of protein kinase C. Experimental brain research *71*, 227-230. 10.1007/BF00247540.
129. Anwyl, R. (1999). Metabotropic glutamate receptors: electrophysiological properties and role in plasticity. Brain Res Brain Res Rev *29*, 83-120.
130. Bashir, Z.I., Bortolotto, Z.A., Davies, C.H., Berretta, N., Irving, A.J., Seal, A.J., Henley, J.M., Jane, D.E., Watkins, J.C., and Collingridge, G.L. (1993). Induction of LTP in the hippocampus needs synaptic activation of glutamate metabotropic receptors. Nature *363*, 347-350. 10.1038/363347a0.
131. Bortolotto, Z.A., and Collingridge, G.L. (2000). A role for protein kinase C in a form of metaplasticity that regulates the induction of long-term potentiation at CA1 synapses of

the adult rat hippocampus. Eur J Neurosci *12*, 4055-4062. 10.1046/j.1460-9568.2000.00291.x.
132. Bortolotto, Z.A., and Collingridge, G.L. (1998). Involvement of calcium/calmodulin-dependent protein kinases in the setting of a molecular switch involved in hippocampal LTP. Neuropharmacology *37*, 535-544. 10.1016/s0028-3908(98)00058-6.
133. Bortolotto, Z.A., and Collingridge, G.L. (1993). Characterisation of LTP induced by the activation of glutamate metabotropic receptors in area CA1 of the hippocampus. Neuropharmacology *32*, 1-9. 10.1016/0028-3908(93)90123-k.
134. Reymann, K.G., and Frey, J.U. (2007). The late maintenance of hippocampal LTP: requirements, phases, 'synaptic tagging', 'late-associativity' and implications. Neuropharmacology *52*, 24-40. 10.1016/j.neuropharm.2006.07.026.
135. de Vries, P.H., and van Slochteren, K.R. (2008). The nature of the memory trace and its neurocomputational implications. J Comput Neurosci *25*, 188-202.
136. Turrigiano, G.G. (2008). The self-tuning neuron: synaptic scaling of excitatory synapses. Cell *135*, 422-435.
137. Sullivan, T.J., and de Sa, V.R. (2008). Sleeping our way to weight normalization and stable learning. Neural Comput *20*, 3111-3130.
138. Sullivan, T.J., and de Sa, V.R. (2006). Homeostatic synaptic scaling in self-organizing maps. Neural Netw *19*, 734-743.
139. Nelson, S.B., and Turrigiano, G.G. (2008). Strength through diversity. Neuron *60*, 477-482.
140. Davis, G.W. (2006). Homeostatic control of neural activity: from phenomenology to molecular design. Annu Rev Neurosci *29*, 307-323.
141. Cannon, W.B.R., A. (1949). The supersensitivity of denervated structure.
142. O'Brien, R.J., Kamboj, S., Ehlers, M.D., Rosen, K.R., Fischbach, G.D., and Huganir, R.L. (1998). Activity-dependent modulation of synaptic AMPA receptor accumulation. Neuron *21*, 1067-1078.
143. Turrigiano, G.G., Leslie, K.R., Desai, N.S., Rutherford, L.C., and Nelson, S.B. (1998). Activity-dependent scaling of quantal amplitude in neocortical neurons. Nature *391*, 892-896.
144. Shepherd, J.D., Rumbaugh, G., Wu, J., Chowdhury, S., Plath, N., Kuhl, D., Huganir, R.L., and Worley, P.F. (2006). Arc/Arg3.1 mediates homeostatic synaptic scaling of AMPA receptors. Neuron *52*, 475-484.
145. Soares, C., Lee, K.F., Nassrallah, W., and Beique, J.C. (2013). Differential subcellular targeting of glutamate receptor subtypes during homeostatic synaptic plasticity. J Neurosci *33*, 13547-13559. 10.1523/JNEUROSCI.1873-13.2013.
146. Watt, A.J., van Rossum, M.C., MacLeod, K.M., Nelson, S.B., and Turrigiano, G.G. (2000). Activity coregulates quantal AMPA and NMDA currents at neocortical synapses. Neuron *26*, 659-670.
147. Turrigiano, G.G., and Nelson, S.B. (2004). Homeostatic plasticity in the developing nervous system. Nat Rev Neurosci *5*, 97-107.
148. Turrigiano, G.G., and Nelson, S.B. (2000). Hebb and homeostasis in neuronal plasticity. Curr Opin Neurobiol *10*, 358-364.
149. Burrone, J., and Murthy, V.N. (2003). Synaptic gain control and homeostasis. Curr Opin Neurobiol *13*, 560-567.

150. Burrone, J., O'Byrne, M., and Murthy, V.N. (2002). Multiple forms of synaptic plasticity triggered by selective suppression of activity in individual neurons. Nature *420*, 414-418.
151. Gong, B., Wang, H., Gu, S., Heximer, S.P., and Zhuo, M. (2007). Genetic evidence for the requirement of adenylyl cyclase 1 in synaptic scaling of forebrain cortical neurons. Eur J Neurosci *26*, 275-288.
152. Stellwagen, D., and Malenka, R.C. (2006). Synaptic scaling mediated by glial TNF-alpha. Nature *440*, 1054-1059.
153. Maghsoodi, B., Poon, M.M., Nam, C.I., Aoto, J., Ting, P., and Chen, L. (2008). Retinoic acid regulates RARalpha-mediated control of translation in dendritic RNA granules during homeostatic synaptic plasticity. Proc Natl Acad Sci U S A *105*, 16015-16020.
154. Seeburg, D.P., Feliu-Mojer, M., Gaiottino, J., Pak, D.T., and Sheng, M. (2008). Critical role of CDK5 and Polo-like kinase 2 in homeostatic synaptic plasticity during elevated activity. Neuron *58*, 571-583.
155. Sutton, M.A., Ito, H.T., Cressy, P., Kempf, C., Woo, J.C., and Schuman, E.M. (2006). Miniature neurotransmission stabilizes synaptic function via tonic suppression of local dendritic protein synthesis. Cell *125*, 785-799.
156. Deeg, K.E. (2009). Synapse-specific homeostatic mechanisms in the hippocampus. J Neurophysiol *101*, 503-506.
157. Kim, J., and Tsien, R.W. (2008). Synapse-specific adaptations to inactivity in hippocampal circuits achieve homeostatic gain control while dampening network reverberation. Neuron *58*, 925-937.
158. Beique, J.C. (2009). Homeostatic plasticity in a reward processing region: accumbens neurons scale too! Eur J Neurosci.
159. Rabinowitch, I., and Segev, I. (2008). Two opposing plasticity mechanisms pulling a single synapse. Trends Neurosci *31*, 377-383.
160. Rabinowitch, I., and Segev, I. (2006). The endurance and selectivity of spatial patterns of long-term potentiation/depression in dendrites under homeostatic synaptic plasticity. J Neurosci *26*, 13474-13484.
161. Rabinowitch, I., and Segev, I. (2006). The interplay between homeostatic synaptic plasticity and functional dendritic compartments. J Neurophysiol *96*, 276-283.
162. Turrigiano, G.G. (1999). Homeostatic plasticity in neuronal networks: the more things change, the more they stay the same. Trends Neurosci *22*, 221-227.
163. Thiagarajan, T.C., Lindskog, M., and Tsien, R.W. (2005). Adaptation to synaptic inactivity in hippocampal neurons. Neuron *47*, 725-737.
164. Thiagarajan, T.C., Lindskog, M., Malgaroli, A., and Tsien, R.W. (2007). LTP and adaptation to inactivity: overlapping mechanisms and implications for metaplasticity. Neuropharmacology *52*, 156-175.
165. Echegoyen, J., Neu, A., Graber, K.D., and Soltesz, I. (2007). Homeostatic plasticity studied using in vivo hippocampal activity-blockade: synaptic scaling, intrinsic plasticity and age-dependence. PloS one *2*, e700.
166. Beique, J.C., Na, Y., Kuhl, D., Worley, P.F., and Huganir, R.L. (2011). Arc-dependent synapse-specific homeostatic plasticity. Proc Natl Acad Sci U S A *108*, 816-821.
167. Amit, D.J. (1989). Modeling Brain Function (Cambridge University Press).
168. Fusi, S., and Abbott, L.F. (2007). Limits on the memory storage capacity of bounded synapses. Nat Neurosci *10*, 485-493.

169. Fusi, S., Drew, P.J., and Abbott, L.F. (2005). Cascade models of synaptically stored memories. Neuron *45*, 599-611.
170. Fusi, S. (2002). Hebbian spike-driven synaptic plasticity for learning patterns of mean firing rates. Biol Cybern *87*, 459-470.
171. Arendt, K.L., Sarti, F., and Chen, L. (2013). Chronic inactivation of a neural circuit enhances LTP by inducing silent synapse formation. J Neurosci *33*, 2087-2096. 10.1523/JNEUROSCI.3880-12.2013.
172. Wierenga, C.J., Walsh, M.F., and Turrigiano, G.G. (2006). Temporal regulation of the expression locus of homeostatic plasticity. J Neurophysiol *96*, 2127-2133.
173. Desai, N.S., Cudmore, R.H., Nelson, S.B., and Turrigiano, G.G. (2002). Critical periods for experience-dependent synaptic scaling in visual cortex. Nat Neurosci *5*, 783-789.
174. Montgomery, J.M., and Madison, D.V. (2002). State-dependent heterogeneity in synaptic depression between pyramidal cell pairs. Neuron *33*, 765-777.
175. Jedlicka, P. (2002). Synaptic plasticity, metaplasticity and BCM theory. Bratisl Lek Listy *103*, 137-143.
176. Abraham, W.C., and Bear, M.F. (1996). Metaplasticity: the plasticity of synaptic plasticity. Trends Neurosci *19*, 126-130.
177. Deisseroth, K., Bito, H., Schulman, H., and Tsien, R.W. (1995). Synaptic plasticity: A molecular mechanism for metaplasticity. Curr Biol *5*, 1334-1338.
178. Levy, W.B., and Steward, O. (1979). Synapses as associative memory elements in the hippocampal formation. Brain Res *175*, 233-245. 10.1016/0006-8993(79)91003-5.
179. Lynch, G., Browning, M., and Bennett, W.F. (1979). Biochemical and physiological studies of long-term synaptic plasticity. Fed Proc *38*, 2117-2122.
180. Martin, S.J., Grimwood, P.D., and Morris, R.G. (2000). Synaptic plasticity and memory: an evaluation of the hypothesis. Annu Rev Neurosci *23*, 649-711. 10.1146/annurev.neuro.23.1.649.
181. Tsien, J.Z. (2000). Linking Hebb's coincidence-detection to memory formation. Curr Opin Neurobiol *10*, 266-273. 10.1016/s0959-4388(00)00070-2.
182. Dringenberg, H.C. (2020). The history of long-term potentiation as a memory mechanism: Controversies, confirmation, and some lessons to remember. Hippocampus *30*, 987-1012. 10.1002/hipo.23213.
183. Winnubst, J., and Lohmann, C. (2012). Synaptic clustering during development and learning: the why, when, and how. Front Mol Neurosci *5*, 70. 10.3389/fnmol.2012.00070.
184. Losonczy, A., and Magee, J.C. (2006). Integrative properties of radial oblique dendrites in hippocampal CA1 pyramidal neurons. Neuron *50*, 291-307.
185. Losonczy, A., Makara, J.K., and Magee, J.C. (2008). Compartmentalized dendritic plasticity and input feature storage in neurons. Nature *452*, 436-441.
186. Larkum, M.E., and Nevian, T. (2008). Synaptic clustering by dendritic signalling mechanisms. Curr Opin Neurobiol *18*, 321-331.
187. Tazerart, S., Mitchell, D.E., Miranda-Rottmann, S., and Araya, R. (2020). A spike-timing-dependent plasticity rule for dendritic spines. Nat Commun *11*, 4276. 10.1038/s41467-020-17861-7.
188. Harvey, C.D., and Svoboda, K. (2007). Locally dynamic synaptic learning rules in pyramidal neuron dendrites. Nature *450*, 1195-1200.
189. Govindarajan, A., Kelleher, R.J., and Tonegawa, S. (2006). A clustered plasticity model of long-term memory engrams. Nat Rev Neurosci *7*, 575-583.

190. Kirchner, J.H., and Gjorgjieva, J. (2021). Emergence of local and global synaptic organization on cortical dendrites. Nat Commun *12*, 4005. 10.1038/s41467-021-23557-3.
191. Mel, B.W. (1993). Synaptic integration in an excitable dendritic tree. J Neurophysiol *70*, 1086-1101. 10.1152/jn.1993.70.3.1086.
192. Poirazi, P., Brannon, T., and Mel, B.W. (2003). Pyramidal neuron as two-layer neural network. Neuron *37*, 989-999. 10.1016/s0896-6273(03)00149-1.
193. Poirazi, P., and Mel, B.W. (2001). Impact of active dendrites and structural plasticity on the memory capacity of neural tissue. Neuron *29*, 779-796. 10.1016/s0896-6273(01)00252-5.
194. Druckmann, S., Feng, L., Lee, B., Yook, C., Zhao, T., Magee, J.C., and Kim, J. (2014). Structured synaptic connectivity between hippocampal regions. Neuron *81*, 629-640. 10.1016/j.neuron.2013.11.026.
195. Rescorla, R.A. (1988). Behavioral studies of Pavlovian conditioning. Annu Rev Neurosci *11*, 329-352. 10.1146/annurev.ne.11.030188.001553.
196. Barnes, C.A., and McNaughton, B.L. (1985). An age comparison of the rates of acquisition and forgetting of spatial information in relation to long-term enhancement of hippocampal synapses. Behav Neurosci *99*, 1040-1048. 10.1037//0735-7044.99.6.1040.
197. Migaud, M., Charlesworth, P., Dempster, M., Webster, L.C., Watabe, A.M., Makhinson, M., He, Y., Ramsay, M.F., Morris, R.G., Morrison, J.H., et al. (1998). Enhanced long-term potentiation and impaired learning in mice with mutant postsynaptic density-95 protein. Nature *396*, 433-439. 10.1038/24790.
198. Rogan, M.T., Staubli, U.V., and LeDoux, J.E. (1997). AMPA receptor facilitation accelerates fear learning without altering the level of conditioned fear acquired. J Neurosci *17*, 5928-5935. 10.1523/JNEUROSCI.17-15-05928.1997.
199. McKernan, M.G., and Shinnick-Gallagher, P. (1997). Fear conditioning induces a lasting potentiation of synaptic currents in vitro. Nature *390*, 607-611. 10.1038/37605.
200. Whitlock, J.R., Heynen, A.J., Shuler, M.G., and Bear, M.F. (2006). Learning induces long-term potentiation in the hippocampus. Science *313*, 1093-1097. 10.1126/science.1128134.
201. Pavlowsky, A., Wallace, E., Fenton, A.A., and Alarcon, J.M. (2017). Persistent modifications of hippocampal synaptic function during remote spatial memory. Neurobiol Learn Mem *138*, 182-197. 10.1016/j.nlm.2016.08.015.
202. Habib, D., Tsui, C.K., Rosen, L.G., and Dringenberg, H.C. (2014). Occlusion of low-frequency-induced, heterosynaptic long-term potentiation in the rat hippocampus in vivo following spatial training. Cereb Cortex *24*, 3090-3096. 10.1093/cercor/bht174.
203. Gruart, A., Munoz, M.D., and Delgado-Garcia, J.M. (2006). Involvement of the CA3-CA1 synapse in the acquisition of associative learning in behaving mice. J Neurosci *26*, 1077-1087. 10.1523/JNEUROSCI.2834-05.2006.
204. Butcher, S.P., Hamberger, A., and Morris, R.G. (1991). Intracerebral distribution of DL-2-amino-phosphonopentanoic acid (AP5) and the dissociation of different types of learning. Experimental brain research *83*, 521-526. 10.1007/BF00229829.
205. Morris, R.G., Anderson, E., Lynch, G.S., and Baudry, M. (1986). Selective impairment of learning and blockade of long-term potentiation by an N-methyl-D-aspartate receptor antagonist, AP5. Nature *319*, 774-776. 10.1038/319774a0.

206. Staubli, U., Thibault, O., DiLorenzo, M., and Lynch, G. (1989). Antagonism of NMDA receptors impairs acquisition but not retention of olfactory memory. Behav Neurosci *103*, 54-60. 10.1037//0735-7044.103.1.54.
207. Morris, R.G. (1989). Synaptic plasticity and learning: selective impairment of learning rats and blockade of long-term potentiation in vivo by the N-methyl-D-aspartate receptor antagonist AP5. J Neurosci *9*, 3040-3057. 10.1523/JNEUROSCI.09-09-03040.1989.
208. Stevens, C.F., Tonegawa, S., and Wang, Y. (1994). The role of calcium-calmodulin kinase II in three forms of synaptic plasticity. Curr Biol *4*, 687-693. 10.1016/s0960-9822(00)00153-6.
209. Hinds, H.L., Tonegawa, S., and Malinow, R. (1998). CA1 long-term potentiation is diminished but present in hippocampal slices from alpha-CaMKII mutant mice. Learn Mem *5*, 344-354.
210. Tsien, J.Z., Huerta, P.T., and Tonegawa, S. (1996). The essential role of hippocampal CA1 NMDA receptor-dependent synaptic plasticity in spatial memory. Cell *87*, 1327-1338. 10.1016/s0092-8674(00)81827-9.
211. McNaughton, B.L., Barnes, C.A., Rao, G., Baldwin, J., and Rasmussen, M. (1986). Long-term enhancement of hippocampal synaptic transmission and the acquisition of spatial information. J Neurosci *6*, 563-571. 10.1523/JNEUROSCI.06-02-00563.1986.
212. Castro, C.A., Silbert, L.H., McNaughton, B.L., and Barnes, C.A. (1989). Recovery of spatial learning deficits after decay of electrically induced synaptic enhancement in the hippocampus. Nature *342*, 545-548. 10.1038/342545a0.
213. Nabavi, S., Fox, R., Proulx, C.D., Lin, J.Y., Tsien, R.Y., and Malinow, R. (2014). Engineering a memory with LTD and LTP. Nature *511*, 348-352. 10.1038/nature13294.
214. Kim, W.B., and Cho, J.H. (2017). Encoding of Discriminative Fear Memory by Input-Specific LTP in the Amygdala. Neuron *95*, 1129-1146 e1125. 10.1016/j.neuron.2017.08.004.
215. Abdou, K., Shehata, M., Choko, K., Nishizono, H., Matsuo, M., Muramatsu, S.I., and Inokuchi, K. (2018). Synapse-specific representation of the identity of overlapping memory engrams. Science *360*, 1227-1231. 10.1126/science.aat3810.
216. Vetere, G., Tran, L.M., Moberg, S., Steadman, P.E., Restivo, L., Morrison, F.G., Ressler, K.J., Josselyn, S.A., and Frankland, P.W. (2019). Memory formation in the absence of experience. Nat Neurosci *22*, 933-940. 10.1038/s41593-019-0389-0.
217. Chang, J.Y., Parra-Bueno, P., Laviv, T., Szatmari, E.M., Lee, S.R., and Yasuda, R. (2017). CaMKII Autophosphorylation Is Necessary for Optimal Integration of Ca(2+) Signals during LTP Induction, but Not Maintenance. Neuron *94*, 800-808 e804. 10.1016/j.neuron.2017.04.041.
218. Jain, A., Nakahata, Y., Watabe, T., Rusina, P., South, K., Adachi, K., Yan, L., Simorowski, N., Furukawa, H., and Yasuda, R. (2023). Dendritic, delayed, and stochastic CaMKII activation underlies behavioral time scale plasticity in CA1 synapses. bioRxiv. 10.1101/2023.08.01.549180.
219. Hong, S.Z., Mesik, L., Grossman, C.D., Cohen, J.Y., Lee, B., Severin, D., Lee, H.K., Hell, J.W., and Kirkwood, A. (2022). Norepinephrine potentiates and serotonin depresses visual cortical responses by transforming eligibility traces. Nat Commun *13*, 3202. 10.1038/s41467-022-30827-1.

220. Gerstner, W., Lehmann, M., Liakoni, V., Corneil, D., and Brea, J. (2018). Eligibility Traces and Plasticity on Behavioral Time Scales: Experimental Support of NeoHebbian Three-Factor Learning Rules. Front Neural Circuits *12*, 53. 10.3389/fncir.2018.00053.
221. He, K., Huertas, M., Hong, S.Z., Tie, X., Hell, J.W., Shouval, H., and Kirkwood, A. (2015). Distinct Eligibility Traces for LTP and LTD in Cortical Synapses. Neuron *88*, 528-538. 10.1016/j.neuron.2015.09.037.
222. Bittner, K.C., Milstein, A.D., Grienberger, C., Romani, S., and Magee, J.C. (2017). Behavioral time scale synaptic plasticity underlies CA1 place fields. Science *357*, 1033-1036. 10.1126/science.aan3846.
223. Magee, J.C., and Grienberger, C. (2020). Synaptic Plasticity Forms and Functions. Annu Rev Neurosci *43*, 95-117. 10.1146/annurev-neuro-090919-022842.
224. Milstein, A.D., Li, Y., Bittner, K.C., Grienberger, C., Soltesz, I., Magee, J.C., and Romani, S. (2021). Bidirectional synaptic plasticity rapidly modifies hippocampal representations. eLife *10*. 10.7554/eLife.73046.
225. Grienberger, C., and Magee, J.C. (2022). Entorhinal cortex directs learning-related changes in CA1 representations. Nature *611*, 554-562. 10.1038/s41586-022-05378-6.
226. Abbott, L.F., and Regehr, W.G. (2004). Synaptic computation. Nature *431*, 796-803. 10.1038/nature03010.
227. Trinh, A.T., Girardi-Schappo, M., Beique, J.C., Longtin, A., and Maler, L. (2023). Adaptive spike threshold dynamics associated with sparse spiking of hilar mossy cells are captured by a simple model. J Physiol *601*, 4397-4422. 10.1113/JP283728.
228. Hashimotodani, Y., Nasrallah, K., Jensen, K.R., Chavez, A.E., Carrera, D., and Castillo, P.E. (2017). LTP at Hilar Mossy Cell-Dentate Granule Cell Synapses Modulates Dentate Gyrus Output by Increasing Excitation/Inhibition Balance. Neuron *95*, 928-943 e923. 10.1016/j.neuron.2017.07.028.
229. Maroto, I.B., Costas-Insua, C., Berthoux, C., Moreno, E., Ruiz-Calvo, A., Montero-Fernandez, C., Macias-Camero, A., Martin, R., Garcia-Font, N., Sanchez-Prieto, J., et al. (2023). Control of a hippocampal recurrent excitatory circuit by cannabinoid receptor-interacting protein Gap43. Nat Commun *14*, 2303. 10.1038/s41467-023-38026-2.
230. Lutzu, S., Alvina, K., Puente, N., Grandes, P., and Castillo, P.E. (2023). Target cell-specific plasticity rules of NMDA receptor-mediated synaptic transmission in the hippocampus. Front Cell Neurosci *17*, 1068472. 10.3389/fncel.2023.1068472.
231. Cruikshank, S.J., Urabe, H., Nurmikko, A.V., and Connors, B.W. (2010). Pathway-specific feedforward circuits between thalamus and neocortex revealed by selective optical stimulation of axons. Neuron *65*, 230-245. 10.1016/j.neuron.2009.12.025.
232. Crandall, S.R., Cruikshank, S.J., and Connors, B.W. (2015). A corticothalamic switch: controlling the thalamus with dynamic synapses. Neuron *86*, 768-782. 10.1016/j.neuron.2015.03.040.
233. Naud, R., and Sprekeler, H. (2018). Sparse bursts optimize information transmission in a multiplexed neural code. Proc Natl Acad Sci U S A *115*, E6329-E6338. 10.1073/pnas.1720995115.
234. Kauer, J.A., and Malenka, R.C. (2007). Synaptic plasticity and addiction. Nat Rev Neurosci *8*, 844-858.
235. Volk, L., Chiu, S.L., Sharma, K., and Huganir, R.L. (2015). Glutamate synapses in human cognitive disorders. Annu Rev Neurosci *38*, 127-149. 10.1146/annurev-neuro-071714-033821.

236. Hyman, S.E., Malenka, R.C., and Nestler, E.J. (2006). Neural mechanisms of addiction: the role of reward-related learning and memory. Annu Rev Neurosci *29*, 565-598.
237. Murphy, T.H., and Corbett, D. (2009). Plasticity during stroke recovery: from synapse to behaviour. Nat Rev Neurosci *10*, 861-872.
238. Grueter, B.A., Rothwell, P.E., and Malenka, R.C. (2012). Integrating synaptic plasticity and striatal circuit function in addiction. Curr Opin Neurobiol *22*, 545-551. 10.1016/j.conb.2011.09.009.
239. Frank, R.A., and Grant, S.G. (2017). Supramolecular organization of NMDA receptors and the postsynaptic density. Curr Opin Neurobiol *45*, 139-147. 10.1016/j.conb.2017.05.019.
240. Lynch, G., Cox, C.D., and Gall, C.M. (2014). Pharmacological enhancement of memory or cognition in normal subjects. Front Syst Neurosci *8*, 90. 10.3389/fnsys.2014.00090.
241. Ingvar, M., Ambros-Ingerson, J., Davis, M., Granger, R., Kessler, M., Rogers, G.A., Schehr, R.S., and Lynch, G. (1997). Enhancement by an ampakine of memory encoding in humans. Exp Neurol *146*, 553-559. 10.1006/exnr.1997.6581.
242. Lynch, G. (1998). Memory and the brain: unexpected chemistries and a new pharmacology. Neurobiol Learn Mem *70*, 82-100. 10.1006/nlme.1998.3840.
243. Grieco, S.F., Castren, E., Knudsen, G.M., Kwan, A.C., Olson, D.E., Zuo, Y., Holmes, T.C., and Xu, X. (2022). Psychedelics and Neural Plasticity: Therapeutic Implications. J Neurosci *42*, 8439-8449. 10.1523/JNEUROSCI.1121-22.2022.
244. Dong, C., Ly, C., Dunlap, L.E., Vargas, M.V., Sun, J., Hwang, I.W., Azinfar, A., Oh, W.C., Wetsel, W.C., Olson, D.E., and Tian, L. (2021). Psychedelic-inspired drug discovery using an engineered biosensor. Cell *184*, 2779-2792 e2718. 10.1016/j.cell.2021.03.043.
245. Olson, D.E. (2018). Psychoplastogens: A Promising Class of Plasticity-Promoting Neurotherapeutics. J Exp Neurosci *12*, 1179069518800508. 10.1177/1179069518800508.
246. Rumbaugh, G., Adams, J.P., Kim, J.H., and Huganir, R.L. (2006). SynGAP regulates synaptic strength and mitogen-activated protein kinases in cultured neurons. Proc Natl Acad Sci U S A *103*, 4344-4351. 10.1073/pnas.0600084103.
247. Kim, J.H., Liao, D., Lau, L.F., and Huganir, R.L. (1998). SynGAP: a synaptic RasGAP that associates with the PSD-95/SAP90 protein family. Neuron *20*, 683-691. 10.1016/s0896-6273(00)81008-9.
248. Araki, Y., Gerber, E.E., Rajkovich, K.E., Hong, I., Johnson, R.C., Lee, H.K., Kirkwood, A., and Huganir, R.L. (2023). Mouse models of SYNGAP1 -related intellectual disability. bioRxiv. 10.1101/2023.05.25.542312.
249. Araki, Y., Zeng, M., Zhang, M., and Huganir, R.L. (2015). Rapid dispersion of SynGAP from synaptic spines triggers AMPA receptor insertion and spine enlargement during LTP. Neuron *85*, 173-189. 10.1016/j.neuron.2014.12.023.
250. Richards, B.A., Lillicrap, T.P., Beaudoin, P., Bengio, Y., Bogacz, R., Christensen, A., Clopath, C., Costa, R.P., de Berker, A., Ganguli, S., et al. (2019). A deep learning framework for neuroscience. Nat Neurosci *22*, 1761-1770. 10.1038/s41593-019-0520-2.
251. Lillicrap, T.P., Santoro, A., Marris, L., Akerman, C.J., and Hinton, G. (2020). Backpropagation and the brain. Nat Rev Neurosci *21*, 335-346. 10.1038/s41583-020-0277-3.

252. Francioni, V., Tang, V.D., Brown, N.J., Toloza, E.H.S., and Harnett, M. (2023). Vectorized instructive signals in cortical dendrites during a brain-computer interface task. bioRxiv. 10.1101/2023.11.03.565534.
253. Payeur, A., Guerguiev, J., Zenke, F., Richards, B.A., and Naud, R. (2021). Burst-dependent synaptic plasticity can coordinate learning in hierarchical circuits. Nat Neurosci *24*, 1010-1019. 10.1038/s41593-021-00857-x.
254. Guerguiev, J., Lillicrap, T.P., and Richards, B.A. (2017). Towards deep learning with segregated dendrites. eLife *6*. 10.7554/eLife.22901.

MANUSCRIPT II

Low throughput screening in Neuroscience: studying central synapses one at a time.

Léa Caya-Bissonnette, Jean-Claude Béïque*
***Corresponding authors.**

This opinion manuscript was published in Neurophotonics in October 2023:
Caya-Bissonnette L, Béïque JC. Low throughput screening in neuroscience: using light to study central synapses one at a time. Neurophotonics. 2023 Oct;10(4):044407. doi: 10.1117/1.NPh.10.4.044407. Epub 2023 Oct 24. PMID: 37881180; PMCID: PMC10594030.

Authors contributions: L.C.B. wrote the first draft and assembled figures. J.C.B. edited the text.

Keywords: 2P uncaging; synapse; plasticity; AMPAR; NMDAR; dendrites

Abstract

The field of neurophotonics has witnessed substantial progress in recent years, particularly in the development of 2P uncaging techniques that allow for precise manipulation and observation of neural processes. Here, we explore how 2P uncaging emerges at the intersection of chemistry, optics, and electrophysiology to enable the precise use of caged molecules and photoactivation for studying functional aspects of synaptic transmission and dendritic integration. We discuss the limitations of traditional microscopy techniques and the advantages offered by multiphoton microscopy, by emphasizing on MNI-Glutamate, a caged compound that enables controlled uncaging of glutamate onto synaptic spines, and activation of endogenous glutamate receptors. Amongst other advancement, this approach has contributed to understanding subcellular regulation of receptor subtypes, the presence of silent synapses, AMPA receptor desensitization, spine calcium behavior, and synaptic plasticity.

Main

Scientists need to be many things, including pedagogues. In doing so, they often rely on intuitive and historically prominent imagery to capture the imagination of their audience (and their own) and to convey a sense of meaning and importance. For instance, in this exercise, many cellular neuroscientists will readily show the drawings of Ramon y Cajal's neuron (Cajal, 1909) that instill a profound sense of wonder and puzzlement, still more than 100 years later. Other cellular neuroscientists, those with perhaps a more abstract mind, will rather intuitively converge to the iconic voltage traces of the action potential from Hodgkin and Huxley as the expression of the elemental essence of the brain in action., Others may think of the banal looking blips analyzed by Sir Bernard Katz in the 1950's that established the foundation of how we still conceptualize information transfer at synapses. Yet, for decades the experimental approaches of cellular electrophysiology and imaging were largely progressing in parallel, with little direct cross-pollination. The development of multiphoton microscopy, along with key progress in synthetic chemistry, has coalesced these disciplines wherein experimenters can both *observe* and *manipulate* neural processes. By allowing the activation of individual brain synapses with exquisite spatial and temporal control, two-photon (2P) uncaging of caged molecules provides a compelling illustration of substantial progress in our understanding of neural function afforded by the still expanding field of Neurophotonics.

Where chemistry, optics and electrophysiology collide

At their core, individual neurons are analog-to-digital converters. They harbor at times tens of thousands of individual synapses and continuously integrate the tiny electrical synaptic events by means of a complex mixture of linear and non-linear operations to render a digital decision: a spike. Yet, any student of the brain knows that synaptic transmission is partly a chemical process, offering corollary practical experimental opportunities. Indeed, it is fairly straightforward to synthesize neurotransmitters and several methods have been developed over the years to provide means for their local and rapid application to study synaptic mimicry. However, these methods (*e.g.,* iontophoresis) inherently present spatial and/or temporal limitations. The development of photolabile 'caged' molecules, combined with the relative ease of controlling light in space and time, offers a powerful approach to (at least partly) address these limitations. A biologically active molecule is said to be caged when it is made inert by the covalent bond of a photochemical group

(Ellis-Davies, 2000). In the late 1970's Kaplan et al., (1978) synthesized the first 'caged' compound, caged ATP. Photolysis of the caged ATP compound (or 'release' of the active molecule) was induced with near-UV light and was instrumental in elucidating important functional aspects of the Na^+/K^+ ATPase pump. In the next decade, the first caged neurotransmitters, including for glutamate, the primary excitatory neurotransmitter in the brain, were developed by the Hess group (Wilcox et al., 1990; Wieboldt et al., 1994a, 1994b, Niu et al., 1996). While the use of these photoactivated caged compounds were useful for molecular biology studies, several of their features made them sub-optimal for direct neuroscience applications.

A common limitation of one photon (1P) microscopy lies in the scattering of light in tissue such as the brain (and resulting degradation of the associated diffraction limited spot). For neurotransmitter uncaging purposes, this limitation is further compounded by the fact that the uncaging event *per se* is not restricted to the focal plane, but rather occurs along the entire length of the excitation light path in the sample. While multiphoton microscopy not only improves the spot quality for imaging in tissue, it also enables the uncaging event to be limited to a volume roughly that of a diffraction-limited spot and therefore, approximating the point-source diffusion of endogenous vesicle release at synapses *in situ*. Yet, the full realization of this approach could only be realized with the development of caged-molecules exhibiting a favorable 2P cross-section, along with a broad set of parallel advantageous functional and practical features (stability, quantum yield, receptor affinity, and others). For synaptic physiology purposes, an important milestone was achieved with the development of MNI-Glutamate (Ellis-Davies, 1998; Ellis-Davies, 1999; Papageorgiou & Corrie, 2000) that allowed the uncaging of glutamate onto visually-identified synaptic spines to trigger excitatory postsynaptic currents and potentials (Figure 1A; Matsuzaki et al., 2001; Béïque et al., 2006; Béïque et al., 2011; Soares et al., 2013).

Synaptic function and dendritic integration

The hardware required to implement 2P imaging dovetails well with that of traditional cellular electrophysiology. While the uncaging approach has been used for several neurotransmitters, we briefly here mention some of the advances that were derived from the use of MNI-Glutamate. In a typical experiment (Figure 1), neurons are recorded in the whole-cell configuration thereby allowing the dialysis of the intracellular compartment with fluorescent dyes in order to either delineate subcellular compartments (*e.g.*, spines) or to monitor some dynamical

process (*e.g.*, intracellular calcium transients). A brief (0.5 ms - 1 ms) illumination with a Ti:saphire laser (tuned at ~720 nm) achieves an effective focal release of glutamate with a roughly < 2 µm (x, y) spot size (Béïque et al., 2006; Soares et al., 2013; Figure 1B,C). The experimenter calibrates the laser power such that the amplitude of synaptic currents closely matches that of those triggered by endogenously released glutamate (*ca*., 5 pA -20 pA). In these conditions, the effective volume of uncaging (which is a convolution of the size of the diffraction limited spot and diffusion) is greater than that resulting from the vesicular release of glutamate (Soares et al., 2019); and unpublished observation), and needs to be carefully considered. Nonetheless, this process readily activates endogenous glutamate receptors of the α-amino-3-hydroxy-5-methyl-4-isoxazolepropionic acid (AMPA) and N-methyl-D-aspartate (NMDA) subtypes, exhibiting a kinetic profile that reasonably well approaches that of when these receptors are activated by release of endogenous glutamate (Figure 1D).

By allowing unparalleled spatial and temporal control of glutamate receptor activation, this broad approach has been conducive to substantial progress. The sole ability to activate AMPA receptors (AMPARs) in a controlled and deterministic fashion provides a useful means to parameterize several of their biophysical features *in situ*. For instance, this overall approach contributed to the demonstration that the desensitization of AMPARs (occurring for instance during burst transmission) is at least partly offset by the lateral diffusion of these receptors along the surface of dendritic/synaptic membrane (Heine et al., 2008). The ability to activate glutamate receptors on different subcellular compartments of neurons (*e.g.*, spine *vs* dendritic compartment) was also used to demonstrate that the homeostatic synaptic plasticity process differentially regulates the subcellular expression of AMPAR and NMDA receptors (NMDARs). As a last example, it is known that a subset of synapses are devoid of NMDARs, and are therefore called 'silent' synapses. While their existence has been demonstrated using traditional electrical stimulation in slices (Isaac et al., 1995; Liao et al., 1995; Vincent-Lamarre et al., 2018), 2P uncaging experiments established that silent synapses were found on thin filopodia protrusions (Béïque et al., 2006; Vardalaki et al., 2022). Analogous experimental approaches were used to map the distribution of silent synapses onto developing dendritic arbor, revealing a striking clustered distribution that is believed to be a manifestation of cooperative plasticity rules (Figure 1E; Lee et al., 2016).

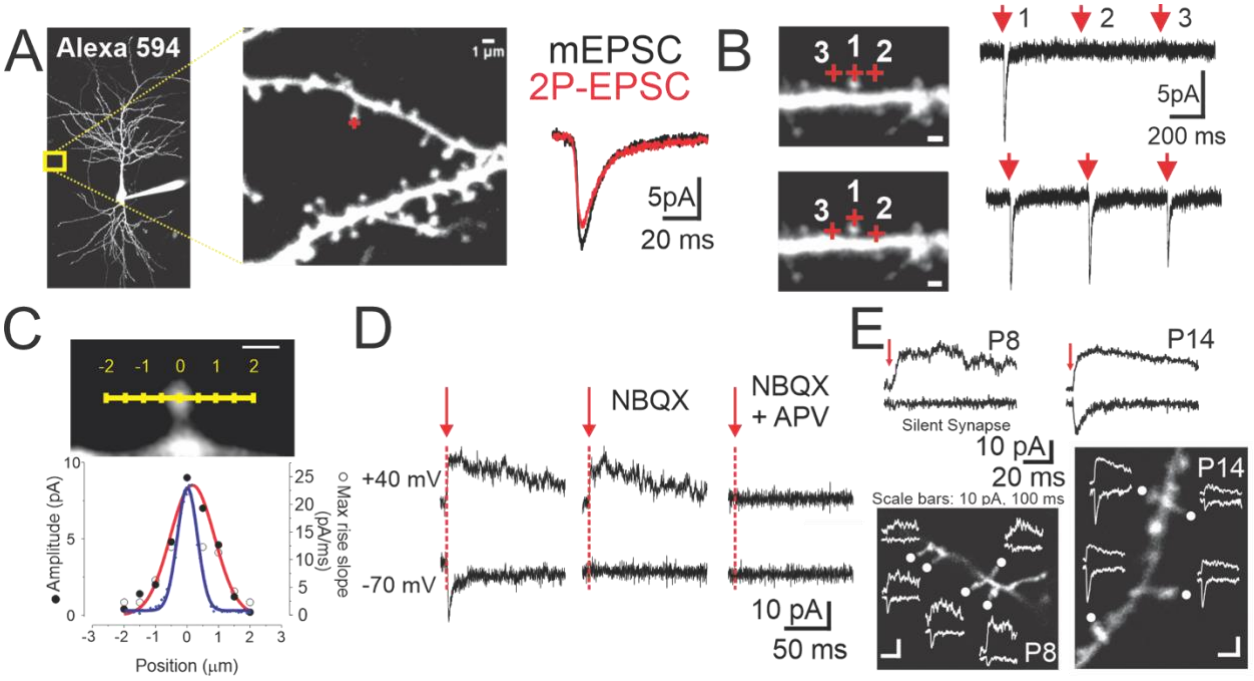

Figure 1. 2P MNI-Glutamate Uncaging. **A.** 2P EPSCs were induced by brief laser illuminations onto a single spine (denoted with the red cross hair) from a CA1 neurons in a hippocampal slice. The neuron was filled with Alexa 594 to outline neuronal morphology (spines, dendrites; note the recording electrode extending from the soma). The light-evoked EPSCs exbibit similar temporal dynamics (rise and decay) to those of EPSCs induced by endogenously released glutamate (miniature EPSCs; mEPSC). **B.** Glutamate uncaging induced on a spine or from varying distances from a dendritic surface (top vs bottom panel) provides an estimate of the effective resolution of the uncaging process. **C.** A similar experiment was carried out, but from uncaging along the orthogonal axis of a dendritic spine. The amplitude (red trace) and max rise slope of the evoked 2P EPSC is shown on the bottom panel, overlayed on the fluorescence profile of the spine (blue trace) **D.** 2P uncaging of MNI-Glu induced the activation of Glutamate receptors of both the AMPA and NMDA subtypes, blocked by NBQX and APV respectively. **E.** Glutamate uncaging detects developmentally regulated silent synapses, that is synapses that harbor NMDA, but no AMPARs. This method is amenable to determine the spatial distribution of synapses of different weights along dendritic arbors. A, C adapted from Soares et al., 2013; B and E adapted from Lee et al., 2016.

2P uncaging allows to test the impact of different spatial and temporal patterns of synaptic input by systematically positioning several uncaging spots along various length of dendritic segments. One area of research that has substantially benefited from such ability is dendritic integration. While a review of these contributions is beyond the scope of this paper, it is noteworthy that uncaging approaches have been central in providing key experimental confirmation of several non-linear dendritic operations that had been proposed by earlier computational approaches. As a mere example, influential work from the early 1990's had proposed that clustered, as opposed to distributed, synaptic inputs would be subjected to non-linear amplification and thereby have a privileged influence on action potential output (Mel, 1993). The experimental confirmation that this class of dendritic operation occurred in neurons, along with mechanistic insights, was made possible by 2P uncaging approaches (Figure 2A; Losonczy and Magee 2006; Harnett et al., 2012; Lee et al., 2016; Tazerart et al., 2020; Dembrow & Spain, 2022). The combination of these experimental advances with modern computational approaches is beginning to uncover the catalog and full algorithmic role of these dendritic operations in controlling neural and network dynamics.

The study of spine behavior was further explored by 2P uncaging, but paired with 2P calcium imaging (Figure 2B). Amongst other advances, these studies have shown the existence of calcium compartmentalization in spines (Noguchi et al., 2005), how this behavior of calcium signals is regulated across postnatal development (Lee et al., 2016) and during synaptic plasticity (*e.g.*, Behavioural Timescale Synaptic Plasticity; Caya-Bissonnette et al., 2023).

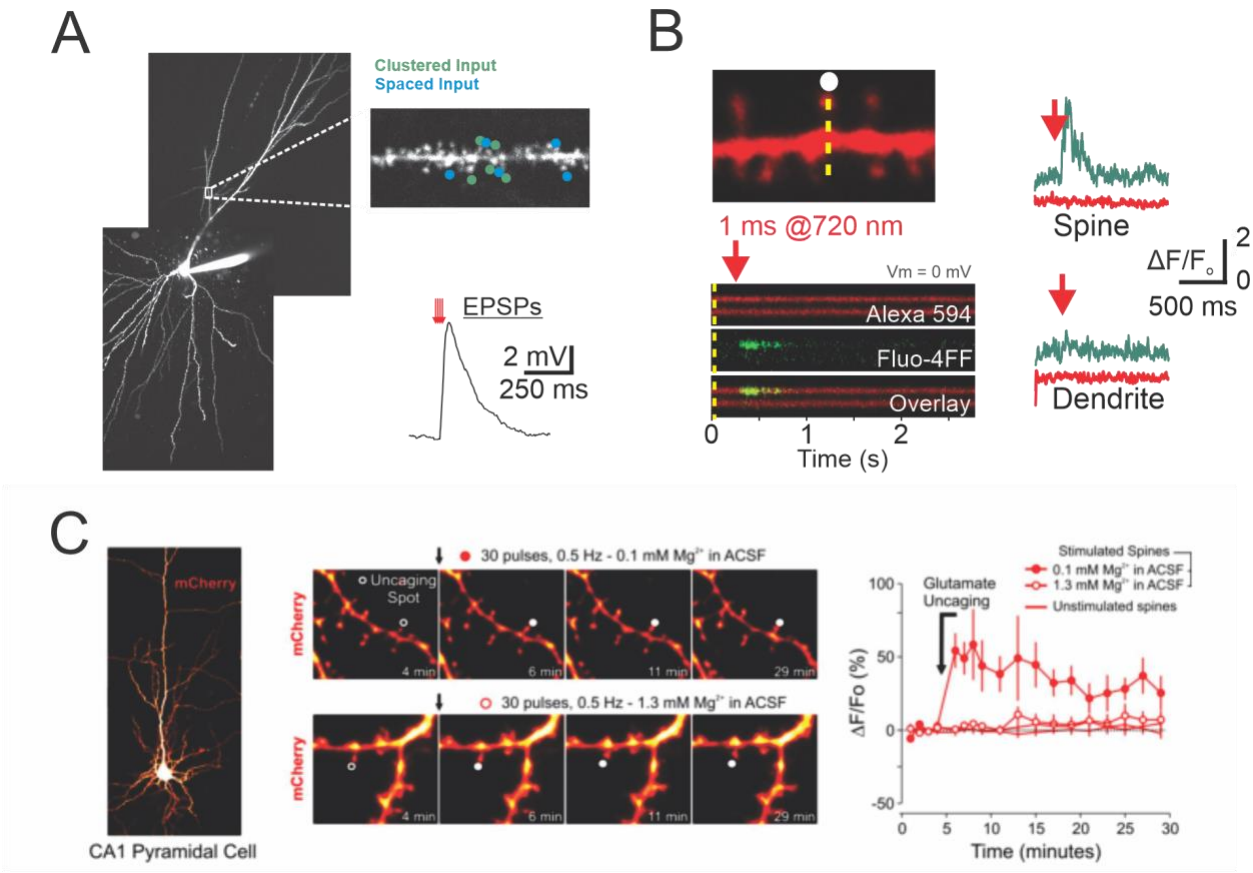

Figure 2. A. 2P MNI-Glu uncaging can be done quasi-simultaneously on closely localised (*i.e.*, clustered) spines using traditional galvo-based beam steering. **B.** Continuous line scan acquisition over a region spanning both spine and dendrite (measured using a low affinity Ca^{2+} fluorescent dye, Fluo-4FF) shows Ca^{2+} dynamics in response to single spine uncaging. The Ca^{2+} signals reflect Ca^{2+} entry mainly through activation of NMDARs (not shown). **C.** All-optical structural plasticity. A neuron expressing the fluorescent protein mCherry was targeted for single synapses uncaging. Repetitive uncaging onto a single spine in conditions favoring the opening of NMDARs (0.1 mM Mg^{2+}; top middle panel) lead to a persistent spine enlargement (far right panel). Note that this structural plasticity in these conditions is spine-specific since closely localised spines do not exhibit shape alterations. C. adapted from Soares et al., 2017.

Synaptic plasticity

Since Bliss and Lømo's breakthrough experiments (Bliss & Lømo, 1973), the ability of synapses to undergo stable and long-term alterations constitutes the mainstay of current models of learning and memory. Traditionally, synaptic strength in slice experiments is monitored by electrically stimulating an unknown number of axons with largely undefined spatial location. Not surprisingly, 2P uncaging approaches have been used to study plasticity induction on identified spines (Figure 2C), and directly demonstrated the existence of structural plasticity (Matsuzaki et al., 2004), where the volume of dendritic spines increased following plasticity induction along with other structural features (*e.g.*, Araya et al., 2014). The ability to activate individual synapses has further been used to study molecular aspects of plasticity, for instance by investigating the effects of molecular manipulations on the expression of structural plasticity or surface expression of AMPARs (determined by the detection of Phluorin-tagged AMPAR subunits (*e.g.*, George et al., 2015). While in principle 2P uncaging approaches can be used to directly monitor the function of endogenous AMPARs following plasticity induction, these experiments are nonetheless highly challenging. Indeed, given the small volume of the uncaging spot, minute spatial drift over prolonged experiments (typically >30 minutes) in principle may lead to high variability in the effective amount of glutamate reaching the spine under study, thereby introducing artifactual changes in EPSC amplitudes. To address this issue, Soares et al., 2017, made use of the iGluSNFR, a genetically encoded fluorescent indicator of glutamate release (Figure 3), to longitudinally monitor the amount of glutamate reaching the spine simultaneously with the magnitude of the EPSC induced by the photolysis event. This combined approach controlled for spatial drift and showed that endogenous AMPARs were rapidly trafficked to spines (Soares et al., 2017).

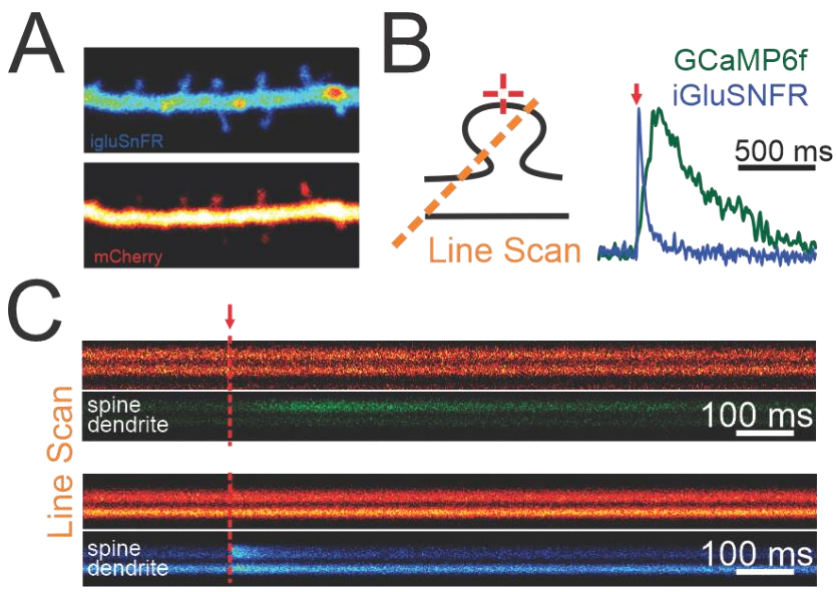

Figure 3. 2P MNI-Glu uncaging used in combination with imaging of genetically encoded sensors **A.** Dendritic and spine expression of the glutamate sensor iGluSNFR expressed in a CA1 pyramidal neuron. **B.** Local photolysis of glutamate by 2P uncaging triggered a rapid fluorescence signal from the glutamate sensor iGluSNFR. Parallel experiments showed a far slower response when NMDAR-dependent Ca^{2+} influx induced by MNI-Glu uncaging was monitored using the GCaMP6f sensor. **C.** The same experiments as in B are plotted showing fluorescence of GCaMP6f (green) and iGluSNFR (blue) over time. The red vertical lines indicate the time of uncaging. Adapted from Soares et al., 2019.

Conclusion

While one can be at once a disciple of both Cajal and of the famed baseball legend Yogi Berra who pointed out that '*Sometimes you can tell a lot about something just by watching*', simply looking is not always enough. How can we know how neurons, with their complex arborization and their odd-looking protuberances such as the mysterious and initially controversial *espinas*, really work? The advent of 2P uncaging approaches allows to manipulate the activity of visually identified single synapses with unmatched ease and precision. Of course, it is not perfect, and brings its share of inevitable compromises. For instance, one would want more, and smaller, uncaging spots, along with far greater and flexible spatial and temporal control of broad arrays of activation arrays, including for *in vivo* application (Noguchi et al., 2019). Yet, considering the progress made in Neurophotonics in recent decades, we only need a bit of patience, as the future is bright.

Conflicts of Interest: All authors declare that they have no conflicts of interest.

References:

Araya, R., Vogels, T. P., & Yuste, R. (2014). Activity-dependent dendritic spine neck changes are correlated with synaptic strength. *Proceedings of the National Academy of Sciences, 111*(28), E2895-E2904. https://doi.org/10.1073/pnas.1321869111

Béïque, J.-C., Lin, D.-T., Kang, M.-G., Aizawa, H., Takamiya, K., & Huganir, R. L. (2006). Synapse-specific regulation of AMPA receptor function by PSD-95. *Proceedings of the National Academy of Sciences*, *103*(51), 19535-19540. https://doi.org/10.1073/pnas.0608492103

Béïque, J.-C., Na, Y., Kuhl, D., Worley, P. F., & Huganir, R. L. (2011). Arc-dependent synapse-specific homeostatic plasticity. *Proceedings of the National Academy of Sciences*, *108*(2), 816-821. https://doi.org/10.1073/pnas.1017914108

Bliss, T. V. P., & Lømo, T. (1973). Long-lasting potentiation of synaptic transmission in the dentate area of the anaesthetized rabbit following stimulation of the perforant path. *The Journal of Physiology*, *232*(2), 331-356.

Ramón, & Cajal (1909). Histology of the Nervous System of Man and Vertebrates [Histology of the Nervous System of Man and Vertebrates]. Paris A. Maloine. - References - Scientific Research Publishing, s. d.

Caya-Bissonnette L, Naud R, Béïque JC, Cellular Substrate of Eligibility Traces during Behavioral Timescale Synaptic Plasticity. BioarXive. 2023.

Dembrow, N. C., & Spain, W. J. (2022). Input rate encoding and gain control in dendrites of neocortical pyramidal neurons. *Cell Reports*, *38*(7), 110382. https://doi.org/10.1016/j.celrep.2022.110382

Ellis-Davies, G. C. R. (1998). Synthesis of photosensitive EGTA derivatives. *Tetrahedron Letters*, *39*(9), 953-956. https://doi.org/10.1016/S0040-4039(97)10668-2

Ellis-Davies G. C. R. (1999). Localized photolysis of caged compounds. J. Gen. Physiol. 114:1a.

Ellis-Davies G. C. R. (2000). Basics of photoactivation in Imaging Living Cells: A Laboratory Manual, eds Yuste R., Konnerth A. (Cold Spring Harbor, NY: Cold Spring Harbor Press;), 300–320

George, J., Soares, C., Montersino, A., Beique, J.-C., & Thomas, G. M. (2015). Palmitoylation of LIM Kinase-1 ensures spine-specific actin polymerization and morphological plasticity. *eLife*, *4*, e06327. https://doi.org/10.7554/eLife.06327

Harnett, M. T., Makara, J. K., Spruston, N., Kath, W. L., & Magee, J. C. (2012). Synaptic amplification by dendritic spines enhances input cooperativity. *Nature*, *491*(7425), 599-602. https://doi.org/10.1038/nature11554

Heine, M., Groc, L., Frischknecht, R., Béïque, J.-C., Lounis, B., Rumbaugh, G., Huganir, R. L., Cognet, L., & Choquet, D. (2008). Surface mobility of postsynaptic AMPARs tunes synaptic transmission. *Science (New York, N.Y.)*, *320*(5873), 201-205. https://doi.org/10.1126/science.1152089

Isaac, J. T., Nicoll, R. A., & Malenka, R. C. (1995). Evidence for silent synapses : Implications for the expression of LTP. *Neuron*, *15*(2), 427-434. https://doi.org/10.1016/0896-6273(95)90046-2

Kaplan, J. H., Forbush, B., & Hoffman, J. F. (1978). Rapid photolytic release of adenosine 5'-triphosphate from a protected analogue : Utilization by the Na:K pump of human red blood cell ghosts. *Biochemistry*, *17*(10), 1929-1935. https://doi.org/10.1021/bi00603a020

Lee, K. F. H., Soares, C., Thivierge, J.-P., & Béïque, J.-C. (2016). Correlated Synaptic Inputs Drive Dendritic Calcium Amplification and Cooperative Plasticity during Clustered Synapse Development. *Neuron*, *89*(4), 784-799. https://doi.org/10.1016/j.neuron.2016.01.012

Liao, D., Hessler, N. A., & Malinow, R. (1995). Activation of postsynaptically silent synapses during pairing-induced LTP in CA1 region of hippocampal slice. *Nature*, *375*(6530), 400-404. https://doi.org/10.1038/375400a0

Matsuzaki, M., Ellis-Davies, G. C. R., Nemoto, T., Miyashita, Y., Iino, M., & Kasai, H. (2001). Dendritic spine geometry is critical for AMPA receptor expression in hippocampal CA1 pyramidal neurons. *Nature Neuroscience*, *4*(11), Article 11. https://doi.org/10.1038/nn736

Matsuzaki, M., Honkura, N., Ellis-Davies, G. C. R., & Kasai, H. (2004). Structural basis of long-term potentiation in single dendritic spines. *Nature*, *429*(6993), 761-766. https://doi.org/10.1038/nature02617

Mel, B. W. (1993). Synaptic integration in an excitable dendritic tree. *Journal of Neurophysiology*, *70*(3), 1086-1101. https://doi.org/10.1152/jn.1993.70.3.1086

Niu, L., Gee, K. R., Schaper, K., & Hess, G. P. (1996). Synthesis and Photochemical Properties of a Kainate Precursor and Activation of Kainate and AMPA Receptor Channels on a Microsecond Time Scale. *Biochemistry*, *35*(6), 2030-2036. https://doi.org/10.1021/bi9516485

Noguchi, J., Matsuzaki, M., Ellis-Davies, G. C. R., & Kasai, H. (2005). Spine-neck geometry determines NMDA receptor-dependent Ca2+ signaling in dendrites. *Neuron*, *46*(4), 609-622. https://doi.org/10.1016/j.neuron.2005.03.015

Noguchi, J., Nagaoka, A., Hayama, T., Ucar, H., Yagishita, S., Takahashi, N., & Kasai, H. (2019). Bidirectional in vivo structural dendritic spine plasticity revealed by two-photon glutamate uncaging in the mouse neocortex. *Scientific Reports*, *9*(1), Article 1. https://doi.org/10.1038/s41598-019-50445-0

Papageorgiou, G., & Corrie, J. E. T. (2000). Effects of Aromatic Substituents on the Photocleavage of 1-Acyl-7-nitroindolines. *Tetrahedron*, *56*(41), 8197-8205. https://doi.org/10.1016/S0040-4020(00)00745-6

Soares, C., Lee, K. F. H., & Béïque, J.-C. (2017). Metaplasticity at CA1 Synapses by Homeostatic Control of Presynaptic Release Dynamics. *Cell Reports*, *21*(5), 1293-1303. https://doi.org/10.1016/j.celrep.2017.10.025

Soares, C., Lee, K. F. H., Nassrallah, W., & Béïque, J.-C. (2013). Differential Subcellular Targeting of Glutamate Receptor Subtypes during Homeostatic Synaptic Plasticity. *The Journal of Neuroscience*, *33*(33), 13547-13559. https://doi.org/10.1523/JNEUROSCI.1873-13.2013

Soares, C., Trotter, D., Longtin, A., Béïque, J.-C., & Naud, R. (2019). Parsing Out the Variability of Transmission at Central Synapses Using Optical Quantal Analysis. *Frontiers in Synaptic Neuroscience*, *11*, 22. https://doi.org/10.3389/fnsyn.2019.00022

Tazerart, S., Mitchell, D. E., Miranda-Rottmann, S., & Araya, R. (2020). A spike-timing-dependent plasticity rule for dendritic spines. *Nature Communications*, *11*(1), Article 1. https://doi.org/10.1038/s41467-020-17861-7

Vardalaki, D., Chung, K., & Harnett, M. T. (2022). Filopodia are a structural substrate for silent synapses in adult neocortex. *Nature*, *612*(7939), Article 7939. https://doi.org/10.1038/s41586-022-05483-6

Vincent-Lamarre, P., Lynn, M., & Béïque, J.-C. (2018). The Eloquent Silent Synapse. *Trends in Neurosciences*, *41*(9), 557-559. https://doi.org/10.1016/j.tins.2018.07.002

a. Wieboldt, R., Gee, K. R., Niu, L., Ramesh, D., Carpenter, B. K., & Hess, G. P. (1994). Photolabile precursors of glutamate : Synthesis, photochemical properties, and activation of

glutamate receptors on a microsecond time scale. *Proceedings of the National Academy of Sciences*, *91*(19), 8752-8756. https://doi.org/10.1073/pnas.91.19.8752

b. Wieboldt, R., Ramesh, D., Carpenter, B. K., & Hess, G. P. (1994). Synthesis and Photochemistry of Photolabile Derivatives of .gamma.-Aminobutyric Acid for Chemical Kinetic Investigations of the .gamma.-Aminobutyric Acid Receptor in the Millisecond Time Region. *Biochemistry*, *33*(6), 1526-1533. https://doi.org/10.1021/bi00172a032

Wilcox, M., Viola, R. W., Johnson, K. W., Billington, A. P., Carpenter, B. K., McCray, J. A., Guzikowski, A. P., & Hess, G. P. (1990). Synthesis of photolabile precursors of amino acid neurotransmitters. *The Journal of Organic Chemistry*, *55*(5), 1585-1589. https://doi.org/10.1021/jo00292a038

MANUSCRIPT III

Heterosynaptic Plasticity in Cortical Interneurons

Léa Caya-Bissonnette[1]

[1] University of Ottawa Brain and Mind Research Institute's Centre for Neural Dynamics

Review of: Chistiakova M, Ilin V, Roshchin M, Bannon N, Malyshev A, Kisvárday Z, Volgushev M (2019) Distinct Heterosynaptic Plasticity in Fast Spiking and Non-Fast-Spiking Inhibitory Neurons in Rat Visual Cortex. J Neurosci 35:6865-6878.

This manuscript was published in the Journal of Neurosciences in 2020:
Caya-Bissonnette, L. (February 26 2020). Heterosynaptic Plasticity in Cortical Interneurons. Journal of Neurosciences. 40(9):1793-1794. DOI: https://doi.org/10.1523/JNEUROSCI.2567-19.2020

Main

Persistent alteration of synaptic strength in response to neuronal activity has long been considered a substrate of learning and memory (Hebb, 1949). Classical Hebbian plasticity results from near-coincidental pre- and postsynaptic action potentials (APs), with the precise order of spiking, either pre-post or post-pre, yielding an increase (long-term potentiation; LTP) and a decrease (long-term depression; LTD) of synaptic weights, respectively (Bliss and Lomo, 1973; Hebb, 1949; Levy and Steward, 1983; Malenka and Nicoll, 1993; Markram et al., 1997). When input-specific, this type of synaptic plasticity is referred to as homosynaptic plasticity. Hebbian forms of plasticity are central to cellular models of learning, but it presents a fundamental problem regarding the stability of neural networks. Specifically, unconstrained LTP expression may produce a pernicious positive-feedback loop and runaway excitation, whereas LTD can lead to extreme depression and synaptic demise.

Two forms of plasticity have been proposed to solve the network stability problem and counteract runaway dynamics that might otherwise arise with homosynaptic LTP and LTD: homeostatic plasticity (Lee et al., 2014) and some forms of heterosynaptic plasticity (Royer and Paré, 2003). Heterosynaptic plasticity occurs at synaptic connections not activated by the presynaptic neuron and therefore does not exhibit strict input-specificity (unlike Hebbian plasticity). In some cases, the polarity of heterosynaptic plasticity leads to synaptic weight normalization (Royer and Paré, 2003) and thus contributes to network stabilization. Heterosynaptic plasticity has been reported mainly in synaptic connections between excitatory neurons. In a recent paper published in *The Journal of Neuroscience*, Chistiakova et al. (2019) investigated the presence of heterosynaptic plasticity at synapses between excitatory and inhibitory neurons of the visual cortex of young male rats.

The authors used extracellular electrodes to stimulate two sets of excitatory inputs onto a single inhibitory neuron whose activity was monitored in whole-cell intracellular recordings. Classic homosynaptic plasticity was induced at one set of inputs by pairing each of 30 excitatory presynaptic spikes with 5 postsynaptic APs (paired input). The second set of excitatory inputs was not activated during postsynaptic APs (unpaired input), thereby allowing the authors to monitor the presence of heterosynaptic plasticity at these synapses. This protocol induced mixed plasticity (*i.e.*, LTP, LTD or no change) at both paired and unpaired inputs. Precisely, if the paired input yielded LTD in a given neuron, the unpaired input onto that same neuron could express LTP or

LTD. These results provided evidence of heterosynaptic plasticity. The authors then showed that activating the postsynaptic neuron with 30 bursts of 5 APs, in the absence of any presynaptic stimulation, was sufficient to induce heterosynaptic plasticity at excitatory inputs, again of mixed polarity. These results therefore hint towards a postsynaptic site of induction for this plasticity mechanism, leaving unanswered the site of expression.

Chistiakova et al. (2019) proceeded to examine whether cell type could account for the plasticity variability observed. They classified the recorded cells as fast-spiking (FS) or non-fast-spiking (non-FS) neurons, the two major classes of cortical inhibitory neurons (Kawaguchi and Kubota, 1997). Burst firing alone in FS neurons, without concurrent synaptic stimulation, induced mixed synaptic weight modifications: LTP (32%), LTD (34%) or no change (34%). These proportions are similar to those previously reported for excitatory synapses onto pyramidal neurons undergoing a similar protocol (Volgushev et al., 2016). Remarkably, excitatory synapses onto non-FS neurons responded differently in that they were preferentially potentiated (47%) in response to postsynaptic bursts alone, with only 15% of synapses expressing LTD and 38% expressing no change. Synapses onto non-FS neurons averaged 116±4.9% potentiation compared to 106±3.7% in FS neurons. Collectively, these results demonstrated important differences in the direction of heterosynaptic plasticity between interneuron subtypes.

The authors then examined mechanisms that might account for these differences. Specifically, they looked for predictors of the direction of plasticity, focusing on animal age, cortical layer, initial release probability, as well as baseline EPSP amplitude, latency, and slope. Of these, the initial release probability of synapses (determined by the ratio of a 50-ms interval paired-pulse) was found to be the strongest predictor of plasticity direction: synapses with initial low release probability (high paired-pulse ratio; PPR) were more likely to undergo LTP, whereas those with high release probability (low PPR) tended to undergo LTD. The relationship between initial PPR and the sign of plasticity suggests a weight-dependent heterosynaptic plasticity, which favors the hypothesis that heterosynaptic plasticity can act to normalize synaptic weights. This is because synapses with low release probability are relatively unlikely to respond to a single stimulus. These weak synapses tend to be reinforced by this form of LTP, whereas synapses with high release probability are more likely to be depressed. As a result, the total synaptic weight tends to be largely unchanged, thereby enacting a form of weight normalization. Importantly, synapses

onto non-FS neurons on average had lower release probability than those onto FS neurons, which may explain the enhanced propensity of synapses onto non-FS neurons to potentiate.

The results outlined above do not formally address the site of expression of this form of plasticity. To this end, Chistiakova et al. (2019) further dissected the relationship between the release probability of the synapse and the direction of heterosynaptic plasticity. The authors found that, even during strictly postsynaptic activation, heterosynaptic LTP was mediated at least partly by an increase in release probability, whereas LTD was mediated by a decrease in release probability. These results indicate that, although the plasticity is induced by postsynaptic spiking alone, it is mediated by presynaptic changes. Such plasticity would necessarily require transsynaptic interactions. This interaction could be mediated by postsynaptic release of a retrograde messenger that activates presynaptic receptors after strong postsynaptic depolarization (Zilberter et al., 1999). Multiple retrograde messengers have been shown to induce long-term changes in synaptic weights by modifying presynaptic release probability (Nugent et al., 2007; Zilberter et al., 1999). Chistiakova et al. (2019) discussed nitric oxide as a possible candidate (Volgushev et al., 2000), although more than one retrograde messenger may be involved. Another possibility is that GABA is dendritically released from the postsynaptic neuron and acts on $GABA_B$ receptors located on the presynaptic terminal of excitatory neurons (Gonchar et al., 2001; Zilberter et al., 1999). Indeed, $GABA_B$ receptors are present at the presynaptic extracellular synaptic sites of excitatory neurons of the visual cortex (Gonchar et al., 2001). In other cell types, activation of $GABA_B$ receptors at the presynaptic terminal has been shown to suppress the activity of voltage-sensitive calcium channels and thus reduce glutamate release onto several cell types (Dolphin and Scott, 1986; Geddes et al., 2016; Gonchar et al., 2001). Determining which retrograde messengers are involved is imperative to determining the mechanism enabling the presynaptically-expressed heterosynaptic plasticity observed by Chistiakova et al. (2019).

Another important question is how the heterosynaptic plasticity observed here is determined by the initial release probability of the synapse. The interaction of retrograde messengers with specific receptors at the presynaptic membrane has been shown, in some cases, to yield presynaptic LTP or LTD (Pelkey et al., 2005). In this way, receptors may be up- and down regulated according to the state of the synapse, and allow retrograde signaling to modify the synaptic weight accordingly (Crosby et al., 2011). Alternatively, proteins like protein kinase C, whose activity regulates the size of the readily releasable pool of vesicles (Stevens and Sullivan,

1998), which correlates with synaptic release probability (Dobrunz 2002), could mediate the effects of the retrograde signal. Future research will be required to dissect the mechanism underlying the weight-dependence of heterosynaptic plasticity as a means to implement synaptic weight normalization.

The study of Chistiakova et al. (2019) supports the generality of heterosynaptic plasticity and supports the hypothesis that this form of plasticity helps to stabilize total synaptic weights. Future work, likely relying in part on computational modeling of neural networks, is necessary to determine how homeostatic plasticity and weight-dependent heterosynaptic plasticity mechanisms at both pre- and postsynaptic sites interact to maintain neural network stability.

Acknowledgments:

The author is a trainee in the laboratory of Dr. Jean-Claude Béïque who is funded by the Natural Sciences and Engineering Research Council of Canada and the Canadian Institutes of Health Research. I thank Dr. Béïque and lab members for the ongoing training and exciting discussion that continuously shapes my research interests and professional development. I also thank Philippe Vincent-Lamarre for providing useful comments.

References:

Bliss TV, Lomo T (1973) Long-lasting potentiation of synaptic transmission in the dentate area of the anaesthetized rabbit following stimulation of the perforant path. J Physiol 232:331–56.

Chistiakova M, Ilin V, Roshchin M, Bannon N, Malyshev A, Kisvárday Z, Volgushev M (2019) Distinct Heterosynaptic Plasticity in Fast Spiking and Non-Fast-Spiking Inhibitory Neurons in Rat Visual Cortex. J Neurosci 35:6865-6878.

Crosby KM, Inoue W, Pittman QJ, Bains JS (2011) Endocannabinoids gate state-dependent plasticity of synaptic inhibition in feeding circuits. Neuron 71:529–541.

Dobrunz LE (2002) Release probability is regulated by the size of the readily releasable vesicle pool at excitatory synapses in hippocampus. Int J Dev Neurosci. 20(3-5):225-36.

Dolphin AC, Scott RH (1986) Inhibition of calcium currents in cultured rat dorsal root ganglion neurons by (-)-baclofen. Br J Pharmac 88:213-220.

Geddes SD, Assadzada S, Lemelin D, Sokolovski A, Bergeron R, Haj-Dahmane S, Béïque JC (2016) Target-specific modulation of the descending prefrontal cortex inputs to the dorsal raphe nucleus by cannabinoids. Proc Natl Acad Sci 113(19):5429-34.

Gonchar Y, Pang L, Malitschek B, Bettler B, Burkhalter A (2001) Subcellular localization of GABA(B) receptor subunits in rat visual cortex. J Comp Neurol 431:182–197.

Hebb DO (1949) The organization of behavior: a neuropsychological theory. New York, NY: John Wiley & Sons

Kawaguchi Y, Kubota Y (1997) GABAergic cell subtypes and their synaptic connections in rat frontal cortex. Cereb Cortex 7:476–486.

Lee KF, Soares C, Béïque JC (2014) Tuning into diversity of homeostatic synaptic plasticity. Neuropharmacology 78:31-7. doi: 10.1016/j.neuropharm.2013.03.016.

Levy WB, Steward O (1983) Temporal contiguity requirements for long-term associative potentiation/depression in the hippocampus. Neuroscience 8(4):791–7.

Malenka RC, Nicoll RA (1993) NMDA-receptor-dependent synaptic plasticity: multiple forms and mechanisms. Trends Neurosci 16(12):521-7.

Markram H, Lübke J, Frotscher M, Sakmann B (1997) Regulation of synaptic efficacy by coincidence of postsynaptic APs and EPSPs. Science 275(5297):213-5.

Nugent FS, Penick EC, Kauer JA (2007) Opioids block long-term potentiation of inhibitory synapses. Nature 446:1086–1090 10.1038/nature05726

Pelkey KA, Lavezzari G, Racca C, Roche KW, McBain CJ (2005) mGluR7 is a metaplastic switch controlling bidirectional plasticity of feedforward inhibition. Neuron 46(1):89-102.

Royer S, Paré D (2003) Conservation of total synaptic weight through balanced synaptic depression and potentiation. Nature 422:518–522. doi:10.1038/nature01530

Stevens CF, Sullivan JM (1998) Regulation of the Readily Releasable Vesicle Pool by Protein Kinase C. Neuron 21(4):885-893.

Volgushev M, Balaban P, Chistiakova M, Eysel UT (2000) Retrograde signaling with nitric oxide at neocortical synapses. Eur J Neurosci 12:4255–4267.

Volgushev M, Chen JY, Ilin V, Goz R, Chistiakova M, Bazhenov M (2016) Partial breakdown of input specificity of STDP at individual synapses promotes new learning. J Neurosci 36:8842–8855.

Zilberter Y, Kaiser KM, Sakmann B (1999) Dendritic GABA release depresses excitatory transmission between layer 2/3 pyramidal and bitufted neurons in rat neocortex. Neuron 24:979–988.

MANUSCRIPT IV

Cellular Substrate of Eligibility Traces

This paper is currently in revision.

Authors:

Léa Caya-Bissonnette[1], Richard Naud[1,2,3,4], Jean-Claude Béïque[1,2,3*]

Affiliations:

[1] Department of Cellular and Molecular Medicine, University of Ottawa, Ottawa, ON K1H 8M5, Canada

[2] Centre for Neural Dynamics and AI, University of Ottawa, Ottawa, ON K1H 8M5, Canada

[3] Brain and Mind Research Institute, University of Ottawa, ON K1H 8M5, Canada

[4] Department of Physics, STEM Complex, Room 336, 150 Louis Pasteur Private, University of Ottawa, Ottawa, ON K1N 6N5, Canada

Corresponding Authors:

* Correspondence: jbeique@uottawa.ca (J.C.B.)

Author contribution: L.C.B. and J.C.B. conceptualized and designed the experimental research. L.C.B. acquired and analyzed the experimental data. L.C.B. and R.N. designed the computational model. L.C.B. implemented the computational model. L.C.B., R.N. and J.C.B interpreted the data and wrote the manuscript.

Data/code availability statement:

The datasets generated during the current study are available from the corresponding author on reasonable request. / The codes generated during the current study are available from the corresponding author on reasonable request.

ABSTRACT

The ability of synapses to undergo associative, activity-dependent weight changes constitutes a linchpin of current cellular models of learning and memory. It is, however, unclear whether canonical forms of Hebbian plasticity, which inherently detect correlations of cellular events occurring over short time scales, can solve the temporal credit assignment problem proper to learning driven by delayed behavioral outcomes. Recent evidence supports the existence of synaptic eligibility traces, a time decaying process that renders synapses momentarily eligible for a weight update by a delayed instructive signal. While eligibility traces offer a means of retrospective credit assignment, their material nature is unknown. Here, we combined whole-cell recordings with two-photon uncaging, calcium imaging and biophysical modeling to address this question. We observed and parameterized a form of behavioral timescale synaptic plasticity (BTSP) in layer 5 pyramidal neurons of mice prefrontal areas wherein the pairing of temporally separated pre- and postsynaptic events (0.5 s – 1 s), irrespective of order, induced synaptic potentiation. By imaging calcium in apical oblique dendrites, we reveal a short-term and associative plasticity of calcium dynamics (STAPCD) whose time-dependence mirrored the induction rules of BTSP. We identified a core set of molecular players that were essential for both STAPCD and BTSP and that, together with computational simulations, support a model wherein the dynamics of intracellular handling of calcium by the endoplasmic reticulum (ER) provides a latent memory trace of neural activity that instantiates synaptic weight updates upon a delayed instructive signal. By satisfying the requirements expected of eligibility traces, this mechanism accounts for how individual neurons can conjunctively bind cellular events that are separated by behaviorally relevant temporal delays, and thus offers a cellular model of reinforced learning.

MAIN

Long-term synaptic plasticity is widely believed to contribute to the ability of the brain to learn [1,2,3,4]. While the elucidation of the molecular and cellular underpinnings of synaptic plasticity mechanisms has received sustained attention over the last few decades, it remains unclear whether the canonical plasticity rules studied in experimentally tractable systems approximate well those guiding behaviorally relevant associative learning. For instance, while spike-timing-dependent plasticity (STDP) encapsulates key Hebbian postulates, it inherently relies on the correlation detection of cellular events occurring over time scales (tens of milliseconds [5,6,7,8,9]) that are fundamentally distinct to those required for the processing of behaviorally relevant credit signal (at least hundreds of milliseconds [1,10]). As such, when instructive signals are delayed, a temporal credit assignment problem arises for which no unified solutions have yet emerged.

Eligibility traces are primarily a theoretical construct used in machine learning to implement credit assignment [11]. In turn, they offer a useful heuristic to appraise synaptic models of associative encoding where they can be conceptualized as a silent process that keeps a time-decaying record of a synapse's activity (*i.e.,* a short-lived local flag), rendering it temporarily 'eligible' for weight update upon a delayed instructive signal. Protracted eligibility traces would thereby allow individual neurons to solve the temporal credit assignment problem by binding cues that are separated by behaviorally relevant temporal delays. An emerging literature is beginning to identify forms of synaptic plasticity that exhibit temporal features that are consistent with the existence of a neural correlate of eligibility traces [12,13,14,15,16,10]. In particular, important recent work in the hippocampus has outlined the presence of a novel form of synaptic plasticity, termed Behavioral Timescales Synaptic Plasticity (BTSP), that emerges following the pairing of synaptic and cellular events that are separated by up to ~ 2 seconds [17,18,19]. While this form of plasticity was shown to be involved in the rapid emergence of place representation in CA1 neurons, the timescale of its induction rules alone provides direct evidence supporting the existence of eligibility traces in the brain. Yet, their material nature is unknown, and so are the details concerning the dynamical rules regulating their deployment.

Here, we show that the pairing of pre- and postsynaptic events with behaviorally relevant temporal delays induced synaptic potentiation in L5 pyramidal neurons of mice prefrontal areas

(medial prefrontal cortex; mPFC) reminiscent of BTSP observed in the hippocampus. The protracted timescales of the plasticity induction preclude the involvement of canonical cellular mechanisms of plasticity. A series of two-photon (2P) glutamate uncaging and calcium (Ca^{2+}) imaging experiments highlighted a spatially constrained, dendritic compartment specific, form of short-term associative plasticity of Ca^{2+} dynamics (termed here STAPCD) that emerged following the temporally discontiguous pairing of pre- and postsynaptic activity. Temporal parameterization, pharmacological experiments and computational modeling highlighted a mechanism wherein the endoplasmic reticulum (ER), through the concerted interplay between glutamate receptors of the N-methyl-D-aspartate receptor (NMDAR) and metabotropic glutamate receptor (mGluR) subtypes and ER Ca^{2+} channels of the ryanodine and inositol trisphosphate (IP_3) subtypes, implement a delayed amplification of intracellular Ca^{2+}. Blocking any of the core molecular players involved in STAPCD blocked BTSP, thereby pointing towards a causal relationship. These results thus describe a mechanism that holds a latent memory trace of cellular activity to participate in instantiating synaptic weight updates by a delayed instructive cue, and thus satisfies the features expected of eligibility traces.

RESULTS

BTSP in L5 pyramidal neuron of the mPFC

The experimental tractability of BTSP provides an opportunity not only to parametrize important dynamical features of eligibility traces, but also to determine their material nature. As an important corollary, we also sought to determine whether BTSP was solely operating in the hippocampus by examining whether qualitatively analogous protocols could induce plasticity in cortex. To achieve these goals, we prepared acute brain slices of the mPFC and carried out whole-cell recordings of layer 5 (L5) pyramidal neurons of male and female mice (Fig. 1A) using a potassium (K^+)-Gluconate intracellular solution supplemented with picrotoxin (PTX), a γ-aminobutyric acid $(GABA)_A$ receptor blocker, to isolate excitatory postsynaptic currents (EPSCs; see Fig. S1). We first examine the effects of a standard STDP protocol validated at other synapses [9,20,21] (*i.e.,* 120 pairings of a single synaptic input followed by 2 APs induced by a 50 ms current injection, with a 20 ms delay) and found, in keeping with previous reports [12,22] that it did not induce

significant potentiation of proximal synapses onto L5 PFC pyramidal neurons, even in young mice (P15 - P16; Fig. S2A; 96.71 ± 5.36 %) whose synapses are typically considered more plastic [23]. Since bursting uncovers BTSP in hippocampus and regulates plasticity in cortex [9,17,20,21], we next induced a presynaptic train of synaptic inputs (10 stimulations at 20 Hz; pre_t) immediately prior to a burst of backpropagating action potentials (bAPs) induced by direct 300 ms current injection ($post_b$), and found that it triggered robust potentiation in response to only 5 pairings (Fig. S2A; 160.98 ± 3.21 % of baseline). This burst-STDP (pre_t-$post_b$) was not restricted to younger animals as it was observed in mice P21 to P36 (Fig. S2A). Thus, a burst-STDP protocol not only induced potentiation at synapses that are otherwise resistant to potentiation by canonical STDP protocols, but did so following a far lower number of repetitions (5 *vs* 120).

We then asked whether bursting in L5 pyramidal neurons would bend the canonical temporal rules of STDP induction into the realm of BTSP (*i.e.*, delays in the hundreds of milliseconds). We thus extended the temporal delay between presynaptic and postsynaptic stimulations to 500 ms, a timescale far outlasting that of STDP induction [6,7,8,24,25], and found, strikingly, that this protocol induced potentiation (Fig. 1B; 140.87 ± 5.43 % of baseline). This plasticity was dependent on postsynaptic Ca^{2+} and NMDARs as it was abolished by the fast Ca^{2+} buffer BAPTA (20 mM) as well as by bath administration of the NMDAR antagonist D-AP5 (100 µM), respectively (Fig. 1B). Importantly, neither presynaptic trains alone, nor postsynaptic bursts alone, yielded potentiation (Fig. 1C), confirming that this form of plasticity at extended timescale is associative in nature.

To investigate with greater granularity the induction rules of BTSP in L5 neurons, we parameterized the timing delay between pre- and postsynaptic events (0 s – 1.25 s). While the pre_t-$post_b$ protocol induced a significant potentiation at short- (0 ms - 50 ms) and extended- (500 ms - 800 ms) time intervals, it induced no plasticity at intermediate timings (125 ms - 250 ms; Fig. 1D). Since the polarity of the synaptic changes induced by canonical STDP is determined by the relative order of pre- and postsynaptic spiking [6,7], we naturally next investigated the effects of reversing the order of pre- and postsynaptic firing. The temporal profiles of both induction protocols (*i.e.*, pre_t-$post_b$ and $post_b$-pre_t) were remarkably symmetrical at extended timescale, with both showing strong potentiation between 500 ms – 800 ms (Fig. 1D). We next explored induction singularities of BTSP at timescales that induced potentiation (*i.e.*, 500 ms - 800 ms). The paired-pulse ratio

(PPR) of baseline *vs* post-pairing EPSCs, an index of presynaptic release probability [28], did not change significantly, suggesting a postsynaptic locus of expression (Fig. S2B). We found that the magnitude of BTSP showed a small positive correlation (pearson correlation coefficient = 0.34, p = 0.04) with the magnitude of short-term facilitation of the stimulated synapses (Fig. S3B). It was otherwise not dependent on a range of experimental variables, including age and sex of the animals, as well as Ih currents and spike frequency adaptation (see Fig. S3), implying a generalization and robustness of these plasticity rules across L5 pyramidal neuron subtypes [26,27].

Collectively, these results show that L5 neurons can bind pre- and postsynaptic events, presented in indiscriminate order, that are separated by time intervals far longer than those of canonical STDP and of typical membrane time constants [6,25]. The timescale and symmetry of this form of BTSP makes it non-Hebbian in nature and represent a direct manifestation of protracted synaptic eligibility traces in L5 pyramidal neurons.

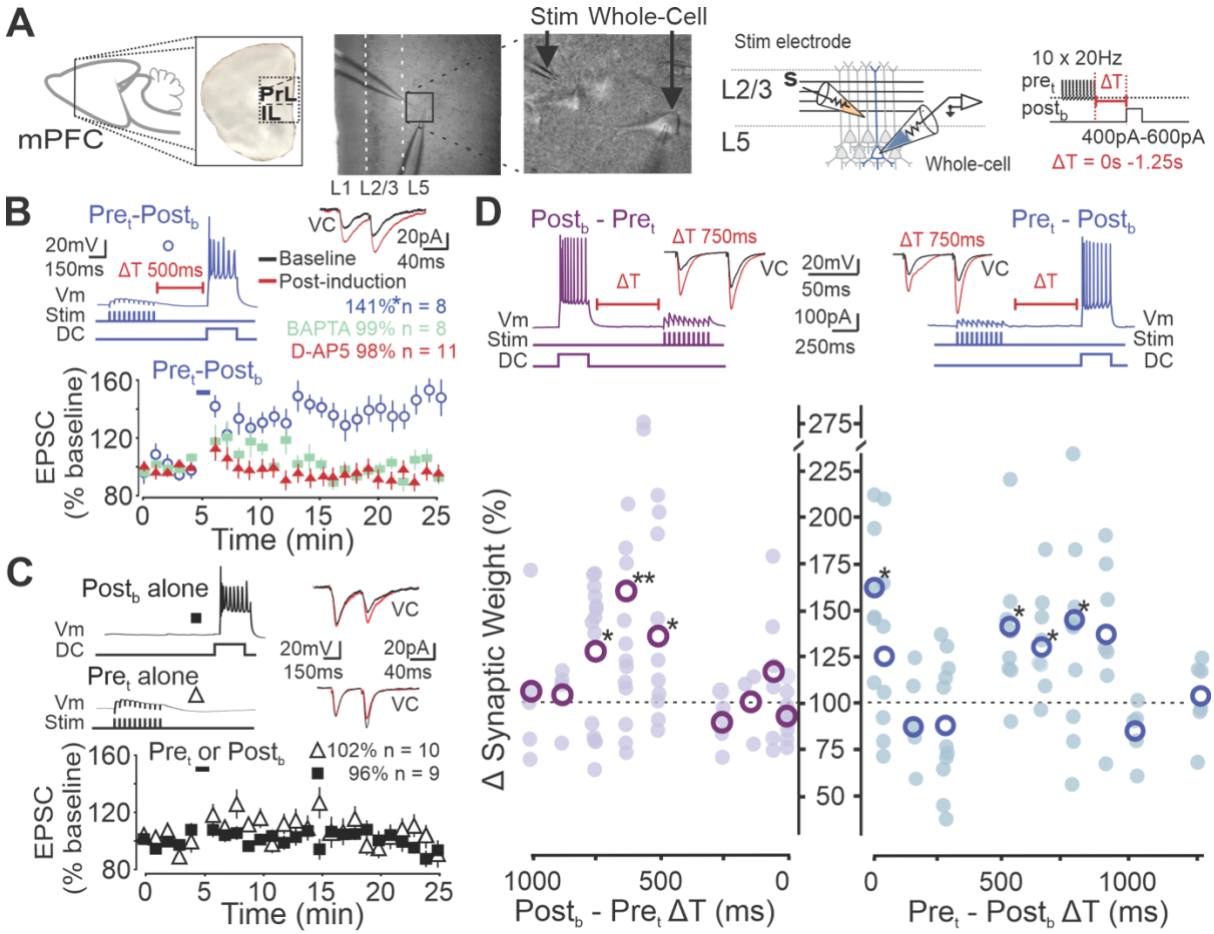

Figure 1. Synapses onto mPFC L5 pyramidal neurons undergo BTSP. (A) Schematic of experimental approach: a stimulating electrode (s) is placed proximal to L5 neuron apical dendrites and a recording electrode in whole-cell patch clamp records from a L5 pyramidal neuron (PrL; prelimbic, IL; infralimbic) and example image of L5 pyramidal neurons of the mPFC using 5 X lens (left), 40 X submersive lens (right). (B) Representative trace of pre_t-$post_b$ pairings at 500 ms delay and EPSCs (top). Resulting normalized EPSC change over time (bottom) for control (blue, n = 8 neurons, p = 0.016), with bath-application of D-AP5 (red, n = 11 neurons, p = 1.0) or intracellular BAPTA (green, n = 8 neurons, p = 0.91). (C) Representative trace of $post_b$ (top, squares) or pre_t (bottom, triangles) induced alone (top left) and EPSCs (top right). Resulting normalized EPSC change over time (bottom, $post_b$: n = 9 neurons, p = 0.82, pre_t: n = 10 neurons, p = 0.92). (D) Representative trace of the pre_t-$post_b$ pairings and $post_b$-pre_t pairings and EPSCs (top). Resulting mean synaptic weight change induced at different timing intervals from 0 ms to 1.25 s (pre_t-$post_b$ 0 ms: n = 6 neurons, p = 0.031, 50 ms: n = 7 neurons, p = 0.47, 125 ms: n = 5 neurons, p = 0.44, 250 ms: n = 11 neurons, p = 0.37, 500 ms: as shown in B, 625 ms: n = 8 neurons, p = 0.039, 750 ms: n = 9 neurons, p = 0.027, 875 ms: n = 7 neurons, p = 0.11, 1000 ms: n = 5 neurons, p = 0.13, 1250 ms: n = 6 neurons, p = 0.84; $post_b$-pre_t 0 ms: n = 9 neurons, p = 0.13, 50 ms: n = 6 neurons, p = 0.44, 125 ms: n = 3 neurons, p = 1.0, 250 ms: n = 5 neurons, p = 0.19, 500 ms: n = 10 neurons, p = 0.048, 625 ms: n = 15 neurons, p = 0.0083, 750 ms: n = 14 neurons, p = 0.017, 875 ms: n = 4 neurons, p = 0.86, 1000 ms: n = 5 neurons, p = 1.0). bsl; baseline. ** p < 0.01, *p < 0.05; Data are shown as mean ± sem.

Short-Term Plasticity of Ca^{2+} Dynamics

While eligibility traces have provided a useful framework to formalize several computational implementations of plasticity [12,10,29], their material nature has not been established. Since mPFC synapses contain a high proportion of high affinity, slow, GluN2B-containing NMDARs [30,31], we wondered whether singularly protracted NMDAR-dependent Ca^{2+} influx may underlie the extended coincident detection between pre- and postsynaptic bursting of BTSP. We thus carried out simultaneous 2P uncaging of MNI-glutamate and Ca^{2+} imaging of the low affinity dye Fluo-4FF. These experiments revealed that the decay of Ca^{2+} transients (218 ms ± 41 ms) on single spines of proximal apical dendrites of L5 pyramidal neurons were: 1) broadly similar to those observed at canonical mature CA1 synapses [31,32,33,34] , and; 2) significantly faster than the time interval of effective BTSP with pre_t-$post_b$ protocols (Fig. S4A). In an attempt to more closely mimic our pre_t-$post_b$ BTSP experiments, we also assessed the decay of Ca^{2+} transients following the repetitive synaptic stimulation (10 uncaging stimulations at 20 Hz) of spatially clustered spines (5 - 6 spines) in current clamp mode ($uPre_t$; Fig. S4B) and found that Ca^{2+} transients were still substantially shorter than the typical delay of paired inputs during BTSP (Fig. S4C). Given that the decay of fluorescence, even when using a low affinity dye, likely overestimates the lifetime of phasic cytosolic Ca^{2+} *in situ* [33,35], these results suggest that the cytosolic Ca^{2+} triggered by synaptic activation onto L5 pyramidal neurons has largely subsided by the time the $post_b$ invades the dendritic arbor during effective BTSP induction, especially for the longer intervals (500 ms to 1000 ms). A protracted, synaptically-induced, cytosolic Ca^{2+} trace is therefore an unlikely candidate for enacting an eligibility trace in L5 mPFC neurons.

For canonical forms of Hebbian plasticity, much of the scrutiny has historically focused on the dynamics of NMDAR-dependent Ca^{2+} entry occurring during the ephemeral coincident detection phase of plasticity induction [32,33,36]. Here, the Ca^{2+} entering during the delayed instructive event (either synaptic or bAPs) may, in principle, act as the plasticity signaling molecule permissive to synaptic potentiation during BTSP. We thus re-focused our attention and examined features of the Ca^{2+} transients triggered by the delayed instructive postsynaptic burst occurring during pre_t-$post_b$ BTSP induction. Using 2P Ca^{2+} imaging, we first established the Ca^{2+} profile at proximal apical dendrites and associated spines induced by a burst of bAPs alone ($post_b$ alone; denominated as 'I.' in Fig. 2A, S5A-B). We restricted our experiments to primary oblique dendrites and did not observe branch point failures of bAP propagation (at least as inferred from

Ca^{2+} imaging). Following a 30 second rest period, we re-imaged the same dendritic segment in response to $post_b$, but when it was *preceded* by synaptic activation (by 500 ms - 750 ms), achieved here by glutamate uncaging onto a cluster of closely positioned spines ($uPre_t$) (mimicking pre_t-$post_b$ BTSP induction; denoted 'II.' in Fig. 2A, S5A-B). Remarkably, we found that the decay time constant of dendritic Ca^{2+} triggered by a burst of bAPs ($post_b$) significantly increased when the burst of bAPs was preceded by clustered synaptic activation (compared to $post_b$ alone; II. *vs* I.; Fig. 2A). This robust augmentation of Ca^{2+} transients was manifest in the dendrites, but not in the stimulated spines, suggesting a dendritic origin (Fig. S5C). When probed following another 30 second rest period, the decay of the Ca^{2+} transients induced by $post_b$ alone (III.) typically returned to that of the initial isolated $post_b$ (III. *vs* I.; Fig. S5), suggesting that the cellular phenomenon supporting this synaptically-induced prolongation of Ca^{2+} signals induced by bAPs is short-lived. We have formalized this general observation as an exclusion criterion to restrict our analysis to healthy recordings (*i.e.*, where the baseline value (I.) and post-paring value (III.) were within 35 % of each other; see Methods). Not surprisingly, the administration of D-AP5 blocked the uncaging-induced synaptic Ca^{2+} transients (Fig. S4) and did not influence the profile of the Ca^{2+} transients induced by $post_b$ alone. However, it blocked the lengthening of bAPs burst-triggered Ca^{2+} transients induced by preceding synaptic activation (Fig. 2B; Fig. S5E). Thus, these results imply that the Ca^{2+} transients triggered by bursts of bAPs are increased when preceded (500 ms - 750 ms before) by a bout of synaptic activation, which effect is dependent on NMDARs. The plasticity of Ca^{2+} transients represent a plausible and intriguing mechanism for enacting an eligibility trace for binding pre- and postsynaptic inputs at behavioral timescales. For simplicity and ease, we will heretofore refer to this phenomenon as Short-Term Associative Plasticity of Ca^{2+} Dynamics (STAPCD).

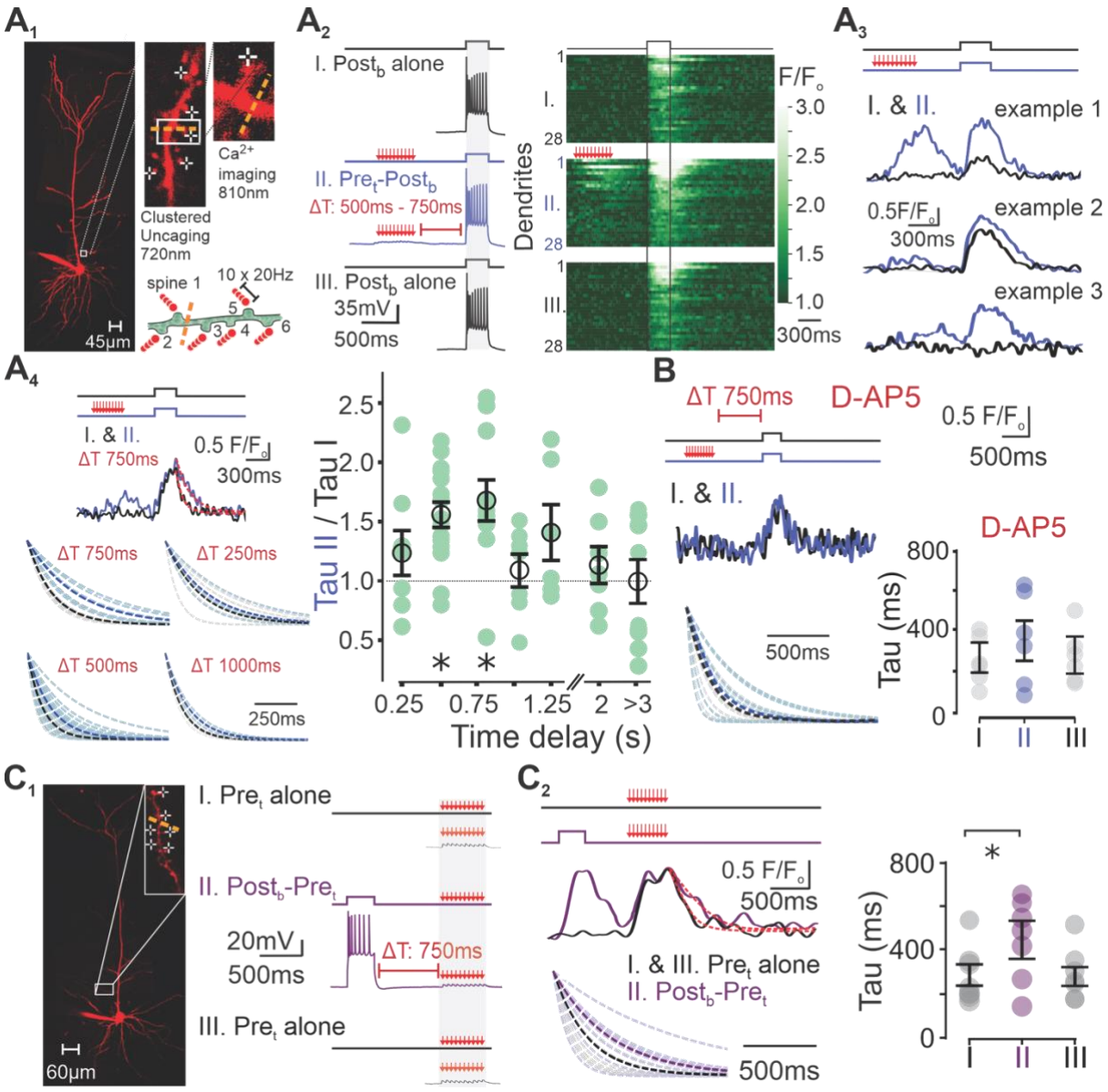

Figure 2. Synaptically-driven short-term associative plasticity of Ca^{2+} dynamics. (A) A_1 Example image of L5 pyramidal neuron and proximal apical dendrite for which glutamate uncaging on clustered spines and line scans on dendrites were performed. A_2 Example of electrophysiology recording induced with 2P uncaging and whole-cell patch clamp for three $post_b$ given at 30 s intervals with a $uPre_t$ given 500 ms - 750 ms prior to the second $post_b$ (left) and resulting 2P line scans recording using Fluo-4FF dye. A_3 Example Ca^{2+} traces measured by line scans using Fluo-4FF. We have not included traces such as example 3 in our analyses do to difficulty with fitting decays, and rare occurences. A_4 Resulting decay traces and normalized relative decay time constants of $post_b$ preceded by $uPre_t$ (II.) compared to the first $post_b$ given alone (I.; 250 ms: n = 8 dendrites, p = 0.31, 500 ms: n = 18 dendrites, p = 0.030, 750 ms: n = 11 dendrites, p = 0.024, 1000 ms: n = 7 dendrites, p = 0.81, 1250 ms: n = 6 dendrites, p = 0.31, 2000 ms: n = 7 dendrites, p = 0.81, > 3000 ms: n = 10 dendrites, p = 0.96). (B) Representative Ca^{2+} trace of protocol shown in A, except in the presence of D-AP5, and decay traces (left) and tau values (right; n = 6 dendrites, p = 0.44). (C) Representative voltage and Ca^{2+} traces of three $uPre_t$ given at 30 s

intervals with the second $uPre_t$ preceded by $post_b$ 750 ms prior induced on L5 proximal apical dendrites and resulting decay traces and time constants (n = 7 dendrites, p = 0.031). *p < 0.05; Data are shown as mean ± sem.

Induction Rules of STAPCD abide by those of BTSP

As a minimal necessary condition for a causal relationship inference between STAPCD and BTSP, their temporal induction rules should be broadly similar. We therefore investigated with increased granularity the temporal contingencies of the delays between the synaptic activation and the burst of bAPs (0.25 s – 4.5 s) and found that STAPCD was readily expressed following extended intervals (0.5 s - ~1 s), but not at 250 ms, a temporal profile closely matching BTSP induction in these neurons (Fig. 2A). STAPCD was also expressed as an amplification in the amplitude (ΔF/F) *per se* of the Ca^{2+} signal for a temporal window of up to ~ 1 s (Fig. S5; see Ca^{2+} model below). We next examined the bidirectionality of STAPCD by determining whether, like BTSP, it was induced when a burst of bAPs ($post_b$) preceded synaptic activation ($post_b$-$uPre_t$). We thus established the baseline profile of synaptic Ca^{2+} transients (again induced by 2P uncaging of MNI-glutamate onto visually identified clustered spines; $uPre_t$), and repeated the procedure 30 seconds later but with the uncaging stimulation ($uPre_t$) preceded by burst of bAPs ($post_b$; 750 ms before). The decay of Ca^{2+} transients induced by the uncaging trains that were preceded by bursts of bAPs were significantly longer than those triggered by synaptic trains alone (*i.e.*, baseline conditions measured 30 seconds before and after the $post_b$-$uPre_t$ pairing; Fig. 2C; Fig. S6). Altogether, the bidirectionality and the temporal requirements of STAPCD closely matches those of BTSP.

We next parameterized some of the salient features of STAPCD. First, we determined its spatial profile and found that the synaptically-induced amplification of bAPs burst-induced Ca^{2+} transients was largely restricted to the dendritic segment of the activated spine cluster (average 7.98 µm; n = 30 dendrites), sharply decreasing with increasing distance along the dendrite (length constant of ~12.5 µm from and including the cluster centroid; Fig. 3B; Fig. S7A). Second, we observed that STAPCD depended on cooperativity between spatially clustered spines since train stimulations of a single spine did not significantly alter the Ca^{2+} transients induced by bursts of bAPs (Fig. 3C; Fig. S7C). Third, this associative form of Ca^{2+} plasticity showed cellular compartment specificity: it was readily observed at proximal apical oblique dendrites but not at basal dendrites (Fig. 3D, Fig. S7B). This result suggests that the manifestation of STAPCD rely

on a minimal amount of Ca^{2+} influx during the synaptic cue. Consistent with this idea, the magnitude of STAPCD was slightly correlated to the amplitude of the initial Ca^{2+} transients induced by clustered synaptic activation ($uPre_t$; Fig. S8D). The extent of STAPCD appeared to be somewhat bounded since the Ca^{2+} amplification was of a lesser magnitude in cases where the bAPs displayed longer Ca^{2+} transients to begin with (i.e., 'I"; Fig. S8B).

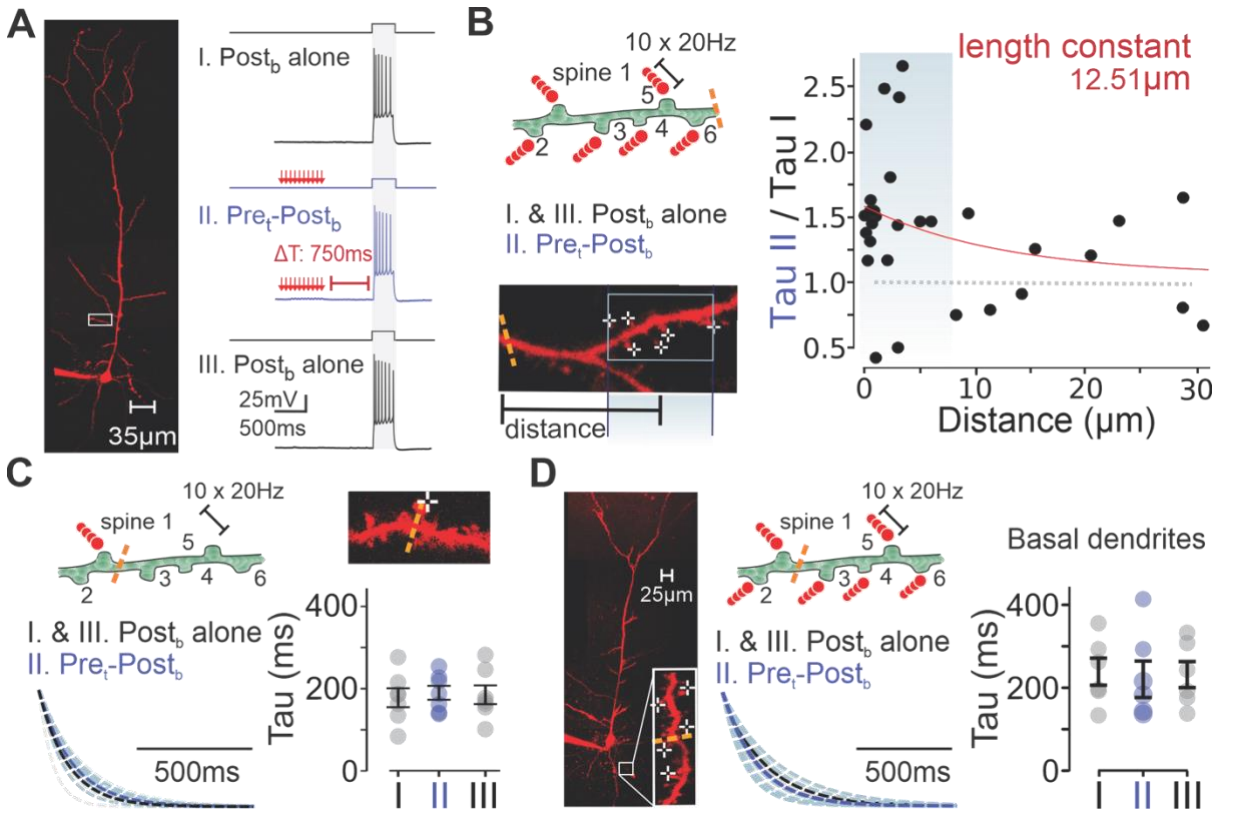

Figure 3. Properties of STAPCD during effective BTSP. (A) Representative voltage trace of three $post_b$ given at 30 s intervals with the second $post_b$ preceded by $uPre_t$ 500 ms - 750 ms prior. (B) Distance dependence of normalized relative decay time constants. Length constant was measured by mono-exponential fit. Data in blue from Fig 2A. (C) Experimental setup and decay traces resulting from three $post_b$ given at 30 s intervals with the second $post_b$ preceded by $uPre_t$ given on a single spine 750 ms prior (left). Resulting time constants (right: n = 7 dendrites, p = 0.81). (D) Example image of L5 pyramidal neuron and a proximal basal dendrite (left). Representative cartoon and resulting decay traces measured on basal dendrites during three $post_b$ given at 30 s intervals with the second $post_b$ preceded by $uPre_t$ 750 ms prior (middle), and resulting time constants (right: n = 6 dendrites, p = 0.56). Data are shown as mean ± sem.

We finally report a range of experimental parameters that were not correlated with the manifestation of STAPCD (see Fig. S8). Collectively, these results outline a set of core features of a novel form of intracellular Ca^{2+} plasticity. We found that STAPCD: 1) is triggered by the conjunctive actions of synaptic and bAP events occurring over protracted time scales, 2) is spatially compartmentalized, and; 3) showed induction rules that closely parallel those of BTSP.

Intracellular Ca^{2+} Stores are involved in the expression of STAPCD

Pondering on the temporal and associative features of the intracellular Ca^{2+} plasticity outlined above, we conjectured that intracellular Ca^{2+} stores may be involved in its manifestation. Indeed, the smooth ER is involved in intracellular Ca^{2+} homeostasis, is found as an anastomosing network in dendrites of pyramidal neurons [37,38,39] and, at times, in spines [38,40]. The ER regulates intracellular Ca^{2+} dynamics through seemingly opposing uptake and release mechanisms (*i.e.*, involving either Ca^{2+} uptake/extrusion from, or release into, the cytoplasm) [41,42,43,44]. In neurons, ER-mediated mechanisms have been shown to regulate in some conditions the profile of both synaptically-induced and spiking-induced cytosolic Ca^{2+} entry [32,45,46,47], and to be involved in several forms of synaptic plasticity [32,48]. In order to ultimately determine whether ER Ca^{2+} stores are involved in STAPCD, we first began by determining the contribution of ER stores to the profile of Ca^{2+} induced by either synaptic trains or bursts of bAPs alone in L5 mPFC neurons. We thus incubated slices in CPA, a Sarco/Endoplasmic Reticulum Ca^{2+}-ATPase (SERCA) pump blocker, for at least 1 h prior to recordings. While CPA did not alter the Ca^{2+} dynamics induced by $post_b$, it modestly, but significantly, increased the decay time constant of dendritic Ca^{2+} profile induced by trains of 2P synaptic activation ($uPre_t$) (Fig. S9A-B). These results suggest that SERCA pumps uptake cytosolic Ca^{2+} that enters following trains of glutamate release in proximal apical dendrites of L5 pyramidal neurons in baseline conditions. In agreement with previous studies (Markram et al., 1995; Majewska et al., 2000), this suggest that ER stores thus slightly constrains the temporal profile of cytosolic Ca^{2+}. Next, given that ER stores can in certain conditions amplify cytosolic Ca^{2+} by a process known as Ca^{2+}-induced Ca^{2+}-release (CICR), we examined the effects of blocking CICR by including ryanodine in the intracellular recording solution. In our conditions, the temporal profile of dendritic Ca^{2+} elicited by either burst of bAPs or synaptic inputs were not

altered by ryanodine (Fig. S9A-B), thus suggesting that ER stores do not appreciably sustain CICR in response to isolated pre- or post-synaptic events.

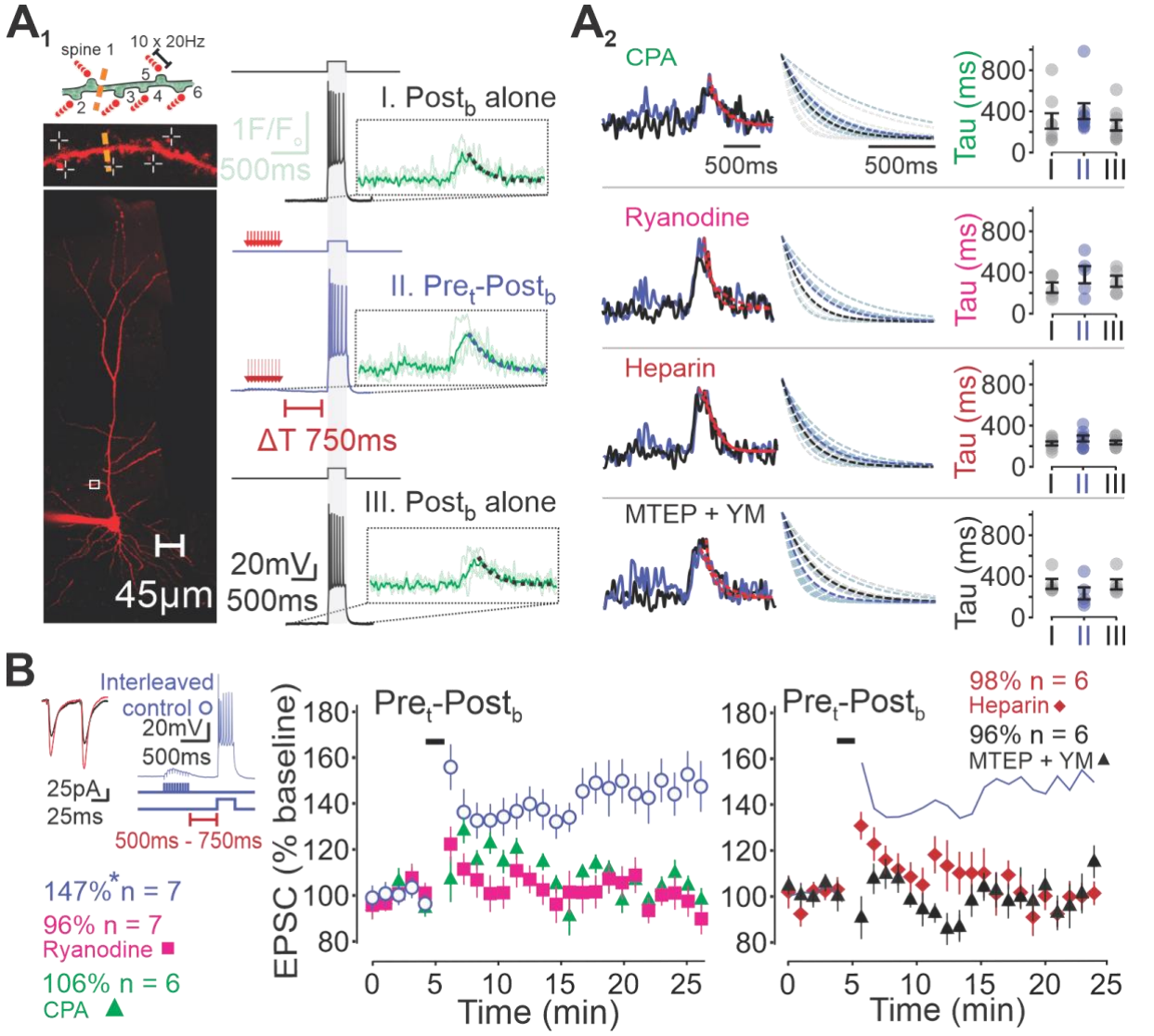

Figure 4. Ca^{2+} stores sustain STAPCD. (A) A_1 Representative voltage trace of three $post_b$ given at 30 s intervals with the second $post_b$ preceded by $uPre_t$ 750 ms prior in the presence of bath-applied drugs. A_2 Example Ca^{2+} traces and resulting decay traces and time constants in the presence of extracellular CPA (n = 8 dendrites, p = 0.15), intracellular ryanodine (pink: n = 7 dendrites, p = 0.13), intracellular heparin (red: n = 8 dendrites, p = 0.15), or extracellular mGluR antagonists, MTEP and YM-298198 (black: n = 5 dendrites, p = 0.063; bottom). (B) Representative trace of BTSP induction and EPSCs for interleaved control, and resulting normalized EPSC change over time (blue: n = 7 neurons, p = 0.032) and with bath-application of CPA (green: n = 6 neurons, p = 0.44), with intracellular ryanodine (pink: n = 7 neurons, p = 0.69), heparin (red: n = 6 neurons, p = 0.57) or bath-application of MTEP and YM-298198 (black: n = 6 neurons, p = 0.68). *p < 0.05. Data are shown as mean ± sem.

An intuition that naturally emerges from the minimal contribution of CICR to synaptic and bursts of bAPs events in baseline conditions, along with the Ca^{2+} uptake by SERCA pumps, is that the ER stores may exhibit a conditional, state-dependent, CICR capacity that would manifest itself following temporally paired Ca^{2+} events. To begin addressing this possibility, we determined the effects of blocking the SERCA pumps on STAPCD and found that CPA prevented it ($uPre_t$ 750 ms before $post_b$; Fig. 4A; Fig. S9C). In line with a role of CICR, intracellular ryanodine significantly reduced STAPCD, but ostensibly only partially (Fig. 4A; Fig. S9C). Thus, the expression of STAPCD requires intact ER stores through a mechanism that, at least partially, involves CICR.

In order to delineate more precisely the involvement of ER in STAPCD, we wondered whether the partial block by ryanodine may reflect the parallel involvement of IP_3-induced Ca^{2+}-Release (IICR) [41], especially given the second-long timescale of action of IP_3 [42,49]. We thus blocked IP_3 receptors (IP_3Rs) with intracellular heparin and found that it abolished STAPCD (Fig. 4A; Fig. S9C). The involvement of IP_3Rs was unsuspected in that it suggests the involvement of a Gq-coupled receptor signaling pathway [50,51]. As a first candidate, we blocked mGluRs of the mGluR1/5 subtype with bath-administration of MTEP and YM-298198, and found that it abolished STAPCD (Fig. 4A; Fig. S9C). Collectively, these results thus far demonstrate that STAPCD requires activation of glutamate receptors of the NMDAR and mGluR subtypes, as well as CICR triggered by activation of ryanodine receptors (RyRs) and IP_3Rs on intact ER stores.

The results from our pharmacological investigation and simulations identified a set of core molecular players involved in STAPCD along with a plausible mechanistic and dynamical model for the role of the ER in STAPCD. In turn, this level of description provides an opportunity to explore the causal relationship between STAPCD and BTSP and, as a corollary, whether STAPCD enact an eligibility trace in cortex. As an obligatory requirement for a causal relationship, the pharmacological blockade of every molecular component known to be involved in STAPCD in isolation, should abolish BTSP. We tested this conjecture and found that individually blocking: 1) NMDARs (with D-AP5; Fig. 1B); 2) SERCA pumps (with CPA; Fig. 4B); 3) RyRs (with intracellular ryanodine; Fig. 4B); 4) IP_3Rs (with intracellular heparin; Fig. 4B) or; 5) mGluRs (with MTEP and YM-298198; Fig. 4B) abolished BTSP.

Activity-dependent state transition of ER Ca^{2+} stores accounts for STAPCD.

While the results outlined above identified a set of core molecular players involved in STAPCD, they however fall short of providing a dynamical and mechanistic account of STAPCD. We thus turned to computational simulations to determine whether the salient features of STAPCD could be modeled by a parsimonious set of experimentally grounded parameters. In particular, we sought to capture the observations that suggest that while ER stores, in baseline conditions, primarily uptake (as opposed to release) Ca^{2+}, they can conditionally amplify the Ca^{2+} transient induced by a delayed signal. We thus modeled cytosolic Ca^{2+} (c) as reflecting direct entry arising from synaptic (I_{syn}) and bAPs (I_{AP}) sources, as well as indirect contribution by intracellular Ca^{2+} stores through cytosolic uptake/extrusion (ER loading) and release (ER unloading) mechanisms (Fig. 5A-B; see Methods for details). The ER amplification of cytosolic Ca^{2+} (*i.e.*, ER unloading) by a delayed instructive cue is temporally constrained to a period of ER release eligibility (*i.e.*, ~ 1 s; experimentally determined in Fig. 2A) and consists in a linear modification in cytosolic Ca^{2+} amplitude (A_{ER}) and a non-linear modification in Ca^{2+} decay time constant (T_{ER}). A_{ER} reflects Ca^{2+} release through IICR and CICR, while the non-linearity of T_{ER} reflects a previously reported concentration-dependent non-linear rate of Ca^{2+} transport by SERCA pumps [43,44].

Simulations deployed from our model captured the temporal rules of STAPCD induction (Fig. 5C-G; Table S1) that were determined experimentally. We further simulated the effects of blocking NMDARs with D-AP5 by setting I_{syn} to 0, and the model reproduced our experimental data in amplitude and decay time constant (Fig. 5H-I). To simulate our experiments blocking SERCA pumps with CPA, we have set both the A_{ER} and T_{ER} parameters to 0, and the model once again reproduced the experimental data (Fig. 5J-K). Together, our experiments and model simulations suggest a mechanistic scenario underlying STAPCD: Ca^{2+} entry triggered by synaptic inputs or postsynaptic firing alters the state of the ER by rendering it momentarily (*i.e.*, ~ 1 second) eligible to sustain RyR- and IP_3R-mediated intracellular Ca^{2+} release, that is triggered by a secondary, time delayed, Ca^{2+} entry associated with an instructive cue. As such, the ER effectively retains a memory of previous activity on a second-long timescale, yielding STAPCD.

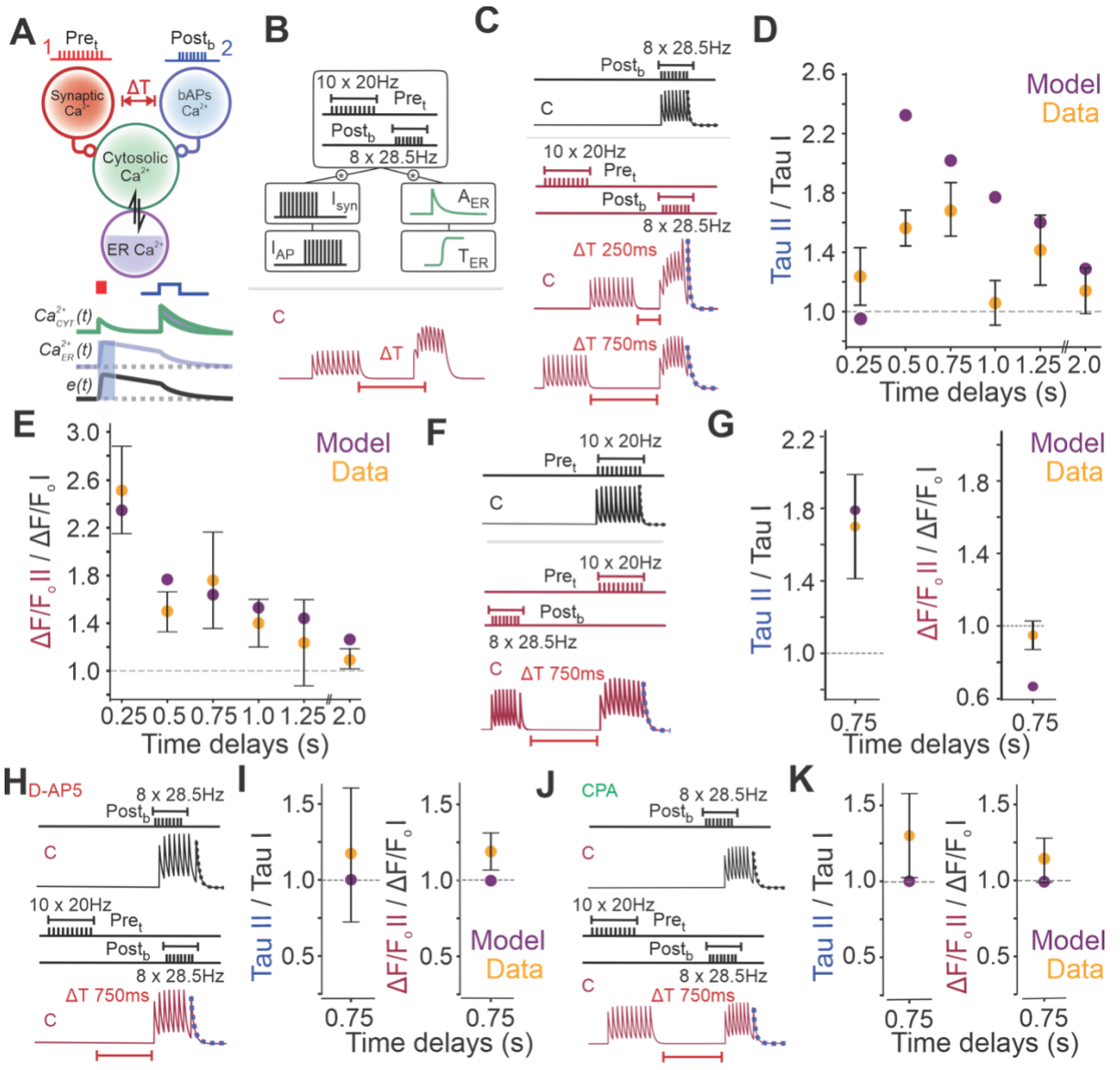

Figure 5. Plasticity of Ca^{2+} dynamics are captured by combining synaptic and bAPs Ca^{2+} with ER modulation. (A) Schematic depicting the relationship between synaptic, bAPs, cytosolic and ER Ca^{2+}, and with eligibility traces. (B) Schematic depicting the nonlinear Ca^{2+} dynamics fitted by minimizing least-squares approach. (C) Modeled cytosolic Ca^{2+} traces of post$_b$ (black) and pre$_t$-post$_b$ pairings at 250 ms and 750 ms (red). (D) Relative normalized decay time constants of post$_b$ paired with pre$_t$ compared to post$_b$ induced alone at varying time delays. (E) Same as D except for peak amplitude of Ca^{2+} transient. (F) Modeled Ca^{2+} traces of pre$_t$ (black) and post$_b$-pre$_t$ pairings at 750ms (red). (G) Relative normalized decay time constants (left) and peak amplitude (right) of traces shown in F. (H) Modeled Ca^{2+} traces of post$_b$ (black) and pre$_t$-post$_b$ pairings at 750ms (red) with D-AP5 (I_{syn} is set to 0). (I) Relative normalized decay time constants (left) and peak amplitude (right) of traces shown in H. (J) Modeled Ca^{2+} traces of post$_b$ (black) and pre$_t$-post$_b$ pairings at 750ms (red) with CPA (A_{ER} and T_{ER} are set to 0). (K) Relative normalized decay time constants (left) and peak amplitude (right) of traces shown in J. Data are shown as mean ± sem.

Thus, STAPCD and BTSP in L5 pyramidal neurons abide by similar temporal induction rules and are sustained by an overlapping molecular makeup. Collectively, these results provide convergent evidence for STAPCD as a plausible mechanistic underpinning of BTSP and as a cellular substrate of eligibility traces in cortex. Ergo, STAPCD enacts an eligibility trace that contribute to the binding of temporally separated cues and thus provide an appealing model of associative memory formation.

Discussion

The high number of paired pre- and postsynaptic stimuli required to induce STDP, along with their strict temporal relationships, renders this plasticity model attractive as a statistical correlation detector during periods of high neural activity, for instance those occurring during early circuit development. This form of plasticity is however less attractive to address the temporal credit assignment problem proper to associative few-shot learning on behavioral timescales. Here, we report in L5 pyramidal neuron of the PFC robust synaptic potentiation following the pairing of only a few pre- and postsynaptic events that are separated by periods of time (0.5 s – 1.0 s) that are substantially longer than neuronal membrane time constants and the rate of glutamate unbinding from NMDARs [6,25,30,31]. These temporal features alone exclude the involvement of canonical cellular models of Hebbian plasticity and entail the presence of a latent, slowly decaying process that can bind temporally discontiguous events in single neurons. Using a mixture of simultaneous 2P glutamate uncaging and Ca^{2+} imaging experiments, we observed and parameterized a form of associative short-term plasticity of Ca^{2+} dynamics mediated by internal ER stores that arise from a time-dependent interplay between synaptic and bAP-mediated Ca^{2+} entry. We provide temporal and pharmacological evidence that suggests that this ER-mediated STAPCD bears causal relationships with the BTSP observed at these neurons. Thus, this time-decaying short-term cellular memory process satisfies the requirements expected of synaptic eligibility traces and thus provides a cellular model for associative memory over behavioral timescales.

In agreement with previous findings in juvenile and adult pyramidal neurons in hippocampus [32,33], the profile of cytosolic Ca^{2+} transients in L5 neurons following entry through NMDARs during synaptic activation (or through VGCC during trains of bAPs) was not appreciably amplified by CICR machinery, and rather seemed slightly constrained by SERCA

activity. Our results however show that the contribution of ER stores to cytosolic Ca^{2+} transients is dynamic and depends on the state of the ER. Thus, temporally and spatially constrained synaptic activation of apical, but not basal, L5 dendrites induces a NMDAR-, mGluR-, and RyR/IP_3R-dependent amplification of the intracellular Ca^{2+} transients triggered by a subsequent burst of bAPs inasmuch as they occur within ~1 second. One parsimonious model for STAPCD is that the level *per se* of Ca^{2+} in ER stores is dynamically regulated by Ca^{2+} entry through either synaptic or VGCC sources, rendering them transiently competent to support CICR/IICR release by a subsequent instructive event. The similar time course and induction rules, along with a common set of molecular players point towards store-mediated memory of Ca^{2+} dynamics as enacting eligibility traces that are permissive to the induction of BTSP at L5 pyramidal neurons. Although some evidence supports a role of ER stores in hippocampal BTSP (O'hare et al. 2022), future work will be required to address the universality of ER stores as a mechanism for eligibility traces.

The temporal profile of BTSP induction at L5 pyramidal neurons is broadly reminiscent, but not identical, to that observed at CA1 synapses [17]. While the induction rules of BTSP are symmetrical in both regions (*i.e.*, synaptic potentiation is triggered by temporally discontiguous pairs of pre- and postsynaptic events irrespective of their relative order), those in L5 pyramidal neurons displayed a singular profile where inputs arriving within a short temporal window (100 ms - 300 ms), were not potentiated, but slightly depressed. The simulation from our experimentally parametrized computational model suggests that it likely is a consequence of the non-linearity of Ca^{2+} extrusion mechanism like that of SERCA pump activity previously reported [34,43,44,]. The temporal window for the induction of BTSP may underly a functional significance in the mPFC. In mice, sensorimotor associations require the frontal cortex, in which sensory inputs from recurrent connections to proximal dendrites could see their synaptic weight updated by BTSP instantiated by delayed contextual cues from thalamic inputs on apical dendrites on a timescale of approximately 400 ms to 1 s [19,52,53,54]. Locally instructive cues may arise from the supervisory action of other brain areas, as assumed in computational models of error-driven learning [55,56,57]. Alternatively, locally instructive cues may be features of the late-stage dynamics of response, as assumed in models of self-supervised learning [58]. Future work will be required to formally address these possibilities, and to gain a mechanistic understanding of the behavioral manifestations of BTSP in the PFC.

Experimental evidence that indirectly support the biological existence of eligibility traces came into light only relatively recently and largely rest on two distinct set of experimental evidence: 1) the finding that subthreshold STDP-like protocols are rendered effective when supplemented with a delayed instructive cue in the form of a neuromodulatory input [12,13,59] and; 2) BTSP, where the pairing of temporally discontiguous pre- and postsynaptic activation induces synaptic potentiation [17]. In the former case, the genesis of eligibility traces *per se* is conjunctive in nature since it relies on both pre- and postsynaptic events, a hallmark of STDP protocols. While BTSP and STAPCD are themselves manifestly conjunctive (*i.e.,* none are triggered by pre-or post-synaptic events alone), the underlying eligibility traces are not. Indeed, subthreshold synaptic activation (*i.e.,* that are calibrated such that it does not elicit postsynaptic spiking) can lead to robust synaptic potentiation if followed by delayed instructive postsynaptic bursting (Fig. 1; or plateau potential [19,17]). Admittedly, since the eligibility traces triggered in these conditions rely on activation of NMDARs (and mGluRs), they may be considered as requiring the conjunctive action of synaptic release with a postsynaptic event (*eg.,* a locally induced but poorly propagating dendritic spike), and thus loosely qualify as conjunctive. However, eligibility traces can be induced by trains of postsynaptic spiking alone (Fig. 1D; Fig. 2A) and is therefore manifestly not relying on a conjunctive pre- and postsynaptic operation. In this post/pre implementation, a burst of bAPs thus appears to render a large population of apical synapses eligible for subsequent potentiation, wherein it is the delayed instructive synaptic inputs that are providing synapse specificity for potentiation. Collectively, the plasticity rules involving ER-mediated eligibility traces are fundamentally distinct from those of STDP not only in providing means for how the brain addresses the temporal credit assignment problem, but also by formally identifying combinatorial relationships between firing patterns, temporal coincidence and the synaptic updating that gives rise to learning.

Acknowledgements:

This work was supported by grants from the Fonds de Recherche du Québec (L.C.B.), Natural Sciences and Engineering Research Council of Canada (L.C.B.; J.C.B.), Canadian Institute for Health Research (J.C.B.; R.N.), the uOttawa Brain and Mind Research Institute (L.C.B.; J.C.B.), Brain Canada (J.C.B.), and the Canadian Foundation for Innovation (J.C.B.). We thank members of Drs. Jean-Claude Béïque, Richard Naud and Leonard Maler labs for helpful discussions, and a special thank you to Michael B. Lynn and Dr. Mark Harnett for critically reading our manuscript.

Author contribution:

L.C.B. and J.C.B. conceptualized and designed the experimental research. L.C.B. acquired and analyzed the experimental data. L.C.B. and R.N. designed the computational model. L.C.B. implemented the computational model. L.C.B., R.N. and J.C.B. interpreted the data and wrote the manuscript.

Declaration of interests:

The authors declare no competing interests.

Data/code availability statement:

The datasets generated during the current study are available from the corresponding author on reasonable request. / The codes generated during the current study are available from the corresponding author on reasonable request.

References:

1. Magee, J. C. & Grienberger, C. Synaptic Plasticity Forms and Functions. *Annu. Rev. Neurosci.* **43**, 95–117 (2020).

2. Nicoll, R. A. A Brief History of Long-Term Potentiation. *Neuron* **93**, 281–290 (2017).

3. Tsien, J. Z. Linking Hebb's coincidence-detection to memory formation. *Curr. Opin. Neurobiol.* **10**, 266–273 (2000).

4. Martin, S. J., Grimwood, P. D. & Morris, R. G. Synaptic plasticity and memory: an evaluation of the hypothesis. *Annu. Rev. Neurosci.* **23**, 649–711 (2000).

5. Levy, W. B. & Steward, O. Temporal contiguity requirements for long-term associative potentiation/depression in the hippocampus. *Neuroscience* **8**, 791–797 (1983).

6. Markram, H., Lübke, J., Frotscher, M. & Sakmann, B. Regulation of synaptic efficacy by coincidence of postsynaptic APs and EPSPs. *Science* **275**, 213–215 (1997).

7. Bi, G. & Poo, M. Synaptic Modifications in Cultured Hippocampal Neurons: Dependence on Spike Timing, Synaptic Strength, and Postsynaptic Cell Type. *J. Neurosci.* **18**, 10464–10472 (1998).

8. Sjöström, P. J., Turrigiano, G. G. & Nelson, S. B. Rate, timing, and cooperativity jointly determine cortical synaptic plasticity. *Neuron* **32**, 1149–1164 (2001).

9. Froemke, R. C. & Dan, Y. Spike-timing-dependent synaptic modification induced by natural spike trains. *Nature* **416**, 433–438 (2002).

10. Gerstner, W., Lehmann, M., Liakoni, V., Corneil, D. & Brea, J. Eligibility Traces and Plasticity on Behavioral Time Scales: Experimental Support of NeoHebbian Three-Factor Learning Rules. *Front. Neural Circuits* **12**, (2018).

11. Sutton, R. S. & Barto, A. *Reinforcement learning: an introduction*. (The MIT Press, 2014).

12. He, K. *et al.* Distinct Eligibility Traces for LTP and LTD in Cortical Synapses. *Neuron* **88**, 528–538 (2015).

13. Fuchsberger, T. *et al.* Postsynaptic burst reactivation of hippocampal neurons enables associative plasticity of temporally discontiguous inputs. *eLife* **11**, e81071 (2022).

14. Brzosko, Z., Schultz, W. & Paulsen, O. Retroactive modulation of spike timing-dependent plasticity by dopamine. *eLife* **4**, e09685 (2015).

15. Shuler, M. G. & Bear, M. F. Reward timing in the primary visual cortex. *Science* **311**, 1606–1609 (2006).

16. Yagishita, S. *et al.* A critical time window for dopamine actions on the structural plasticity of dendritic spines. *Science* **345**, 1616–1620 (2014).

17. Bittner, K. C., Milstein, A. D., Grienberger, C., Romani, S. & Magee, J. C. Behavioral time scale synaptic plasticity underlies CA1 place fields. *Science* **357**, 1033–1036 (2017).

18. Milstein, A. D. *et al.* Bidirectional synaptic plasticity rapidly modifies hippocampal representations. *eLife* **10**, e73046 (2021).

19. Grienberger, C. & Magee, J. C. Entorhinal cortex directs learning-related changes in CA1 representations. *Nature* **611**, 554–562 (2022).

20. Froemke, R. C., Tsay, I. A., Raad, M., Long, J. D. & Dan, Y. Contribution of Individual Spikes in Burst-Induced Long-Term Synaptic Modification. *J. Neurophysiol.* **95**, 1620–1629 (2006).

21. Birtoli, B. & Ulrich, D. Firing Mode-Dependent Synaptic Plasticity in Rat Neocortical Pyramidal Neurons. *J. Neurosci.* **24**, 4935–4940 (2004).

22. Louth, E. L., Jørgensen, R. L., Korshoej, A. R., Sørensen, J. C. H. & Capogna, M. Dopaminergic Neuromodulation of Spike Timing Dependent Plasticity in Mature Adult Rodent and Human Cortical Neurons. *Front. Cell. Neurosci.* **15**, (2021).

23. Fox, K. The critical period for long-term potentiation in primary sensory cortex. *Neuron* **15**, 485–488 (1995).

24. Nowak, L., Bregestovski, P., Ascher, P., Herbet, A. & Prochiantz, A. Magnesium gates glutamate-activated channels in mouse central neurones. *Nature* **307**, 462–465 (1984).

25. Koch, C., Rapp, M. & Segev, I. A brief history of time (constants). *Cereb. Cortex N. Y. N 1991* **6**, 93–101 (1996).

26. Dembrow, N. C., Chitwood, R. A. & Johnston, D. Projection-Specific Neuromodulation of Medial Prefrontal Cortex Neurons. *J. Neurosci.* **30**, 16922–16937 (2010).

27. Anastasiades, P. G. & Carter, A. G. Circuit organization of the rodent medial prefrontal cortex. *Trends Neurosci.* **44**, 550–563 (2021).

28. Dobrunz, L. E. & Stevens, C. F. Heterogeneity of Release Probability, Facilitation, and Depletion at Central Synapses. *Neuron* **18**, 995–1008 (1997).

29. Huertas, M. A., Schwettmann, S. E. & Shouval, H. Z. The Role of Multiple Neuromodulators in Reinforcement Learning That Is Based on Competition between Eligibility Traces. *Front. Synaptic Neurosci.* **8**, (2016).

30. Balsara, R. D., Ferreira, A. N., Donahue, D. L., Castellino, F. J. & Sheets, P. L. Probing NMDA receptor GluN2A and GluN2B subunit expression and distribution in cortical neurons. *Neuropharmacology* **79**, 542–549 (2014).

31. Erreger, K., Dravid, S. M., Banke, T. G., Wyllie, D. J. & Traynelis, S. F. Subunit-specific gating controls rat NR1/NR2A and NR1/NR2B NMDA channel kinetics and synaptic signalling profiles. *J. Physiol.* **563**, 345–358 (2005).

32. Lee, K. F. H., Soares, C., Thivierge, J.-P. & Béïque, J.-C. Correlated Synaptic Inputs Drive Dendritic Calcium Amplification and Cooperative Plasticity during Clustered Synapse Development. *Neuron* **89**, 784–799 (2016).

33. Sabatini, B. L., Oertner, T. G. & Svoboda, K. The Life Cycle of Ca2+ Ions in Dendritic Spines. *Neuron* **33**, 439–452 (2002).

34. Scheuss, V., Yasuda, R., Sobczyk, A. & Svoboda, K. Nonlinear [Ca2+] Signaling in Dendrites and Spines Caused by Activity-Dependent Depression of Ca2+ Extrusion. *J. Neurosci.* **26**, 8183–8194 (2006).

35. Svoboda, K. & Yasuda, R. Principles of Two-Photon Excitation Microscopy and Its Applications to Neuroscience. *Neuron* **50**, 823–839 (2006).

36. Durand, G. M., Kovalchuk, Y. & Konnerth, A. Long-term potentiation and functional synapse induction in developing hippocampus. *Nature* **381**, 71–75 (1996).

37. Cooney, J. R., Hurlburt, J. L., Selig, D. K., Harris, K. M. & Fiala, J. C. Endosomal Compartments Serve Multiple Hippocampal Dendritic Spines from a Widespread Rather Than a Local Store of Recycling Membrane. *J. Neurosci.* **22**, 2215–2224 (2002).

38. Spacek, J. & Harris, K. M. Three-Dimensional Organization of Smooth Endoplasmic Reticulum in Hippocampal CA1 Dendrites and Dendritic Spines of the Immature and Mature Rat. *J. Neurosci.* **17**, 190–203 (1997).

39. Terasaki, M., Jaffe, L. A., Hunnicutt, G. R. & Hammer, J. A. Structural change of the endoplasmic reticulum during fertilization: evidence for loss of membrane continuity using the green fluorescent protein. *Dev. Biol.* **179**, 320–328 (1996).

40. Toresson, H. & Grant, S. G. N. Dynamic distribution of endoplasmic reticulum in hippocampal neuron dendritic spines. *Eur. J. Neurosci.* **22**, 1793–1798 (2005).

41. Power, J. M. & Sah, P. Distribution of IP3-mediated calcium responses and their role in nuclear signalling in rat basolateral amygdala neurons. *J. Physiol.* **580**, 835–857 (2007).

42. Nakamura, T., Barbara, J. G., Nakamura, K. & Ross, W. N. Synergistic release of Ca2+ from IP3-sensitive stores evoked by synaptic activation of mGluRs paired with backpropagating action potentials. *Neuron* **24**, 727–737 (1999).

43. Satoh, K. *et al.* Highly cooperative dependence of sarco/endoplasmic reticulum calcium ATPase SERCA2a pump activity on cytosolic calcium in living cells. *J. Biol. Chem.* **286**, 20591–20599 (2011).

44. Lytton, J., Westlin, M., Burk, S. E., Shull, G. E. & MacLennan, D. H. Functional comparisons between isoforms of the sarcoplasmic or endoplasmic reticulum family of calcium pumps. *J. Biol. Chem.* **267**, 14483–14489 (1992).

45. Qin, Z. *et al.* LIM domain only 4 (LMO4) regulates calcium-induced calcium release and synaptic plasticity in the hippocampus. *J. Neurosci. Off. J. Soc. Neurosci.* **32**, 4271–4283 (2012).

46. Emptage, N., Bliss, T. V. P. & Fine, A. Single Synaptic Events Evoke NMDA Receptor–Mediated Release of Calcium from Internal Stores in Hippocampal Dendritic Spines. *Neuron* **22**, 115–124 (1999).

47. Sabatini, B. L., Maravall, M. & Svoboda, K. Ca2+ signaling in dendritic spines. *Curr. Opin. Neurobiol.* **11**, 349–356 (2001).

48. Reyes, M. & Stanton, P. K. Induction of Hippocampal Long-Term Depression Requires Release of Ca2+ from Separate Presynaptic and Postsynaptic Intracellular Stores. *J. Neurosci.* **16**, 5951–5960 (1996).

49. Allbritton, N. L., Meyer, T. & Stryer, L. Range of Messenger Action of Calcium Ion and Inositol 1,4,5-Trisphosphate. *Science* **258**, 1812–1815 (1992).

50. Wootten, D., Christopoulos, A., Marti-Solano, M., Babu, M. M. & Sexton, P. M. Mechanisms of signalling and biased agonism in G protein-coupled receptors. *Nat. Rev. Mol. Cell Biol.* **19**, 638–653 (2018).

51. Ribeiro, F. M., Paquet, M., Cregan, S. P. & Ferguson, S. S. G. Group I Metabotropic Glutamate Receptor Signalling and its Implication in Neurological Disease. *CNS Neurol. Disord. - Drug Targets* **9**, 574–595.

52. Zatka-Haas, P., Steinmetz, N. A., Carandini, M. & Harris, K. D. Sensory coding and the causal impact of mouse cortex in a visual decision. *eLife* **10**, e63163 (2021).

53. Steinmetz, N. A., Zatka-Haas, P., Carandini, M. & Harris, K. D. Distributed coding of choice, action and engagement across the mouse brain. *Nature* **576**, 266–273 (2019).

54. Peters, A. J., Marica, A.-M., Fabre, J. M. J., Harris, K. D. & Carandini, M. Visuomotor learning promotes visually evoked activity in the medial prefrontal cortex. *Cell Rep.* **41**, 111487 (2022).

55. Payeur, A., Guerguiev, J., Zenke, F., Richards, B. A. & Naud, R. Burst-dependent synaptic plasticity can coordinate learning in hierarchical circuits. *Nat. Neurosci.* **24**, 1010–1019 (2021).

56. Roelfsema, P. R. & Holtmaat, A. Control of synaptic plasticity in deep cortical networks. *Nat. Rev. Neurosci.* **19**, 166–180 (2018).

57. Lillicrap, T. P., Cownden, D., Tweed, D. B. & Akerman, C. J. Random synaptic feedback weights support error backpropagation for deep learning. *Nat. Commun.* **7**, 13276 (2016).

58. Halvagal, M. S., Laborieux, A. & Zenke, F. Predictor networks and stop-grads provide implicit variance regularization in BYOL/SimSiam. Preprint at https://doi.org/10.48550/arXiv.2212.04858 (2022).

59. Frémaux, N. & Gerstner, W. Neuromodulated Spike-Timing-Dependent Plasticity, and Theory of Three-Factor Learning Rules. *Front. Neural Circuits* **9**, 85 (2015).

SUPPLEMENTARY MATERIAL

Methods

Experiments

Slice Preparation

Acute brain slices from the PFC of C57BL/6 mice P15 – P16 (STDP experiments) and P16 - P36 (BTSP experiments) were prepared in accordance with the University of Ottawa Animal Care Committee. Mice were obtained from The Jackson Laboratory and had access to food and water *ad libitum*. Acute slices were prepared following similar guidelines as previously described [55]. In brief, mice were anesthetized by inhalation of isoflurane (Baxter Corporation, Canada) and sacrificed by decapitation. The brain was immediately removed and slices were transferred to an ice-cold cutting solution containing (in mM): 119 choline-Cl, 2.5 KCl, 1 $CaCl_2$, 4.3 $MgSO_4$-$7H_2O$, 1 NaH_2PO_4, 1.3 sodium L-ascorbate, 26.2 $NaHCO_3$, and 11 glucose, and equilibrated with 95 % O_2, 5 % CO_2 gas. Slices were sectioned and transferred to a recovery chamber containing artificial cerebrospinal fluid (Ringer) solution (in mM): 119 NaCl, 2.5 $CaCl_2$, 1.3 $MgSO_4$-$7H_2O$, 1 NaH_2PO_4, 26.2 $NaHCO_3$, and 11 glucose, at a temperature of 37 °C, bubbled with 95 % O_2, 5 % CO_2. Slices were left in the recovery chamber for at least 1 hour prior to recordings at room temperature.

Whole-Cell Electrophysiology

L5 pyramidal neurons of the mPFC were visualized using an Olympus BX51W1 microscope with submersive LUMplanFL N 40x/0.8W objective. Slices were continuously perfused with Ringer solution (described in *Slice Preparation* section of the Methods). Whole-cell recordings were performed using borosilicate glass patch electrodes (4-6 MΩ; Sutter Instruments, Florida) pulled on a Narishige PC-10 pipette puller (Narishige, Japan), filled with a K^+-Gluconate-based intracellular solution containing (in mM): 115 potassium gluconate, 20 KCl, 10 sodium phosphocreatine, 10 HEPES, 4 ATP(Mg^{2+}), and 0.5 GTP (pH adjusted with KOH); or if otherwise specified, with a cesium internal solution containing (in mM): 115 cesium methane-sulfonate, 5 tetraethylammonium-Cl, 10 sodium phosphocreatine, 20 HEPES, 2.8 NaCl, 5 QX-314, 0.4 EGTA, 3 ATP (Mg^{2+}), and 0.5 GTP (pH adjusted with CsOH). Both solutions had pH 7.25 and osmolarity of 280 – 290 mOsmol/L. Internal solutions were prepared in advance and kept at -80 °C until day of experiments. Unless specified otherwise, $GABA_A$ receptor mediated currents were blocked with 100µM internal picrotoxin (PTX; Abcam). Whole-cell recordings were carried out using an Axon Multiclamp 700B amplifier, and voltage and current were low-pass filtered at 2 kHz and sampled

at 10 or 20 kHz using a Axon Digidata 1440A (or 1550) digitizer. Experiments were performed at room temperature, except where specified otherwise (30 - 32 °C using an in-line bath heater as well as a stage heater). Access resistance was monitored on each sweep using a 200 ms, 5 mV hyperpolarizing pulse, for voltage clamp recordings, or with a 400 ms, -25 pA current injection for current clamp recordings, each induced at least 800 ms prior to electrical synaptic stimulations. Only recordings with steady access resistance (± 30 %) were included. Liquid junction potential was not compensated for. For experiments conducted in current-clamp, small somatic direct current injection was at times used to maintain membrane potential between -65 mV and -75 mV to reduce probability of spiking by synaptic stimulation (see below).

Electrical Stimulation of L5 Proximal Synapses and LTP Experiments

Synaptic inputs were stimulated with a stimulating electrode proximal to L5 neurons to determine the ability of proximal synapses to undergo plasticity. Electrical stimuli of proximal synapses were delivered through a stimulation electrode (borosilicate glass; 4-6 MΩ), filled with Ringer, located < ~200 µm from the soma of the recorded neuron. The stimulating electrode was controlled with an iso-flex ULC stimulation box and stimuli were 0.1 ms in duration. The amplitude of electrical stimulation were experimentally adjusted so that to induce EPSCs of ~20 pA - 300 pA. For most plasticity experiments, two EPSCs were induced at 50 ms interval in voltage clamp every 20 s for 10 minutes (baseline recordings) and 20 minutes (post-induction recordings). The induction protocol for BTSP experiments were carried out in current clamp mode and consisted of a train of 10 (pre_t) electrical stimulation at 20Hz (alone or) paired with a 300 ms 400 pA - 600 pA ($post_b$) current injection, at variable delays. The BTSP pairing protocol was repeated 5 times every 15 seconds. STDP pairings consisted in a single presynaptic stimulation paired with a 50 ms 300 pA current injection induced 120 times at 33 Hz.

Data Analysis - Electrophysiology

Electrophysiological recordings were analyzed on Clampfit 10.7 (Molecular Devices), and Python programming language (Numpy and Scipy libraries). n refers to the number of cells recorded per experiments and all experiments were conducted on different neurons unless stated otherwise. The first EPSC of the paired-pulse in the baseline and post-induction stimulations were used for plasticity analyses. The magnitude of potentiation/depression was calculated as the mean percent change in EPSC amplitude between baseline and the last 5 minutes of post-induction recordings. Cells whose synaptic weight changed more than 3 times the standard deviation away from the mean were removed from analyses. The amplitude of the first and second EPSC in the paired pulse was used for PPR analysis. The PPR was calculated as the mean change in amplitude of the second EPSC compared to the first for baseline and post-induction recordings (post-induction/baseline).

Two-Photon Microscopy

For Ca^{2+} imaging experiments, 20 µM Alexa Fluor 594 hydrazide (Thermo Fisher Scientific) and 0.2 mM Fluo-4FF (pentapotassium salt; Thermo Fisher Scientific) were added to the recording electrode to visualize morphology and intracellular Ca^{2+}, respectively. For glutamate uncaging experiments, 2.5 mM 4-Methoxy-7-NitroIndolinyl (MNI)-caged-glutamate-trifluoroacetate (Femtonics) was added to the extracellular solution. Two-photon imaging and

glutamate uncaging were performed simultaneously using two Ti:Sapphire pulsed lasers (MaiTai DeepSee, Spectra Physics), with the imaging laser set to 810 nm (Alexa Fluor 594 and Fluo-4FF) and the stationary uncaging laser set to 720 nm (for glutamate uncaging). Independent acousto-optic modulators were coupled to a dual galvanometer scanning system (Olympus MPE-1000; BX61WI upright microscope) with a LUMplanFL N 60x/1.0W lens. Image acquisition and stimulation patterns were controlled using Olympus FV10-ASW software (Version 3). Neurons were imaged >10 min after break-in. Proximal apical dendrites were surveyed to find a dendritic segment within the same XY plane containing at least 5-6 spines. Electrophysiological recordings were performed as described in the *Whole-Cell Electrophysiology* section of the Methods. In voltage-clamp at a holding potential of -70 mV, uncaging stimulations lasted 1 ms, and were tuned to evoke small EPSCs (2 pA - 20 pA) for each stimulated spine, for a resulting compound EPSC of ~ 10 pA - 120 pA for clustered activation. The stimulations were subsequently delivered in current clamp for a resulting compound EPSP of ~ 0.1 mV - 5 mV. These stimulations induced at 20Hz for 500ms, either on their own, or paired with a 300 ms 400 pA - 600 pA somatic current injection. Ca^{2+} imaging was performed simultaneously with uncaging with a line scan probing individual dendritic spines and parent dendrite at ~0.66 kHz (~1.5ms/line). Kalman averaged (2 frames) images were obtained to visualize spine morphology. Z-stacks along the entire apical dendrites were obtained to visualize whole-cell morphology.

Data Analysis - Two-Photon Microscopy

Ca^{2+} signals were analyzed through Python programming language. Ca^{2+} signals were filtered using a smoothing filter based on the convolution of the signal with a scaled window (Hanning function). Uncaging artifacts were removed to analyze synaptic Ca^{2+} signals. Experiments where Ca^{2+} fluorescence exhibited anomalous behavior (*i.e.,* high baseline Ca^{2+} fluorescence or failure to decay) were excluded from analyses to ensure that recordings were restricted to healthy dendrites. We also excluded experiments where the Ca^{2+} signals induced by the baseline burst of bAPs (*i.e.,* 'I') differed from the recovery burst of bAPs (*i.e.,* 'III') by more than 35 %, which we inferred reflected poor dendritic health. To quantify $\Delta[Ca^{2+}]$, we computed $\Delta F/F_o$ to minimize signal-noise variability and to facilitate comparison between neurons. For each scan, the mean baseline fluorescence (F_o) was subtracted from the Ca^{2+} signal (F), which was subsequently divided by the mean baseline fluorescence (F_o): $\Delta F/F_o = (F - F_o) / F_o$. F_o was calculated using the average fluorescence over the 20 lines scans just prior to stimulation. At times, during paired stimulations of presynaptic and postsynaptic spiking, the Ca^{2+} signal failed to completely decay by the time of the second stimulation. Thus, we calculated a mono-exponential fit of Ca^{2+} decay to estimate the baseline (F_o) at the cross-section between the fit and the peak amplitude of the paired Ca^{2+} signal. In case of poor fitting, the baseline fluorescence (F_o) was overshooted by measuring the Ca^{2+} fluorescence at the start of the second (paired) stimulation. The decay time constant (τ) was calculated from a mono-exponential fit of Ca^{2+} signal from the peak fluorescence to the end of the recording (baseline) with zero offset. Fit with an average goodness of fit (R^2) < 0.4 were rejected. Synaptic Ca^{2+} events with $\Delta F/F < 0.1$ were discarded from analyses except for synaptic Ca^{2+} during D-AP5 experiments. For distance dependence experiments, a synaptic $\Delta F/F > 0.1$ was measured in the synaptic cluster before recordings outside of the synaptic cluster. Fits were obtained using the curve_fit method from the Scipy library. Images of entire neurons were analyzed on ImageJ software and assembled on Paint.

Statistics

Normality of data was determined using a Shapiro wilks test on SciPy Stats package in Python. Un-normalized EPSC data (plasticity experiments) followed a normal distribution $p > 0.05$. As such two-sided paired or unpaired Student t-test were used in plasticity experiments to compare before and after EPSCs, and between group data, respectively ($p < 0.05$ indicated with an asterisk (*) to determine statistical significance). Decay time constant and ΔF/F data did not follow a normal distribution ($p < 0.05$), therefore, we used two-sided Mann-Whitney U to compare groups and the two-sided Wilcoxon Signed Rank Test to compare before and after experiments. We used a Bonferroni correction to correct for multiple comparisons where appropriate. Pearson correlation tests were used in correlational analysis. Data are presented as means ± SEM.

Drugs and Chemicals

Drugs were added as described in text. Concentrations used for drugs not described elsewhere for the internal solution were: 20 mM 1,2-bis(o-aminophenoxy)ethane-N,N,N′,N′-tetraacetic acid (BAPTA; tetrapotassium salt); 1 mg/ml Heparin (Sodium salt); 100 µM Ryanodine, and for external solution were: 30 µM Cyclopiazonic Acid (CPA); 100 µM 5-phosphono-D-norvaline (D-AP5); 10 µM 3-[(2-methyl-1,3-thiazol-4-yl)ethynyl]-pyridine (MTEP); 5 µM YM298198 (hydrochloride), 20 µM 6-cyano-7-nitroquinoxaline-2,3-dione (CNQX). All reagents were bought from Abcam (Cambridge, MA).

Model

Model - Ca^{2+} Dynamics

Ca^{2+} dynamics emerging from pre- and postsynaptic spike trains, are defined here as $S_{pre}(t)$ and $S_{pos}(t)$, respectively. We reproduced the presynaptic spiking in our experiments with a spike train consisting of 10 presynaptic spikes at 20 Hz (for pre_t). S_{pos} (for $post_b$) was modeled based on the average number of spikes elicited by the current injection (~ 8 spikes) during experimental recordings, produced regularly during the 300 ms time frame (28.5 Hz) (see Fig. S3).

Pre- and postsynaptic spikes trigger changes in postsynaptic Ca^{2+} approximated respectively by $I_{syn} = k_{syn} S_{pre}$ and $I_{AP} = k_{AP} S_{pos}$, together giving $I_{Ca} = I_{syn} + I_{AP}$. The temporal dynamics of postsynaptic Ca^{2+} (c, baseline corrected) are given by:

$$\tau_c T_{ER}(t) \frac{d}{dt} c(t) = -c(t) + A_{ER}(t) I_{Ca}(t) \quad (1)$$

Where τ_c is the decay time constant of cytosolic Ca^{2+} in the absence of ER contributions. A_{ER} and T_{ER} model the effect of ER on the amplitude and decay time of Ca^{2+} transients, respectively (see below).

ER Ca^{2+} concentration, *e*, is modeled as being filled at the time of the last event, whether presynaptic (t_{pre}) or postsynaptic (t_{pos}). ER Ca^{2+} is assumed to decay exponentially on the time scale of τ_{ER}:

$$e(t) = k_e \left(e^{-\frac{t-t_{pre}}{\tau_{ER}}} + e^{-\frac{t-t_{pos}}{\tau_{ER}}} \right) \qquad (2)$$

Where k_e is the trace strength upon induction.

The factor A_{ER} in Eq. (1) modulates the amplitude of cytosolic Ca^{2+} transients. It is made dynamic so as to give larger amplitudes when the ER is filled. It is modeled as a readout of the state of ER at the time of an instructive signal t_* with $f(t_*) = k_f e^{-t_*/\tau_f}$ representing an exponentially decaying function with an amplitude of k_f, and decay time constant τ_f, that accelerates the effect of decaying *e* in time.

$$A_{ER}(t_*) = 1 + e(t_*)\ f(t_*) \qquad (3)$$

Similarly, the factor T_{ER} modulates the decay time of postsynaptic Ca^{2+} based on a readout of ER state, and a dynamic state *r*.

$$T_{ER}(t_*) = 1 + k_T\ \ e(t_*)\ f(t_*)\ \sigma(r(t_*)) \qquad (4)$$

where σ is the sigmoid function of *r* with sensitivity β, and k_t is a strength modulating factor. The dynamic state *r* relates to the Ca^{2+} dependence of SERCA pumps rate of transport [43,44]. It was introduced to match the observed refractory period. The relative refractory period is modeled as being triggered by previous increases in cytosolic Ca^{2+}:

$$\tau_r \frac{d}{dt} r(t) = -r(t) + k_r\ I_{Ca}(t) \qquad (5)$$

Where k_r controls the coupling between cytosolic Ca^{2+} and the refractory state and τ_r is the decay time constant of *r*.

Model – Fitting

Parameters were fitted using a set of initial parameters and an optimize minimize function using SciPy module in python to obtain the least squared error ($error_c$) between experimental data and the model parameters using the equations below:

$$error_c = \frac{2\left(\sum_i^n (\Delta f/f_{btsp_i} - \Delta f/f_i)^2 + \sum_i^n (\tau_{btsp_i} - \tau_i)^2\right)}{n} \qquad (6)$$

Where *i* is an index labeling each time point tested in the experimental protocol (250 ms - 4.5 s pre_t-$post_b$, 750 ms $post_b$-pre_t), n is the total number of time points across all protocols (n = 7), $\Delta F/F_{btsp}$ and τ_{btsp} are the experimental normalized peak fluorescence and decay time constant, and $\Delta F/F$ and τ are the values for the normalized peak Ca^{2+} and decay time constant obtained during parameter fitting for the model.

The decay time constant was obtained using the same fitting method as for the experimental data, except that in experimental recordings the fit was obtained from the peak of Ca^{2+} due to low temporal resolution of the dye, whereas in computational experiments, the decay was fitted from the last spike in the event.

We found a single set of parameters that reproduced our Ca^{2+} data in all three protocols and across all tested timescales (Fig. 5C-K; Table S1).

GENERAL DISCUSSION

How do we acquire new knowledge, store it, and retrieve it when needed? What neural mechanisms underlie these complex cognitive functions? Here, we integrated various concepts from neurobiology and computational modeling, and embarked on an extensive exploration of synaptic plasticity, eligibility traces, and one-shot learning in an attempt to reconcile features of synaptic and behavioral forms of learning.

Manuscript I-III provide a comprehensive overview of the current state and challenges of synaptic plasticity research. Manuscript I delves into the history of LTP, exploring its induction and expression mechanisms (early and late phases), its role in learning and memory, and the requirements for weight stabilization. Manuscript II focuses on the techniques employed in the study of dendrites and synapses, specifically utilizing 2-Photon (2P) Ca^{2+} imaging and glutamate uncaging. In Manuscript III, I describe recent findings showing evidence of heterosynaptic plasticity in interneurons of the visual cortex. In these neurons, sole postsynaptic bAPs are able to trigger presynaptically expressed bidirectional plasticity. The sign of plasticity is best predicted by the initial state of the synapses; weak synapses are more likely to undergo LTP, while strong synapses are more likely to experience LTD, supporting a role of heterosynaptic plasticity in weight normalization.

Manuscripts IV and V (Appendix A) address three fundamental problems in cellular models of learning. Firstly, we provide evidence that synapses can associate temporally discontiguous cues by establishing the existence of BTSP in the neocortex, and thus provide a line of solution to the temporal credit assignment problem in higher-order cognitive areas. Secondly, we uncover a biological substrate of eligibility traces. This finding provides concrete and direct evidence of *how* neurons can associate cues that are separated in time and opens avenues to understand the contingencies underlying associative learning. It also enhances our ability to simulate more efficient and effective learning algorithms. Lastly, we present evidence of burst-dependent one-shot learning under BTSP. This demonstrates that synapses have evolved to extract important information quickly and efficiently. Together, this thesis put forth evidence of biological eligibility traces, and provides evidence of rapid, and behaviorally relevant associative learning in PFC. In this discussion, I examine the connections and relationships between the findings presented in this thesis. I explore their significance beyond those explored in the manuscripts, and propose potential experimental and theoretical avenues to further expand upon these discoveries.

The biological substate of eligibility traces; properties, implications, and future directions

Understanding the relationship between synaptic plasticity and behavioral learning has been a longstanding challenge. On the one hand, traditional models of associative plasticity, such as STDP, necessitate numerous pairings of coincident pre- and postsynaptic inputs for learning to occur. On the other hand, a simple action, like grabbing a milk bottle, and its resulting outcome (*i.e.,* drinking the milk), are separated by at least several hundreds of milliseconds (200 ms - 2 s), and likely require only a few attempts to incur learning. This raises a crucial question: How can neurons learn to associate actions and outcomes in just a few trials and at behaviorally relevant time intervals?

Our experiments in Manuscript IV and V demonstrate that potentiation can be induced by a single or a few pairings of pre- and postsynaptic inputs arriving between 0 s – 1.25 s delay in the PFC. Our findings establish the presence of a form of BTSP outside the hippocampus, and provide a line of solution to the temporal credit assignment problem, but how are these cues associated in time?

In computational models of reinforcement learning, eligibility traces have been used for decades (Barto, Sutton & Anderson, 1983; Lin, 1992; Tesauro, 1992; Peng & Williams, 1994) as a solution to the temporal credit assignment problem. Eligibility traces act as a critical binding factor, determining how past events impact current ones, but only recently has indirect evidence of their existence in biological networks begun to emerge (Bittner et al., 2017; Gerstner et al., 2018; Yagishita et al., 2014). As such, we asked; what is the cellular substrate of eligibility traces?

Our first hypothesis was that BTSP binds temporally discontiguous cues through extended inactivation kinetics (~ 1 s) of NMDARs, such as those elicited by specific subunit compositions (Vicini et al., 1998). However, we disproved this hypothesis by evidence that NMDARs-mediated Ca^{2+} kinetics measured with Fluo-4FF had a decay time constant of ~ 200 ms, in line with those of canonical CA1 synapses. Instead, we established that ER Ca^{2+} stores act as an eligibility trace for synaptic plasticity on a timescale of seconds. ER stores achieve this through their competing loading and unloading functions.

We found that, during minimal Ca^{2+} events (*i.e.,* synaptic inputs or postsynaptic bursts), ER stores are being at least partially filled. This is consistent with previous findings supporting the role of ER stores as an effective Ca^{2+} sink (Hirabayashi et al., 2017; Markram et al., 1995). However, we found that these minimal Ca^{2+} events effectively transition ER from a net Ca^{2+} sink

to a release mode. This transition is upheld for 1 s, a temporal window that correspond to the one of BTSP induction. We called this effect short-term associative plasticity of Ca^{2+} dynamics (STAPCD). The release is triggered by synaptic trains or postsynaptic bursting, and depends on the conjunctive activation of pre- and postsynaptic neurons (*i.e.*, the eligibility trace cannot be induced and transformed by two synaptic trains or two postsynaptic bursts; see Manuscript V). By employing this clever strategy, ER stores can effectively bind pre- and postsynaptic inputs arriving with a second-long delay, acting as an eligibility trace for BTSP. The enactment of an eligibility trace by ER stores offers a cellular and molecular mechanism for BTSP and a solution to the temporal credit assignment problem, which bear significant implications for the fields of biology, neuroscience, and artificial intelligence (AI).

The release of ER stores was strongly dependent on IP_3Rs, adding the downstream effect of mGluR activation to the mechanism. In part, this finding was surprising since mGluRs are often associated with LTD during STDP pairings (Casimiro et al., 2011; Jo et al., 2008; Nishiyama et al., 2000). Our results imply that IP_3 can act on different timescales, possibly based on different activation patterns, to mediate opposing effects on synaptic weights. In a second part, the kinetics of IP_3 corresponds to many features that we observed in STAPCD and its involvement is therefore not so surprising. First, IP_3 remains effective for IP_3Rs activation on the order of seconds (Allbritton et al., 1992; S. S. Wang et al., 1995), permitting STAPCD to occur under the same temporal contingencies. Second, IP_3 is a long-range second messenger, and is thus able to travel to the dendrites with little degradation (C. R. Rose & Konnerth, 2001; Stuart et al., 2016), where STAPCD is observed. Third, although IP_3 can reach the dendrites, its diffusion remains largely localized, possibly restricting STAPCD to the dendritic segment adjacent to the stimulated spine cluster, and plastic modification to local synapses (Finch & Augustine, 1998; Takechi et al., 1998; S. S. Wang & Augustine, 1995).

Although Ca^{2+} stores are present in basal dendrites of L5 PFC pyramidal neurons (Milojkovic et al., 2007), some evidence suggest that they operate differently (Nakamura et al., 1999; O'Hare et al., 2022). This is consistent with our results in which we did not observe STAPCD in basal dendrites, suggesting that BTSP may be compartment specific (*i.e.*, restricted to apical dendrites). We also found that eligibility traces induction depended on clustered synaptic inputs. Single spine stimulation, albeit stimulated 10 times at 20 Hz, did not induce STAPCD. This is interesting because clustered inputs tend to carry information that are closely related in terms of content

(Losonczy & Magee, 2006, Mel, 1993, Polsky et al., 2004; Lee et al., 2016; Adoff et al., 2021; Larkum & Nevian, 2008), providing a sort of selectivity filter regarding which inputs can trigger ER-mediated eligibility traces. It also reduces the probability of random inputs to undergo BTSP, which may be critically important given the propensity of BTSP to induce strong potentiation.

The role of ER stores in BTSP corresponds well to recently published data in the hippocampus. Indeed, O'Hare et al., (2022) demonstrated that ER stores on apical, and not basal, dendrites of CA1 neurons, likely activated by clustered inputs, are important for place cells formation *in vivo*, suggesting that it may be linked to BTSP in the hippocampus. Combining these findings with ours, it suggests that ER stores may be important mediators of second-long eligibility traces in different brain regions.

One question that arises is how the dendritic signal carried out by ER stores is relocated to the synapses for synaptic weight change. Recent evidence suggests that BTSP in the hippocampus depends on CaMKII (Xiao et al., 2023). This is not entirely surprising since CaMKII has been involved in many forms of synaptic plasticity (Herring & Nicoll, 2016; Lisman et al., 2012). In addition, CaMKII can be activated in dendrites and translocate back into the spines (Lu et al., 2014; K. Shen & Meyer, 1999), and thus might bridge the spatial gap between STAPCD and synaptic weight change.

The synaptic effect of eligibility traces also raises the question of synapse specificity. Since $post_b$-pre_t protocols elicited STAPCD and BTSP, it suggests that eligibility traces can be set at each synapse upon postsynaptic bursting. For long, eligibility traces have been thought of as synaptic traces that inherently maintained synapse specificity. This concept originated from reinforcement learning models where eligibility traces appear at the connections between activated "neurons". Early evidence of eligibility traces in the brain (He et al., 2015; Yagishita et al., 2014) also implied synapse specificity, since STDP pairings were used to induce eligibility traces. However, the fundamental properties of BTSP imply that postsynaptic firing can elicit an eligibility trace at all synapses, but their transformations into potentiation are specific to recently activated synapses (up to ~ 1 s later). This feature is made possible by ER stores: Postsynaptic firing can induce Ca^{2+} influx and fill dendritic stores on a large scale, inducing an eligibility trace that is not synapse-specific. However, upon synaptic inputs, activated IP_3Rs and RyR can induce localized release, regaining synapse-specificity for plasticity.

In our quest to find a biological substrate of eligibility traces, we answer many important questions. We first established their material nature, that is their materializations by ER stores, their induction contingencies (requirements of clustered inputs, dendritic compartment specificity, length constant), and address the problem in which the eligibility trace does not appear to be synapse specific in post-pre induction paradigms. However, many questions remain. For instance, do ER stores substantiate eligibility traces in other brain regions? Can eligibility traces, and BTSP, be induced presynaptically (Bezprozvanny & Kavalali, 2020)? Are BTSP and ER-store mediated eligibility traces present in interneurons (Vullhorst et al., 2023)? Future studies will have to investigate the generality of eligibility traces to many aspects of the brain and evaluate their role in circuit, cellular and synaptic computations.

Intrinsic and Extrinsic Modulation of BTSP

Animals have remarkable ability to learn and adapt to new environments. Individuals are able to acquire and generalize knowledge from a single exposure to a stimulus or a task. Yet, reconciling this ability to our understanding of synaptic plasticity has been a challenge in the field. We examined the competency of synapses to undergo rapid changes during BTSP. Here, I provide evidence that the pairing of presynaptic trains with postsynaptic bursting at extended timescales can yield potentiation in a single pairing (Manuscript V). This induction was contingent on the presence of strong stimulations from both pre- and postsynaptic neurons as I found no plasticity when inducing a single pairing of a single presynaptic input with a postsynaptic burst (pre_s-$post_b$). STAPCD reflected these contingencies; pre_t-$post_b$ induced STAPCD in only one pairing (Manuscript IV), whereas pre_s-$post_b$ did not (Manuscript V), matching BTSP induction rules.

These results imply that neurons are able to undergo one-shot learning in response to specific signal patterns (*i.e.,* train & burst). They also imply that eligibility traces enacted by ER stores follow the same contingencies. Intriguingly, this suggests that a single presynaptic input (albeit clustered) is not sufficient to trigger the ER transition from a net sink to a net release. Instead, the transition is observed after 5 repetitions. Since repetitions were prompted every 15 s, it reveals the presence of a second eligibility trace, one that binds pairs of events through time (>15 s). The exact duration of this second trace could be determined by increasing the time between each repetition, up to the time when STAPCD and BTSP are abolished. Possibly, IP_3 or ER Ca^{2+} accumulate over each repetition before reaching threshold for plasticity-inducing release. To test this hypothesis,

future work could use intraluminal Ca^{2+} dyes and investigate the Ca^{2+} dynamics inside the ER over repeated pairings. Interestingly, the mechanism underlying one-shot learning provides a safekeep to prevent potentiation of synapses during minimal stimulations (*i.e.,* single presynaptic inputs). Collectively, these findings indicate that synapses can support learning from a single exposure, thereby enabling rapid encoding and consolidation of information. The burst-dependency of one-shot learning rules underscores a mechanism that capitalizes on specific information patterns (*i.e.*, trains and burst) to enhance the brain's ability to learn from experiences. Further investigations are needed to determine the behavioral relevance of these input patterns in the mPFC.

Our discovery of STAPCD provides important information on the Ca^{2+} dynamics underlying synaptic plasticity induction. Currently, there is no agreement regarding the mechanism by which Ca^{2+} mediates its dual effects on synaptic potentiation and depression. Arguments regarding amplitude (*i.e.*, where high Ca^{2+} leads to LTP and low Ca^{2+} leads to LTD), duration (*i.e.*, where high and fast Ca^{2+} leads to LTP, and low and long Ca^{2+} leads to LTD), and subcellular location of Ca^{2+} have been posited in the context of frequency-dependent induction of long-term synaptic plasticity and STDP (Evans & Blackwell, 2015). In manuscript IV and V, we modeled the Ca^{2+} dynamics elicited by the ER stores during the pairing of pre- and postsynaptic inputs at various time delays. Our results contradict hypotheses regarding the amplitude and duration of Ca^{2+} required for a switch in the sign of plasticity. We observed fast Ca^{2+} currents of very high and low amplitudes during induction protocols yielding depression, and found high and slow Ca^{2+} currents during induction protocols of potentiation. We have not modeled how these Ca^{2+} dynamics are transformed into synaptic weight changes. However, one hypothesis is that CaMKII integrate slower signal better than faster signals (Chang et al., 2017; S.-J. R. Lee et al., 2009; Yagishita et al., 2014), thus promoting LTP during these Ca^{2+} dynamics. Future modelling studies may include these Ca^{2+} dynamics to understand how they translate into synaptic weight change in the hope to shed light on the dual effects of Ca^{2+} in synaptic plasticity.

An important and intriguing finding in our study was the temporal profile of BTSP induction at L5 pyramidal neurons, which was broadly reminiscent, but not identical, to that observed at CA1 synapses (Manuscript IV; Bittner et al., 2017). While BTSP was symmetrical in both regions (*i.e.,* synaptic potentiation irrespective of relative input order), BTSP induced onto L5 pyramidal neurons displayed a singular profile where inputs arriving within a short temporal window (100 ms - 300 ms), were not potentiated, and even slightly depressed. This apparent

temporal notch filter was however strictly contingent on the presence of presynaptic trains (*i.e.*, pre_s-$post_b$ induced potentiation at all timescales). Using our experimentally parametrized computational model, we were able to account, at least partly, for this feature as a likely consequence of the non-linearity of SERCA pump activity determined by Ca^{2+} gradients (Manuscript IV-V). Pondering on the relevance of the timescales for BTSP (500 ms – 1 s) in the neocortex would be useful to understand its role. For instance, BTSP may be important for associating two discrete events (500 ms – 1 s), while filtering out irrelevant (or continuous) stimuli (125 ms – 300 ms). It has been shown that the sequence of events for sensorimotor associations requires motor planning, execution, sensory feedback and integration. In mice, this sequence of events takes from 400 ms to 1 s, and requires the frontal cortex (Peters et al., 2022; Steinmetz et al., 2019; Zatka-Haas et al., 2021). As such, BTSP could result from delayed coincidence between cues arriving at hundreds of milliseconds delay. It is unclear, however, why single synaptic inputs do not obey this apparent notch filter; but preliminary results (not shown here) may suggest that this switch may be contingent on pairing repetition.

Fundamentals of associative plasticity by BTSP in the neocortex

Although BTSP is a relatively novel concept, recent investigations in the hippocampus have started to formulate its operative model (Bittner et al., 2017; Fan et al., 2023; Grienberger & Magee, 2022). CA1 neurons receive EC3 inputs onto their distal apical dendrites (Suh et al., 2011; Megias et al., 2001; Steward & Scoville., 1976). These inputs carry context-related information, and are crucial in the induction of plateau potentials (Grienberger & Magee, 2022). EC3-induced plateau potentials update proximal CA2/3 inputs, that had been flagged by second-long subthreshold activity, via BTSP, leading to the induction of place cell firing on subsequent trials (Bittner et al., 2015, 2017; Fan et al., 2023). Although positing the role of BTSP in the PFC is of significant challenge, this model can serve as a guiding principle for speculating on the function of BTSP in higher-order association areas.

How may BTSP be useful to neurons in the PFC? There is a general agreement that the PFC can internally represent goals and coordinate sensory and motor processes (Diehl & Redish, 2023; Reinert et al., 2021; Santana & Artigas, 2017), yet it is unclear how neurons can achieve these representations, but may do so in a similar way the hippocampus represent flexible spatial maps (Aru et al., 2023). As opposed to the hippocampus, the PFC connectivity is complex, and not

immediately obviously arranged in an ordered manner. Generally, L5 apical dendrites are enriched by higher order thalamic inputs (Collins et al., 2018; DeNardo et al., 2015; Mair et al., 2021), whereas proximal dendrites are preferentially activated by local PFC inputs related to persistent activity (Anastasiades & Carter, 2021). A recent study has shown that L5 neurons experience a reward-predictive ramp up in membrane voltage ahead of persistent firing during a second-long delay association task (E. Kim et al., 2021). It is possible that proximal synapses evoking second-long subthreshold inputs, can be potentiated (*via* BTSP) by instructive thalamic feedback to distal L5 neurons. This potentiation may facilitate the induction and maintenance of persistent activity.

To test this hypothesis, a series of experimental tests is required. It will be imperative to use voltage indicators and *in vivo* patch clamp techniques to understand fundamental aspects of subthreshold activity and persistent firing during associative learning tasks, and answer a few important questions. First, does subthreshold activity (ramp up) and sustained firing develop during learning? Second, are some spiking events (*i.e.*, error signals) involved in triggering the ramp up in membrane voltage? Finally, which inputs are facilitating these spiking events and subthreshold increase in membrane voltage? If an error signal triggers second-long subthreshold activity and persistent firing, then it might be accomplished *via* BTSP. In this case, *in vivo* optogenetic inhibition of thalamic inputs could be used to assess its role in generating an error signal to induce sustained firing and learning. Likewise, inhibition of proximal PFC inputs can be performed to determine their requirements for sustained activity and task performance. A subsequent *in vitro* study would be important to establish a clear correlation between *in vivo* and *in vitro* findings by testing the dependence of BTSP in the PFC to thalamic and recurrent proximal inputs. This set of experiments will help guide the understanding of the role of BTSP in L5 PFC neurons. In sum, these experiments would help clarify whether thalamic inputs update locally recurrent proximal synapses via BTSP to enable persistent firing during associative learning tasks.

Intriguingly, our results provided an important consideration regarding the nature of the error signal (*i.e.*, signal used to update synaptic weights). In hippocampal neurons, the error signal manifests as a plateau potential (Magee & Grienberger, 2020). However, Manuscript IV and V suggest that plateau potentials are not necessary for BTSP in the PFC. This stems from two main findings. The first is that I induced BTSP in the PFC in the presence of K^+-Gluconate, as opposed to cesium intracellular solution. Cesium, which was used in hippocampal CA1 pyramidal neurons during the induction of BTSP (Bittner et al., 2017), blocks K^+ channels and increase dendritic

impedance, thus promoting the induction of plateau potentials by interfering with repolarization. However, when used in L5 PFC pyramidal neurons, we observed that depolarization induced by somatic current injection does not repolarize within a reasonable timeframe (Appendix B). On average, repolarization to resting membrane potential took 10 s in L5 neurons, forcing the use of K^+-Gluconate instead. Because of this, we were unable to induce a depolarization characteristic of plateaus in these conditions. Surprisingly, we were nonetheless able to induce BTSP, suggesting that plateaus are not required for BTSP in the PFC. The second finding is in Manuscript V. I explored the burst dependence of BTSP, and found that even single spikes (paired with a synaptic train; pre_t-$post_s$) were able to induce potentiation at extended timescale, further supporting that plateaus are not essential in inducing BTSP in the PFC.

Once induce, how does BTSP influence its downstream target? Automatic or stereotyped behaviors are driven by connections between sensory and motor areas, and are bottom-up operation that do not necessitate PFC involvement (*e.g.*, reflexes). However, situations requiring a high degree of flexibility, such as navigating a novel environment or adapting to changing behavioral states, demand PFC engagement, and benefit from its large connectivity (Buschman & Miller, 2007; Miller, 2000; Miller & Cohen, 2001). Pyramidal neurons in PFC are classified by their output projections, which differ by electrophysiological features. Interestingly, we found that BTSP does not depend on electrophysiological characteristic exclusive to different neural type in the PFC (*i.e.*, I_h current and SFA), suggesting a generalization of this form of plasticity to PFC neurons, regardless of their downstream targets.

Concluding remarks

Here, we provide evidence that neurons can bind temporally separated cues by means of BTSP in cortex, providing a line of solution to the temporal credit assignment problem. The timescale for the induction of BTSP highlights the ability of neurons to make connections between seemingly unrelated information. The timescales obey burst-dependent rules, providing learning flexibility. This novel form of plasticity can rapidly update synaptic weights, and thus enables rapid and efficient one-shot learning. The association of cues in time is made possible by eligibility traces sustained by ER Ca^{2+} stores through dynamic interplay between SERCA pumps, IP_3Rs and RyRs. The Ca^{2+} kinetics by ER stores challenge current models of long-term synaptic plasticity.

Together, these findings provide novel ways by which learning and memory are operated at the synaptic and cellular level, and provide solutions to long existing challenges in understanding the neural basis of associative learning.

References

Adoff, M. D., Climer, J. R., Davoudi, H., Marvin, J. S., Looger, L. L., & Dombeck, D. A. (2021). The functional organization of excitatory synaptic input to place cells. *Nature Communications*, *12*(1), Article 1. https://doi.org/10.1038/s41467-021-23829-y

Allbritton, N. L., Meyer, T., & Stryer, L. (1992). Range of Messenger Action of Calcium Ion and Inositol 1,4,5-Trisphosphate. *Science*, *258*(5089), 1812–1815. https://doi.org/10.1126/science.1465619

Anastasiades, P. G., & Carter, A. G. (2021). Circuit organization of the rodent medial prefrontal cortex. *Trends in Neurosciences*, *44*(7), 550–563. https://doi.org/10.1016/j.tins.2021.03.006

Anggono V., Huganir R. L. (2012). Regulation of AMPA receptor trafficking and synaptic plasticity. *Curr. Opin. Neurobiol.* 22, 461–469. 10.1016/j.conb.2011.12.006

Armitage, B. A., & Siegelbaum, S. A. (1998). Presynaptic induction and expression of homosynaptic depression at Aplysia sensorimotor neuron synapses. *The Journal of Neuroscience: The Official Journal of the Society for Neuroscience*, *18*(21), 8770–8779. https://doi.org/10.1523/JNEUROSCI.18-21-08770.1998

Aru, J., Drüke, M., Pikamäe, J., & Larkum, M. E. (2023). Mental navigation and the neural mechanisms of insight. *Trends in Neurosciences*, *46*(2), 100–109. https://doi.org/10.1016/j.tins.2022.11.002

Ashby, M.C., Tepikin. A.V. (2001). ER calcium and the functions of intracellular organelles. *Seminars in Cell & Developmental Biology.* 12(1). 11-17, https://doi.org/10.1006/scdb.2000.0212.

Ascher, P., & Nowak, L. (1988). The role of divalent cations in the N-methyl-D-aspartate responses of mouse central neurones in culture. *The Journal of Physiology*, *399*, 247–266. https://doi.org/10.1113/jphysiol.1988.sp017078

Baddeley, A. D., & Hitch, G. (1974). Working Memory. In G. H. Bower (Ed.), *Psychology of Learning and Motivation* (Vol. 8, pp. 47–89). Academic Press. https://doi.org/10.1016/S0079-7421(08)60452-1

Baker, A., Kalmbach, B., Morishima, M., Kim, J., Juavinett, A., Li, N., & Dembrow, N. (2018). Specialized Subpopulations of Deep-Layer Pyramidal Neurons in the Neocortex: Bridging Cellular Properties to Functional Consequences. *Journal of Neuroscience*, *38*(24), 5441–5455. https://doi.org/10.1523/JNEUROSCI.0150-18.2018

Bakin, J. S., & Weinberger, N. M. (1996). Induction of a physiological memory in the cerebral cortex by stimulation of the nucleus basalis. *Proceedings of the National Academy of Sciences of the United States of America*, *93*(20), 11219–11224. https://doi.org/10.1073/pnas.93.20.11219

Bandura, A. (1977). *Social learning theory*. Prentice Hall. http://www.gbv.de/dms/bowker/toc/9780138167448.pdf

Barakan, T. H., Downman, C. B. B., & Eccles, J. C. (1949). ELECTRIC POTENTIALS GENERATED BY ANTIDROMIC VOLLEYS IN QUADRICEPS AND HAMSTRING MOTONEURONES. *Journal of Neurophysiology*, *12*(6), 393–424. https://doi.org/10.1152/jn.1949.12.6.393

Bari, B. A., Grossman, C. D., Lubin, E. E., Rajagopalan, A. E., Cressy, J. I., & Cohen, J. Y. (2019). Stable Representations of Decision Variables for Flexible Behavior. *Neuron*, *103*(5), 922-933.e7. https://doi.org/10.1016/j.neuron.2019.06.001

Barto, A. G., Sutton, R. S., & Anderson, C. W., (1983). Neuronlike elements that can solve difficult learning control problems. *IEEE Trans. on Systems, Man, and Cybernetics*, 13, 835-846.

Bedwell, S. A., Billett, E. E., Crofts, J. J., & Tinsley, C. J. (2014). The topology of connections between rat prefrontal, motor and sensory cortices. *Frontiers in Systems Neuroscience*, *8*. https://www.frontiersin.org/articles/10.3389/fnsys.2014.00177

Bedwell, S. A., & Tinsley, C. J. (2018). Mapping of fine-scale rat prefrontal cortex connections: Evidence for detailed ordering of inputs and outputs connecting the temporal cortex and sensory-motor regions. *European Journal of Neuroscience*, *48*(3), 1944–1963. https://doi.org/10.1111/ejn.14068

Bekkers, J. M., & Stevens, C. F. (1989). NMDA and non-NMDA receptors are co-localized at individual excitatory synapses in cultured rat hippocampus. *Nature*, *341*(6239), 230–233. https://doi.org/10.1038/341230a0

Bell, C. C., Han, V. Z., Sugawara, Y., & Grant, K. (1997). Synaptic plasticity in a cerebellum-like structure depends on temporal order. *Nature*, *387*(6630), Article 6630. https://doi.org/10.1038/387278a0

Ben-Ari, Y. (1992). *ProteinkinaseCmodulationof NMDAcurrents:an important linkforLTPindudion*. *15*(9).

Berridge, M. J. (1998). Neuronal calcium signaling. *Neuron*, *21*(1), 13–26. https://doi.org/10.1016/s0896-6273(00)80510-3

Bezprozvanny, I., & Kavalali, E. T. (2020). Presynaptic endoplasmic reticulum and neurotransmission. *Cell Calcium*, *85*, 102133. https://doi.org/10.1016/j.ceca.2019.102133

Bi, G., & Poo, M. (1998). Synaptic Modifications in Cultured Hippocampal Neurons: Dependence on Spike Timing, Synaptic Strength, and Postsynaptic Cell Type. *Journal of Neuroscience*, *18*(24), 10464–10472. https://doi.org/10.1523/JNEUROSCI.18-24-10464.1998

Bittner, K. C., Grienberger, C., Vaidya, S. P., Milstein, A. D., Macklin, J. J., Suh, J., Tonegawa, S., & Magee, J. C. (2015). Conjunctive input processing drives feature selectivity in hippocampal CA1 neurons. *Nature Neuroscience*, *18*(8), Article 8. https://doi.org/10.1038/nn.4062

Bittner, K. C., Milstein, A. D., Grienberger, C., Romani, S., & Magee, J. C. (2017). Behavioral time scale synaptic plasticity underlies CA1 place fields. *Science (New York, N.Y.)*, *357*(6355), 1033–1036. https://doi.org/10.1126/science.aan3846

Bliss, T. V. P., & Lømo, T. (1973). Long-lasting potentiation of synaptic transmission in the dentate area of the anaesthetized rabbit following stimulation of the perforant path. *The Journal of Physiology*, *232*(2), 331–356.

Boucher-Routhier. M., Zhang., B.L.F., Thivierge, J.P. (2021). Extreme neural machines. Neural Networks. 144:639-647. doi: 10.1016/j.neunet.2021.09.021

Branco, T., & Häusser, M. (2011). Synaptic integration gradients in single cortical pyramidal cell dendrites. *Neuron*, *69*(5), 885–892. https://doi.org/10.1016/j.neuron.2011.02.006

Buschman, T. J., & Miller, E. K. (2007). Top-Down Versus Bottom-Up Control of Attention in the Prefrontal and Posterior Parietal Cortices. *Science*, *315*(5820), 1860–1862. https://doi.org/10.1126/science.1138071

Bush, D., & Jin, Y. (2012). Calcium control of triphasic hippocampal STDP. *Journal of Computational Neuroscience*, *33*(3), 495–514. https://doi.org/10.1007/s10827-012-0397-5

Carbone, E., & Swandulla, D. (1989). Neuronal calcium channels: Kinetics, blockade and modulation. *Progress in Biophysics and Molecular Biology*, *54*(1), 31–58. https://doi.org/10.1016/0079-6107(89)90008-4

Casimiro, T. M., Sossa, K. G., Uzunova, G., Beattie, J. B., Marsden, K. C., & Carroll, R. C. (2011). MGluR and NMDAR activation internalize distinct populations of AMPARs. *Molecular and Cellular Neurosciences*, *48*(2), 161–170. https://doi.org/10.1016/j.mcn.2011.07.007

Castellucci, V. F., & Kandel, E. R. (1974). A quantal analysis of the synaptic depression underlying habituation of the gill-withdrawal reflex in Aplysia. *Proceedings of the National Academy of Sciences of the United States of America*, *71*(12), 5004–5008. https://doi.org/10.1073/pnas.71.12.5004

Cavazzini, M., Bliss, T., & Emptage, N. (2005). Ca2+ and synaptic plasticity. *Cell Calcium*, *38*(3), 355–367. https://doi.org/10.1016/j.ceca.2005.06.013

Caya-Bissonnette, L. (2020). Heterosynaptic Plasticity in Cortical Interneurons. *The Journal of Neuroscience: The Official Journal of the Society for Neuroscience*, *40*(9), 1793–1794. https://doi.org/10.1523/JNEUROSCI.2567-19.2020

Caya-Bissonnette, L., Naud, R., & Béïque, J.-C. (2023). *Cellular Substrate of Eligibility Traces* (p. 2023.06.29.547097). bioRxiv. https://doi.org/10.1101/2023.06.29.547097

Chamberland, S., Evstratova, A., & Tóth, K. (2017). Short-Term Facilitation at a Detonator Synapse Requires the Distinct Contribution of Multiple Types of Voltage-Gated Calcium Channels. *Journal of Neuroscience*, *37*(19), 4913–4927. https://doi.org/10.1523/JNEUROSCI.0159-17.2017

Chandra, S., Kable, E. P., Morrison, G. H., & Webb, W. W. (1991). Calcium sequestration in the Golgi apparatus of cultured mammalian cells revealed by laser scanning confocal microscopy and ion microscopy. *Journal of Cell Science*, *100 (Pt 4)*, 747–752. https://doi.org/10.1242/jcs.100.4.747

Chang, J.-Y., Parra-Bueno, P., Laviv, T., Szatmari, E. M., Lee, S.-J. R., & Yasuda, R. (2017). CaMKII Autophosphorylation is Necessary for Optimal Integration of Ca2+ Signals During LTP

Induction but Not Maintenance. *Neuron, 94*(4), 800-808.e4. https://doi.org/10.1016/j.neuron.2017.04.041

Chemin, J., Girard, C., Duprat, F., Lesage, F., Romey, G., & Lazdunski, M. (2003). Mechanisms underlying excitatory effects of group I metabotropic glutamate receptors via inhibition of 2P domain K+ channels. *The EMBO Journal*, *22*(20), 5403–5411. https://doi.org/10.1093/emboj/cdg528

Chistiakova, M., Bannon, N. M., Bazhenov, M., & Volgushev, M. (2014). Heterosynaptic Plasticity: Multiple Mechanisms and Multiple Roles. *The Neuroscientist : A Review Journal Bringing Neurobiology, Neurology and Psychiatry*, *20*(5), 483–498. https://doi.org/10.1177/1073858414529829

Chistiakova, M., Ilin, V., Roshchin, M., Bannon, N., Malyshev, A., Kisvárday, Z., & Volgushev, M. (2019). Distinct Heterosynaptic Plasticity in Fast Spiking and Non-Fast-Spiking Inhibitory Neurons in Rat Visual Cortex. *The Journal of Neuroscience*, *39*(35), 6865–6878. https://doi.org/10.1523/JNEUROSCI.3039-18.2019

Cho, K., Aggleton, J. P., Brown, M. W., & Bashir, Z. I. (2001). An experimental test of the role of postsynaptic calcium levels in determining synaptic strength using perirhinal cortex of rat. *The Journal of Physiology*, *532*(Pt 2), 459–466. https://doi.org/10.1111/j.1469-7793.2001.0459f.x

Collingridge, G. L., Kehl, S. J., & McLennan, H. (1983). Excitatory amino acids in synaptic transmission in the Schaffer collateral-commissural pathway of the rat hippocampus. *The Journal of Physiology*, *334*, 33–46. https://doi.org/10.1113/jphysiol.1983.sp014478

Collins, D. P., Anastasiades, P. G., Marlin, J. J., & Carter, A. G. (2018). Reciprocal Circuits Linking the Prefrontal Cortex with Dorsal and Ventral Thalamic Nuclei. *Neuron*, *98*(2), 366-379.e4. https://doi.org/10.1016/j.neuron.2018.03.024

Cook, S. G., Buonarati, O. R., Coultrap, S. J., & Bayer, K. U. (2021). CaMKII holoenzyme mechanisms that govern the LTP versus LTD decision. *Science Advances*, *7*(16), eabe2300. https://doi.org/10.1126/sciadv.abe2300

Coombs, J. S., Eccles, J. C., & Fatt, P. (1955). The inhibitory suppression of reflex discharges from motoneurones. *The Journal of Physiology*, *130*(2), 396–413.

Cooney, J. R., Hurlburt, J. L., Selig, D. K., Harris, K. M., & Fiala, J. C. (2002). Endosomal Compartments Serve Multiple Hippocampal Dendritic Spines from a Widespread Rather Than a Local Store of Recycling Membrane. *The Journal of Neuroscience*, *22*(6), 2215–2224. https://doi.org/10.1523/JNEUROSCI.22-06-02215.2002

Constantinidis C, Franowicz MN, Goldman-Rakic PS. Coding specificity in cortical microcircuits: a multiple-electrode analysis of primate prefrontal cortex. J Neurosci. 2001;21:3646–3655

Constantinidis C, Goldman-Rakic PS. Correlated discharges among putative pyramidal neurons and interneurons in the primate prefrontal cortex. J Neurophysiol. 2002;88:3487–3497.).

Cummings, J. A., Mulkey, R. M., Nicoll, R. A., & Malenka, R. C. (1996). Ca2+ signaling requirements for long-term depression in the hippocampus. *Neuron*, *16*(4), 825–833. https://doi.org/10.1016/s0896-6273(00)80102-6

Debanne D., Gähwiler B.H., Thompson S.M., (1998). Long-term synaptic plasticity between pairs of individual CA3 pyramidal cells in rat hippocampal slice cultures. *J. Physiol.* (Lond.). 507: 237-247

del Castillo, J., & Katz, B. (1954). Quantal components of the end-plate potential. *The Journal of Physiology*, *124*(3), 560–573.

Dembrow, N. C., Zemelman, B. V., & Johnston, D. (2015). Temporal Dynamics of L5 Dendrites in Medial Prefrontal Cortex Regulate Integration Versus Coincidence Detection of Afferent Inputs. *Journal of Neuroscience*, *35*(11), 4501–4514. https://doi.org/10.1523/JNEUROSCI.4673-14.2015

DeNardo, L. A., Berns, D. S., DeLoach, K., & Luo, L. (2015). Connectivity of Mouse Somatosensory and Prefrontal Cortex Examined with Trans-synaptic Tracing. *Nature Neuroscience*, *18*(11), 1687–1697. https://doi.org/10.1038/nn.4131

Diehl, G. W., & Redish, A. D. (2023). Differential processing of decision information in subregions of rodent medial prefrontal cortex. *ELife*, *12*, e82833. https://doi.org/10.7554/eLife.82833

Dittman JS, Regehr WG 1998. Calcium dependence and recovery kinetics of presynaptic depression at the climbing fiber to Purkinje cell synapse. *J Neurosci* 18: 6147–6162

Dittman JS, Kreitzer AC, Regehr WG 2000. Interplay between facilitation, depression, and residual calcium at three presynaptic terminals. *J Neurosci* 20: 1374–1385

Dobrunz, L. E. & Stevens, C. F. Heterogeneity of Release Probability, Facilitation, and Depletion at Central Synapses. *Neuron* 18, 995–1008 (1997).

Douglas, R. M., & Goddard, G. V. (1975). Long-term potentiation of the perforant path-granule cell synapse in the rat hippocampus. *Brain Research*, *86*(2), 205–215. https://doi.org/10.1016/0006-8993(75)90697-6

Dudek S.M., Bear M.F. (1992).Homosynaptic long-term depression in area CA1 of hippocampus and effects of N-methyl-D-aspartate receptor blockade. *Proc. Natl. Acad. Sci. USA*, 89, pp. 4363-4367

Duman and Nestler EJ. Signal transduction pathways for catecholamine receptors. In: Bloom FE, Kupfer DJ, editors. Psychopharmacology: The Fourth Generation of Progress. N.Y: Raven Press; 1995. pp. 303–320

Dunfield. D., Haas. K., (2009). Metaplasticity Governs Natural Experience-Driven Plasticity of Nascent Embryonic Brain Circuits. *Neuron* 64, 240–250 DOI 10.1016/j.neuron.2009.08.034

Dunlap, K., Luebke, J. I., & Turner, T. J. (1995). Exocytotic Ca2+ channels in mammalian central neurons. *Trends in Neurosciences*, *18*(2), 89–98.

El-Hassar, L., Hagenston, A. M., D'Angelo, L. B., & Yeckel, M. F. (2011). Metabotropic glutamate receptors regulate hippocampal CA1 pyramidal neuron excitability via Ca2+ wave-dependent activation of SK and TRPC channels. *The Journal of Physiology*, *589*(Pt 13), 3211–3229. https://doi.org/10.1113/jphysiol.2011.209783

Emptage, N., Bliss, T. V. P. & Fine, A. Single Synaptic Events Evoke NMDA Receptor–Mediated Release of Calcium from Internal Stores in Hippocampal Dendritic Spines. *Neuron* 22, 115–124 (1999).

Epsztein, J., Brecht, M., & Lee, A. K. (2011). Intracellular determinants of hippocampal CA1 place and silent cell activity in a novel environment. *Neuron*, *70*(1), 109–120. https://doi.org/10.1016/j.neuron.2011.03.006

Evans, R. C., & Blackwell, K. T. (2015). Calcium: Amplitude, duration, or location? *The Biological Bulletin*, *228*(1), 75–83. https://doi.org/10.1086/BBLv228n1p75

Evstratova, A., Tóth. K,. (2011). Synaptically evoked Ca2+ release from intracellular stores is not influenced by vesicular zinc in CA3 hippocampal pyramidal neurones *JPhysiol.* 589(Pt 23):5677-89. doi: 10.1113/jphysiol.2011.216598.

Fan, L. Z., Kim, D. K., Jennings, J. H., Tian, H., Wang, P. Y., Ramakrishnan, C., Randles, S., Sun, Y., Thadhani, E., Kim, Y. S., Quirin, S., Giocomo, L., Cohen, A. E., & Deisseroth, K. (2023). All-optical physiology resolves a synaptic basis for behavioral timescale plasticity. *Cell*, *186*(3), 543-559.e19. https://doi.org/10.1016/j.cell.2022.12.035

Fatt, P., & Katz, B. (1952). Spontaneous subthreshold activity at motor nerve endings. *The Journal of Physiology*, *117*(1), 109–128.

Fayuk D, Yakel JL. (2007). Dendritic Ca2+ signalling due to activation of alpha7-containing nicotinic acetylcholine receptors in rat hippocampal neurons. J Physiol.;582:597–611.

Fei-Fei, L., Fergus, R., & Perona, P. (2006). One-shot learning of object categories. *IEEE Transactions on Pattern Analysis and Machine Intelligence*, *28*(4), 594–611. https://doi.org/10.1109/TPAMI.2006.79

Field, R. E., D'amour, J. A., Tremblay, R., Miehl, C., Rudy, B., Gjorgjieva, J., & Froemke, R. C. (2020). Heterosynaptic Plasticity Determines the Set Point for Cortical Excitatory-Inhibitory Balance. *Neuron*, *106*(5), 842-854.e4. https://doi.org/10.1016/j.neuron.2020.03.002

Finch, E. A., & Augustine, G. J. (1998). Local calcium signalling by inositol-1,4,5-trisphosphate in Purkinje cell dendrites. *Nature*, *396*(6713), 753–756. https://doi.org/10.1038/25541

Fino, E., Glowinski, J., & Venance, L. (2005). Bidirectional Activity-Dependent Plasticity at Corticostriatal Synapses. *Journal of Neuroscience*, *25*(49), 11279–11287. https://doi.org/10.1523/JNEUROSCI.4476-05.2005

Fitzjohn, S. M., Irving, A. J., Palmer, M. J., Harvey, J., Lodge, D., & Collingridge, G. L. (1996). Activation of group I mGluRs potentiates NMDA responses in rat hippocampal slices. *Neuroscience Letters*, *203*(3), 211–213. https://doi.org/10.1016/0304-3940(96)12301-6

Frank, L. M., Brown, E. N., & Wilson, M. (2000). Trajectory encoding in the hippocampus and entorhinal cortex. *Neuron*, *27*(1), 169–178. https://doi.org/10.1016/s0896-6273(00)00018-0

Froemke, R. C., Carcea, I., Barker, A. J., Yuan, K., Seybold, B. A., Martins, A. R. O., Zaika, N., Bernstein, H., Wachs, M., Levis, P. A., Polley, D. B., Merzenich, M. M., & Schreiner, C. E. (2013). Long-term modification of cortical synapses improves sensory perception. *Nature Neuroscience*, *16*(1), 79–88. https://doi.org/10.1038/nn.3274

Froemke, R. C., Merzenich, M. M., & Schreiner, C. E. (2007). A synaptic memory trace for cortical receptive field plasticity. *Nature*, *450*(7168), Article 7168. https://doi.org/10.1038/nature06289

Froemke, R. C., Poo, M.-M., & Dan, Y. (2005). Spike-timing-dependent synaptic plasticity depends on dendritic location. *Nature*, *434*(7030), 221–225. https://doi.org/10.1038/nature03366

Fuchsberger, T., Clopath, C., Jarzebowski, P., Brzosko, Z., Wang, H., & Paulsen, O. (2022). Postsynaptic burst reactivation of hippocampal neurons enables associative plasticity of temporally discontiguous inputs. *ELife*, *11*, e81071. https://doi.org/10.7554/eLife.81071

Fuster, J. M. (1973). Unit activity in prefrontal cortex during delayed-response performance: Neuronal correlates of transient memory. *Journal of Neurophysiology*, *36*(1), 61–78. https://doi.org/10.1152/jn.1973.36.1.61

Fuster JM, Alexander GE. Neuron activity related to short-term memory. *Science.* 1971;173:652–654.;

Fuster JM. The prefrontal cortex, mediator of cross-temporal contingencies. *Hum Neurobiol.* 1985;4:169–179.

Fyhn, M., Molden, S., Witter, M. P., Moser, E. I., & Moser, M.-B. (2004). Spatial representation in the entorhinal cortex. *Science (New York, N.Y.)*, *305*(5688), 1258–1264. https://doi.org/10.1126/science.1099901

Galakhova, A. A., Hunt, S., Wilbers, R., Heyer, D. B., Kock, C. P. J. de, Mansvelder, H. D., & Goriounova, N. A. (2022). Evolution of cortical neurons supporting human cognition. *Trends in Cognitive Sciences*, *26*(11), 909–922. https://doi.org/10.1016/j.tics.2022.08.012

Geddes SD, Assadzada S, Lemelin D, Sokolovski A, Bergeron R, Haj-Dahmane S, Béïque JC (2016) Target-specific modulation of the descending prefrontal cortex inputs to the dorsal raphe nucleus by cannabinoids. *Proc Natl Acad Sci* 113(19):5429-34.

Gerstner, W., Lehmann, M., Liakoni, V., Corneil, D., & Brea, J. (2018). Eligibility Traces and Plasticity on Behavioral Time Scales: Experimental Support of NeoHebbian Three-Factor Learning Rules. *Frontiers in Neural Circuits*, *12*. https://www.frontiersin.org/articles/10.3389/fncir.2018.00053

Giorgi, C., Marchi, S., & Pinton, P. (2018). The machineries, regulation and cellular functions of mitochondrial calcium. *Nature Reviews Molecular Cell Biology*, *19*(11), Article 11. https://doi.org/10.1038/s41580-018-0052-8

Glanzman, D. L. (2006). The cellular mechanisms of learning in Aplysia: Of blind men and elephants. *The Biological Bulletin*, *210*(3), 271–279. https://doi.org/10.2307/4134563

Goldman-Rakic, P. S. (1995). Cellular basis of working memory. *Neuron*, *14*(3), 477–485. https://doi.org/10.1016/0896-6273(95)90304-6

Graupner, M., & Brunel, N. (2012). Calcium-based plasticity model explains sensitivity of synaptic changes to spike pattern, rate, and dendritic location. *Proceedings of the National Academy of Sciences*, *109*(10), 3991–3996. https://doi.org/10.1073/pnas.1109359109

Grienberger, C., Chen, X., & Konnerth, A. (2015). Dendritic function in vivo. *Trends in Neurosciences*, *38*(1), 45–54. https://doi.org/10.1016/j.tins.2014.11.002

Grienberger, C., & Magee, J. C. (2022). Entorhinal cortex directs learning-related changes in CA1 representations. *Nature*, *611*(7936), 554–562. https://doi.org/10.1038/s41586-022-05378-6

Grueter, B. A., & Winder, D. G. (2009). Metabotropic Glutamate Receptors (mGluRs): Functions. In L. R. Squire (Ed.), *Encyclopedia of Neuroscience* (pp. 795–800). Academic Press. https://doi.org/10.1016/B978-008045046-9.01208-0

Haas K., Cline, K., Malinow, R., (1998). No change in NMDA receptor-mediated response rise-time during development: evidence against transmitter spillover. *Neuropharmacology.* 37(10);1393-1398 DOI: 10.1016/S0028-3908(98)00137-3

Hafting, T., Fyhn, M., Molden, S., Moser, M.-B., & Moser, E. I. (2005). Microstructure of a spatial map in the entorhinal cortex. *Nature*, *436*(7052), 801–806. https://doi.org/10.1038/nature03721

Han, V. Z., Grant, K., & Bell, C. C. (2000). Reversible associative depression and nonassociative potentiation at a parallel fiber synapse. *Neuron*, *27*(3), 611–622. https://doi.org/10.1016/s0896-6273(00)00070-2

Hansel, C., Artola, A., & Singer, W. (1996). Different threshold levels of postsynaptic [Ca2+]i have to be reached to induce LTP and LTD in neocortical pyramidal cells. *Journal of Physiology-Paris*, *90*(5), 317–319. https://doi.org/10.1016/S0928-4257(97)87906-5

Harvey, C. D., Collman, F., Dombeck, D. A., & Tank, D. W. (2009). Intracellular dynamics of hippocampal place cells during virtual navigation. *Nature*, *461*(7266), Article 7266. https://doi.org/10.1038/nature08499

Harvey-Girard, E., Lewis, J., & Maler, L. (2010). Burst-Induced Anti-Hebbian Depression Acts through Short-Term Synaptic Dynamics to Cancel Redundant Sensory Signals. *The Journal of Neuroscience*, *30*(17), 6152–6169. https://doi.org/10.1523/JNEUROSCI.0303-10.2010

He, K., Huertas, M., Hong, S. Z., Tie, X., Hell, J. W., Shouval, H., & Kirkwood, A. (2015). Distinct Eligibility Traces for LTP and LTD in Cortical Synapses. *Neuron*, *88*(3), 528–538. https://doi.org/10.1016/j.neuron.2015.09.037

Hebb, D. O. (1949). *The organization of behavior; a neuropsychological theory* (pp. xix, 335). Wiley.

Herring, B. E., & Nicoll, R. A. (2016). Long-Term Potentiation: From CaMKII to AMPA Receptor Trafficking. *Annual Review of Physiology*, *78*, 351–365. https://doi.org/10.1146/annurev-physiol-021014-071753

Hildebrand, M. E., Isope, P., Miyazaki, T., Nakaya, T., Garcia, E., Feltz, A., Schneider, T., Hescheler, J., Kano, M., Sakimura, K., Watanabe, M., Dieudonné, S., & Snutch, T. P. (2009). Functional Coupling between mGluR1 and Cav3.1 T-Type Calcium Channels Contributes to Parallel Fiber-Induced Fast Calcium Signaling within Purkinje Cell Dendritic Spines. *The Journal of Neuroscience*, *29*(31), 9668–9682. https://doi.org/10.1523/JNEUROSCI.0362-09.2009

Hirabayashi, Y., Kwon, S.-K., Paek, H., Pernice, W. M., Paul, M. A., Lee, J., Erfani, P., Raczkowski, A., Petrey, D. S., Pon, L. A., & Polleux, F. (2017). ER-mitochondria tethering by PDZD8 regulates Ca2+ dynamics in mammalian neurons. *Science (New York, N.Y.)*, *358*(6363), 623–630. https://doi.org/10.1126/science.aan6009

Hodgkin, A. L., & Huxley, A. F. (1952). Currents carried by sodium and potassium ions through the membrane of the giant axon of Loligo. *The Journal of Physiology*, *116*(4), 449–472. https://doi.org/10.1113/jphysiol.1952.sp004717

Hollmann, M., Hartley, M. & Heinemann, S. (1991). Ca2+ permeability of KA-AMPA-gated glutamate receptor channels depends on subunit composition. *Science* 252, 851–853.

Houchin, J. (1973). Procion Yellow electrodes for intracellular recording and staining of neurones in the somatosensory cortex of the rat. *The Journal of Physiology*, *232*(2), 67P-69P.

Huguenard, J. R. (1996). Low-threshold calcium currents in central nervous system neurons. *Annual Review of Physiology*, *58*, 329–348. https://doi.org/10.1146/annurev.ph.58.030196.001553

Huganir R. L., Nicoll R. A. (2013). AMPARs and synaptic plasticity: the last 25 years. *Neuron* 80, 704–717. 10.1016/j.neuron.2013.10.025

Hull, C. L. (1943). *Principles of behavior: An introduction to behavior theory* (pp. x, 422). Appleton-Century.

Hume, R. I., Dingledine, R. & Heinemann, S. F. (1991). Identification of a site in glutamate receptor subunits that controls calcium permeability. *Science* 253, 1028–1031.

Igarashi, K. M., Lee, J. Y., & Jun, H. (2022). Reconciling neuronal representations of schema, abstract task structure, and categorization under cognitive maps in the entorhinal-hippocampal-frontal circuits. *Current Opinion in Neurobiology*, *77*, 102641. https://doi.org/10.1016/j.conb.2022.102641

Inglebert, Y., Aljadeff, J., Brunel, N., & Debanne, D. (2020). Synaptic plasticity rules with physiological calcium levels. *Proceedings of the National Academy of Sciences of the United States of America*, *117*(52), 33639–33648. https://doi.org/10.1073/pnas.2013663117

Isaacson, J. S., & Murphy, G. J. (2001). Glutamate-mediated extrasynaptic inhibition: Direct coupling of NMDA receptors to Ca(2+)-activated K+ channels. *Neuron*, *31*(6), 1027–1034. https://doi.org/10.1016/s0896-6273(01)00428-7

Ito. M. (1989). Long term depression. *Ann. Rev. Neurosci*, 12, pp. 85-102

Ito. M., Sakurai, M., Tongroach. P. (1982). Climbing fibre induced depression of both mossy fibre responsiveness and glutamate sensitivity of cerebellar Purkinje cells. *J. Physiol*, 324, pp. 113-134

Jo, J., Heon, S., Kim, M. J., Son, G. H., Park, Y., Henley, J. M., Weiss, J. L., Sheng, M., Collingridge, G. L., & Cho, K. (2008). Metabotropic Glutamate Receptor-Mediated LTD Involves Two Interacting Ca2+ Sensors, NCS-1 and PICK1. *Neuron*, *60*(6), 1095–1111. https://doi.org/10.1016/j.neuron.2008.10.050

Kampa, B. M., Clements, J., Jonas, P., & Stuart, G. J. (2004). Kinetics of Mg2+ unblock of NMDA receptors: Implications for spike-timing dependent synaptic plasticity. *The Journal of Physiology*, *556*(Pt 2), 337–345. https://doi.org/10.1113/jphysiol.2003.058842

Kandel, E. R. (1976). *Cellular basis of behavior: An introduction to behavioral neurobiology* (pp. xx, 727). W. H. Freeman.

Kandel, E. R., Schwartz, J. H., & Jessell, T. M. (2000). *Principles of neural science* (4th ed). McGraw-Hill, Health Professions Division. http://catdir.loc.gov/catdir/toc/mh023/99044479.html

Katz, B., & Miledi, R. (1967). A study of synaptic transmission in the absence of nerve impulses. *The Journal of Physiology*, *192*(2), 407–436.

Keller, D. X., Franks, K. M., Jr, T. M. B., & Sejnowski, T. J. (2008). Calmodulin Activation by Calcium Transients in the Postsynaptic Density of Dendritic Spines. *PLOS ONE*, *3*(4), e2045. https://doi.org/10.1371/journal.pone.0002045

Kessels H. W., Malinow R. (2009). Synaptic AMPA receptor plasticity and behavior. *Neuron* 61, 340–350. 10.1038/nrn2501

Kilgard, M. P., & Merzenich, M. M. (1998). Cortical map reorganization enabled by nucleus basalis activity. *Science (New York, N.Y.)*, *279*(5357), 1714–1718. https://doi.org/10.1126/science.279.5357.1714

Kim, E., Bari, B. A., & Cohen, J. Y. (2021). Subthreshold basis for reward-predictive persistent activity in mouse prefrontal cortex. *Cell Reports*, *35*(5), 109082. https://doi.org/10.1016/j.celrep.2021.109082

Kim, J. N., & Shadlen, M. N. (1999). Neural correlates of a decision in the dorsolateral prefrontal cortex of the macaque. *Nature Neuroscience*, *2*(2), 176–185. https://doi.org/10.1038/5739

Kim, W. B., & Cho, J.-H. (2020). Encoding of contextual fear memory in hippocampal–amygdala circuit. *Nature Communications*, *11*(1), Article 1. https://doi.org/10.1038/s41467-020-15121-2

Kirkwood A., Dudek S.M., Gold J.T., Aizenman C.D., Bear M.F. (1993). Common forms of synaptic plasticity in the hippocampus and neocortex in vitro. *Science.*; 260: 1518-1521

Klopf, A. H., (1972). Brain function and adaptive systems--A heterostatic theory. Technical Report AFCRL72-0164, *Air Force Cambridge Research Laboratories*, Bedford, MA.

Koch GL. (1990). The endoplasmic reticulum and calcium storage. *Bioessays.* Nov;12(11):527-31. doi: 10.1002/bies.950121105. PMID: 2085319.

Kritzer MF, Goldman-Rakic PS. Intrinsic circuit organization of the major layers and sublayers of the dorsolateral prefrontal cortex in the rhesus monkey. *J Comp Neurol.* 1995;359:131–143.;

Kubota K, Niki H. Prefrontal cortical unit activity and delayed alternation performance in monkeys. *J Neurophysiology.* 1971;34:337–347.;

Kuner, T., & Schoepfer, R. (1996). Multiple structural elements determine subunit specificity of Mg2+ block in NMDA receptor channels. *The Journal of Neuroscience: The Official Journal of the Society for Neuroscience*, *16*(11), 3549–3558. https://doi.org/10.1523/JNEUROSCI.16-11-03549.1996

Lamsa, K. P., Heeroma, J. H., Somogyi, P., Rusakov, D. A., & Kullmann, D. M. (2007). Anti-Hebbian long-term potentiation in the hippocampal feedback inhibitory circuit. *Science (New York, N.Y.)*, *315*(5816), 1262–1266. https://doi.org/10.1126/science.1137450

Larkum, M. E., Kaiser, K. M., & Sakmann, B. (1999). Calcium electrogenesis in distal apical dendrites of layer 5 pyramidal cells at a critical frequency of back-propagating action potentials. *Proceedings of the National Academy of Sciences of the United States of America*, *96*(25), 14600–14604. https://doi.org/10.1073/pnas.96.25.14600

Larkum, M. E., & Nevian, T. (2008). Synaptic clustering by dendritic signalling mechanisms. *Current Opinion in Neurobiology*, *18*(3), 321–331. https://doi.org/10.1016/j.conb.2008.08.013

Larkum, M. E., Nevian, T., Sandler, M., Polsky, A., & Schiller, J. (2009). Synaptic integration in tuft dendrites of layer 5 pyramidal neurons: A new unifying principle. *Science (New York, N.Y.)*, *325*(5941), 756–760. https://doi.org/10.1126/science.1171958

Larkum, M. E., Watanabe, S., Nakamura, T., Lasser-Ross, N., & Ross, W. N. (2003). Synaptically Activated Ca2+ Waves in Layer 2/3 and Layer 5 Rat Neocortical Pyramidal Neurons. *The Journal of Physiology*, *549*(2), 471–488. https://doi.org/10.1113/jphysiol.2002.037614

Laubach, M., Amarante, L. M., Swanson, K., & White, S. R. (2018). What, If Anything, Is Rodent Prefrontal Cortex? *ENeuro*, *5*(5). https://doi.org/10.1523/ENEURO.0315-18.2018

Lee, S. W., O'Doherty, J. P., & Shimojo, S. (2015). Neural Computations Mediating One-Shot Learning in the Human Brain. *PLOS Biology*, *13*(4), e1002137. https://doi.org/10.1371/journal.pbio.1002137

Lee, S.-J. R., Escobedo-Lozoya, Y., Szatmari, E. M., & Yasuda, R. (2009). Activation of CaMKII in single dendritic spines during long-term potentiation. *Nature*, *458*(7236), 299–304. https://doi.org/10.1038/nature07842

Lehmann, M. P., Xu, H. A., Liakoni, V., Herzog, M. H., Gerstner, W., & Preuschoff, K. (2019). One-shot learning and behavioral eligibility traces in sequential decision making. *ELife*, *8*, e47463. https://doi.org/10.7554/eLife.47463

Levy, W. B., & Steward, O. (1979). Synapses as associative memory elements in the hippocampal formation. *Brain Research*, *175*(2), 233–245. https://doi.org/10.1016/0006-8993(79)91003-5

Levy, W. B., & Steward, O. (1983). Temporal contiguity requirements for long-term associative potentiation/depression in the hippocampus. *Neuroscience*, *8*(4), 791–797. https://doi.org/10.1016/0306-4522(83)90010-6

Li, L., Stefan, M. I., & Novère, N. L. (2012). Calcium Input Frequency, Duration and Amplitude Differentially Modulate the Relative Activation of Calcineurin and CaMKII. *PLOS ONE*, *7*(9), e43810. https://doi.org/10.1371/journal.pone.0043810

Liang, H., DeMaria, C. D., Erickson, M. G., Mori, M. X., Alseikhan, B. A., & Yue, D. T. (2003). Unified mechanisms of Ca2+ regulation across the Ca2+ channel family. *Neuron*, *39*(6), 951–960. https://doi.org/10.1016/s0896-6273(03)00560-9

Lin, L. J., (1992). Self-improving reactive agents based on reinforcement learning, planning and teaching. *Machine Learning*, 8(3/4), 293-321.

Lisman, J., Schulman, H., & Cline, H. (2002). The molecular basis of CaMKII function in synaptic and behavioural memory. *Nature Reviews. Neuroscience*, *3*(3), 175–190. https://doi.org/10.1038/nrn753

Lisman, J., & Spruston, N. (2005). Postsynaptic depolarization requirements for LTP and LTD: A critique of spike timing-dependent plasticity. *Nature Neuroscience*, *8*(7), 839–841. https://doi.org/10.1038/nn0705-839

Lisman, J., & Spruston, N. (2010). Questions about STDP as a General Model of Synaptic Plasticity. *Frontiers in Synaptic Neuroscience*, *2*, 140. https://doi.org/10.3389/fnsyn.2010.00140

Lisman, J., Yasuda, R., & Raghavachari, S. (2012). Mechanisms of CaMKII action in long-term potentiation. *Nature Reviews. Neuroscience*, *13*(3), 169–182. https://doi.org/10.1038/nrn3192

Liu, D., Yang, Q., & Li, S. (2013). Activation of extrasynaptic NMDA receptors induces LTD in rat hippocampal CA1 neurons. *Brain Research Bulletin*, *93*, 10–16. https://doi.org/10.1016/j.brainresbull.2012.12.003

Llinás, R., & Hess, R. (1976). Tetrodotoxin-resistant dendritic spikes in avian Purkinje cells. *Proceedings of the National Academy of Sciences of the United States of America*, *73*(7), 2520–2523. https://doi.org/10.1073/pnas.73.7.2520

López-Sanjurjo, C. I., Tovey, S. C., Prole, D. L., & Taylor, C. W. (2013). Lysosomes shape Ins(1,4,5)P3-evoked Ca2+ signals by selectively sequestering Ca2+ released from the

endoplasmic reticulum. *Journal of Cell Science*, *126*(1), 289–300. https://doi.org/10.1242/jcs.116103

Losonczy, A., Magee, J.C. (2006). Integrative properties of radial oblique dendrites in hippocampal CA1 pyramidal neurons. *Neuron*, 50, pp. 291-307

Lu, H. E., MacGillavry, H. D., Frost, N. A., & Blanpied, T. A. (2014). Multiple Spatial and Kinetic Subpopulations of CaMKII in Spines and Dendrites as Resolved by Single-Molecule Tracking PALM. *Journal of Neuroscience*, *34*(22), 7600–7610. https://doi.org/10.1523/JNEUROSCI.4364-13.2014

Lynch, Dunwiddie, T., & Gribkoff, V. (1977). Heterosynaptic depression: A postsynaptic correlate of long-term potentiation. *Nature*, *266*(5604), 737–739. https://doi.org/10.1038/266737a0

Lynch, Larson, J., Kelso, S., Barrionuevo, G., & Schottler, F. (1983). Intracellular injections of EGTA block induction of hippocampal long-term potentiation. *Nature*, *305*(5936), Article 5936. https://doi.org/10.1038/305719a0

MacDermott, A. B., Mayer, M. L., Westbrook, G. L., Smith, S. J., & Barker, J. L. (1986). NMDA-receptor activation increases cytoplasmic calcium concentration in cultured spinal cord neurones. *Nature*, *321*(6069), 519–522. https://doi.org/10.1038/321519a0

Magee, J. C., & Grienberger, C. (2020). Synaptic Plasticity Forms and Functions. *Annual Review of Neuroscience*, *43*(1), 95–117. https://doi.org/10.1146/annurev-neuro-090919-022842

Mair, R. G., Francoeur, M. J., & Gibson, B. M. (2021). Central Thalamic-Medial Prefrontal Control of Adaptive Responding in the Rat: Many Players in the Chamber. *Frontiers in Behavioral Neuroscience*, *15*. https://www.frontiersin.org/articles/10.3389/fnbeh.2021.642204

Major, G., Larkum, M. E., & Schiller, J. (2013). Active properties of neocortical pyramidal neuron dendrites. *Annual Review of Neuroscience*, *36*, 1–24. https://doi.org/10.1146/annurev-neuro-062111-150343

Makara, J. K., & Magee, J. C. (2013). Variable Dendritic Integration in Hippocampal CA3 Pyramidal Neurons. *Neuron*, *80*(6), 1438–1450. https://doi.org/10.1016/j.neuron.2013.10.033

Malenka R. C. (2003). The long-term potential of LTP. *Nat. Rev. Neurosci.* 4, 923–926. 10.1038/nrn1258

Malenka, R. C., & Bear, M. F. (2004). LTP and LTD: An Embarrassment of Riches. *Neuron*, *44*(1), 5–21. https://doi.org/10.1016/j.neuron.2004.09.012

Markram, H., Gerstner, W., & Sjöström, P. J. (2011). A History of Spike-Timing-Dependent Plasticity. *Frontiers in Synaptic Neuroscience*, *3*. https://www.frontiersin.org/articles/10.3389/fnsyn.2011.00004

Markram, H., Helm, P. J., & Sakmann, B. (1995). Dendritic calcium transients evoked by single back-propagating action potentials in rat neocortical pyramidal neurons. *The Journal of Physiology*, *485 (Pt 1)*(Pt 1), 1–20. https://doi.org/10.1113/jphysiol.1995.sp020708

Markram, H., Lübke, J., Frotscher, M., & Sakmann, B. (1997). Regulation of synaptic efficacy by coincidence of postsynaptic APs and EPSPs. *Science (New York, N.Y.)*, *275*(5297), 213–215. https://doi.org/10.1126/science.275.5297.213

Markus, E. J., Qin, Y. L., Leonard, B., Skaggs, W. E., McNaughton, B. L., & Barnes, C. A. (1995). Interactions between location and task affect the spatial and directional firing of hippocampal neurons. *Journal of Neuroscience*, *15*(11), 7079–7094. https://doi.org/10.1523/JNEUROSCI.15-11-07079.1995

Mayer, M. L., Westbrook, G. L., & Guthrie, P. B. (1984). Voltage-dependent block by Mg2+ of NMDA responses in spinal cord neurones. *Nature*, *309*(5965), 261–263. https://doi.org/10.1038/309261a0

Megias M, Emri Z, Freund TF, Gulyas AI. (2001). Total number and distribution of inhibitory and excitatory synapses on hippocampal CA1 pyramidal cells.*Neuroscience*.;102:527–540.

Mel. B.W. Synaptic integration in an excitable dendritic tree. *J. Neurophysiol.*, 70 (1993), pp. 1086-1101

Miller, E. K. (2000). The prefrontal cortex and cognitive control. *Nature Reviews. Neuroscience*, *1*(1), 59–65. https://doi.org/10.1038/35036228

Miller, E. K., & Cohen, J. D. (2001). An integrative theory of prefrontal cortex function. *Annual Review of Neuroscience*, *24*, 167–202. https://doi.org/10.1146/annurev.neuro.24.1.167

Milojkovic, B. A., Zhou, W.-L., & Antic, S. D. (2007). Voltage and calcium transients in basal dendrites of the rat prefrontal cortex. *The Journal of Physiology*, *585*(Pt 2), 447–468. https://doi.org/10.1113/jphysiol.2007.142315

Moita, M. A. P., Rosis, S., Zhou, Y., LeDoux, J. E., & Blair, H. T. (2004). Putting Fear in Its Place: Remapping of Hippocampal Place Cells during Fear Conditioning. *Journal of Neuroscience*, *24*(31), 7015–7023. https://doi.org/10.1523/JNEUROSCI.5492-03.2004

Moser, M.-B., Rowland, D. C., & Moser, E. I. (2015). Place Cells, Grid Cells, and Memory. *Cold Spring Harbor Perspectives in Biology*, *7*(2), a021808. https://doi.org/10.1101/cshperspect.a021808

Mulkey, R. M., Endo, S., Shenolikar, S., & Malenka, R. C. (1994). Involvement of a calcineurin/inhibitor-1 phosphatase cascade in hippocampal long-term depression. *Nature*, *369*(6480), 486–488. https://doi.org/10.1038/369486a0

Mulkey, R. M., & Malenka, R. C. (1992). Mechanisms underlying induction of homosynaptic long-term depression in area CA1 of the hippocampus. *Neuron*, *9*(5), 967–975. https://doi.org/10.1016/0896-6273(92)90248-c

Nabavi, S., Kessels, H. W., Alfonso, S., Aow, J., Fox, R., & Malinow, R. (2013). Metabotropic NMDA receptor function is required for NMDA receptor-dependent long-term depression. *Proceedings of the National Academy of Sciences of the United States of America*, *110*(10), 4027–4032. https://doi.org/10.1073/pnas.1219454110

Nakamura, T., Barbara, J. G., Nakamura, K., & Ross, W. N. (1999). Synergistic release of Ca2+ from IP3-sensitive stores evoked by synaptic activation of mGluRs paired with backpropagating action potentials. *Neuron*, *24*(3), 727–737. https://doi.org/10.1016/s0896-6273(00)81125-3

Naraghi, M., & Neher, E. (1997). Linearized buffered Ca2+ diffusion in microdomains and its implications for calculation of [Ca2+] at the mouth of a calcium channel. *The Journal of Neuroscience: The Official Journal of the Society for Neuroscience*, *17*(18), 6961–6973. https://doi.org/10.1523/JNEUROSCI.17-18-06961.1997

Nevian, T., Larkum, M. E., Polsky, A., & Schiller, J. (2007). Properties of basal dendrites of layer 5 pyramidal neurons: A direct patch-clamp recording study. *Nature Neuroscience*, *10*(2), 206–214. https://doi.org/10.1038/nn1826

Nishiyama, M., Hong, K., Mikoshiba, K., Poo, M. M., & Kato, K. (2000). Calcium stores regulate the polarity and input specificity of synaptic modification. *Nature*, *408*(6812), 584–588. https://doi.org/10.1038/35046067

Nowak, L., Bregestovski, P., Ascher, P., Herbet, A., & Prochiantz, A. (1984). Magnesium gates glutamate-activated channels in mouse central neurones. *Nature*, *307*(5950), Article 5950. https://doi.org/10.1038/307462a0

O'Hare, J. K., Gonzalez, K. C., Herrlinger, S. A., Hirabayashi, Y., Hewitt, V. L., Blockus, H., Szoboszlay, M., Rolotti, S. V., Geiller, T. C., Negrean, A., Chelur, V., Polleux, F., & Losonczy, A. (2022). Compartment-specific tuning of dendritic feature selectivity by intracellular Ca2+ release. *Science*, *375*(6586), eabm1670. https://doi.org/10.1126/science.abm1670

O'Keefe J 1976. Place units in the hippocampus of the freely moving rat. *Exp Neurol* 51: 78–109.

O'Keefe J, Nadel L 1978. The hippocampus as a cognitive map. Clarendon, Oxford.

O'Keefe, J., & Dostrovsky, J. (1971). The hippocampus as a spatial map. Preliminary evidence from unit activity in the freely-moving rat. *Brain Research*, *34*(1), 171–175. https://doi.org/10.1016/0006-8993(71)90358-1

Oliet, S.H., Malenka, R.C., Nicoll. R.A. (1997). Two distinct forms of long-term depression coexist in CA1 hippocampal pyramidal cells. *Neuron*, 18, pp. 969-982

Pavlov, I. P. (1910). *The work of the digestive glands* (2d English ed.). C. Griffin.

Peng, J. & Williams, R. J., (1994). Incremental multi-step Q-learning. In Machine Learning: *Proceedings of the Eleventh International Conference*, pages 226-232. Morgan Kaufmann.

Peters, A. J., Marica, A.-M., Fabre, J. M. J., Harris, K. D., & Carandini, M. (2022). Visuomotor learning promotes visually evoked activity in the medial prefrontal cortex. *Cell Reports*, *41*(3), 111487. https://doi.org/10.1016/j.celrep.2022.111487

Pi, H. J., Otmakhov, N., Lemelin, D., De Koninck, P., & Lisman, J. (2010). Autonomous CaMKII Can Promote either Long-Term Potentiation or Long-Term Depression, Depending on

the State of T305/T306 Phosphorylation. *The Journal of Neuroscience*, *30*(26), 8704–8709. https://doi.org/10.1523/JNEUROSCI.0133-10.2010

Pigott, B. M., & Garthwaite, J. (2016). Nitric Oxide Is Required for L-Type Ca2+ Channel-Dependent Long-Term Potentiation in the Hippocampus. *Frontiers in Synaptic Neuroscience*, *8*. https://www.frontiersin.org/articles/10.3389/fnsyn.2016.00017

Polsky, A., Mel, B.W., Schiller, J. (2004). Computational subunits in thin dendrites of pyramidal cells. *Nat. Neurosci*., 7, pp. 621-627

Power, J. M., & Sah, P. (2007). Distribution of IP3-mediated calcium responses and their role in nuclear signalling in rat basolateral amygdala neurons. *The Journal of Physiology*, *580*(Pt.3), 835–857. https://doi.org/10.1113/jphysiol.2006.125062

Qian, A., Buller, A. L., & Johnson, J. W. (2005). NR2 subunit-dependence of NMDA receptor channel block by external Mg2+. *The Journal of Physiology*, *562*(Pt 2), 319–331. https://doi.org/10.1113/jphysiol.2004.076737

Radulovic, J., Kammermeier, J., & Spiess, J. (1998). Generalization of fear responses in C57BL/6N mice subjected to one-trial foreground contextual fear conditioning. *Behavioural Brain Research*, *95*(2), 179–189. https://doi.org/10.1016/s0166-4328(98)00039-4

Ramaswamy, S., & Markram, H. (2015). Anatomy and physiology of the thick-tufted layer 5 pyramidal neuron. *Frontiers in Cellular Neuroscience*, *9*, 233. https://doi.org/10.3389/fncel.2015.00233

Rao, S. G., Williams, G. V., & Goldman-Rakic, P. S. (2000). Destruction and Creation of Spatial Tuning by Disinhibition: GABAA Blockade of Prefrontal Cortical Neurons Engaged by Working Memory. *Journal of Neuroscience*, *20*(1), 485–494. https://doi.org/10.1523/JNEUROSCI.20-01-00485.2000

Regehr WG, Delaney KR, Tank DW 1994. The role of presynaptic calcium in short-term enhancement at the hippocampal mossy fiber synapse. J Neurosci 14: 523–537

Reinert, S., Hübener, M., Bonhoeffer, T., & Goltstein, P. M. (2021). Mouse prefrontal cortex represents learned rules for categorization. *Nature*, *593*(7859), Article 7859. https://doi.org/10.1038/s41586-021-03452-z

Rhodes, P. (2006). The Properties and Implications of NMDA Spikes in Neocortical Pyramidal Cells. *The Journal of Neuroscience*, *26*(25), 6704–6715. https://doi.org/10.1523/JNEUROSCI.3791-05.2006

Rose, C. R., & Konnerth, A. (2001). Stores Not Just for Storage: Intracellular Calcium Release and Synaptic Plasticity. *Neuron*, *31*(4), 519–522. https://doi.org/10.1016/S0896-6273(01)00402-0

Rose, J. E., & Woolsey, C. N. (1948). The orbitofrontal cortex and its connections with the mediodorsal nucleus in rabbit, sheep and cat. *Research Publications - Association for Research in Nervous and Mental Disease*, *27 (1 vol.)*, 210–232.

Royer, S., & Paré, D. (2003). Conservation of total synaptic weight through balanced synaptic depression and potentiation. *Nature*, *422*(6931), 518–522. https://doi.org/10.1038/nature01530

Rubin, J. E., Gerkin, R. C., Bi, G. Q., & Chow, C. C. (2005). Calcium time course as a signal for spike-timing-dependent plasticity. *Journal of Neurophysiology*, *93*(5), 2600–2613. https://doi.org/10.1152/jn.00803.2004

Samborska, V., Butler, J. L., Walton, M. E., Behrens, T. E. J., & Akam, T. (2022). Complementary task representations in hippocampus and prefrontal cortex for generalizing the structure of problems. *Nature Neuroscience*, *25*(10), 1314–1326. https://doi.org/10.1038/s41593-022-01149-8

Santana, N., & Artigas, F. (2017). Laminar and Cellular Distribution of Monoamine Receptors in Rat Medial Prefrontal Cortex. *Frontiers in Neuroanatomy*, *11*, 87. https://doi.org/10.3389/fnana.2017.00087

Satoh, K., Matsu-Ura, T., Enomoto, M., Nakamura, H., Michikawa, T., & Mikoshiba, K. (2011). Highly cooperative dependence of sarco/endoplasmic reticulum calcium ATPase SERCA2a pump activity on cytosolic calcium in living cells. *The Journal of Biological Chemistry*, *286*(23), 20591–20599. https://doi.org/10.1074/jbc.M110.204685

Schall, J. D., & Hanes, D. P. (1993). Neural basis of saccade target selection in frontal eye field during visual search. *Nature*, *366*(6454), 467–469. https://doi.org/10.1038/366467a0

Schiller, J., Major, G., Koester, H. J., & Schiller, Y. (2000). NMDA spikes in basal dendrites of cortical pyramidal neurons. *Nature*, *404*(6775), 285–289. https://doi.org/10.1038/35005094

Schiller, J., Schiller, Y., Stuart, G., & Sakmann, B. (1997). Calcium action potentials restricted to distal apical dendrites of rat neocortical pyramidal neurons. *The Journal of Physiology*, *505*(Pt 3), 605–616.

Segal, M., Vlachos, A., & Korkotian, E. (2010). The spine apparatus, synaptopodin, and dendritic spine plasticity. *The Neuroscientist: A Review Journal Bringing Neurobiology, Neurology and Psychiatry*, *16*(2), 125–131. https://doi.org/10.1177/1073858409355829

Sejnowski, T. J. (1977). Storing covariance with nonlinearly interacting neurons. *Journal of Mathematical Biology*, *4*(4), 303–321. https://doi.org/10.1007/BF00275079

Sharp, A. H., McPherson, P. S., Dawson, T. M., Aoki, C., Campbell, K. P., & Snyder, S. H. (1993). Differential immunohistochemical localization of inositol 1,4,5-trisphosphate- and ryanodine-sensitive Ca2+ release channels in rat brain. *The Journal of Neuroscience: The Official Journal of the Society for Neuroscience*, *13*(7), 3051–3063. https://doi.org/10.1523/JNEUROSCI.13-07-03051.1993

Shen, J., & Yakel, J. L. (2009). Nicotinic acetylcholine receptor-mediated calcium signaling in the nervous system. *Acta Pharmacologica Sinica*, *30*(6), 673. https://doi.org/10.1038/aps.2009.64

Shen, K., & Meyer, T. (1999). Dynamic Control of CaMKII Translocation and Localization in Hippocampal Neurons by NMDA Receptor Stimulation. *Science*, *284*(5411), 162–167. https://doi.org/10.1126/science.284.5411.162

Sherrington, C. S. (1906). The Integrative Action of the Nervous System. In *Scientific and Medical Knowledge Production, 1796-1918*. Routledge.

Shigemoto, R., Nomura, S., Ohishi, H., Sugihara, H., Nakanishi, S., & Mizuno, N. (1993). Immunohistochemical localization of a metabotropic glutamate receptor, mGluR5, in the rat brain. *Neuroscience Letters*, *163*(1), 53–57. https://doi.org/10.1016/0304-3940(93)90227-C

Shouval, H. Z., Bear, M. F., & Cooper, L. N. (2002). A unified model of NMDA receptor-dependent bidirectional synaptic plasticity. *Proceedings of the National Academy of Sciences of the United States of America*, *99*(16), 10831–10836. https://doi.org/10.1073/pnas.152343099

Siegler Retchless, B., Gao, W., & Johnson, J. W. (2012). A single GluN2 subunit residue controls NMDA receptor channel properties via intersubunit interaction. *Nature Neuroscience*, *15*(3), 406–413, S1-2. https://doi.org/10.1038/nn.3025

Silver, R. A., Traynelis, S. F., & Cull-Candy, S. G. (1992). Rapid-time-course miniature and evoked excitatory currents at cerebellar synapses in situ. *Nature*, *355*(6356), Article 6356. https://doi.org/10.1038/355163a0

Skinner, B. F. (1963). Operant behavior. *American Psychologist*, *18*(8), 503–515. https://doi.org/10.1037/h0045185

Spacek, J., & Harris, K. M. (1997). Three-Dimensional Organization of Smooth Endoplasmic Reticulum in Hippocampal CA1 Dendrites and Dendritic Spines of the Immature and Mature Rat. *Journal of Neuroscience*, *17*(1), 190–203. https://doi.org/10.1523/JNEUROSCI.17-01-00190.1997

Stafstrom, C. E., Schwindt, P. C., Chubb, M. C., & Crill, W. E. (1985). Properties of persistent sodium conductance and calcium conductance of layer V neurons from cat sensorimotor cortex in vitro. *Journal of Neurophysiology*, *53*(1), 153–170. https://doi.org/10.1152/jn.1985.53.1.153

Steinmetz, N. A., Zatka-Haas, P., Carandini, M., & Harris, K. D. (2019). Distributed coding of choice, action and engagement across the mouse brain. *Nature*, *576*(7786), 266–273. https://doi.org/10.1038/s41586-019-1787-x

Steward O, Scoville SA. (1976). Cells of origin of entorhinal cortical afferents to the hippocampus and fascia dentata of the rat. *J Comp Neurol.* 169:347–370.

Stuart, E. by G., Spruston, N., & Hausser, and M. (Eds.). (2016). *Dendrites* (Third Edition, Third Edition). Oxford University Press.

Suh J, Rivest AJ, Nakashiba T, Tominaga T, Tonegawa S. (2011). Entorhinal cortext layer III input to the hippocampus is crucial for temporal association memory. *Science*. 2011;334:1415–1420.

Sutton, R. S., & Barto, A. (2014). *Reinforcement learning: An introduction* (Nachdruck). The MIT Press.

Szabo SI, Zelles T, Lendvai B. (2008). Intracellular Ca2+ dynamics of hippocampal interneurons following nicotinic acetylcholine receptor activation. *Neurochemistry International*.;52:135–41.

Takahashi, H., & Magee, J. C. (2009). Pathway interactions and synaptic plasticity in the dendritic tuft regions of CA1 pyramidal neurons. *Neuron*, *62*(1), 102–111. https://doi.org/10.1016/j.neuron.2009.03.007

Takechi, H., Eilers, J., & Konnerth, A. (1998). A new class of synaptic response involving calcium release in dendritic spines. *Nature*, *396*(6713), 757–760. https://doi.org/10.1038/25547

Tank DW, Regehr WG, Delaney KR 1995. A quantitative analysis of presynaptic calcium dynamics that contribute to short-term enhancement. J Neurosci 15: 7940–7952

Tesauro, G. J., (1992). Practical issues in temporal difference learning. *Machine Learning,* 8(3/4), 257-277.

Thorpe, S., Fize, D., & Marlot, C. (1996). Speed of processing in the human visual system. *Nature*, *381*(6582), 520–522. https://doi.org/10.1038/381520a0

Tóth, K., & McBain, C. J. (1998). Afferent-specific innervation of two distinct AMPA receptor subtypes on single hippocampal interneurons. *Nature Neuroscience*, *1*(7), 572–578. https://doi.org/10.1038/2807

Traynelis, S. F., Wollmuth, L. P., McBain, C. J., Menniti, F. S., Vance, K. M., Ogden, K. K., Hansen, K. B., Yuan, H., Myers, S. J., & Dingledine, R. (2010). Glutamate receptor ion channels: Structure, regulation, and function. *Pharmacological Reviews*, *62*(3), 405–496. https://doi.org/10.1124/pr.109.002451

Trimmer, J. S., & Rhodes, K. J. (2004). Localization of voltage-gated ion channels in mammalian brain. *Annual Review of Physiology*, *66*, 477–519. https://doi.org/10.1146/annurev.physiol.66.032102.113328

Tsien, R. W., Lipscombe, D., Madison, D. V., Bley, K. R., & Fox, A. P. (1988). Multiple types of neuronal calcium channels and their selective modulation. *Trends in Neurosciences*, *11*(10), 431–438. https://doi.org/10.1016/0166-2236(88)90194-4

Usowicz, M. M., Sugimori, M., Cherksey, B., & Llinás, R. (1992). P-type calcium channels in the somata and dendrites of adult cerebellar Purkinje cells. *Neuron*, *9*(6), 1185–1199. https://doi.org/10.1016/0896-6273(92)90076-p

Vaidya, S. P., Chitwood, R. A., & Magee, J. C. (2023). *The formation of an expanding memory representation in the hippocampus* (p. 2023.02.01.526663). bioRxiv. https://doi.org/10.1101/2023.02.01.526663

Verkhratsky, A. (2005). Physiology and pathophysiology of the calcium store in the endoplasmic reticulum of neurons. *Physiological Reviews*, *85*(1), 201–279. https://doi.org/10.1152/physrev.00004.2004

Vicini, S., Wang, J. F., Li, J. H., Zhu, W. J., Wang, Y. H., Luo, J. H., Wolfe, B. B., & Grayson, D. R. (1998). Functional and pharmacological differences between recombinant N-methyl-D-aspartate receptors. *Journal of Neurophysiology*, *79*(2), 555–566. https://doi.org/10.1152/jn.1998.79.2.555

Vullhorst, D., Bloom, M. S., Akella, N., & Buonanno, A. (2023). ER-PM Junctions on GABAergic Interneurons Are Organized by Neuregulin 2/VAP Interactions and Regulated by NMDA Receptors. *International Journal of Molecular Sciences*, *24*(3), Article 3. https://doi.org/10.3390/ijms24032908

Wallis, J. D., Anderson, K. C., & Miller, E. K. (2001). Single neurons in prefrontal cortex encode abstract rules. *Nature*, *411*(6840), Article 6840. https://doi.org/10.1038/35082081

Wang, S. S., Alousi, A. A., & Thompson, S. H. (1995). The lifetime of inositol 1,4,5-trisphosphate in single cells. *The Journal of General Physiology*, *105*(1), 149–171. https://doi.org/10.1085/jgp.105.1.149

Wang, S. S., & Augustine, G. J. (1995). Confocal imaging and local photolysis of caged compounds: Dual probes of synaptic function. *Neuron*, *15*(4), 755–760. https://doi.org/10.1016/0896-6273(95)90167-1

Wang, X. J. (2001). Synaptic reverberation underlying mnemonic persistent activity. *Trends in Neurosciences*, *24*(8), 455–463. https://doi.org/10.1016/s0166-2236(00)01868-3

Wang, Y. T., & Linden, D. J. (2000). Expression of Cerebellar Long-Term Depression Requires Postsynaptic Clathrin-Mediated Endocytosis. *Neuron*, *25*(3), 635–647. https://doi.org/10.1016/S0896-6273(00)81066-1

Weaver, J. (2015). How One-Shot Learning Unfolds in the Brain. *PLOS Biology*, *13*(4), e1002138. https://doi.org/10.1371/journal.pbio.1002138

Weisskopf, M. G., Bauer, E. P., & LeDoux, J. E. (1999). L-Type Voltage-Gated Calcium Channels Mediate NMDA-Independent Associative Long-Term Potentiation at Thalamic Input Synapses to the Amygdala. *The Journal of Neuroscience*, *19*(23), 10512–10519. https://doi.org/10.1523/JNEUROSCI.19-23-10512.1999

Willshaw, D., & Dayan, P. (1990). Optimal plasticity from matrix memories: What goes up must come down. *Neural Computation*, *2*(1), 85–93. https://doi.org/10.1162/neco.1990.2.1.85

Wilson MA, McNaughton BL 1993. Dynamics of the hippocampal ensemble code for space. *Science* 261: 1055–1058.

Wood, E. R., Dudchenko, P. A., Robitsek, R. J., & Eichenbaum, H. (2000). Hippocampal neurons encode information about different types of memory episodes occurring in the same location. *Neuron*, *27*(3), 623–633. https://doi.org/10.1016/s0896-6273(00)00071-4

Wrighton, D. C., Baker, E. J., Chen, P. E., & Wyllie, D. J. A. (2008). Mg2+ and memantine block of rat recombinant NMDA receptors containing chimeric NR2A/2D subunits expressed in Xenopus laevis oocytes. *Journal of Physiology*, *586*(1), 211–225. https://doi.org/10.1113/jphysiol.2007.143164

Xiao, K., Li, Y., Chitwood, R. A., & Magee, J. C. (2023). *A critical role for CaMKII in behavioral timescale synaptic plasticity in hippocampal CA1 pyramidal neurons* (p. 2023.04.18.537377). bioRxiv. https://doi.org/10.1101/2023.04.18.537377

Yagishita, S., Hayashi-Takagi, A., Ellis-Davies, G. C. R., Urakubo, H., Ishii, S., & Kasai, H. (2014). A critical time window for dopamine actions on the structural plasticity of dendritic spines. *Science*, *345*(6204), 1616–1620. https://doi.org/10.1126/science.1255514

Yang, S. N., Tang, Y. G., & Zucker, R. S. (1999). Selective induction of LTP and LTD by postsynaptic [Ca2+]i elevation. *Journal of Neurophysiology*, *81*(2), 781–787. https://doi.org/10.1152/jn.1999.81.2.781

Yang, S.-T., Shi, Y., Wang, Q., Peng, J.-Y., & Li, B.-M. (2014). Neuronal representation of working memory in the medial prefrontal cortex of rats. *Molecular Brain*, *7*, 61. https://doi.org/10.1186/s13041-014-0061-2

Youn, D., Gerber, G., & Sather, W. A. (2013). Ionotropic Glutamate Receptors and Voltage-Gated Ca^{2+} Channels in Long-Term Potentiation of Spinal Dorsal Horn Synapses and Pain Hypersensitivity. *Neural Plasticity*, *2013*, e654257. https://doi.org/10.1155/2013/654257

Yu, W., Kwon, J., Sohn, J., Lee, S. H., Kim, S., & Ho, W. (2018). MGluR5-dependent modulation of dendritic excitability in CA1 pyramidal neurons mediated by enhancement of persistent Na+ currents. *The Journal of Physiology*, *596*(17), 4141–4156. https://doi.org/10.1113/JP275999

Zatka-Haas, P., Steinmetz, N. A., Carandini, M., & Harris, K. D. (2021). Sensory coding and the causal impact of mouse cortex in a visual decision. *ELife*, *10*, e63163. https://doi.org/10.7554/eLife.63163

Zeng, H., Chattarji, S., Barbarosie, M., Rondi-Reig, L., Philpot, B. D., Miyakawa, T., Bear, M. F., & Tonegawa, S. (2001). Forebrain-specific calcineurin knockout selectively impairs bidirectional synaptic plasticity and working/episodic-like memory. *Cell*, *107*(5), 617–629. https://doi.org/10.1016/s0092-8674(01)00585-2

Zito K., Scheuss, V. 2009, NMDA Receptor Function and Physiological Modulation, *Encyclopedia of Neurosciences.* 1157-1164. DOI: 10.1016/B978-008045046-9.01225-0

Zhang, L. I., Tao, H. W., Holt, C. E., Harris, W. A., & Poo, M. (1998). A critical window for cooperation and competition among developing retinotectal synapses. *Nature*, *395*(6697), 37–44. https://doi.org/10.1038/25665

APPENDICES

Appendix A – Manuscript V

This manuscript is in early stage of preparation.

Evidence of burst-dependent one shot-learning in PFC.

Authors: Léa Caya-Bissonnette, Jean-Claude Béïque

Author contribution: L.C.B. conceptualized, designed and carried out the experiments. J.C.B provided fundings.

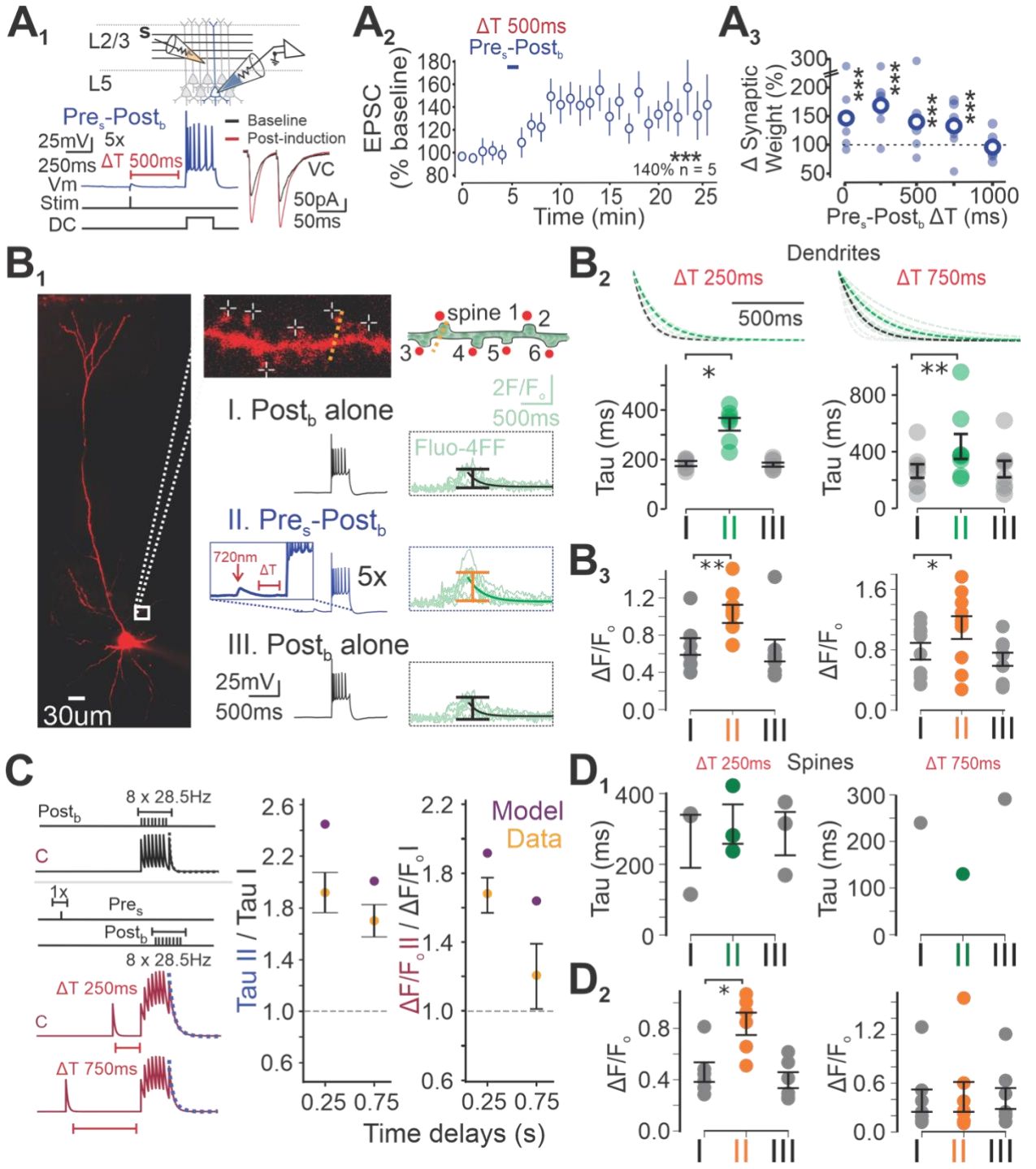

Figure 1. Single synaptic inputs paired with burst firing induce BTSP and STAPCD. (A) A_1 Cartoon (top) and representative trace of a single synaptic inputs paired with a postsynaptic burst at 500 ms delay in current clamp (left) and baseline and post-pairing EPSCs in voltage clamp (VC; right). A_2 Resulting normalized EPSC change over time after 5 pairings (n = 5 neurons, p = 0.00027). A_3 Mean synaptic weight change for protocol at different timing intervals (50 ms: n = 6 neurons, p = 2.64 x 10^{-5}, 250 ms: n = 7 neurons, p = 2.90 x 10^{-16}, 500 ms: as shown in A_2, 750 ms: n = 7 neurons, p = 5.46 x 10^{-7}, 1000 ms: n = 9 neurons, p = 0.43). (B) B_1 Image of L5 PFC neuron

(left). Representative voltage trace and resulting Ca^{2+} traces of three $post_b$ given at 30 s interval with the second $post_b$ preceded by a single glutamate uncaging pulse on spatially clustered spines at varying time intervals, repeated 5 times (right). B_2 Resulting dendritic decay traces and time constants for protocol of 250 ms (n = 7 dendrites, p = 0.016) and 750 ms (n = 8 dendrites, p = 0.0078) delay. B_3 Same as B_2 except for ΔF/F values for 250 ms (n = 8 dendrites, p = 0.0078) and 750 ms (n = 10 dendrites, p = 0.0039) delay. C) Modeled Ca^{2+} traces of $post_b$ (black) and pre_s-$post_b$ pairings at 250ms and 750ms (red) (left). Relative normalized decay time constants (middle) and peak amplitudes (right). D) D_1 same as B_2, except for spine values (250 ms: n = 6 dendrites, p = 0.031, and 750 ms: n = 8 spines, p = 0.46). D_2 Same as D_1, except for tau values (250 ms: n = 3 dendrites, p = 0.75, and 750 ms: n = 1 spine). * $p < 0.05$, ** $p < 0.01$, *** $p < 0.001$. Data shown as mean ± sem.

Textual explanation:

I had previously found that L5 pyramidal neurons of the PFC can undergo BTSP after five pairings of presynaptic trains (10 stimulations at 20 Hz) and postsynaptic bursting (300 ms 600 pA somatic current injection; Manuscript IV). I asked whether this input pattern was crucial to the induction of BTSP, by testing whether a single synaptic input paired with postsynaptic bursting in L5 pyramidal neurons would also induce BTSP (*i.e.*, delays in the hundreds of milliseconds). I thus induced pairings with a temporal delay between presynaptic and postsynaptic stimulations of 500 ms, a timescale far outlasting that of STDP induction (Markram et al., 1997; Bi and Poo, 1998: Nowak et al., 1984; Koch et al.,1996), and found, strikingly, that this protocol induced robust potentiation (Fig. 1A; 140.32 ± 10.08 %). I parameterized the timing delay between pre_s-$post_b$ (0 s – 1 s) and found significant potentiation when burst bAPs arrived with a delay of up to ~1 s (Fig. 1A), suggesting that single synaptic inputs can induce plasticity at behaviorally relevant time interval if paired with a postsynaptic burst.

The binding of pre- and postsynaptic neurons at extended timescales has been shown to be enabled by ER-mediated short-term associative plasticity of Ca^{2+} dynamics (STAPCD), acting as an eligibility trace for BTSP (Manuscript IV). Thus, we next tested whether a similar protocol in which synaptic inputs are induced with glutamate uncaging paired with postsynaptic bursting ($uPre_s$-$post_b$) could elicit STAPCD in L5 PFC pyramidal neurons. We found that a single EPSP (elicited by uncaging onto spatially clustered spines) elicited an amplification of Ca^{2+} transients triggered by subsequent postsynaptic APs (Fig. 1B). This amplification was observed with both intermediate (250 ms) and extended timescales (750 ms), closely matching the temporal contingencies of BTSP induced by the pairing of pre_s-$post_b$. This effect could be simulated by our

model developed in Manuscript IV (Fig. 1C), and was only partially observed in spines (Fig. 1D), as expected from previous results. Together, these results suggest that a single synaptic inputs, albeit stimulating 5-6 clustered spines, is sufficient to induce an eligibility trace observed by evidence of STAPCD and BTSP, if paired with a postsynaptic burst under ~ 1 s.

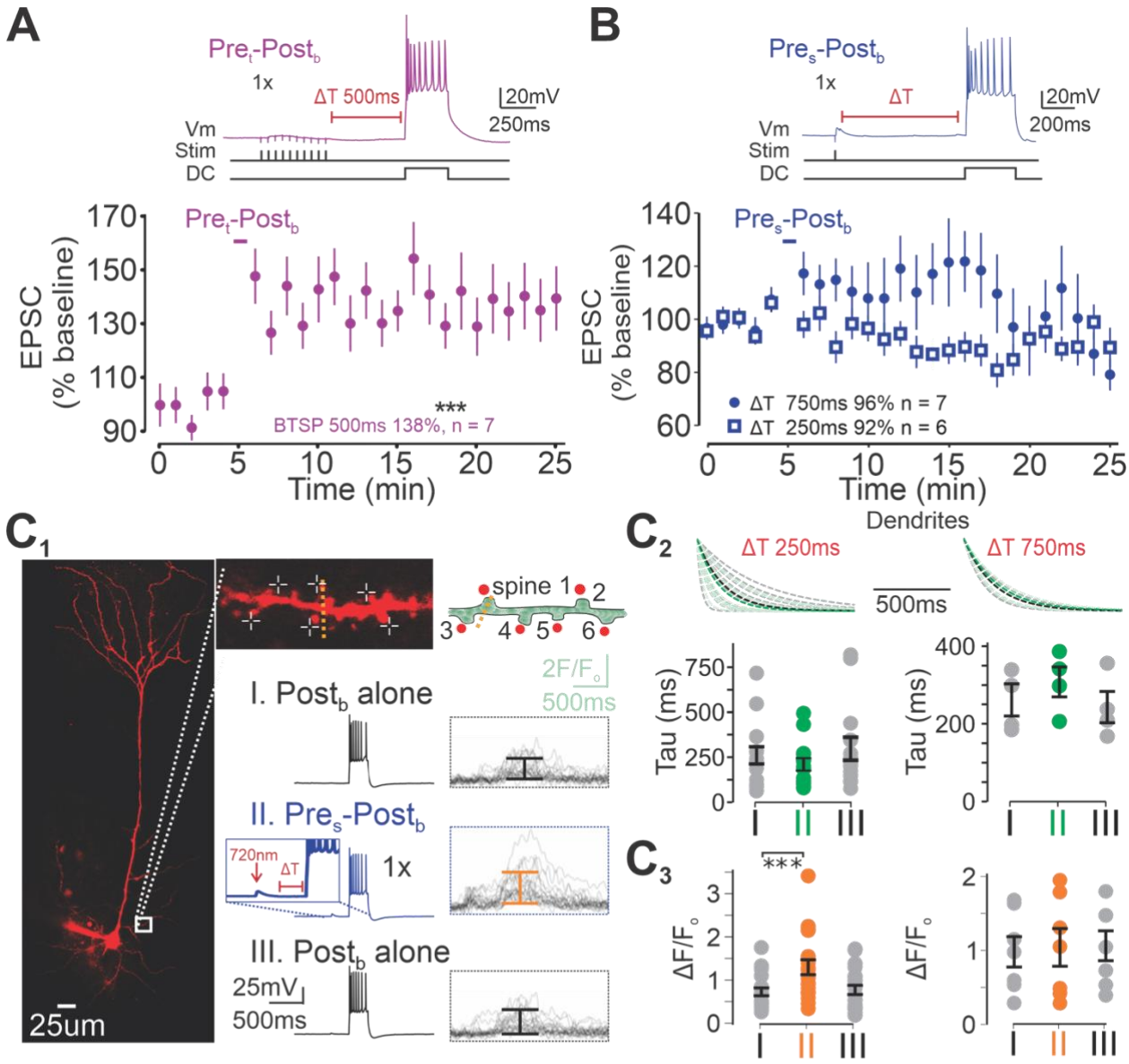

Figure 2. Bursting rules for one shot BTSP and STAPCD. A) Representative trace of a single pairing of a synaptic train with a postsynaptic burst (top). Resulting synaptic weight change (bottom; n = 7 neurons, $p = 4.12 \times 10^{-7}$). B) Same as A, except for the pairing of a single synaptic input instead of a train. C) C_1 Image of L5 PFC neuron (left). Representative voltage trace and resulting Ca^{2+} traces of three post$_b$ given at 30 s interval with the second post$_b$ preceded by a single glutamate uncaging pulse on spatially clustered spines at varying time intervals (right). C_2 Resulting dendritic decay traces and time constants for protocol of 250 ms (n = 13 dendrites, p = 0.22) and 750 ms (n = 4 dendrites, p = 0.71) delay. C_3 Same as C_2 except for ΔF/F values for 250 ms (n = 20 dendrites, $p = 4.77 \times 10^{-5}$) and 750 ms (n = 7 dendrites, p = 0.69) delay. *** $p < 0.001$. Data shown as mean ± sem.

Textual explanation:

Learning simple tasks or information can occur rapidly, sometimes even in a single trial. It is unclear how the brain can achieve such efficient learning, however, the very few pairings required for BTSP induction may provide a solution to this problem. We thus tested whether BTSP can be induced by a single pairing of pre_t-$post_b$ or pre_s-$post_b$. Intriguingly, we found that pre_t-$post_b$, and not pre_s-$post_b$, induced BTSP in a single pairing (Fig 2A-B), suggesting that BTSP can sustain rapid updating of synaptic weights depending on input patterns.

We investigated whether STAPCD was also bound by the same contingencies. In manuscript IV, we were able to induce STAPCD in a single repetition of pre_t-$post_b$. Here, we observed that a single pairing of pre_s-$post_b$ was not sufficient to induce STAPCD (Fig. 2C). Together, these experiments revealed that the eligibility trace can be induce by a single presynaptic train, but not by a single presynaptic input; and, in the latter case, may instead accumulate over a longer timescale such that five repetitions (every 15 s) can induce the eligibility trace.

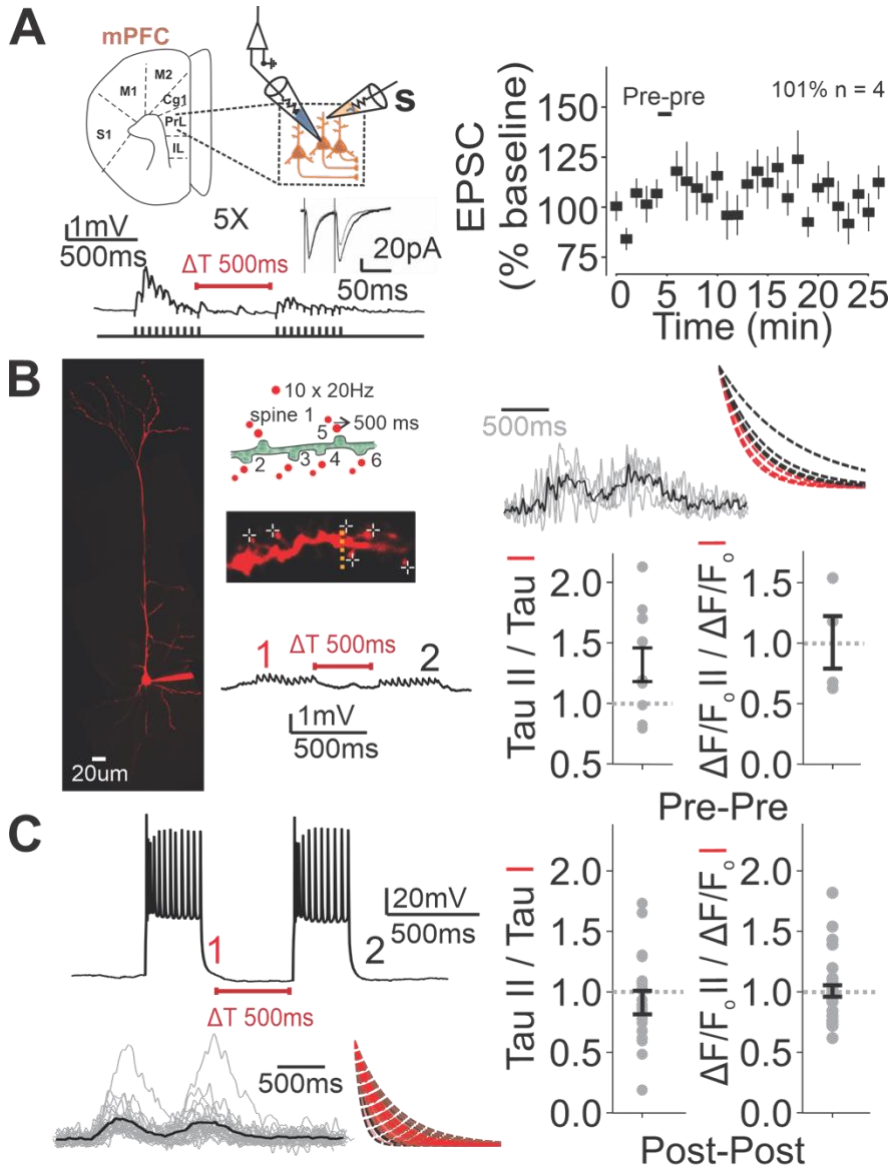
A
mPFC
M2
M1
Cg1
PrL
IL
S1
S
1mV
500ms
5X
20pA
ΔT 500ms
50ms
EPSC (% baseline)
150
125
100
75
Pre-pre
101% n = 4
0 5 10 15 20 25
Time (min)
B
10 x 20Hz
spine 1
500 ms
5
2 3 4 6
20um
1
ΔT 500ms
2
1mV
500ms
500ms
Tau II / Tau I
2.0
1.5
1.0
0.5
ΔF/F0 II / ΔF/F0 I
1.5
1.0
0.5
0.0
Pre-Pre
C
20mV
500ms
1
2
ΔT 500ms
500ms
Tau II / Tau I
2.0
1.5
1.0
0.5
0.0
ΔF/F0 II / ΔF/F0 I
2.0
1.5
1.0
0.5
0.0
Post-Post

Figure 3. Conjunction of pre- and postsynaptic activity is required for BTSP and STAPCD. A) Representative trace of two presynaptic trains paired 5 times at 500 ms delay (left). Resulting synaptic weight changes (right). B) Representative trace of two presynaptic trains paired 5 times at 500 ms delay induced by glutamate uncaging on clustered synapses (left). Resulting Ca^{2+} and decay traces (top right). Resulting decay time constant and $\Delta F/F$ values of the Ca^{2+} influx induced by the second train relative to the first (bottom right). C) Same as B) except for two postsynaptic bursts induced by somatic current injection. Data shown as mean ± sem.

Textual explanation:

Although we had previously found that BTSP was dependent on the association of two inputs (see Manuscript IV), we had not tested whether BTSP induction required the conjunction of pre- and postsynaptic activity. To this end, we induced five pairings of two presynaptic trains at 500 ms, and found no plasticity (Fig. 3A). Although STAPCD acts as an eligibility trace for BTSP, it is possible that it can be induced by two pre- or two postsynaptic spiking activity, but that a third factor is necessary to transform the eligibility trace into synaptic weight change. As such, we next tested whether STAPCD also required conjunctive action of pre- and postsynaptic activity. We found that pairing two synaptic trains or two postsynaptic bursts at 500 ms did not induce an increase in Ca^{2+}, suggesting that STAPCD requires the action of both pre- and postsynaptic inputs for its induction.

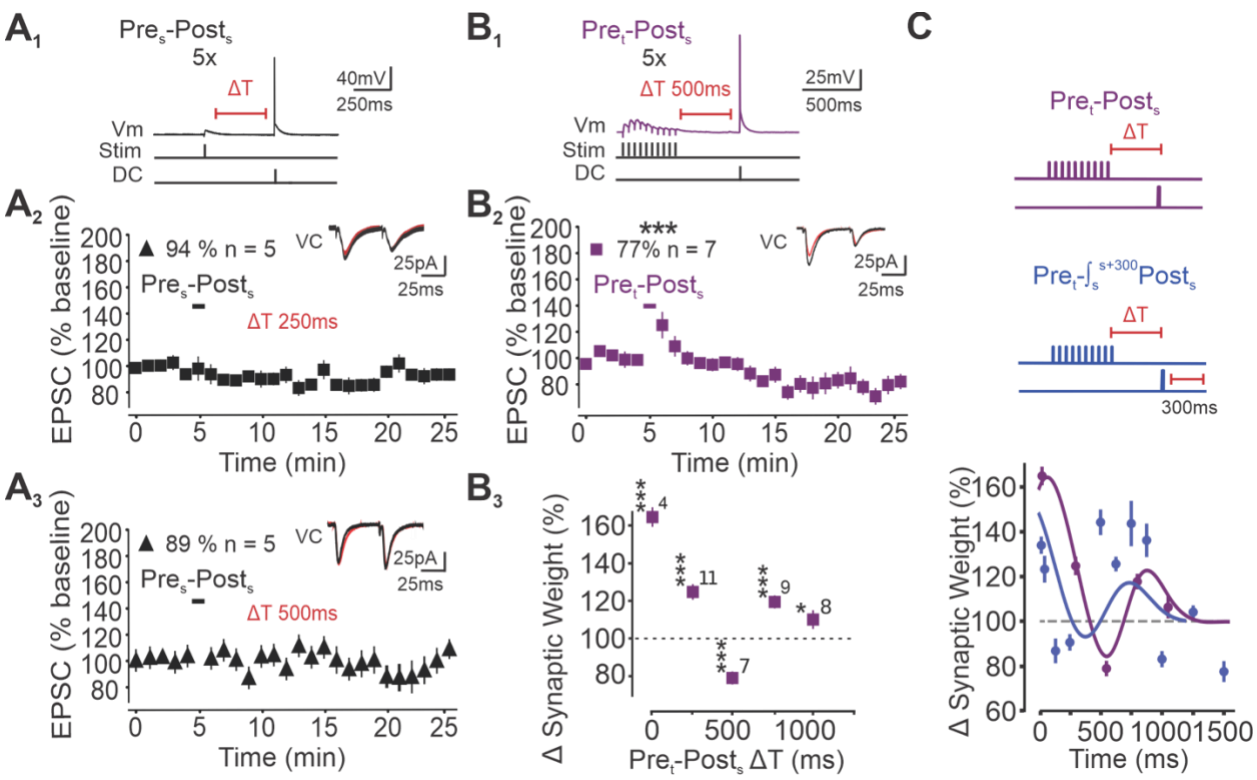

Figure 4. Dependency of BTSP to postsynaptic burst firing. (A) A_1 Representative trace of pre_s-$post_s$ pairings at 500 ms delay in current clamp (left) and baseline and post-pairing EPSCs in voltage clamp (right). A_2 Normalized EPSCs change for protocol shown in A_1 at $\Delta T = 250$ ms (n = 5 neurons, p = 0.075). A_3 Same as A_2, except for $\Delta T = 500$ ms (n = 5 neurons, p = 0.079). (B) B_1 Representative trace of pre_t-$post_s$ pairings (left). B_2 Normalized EPSCs change for protocol shown in B_1 (n = 7 neurons, 1.18×10^{-6}). B_3 Resulting mean synaptic weight change for timing intervals of 0 ms (n = 4 neurons, $p = 1.63 \times 10^{-8}$), 250 ms (n = 11 neurons, $p = 9.94 \times 10^{-7}$), 500 ms (as shown in B_2), 750 ms (n = 9 neurons, $p = 3 \times 10^{-9}$), 1000 ms (n = 8 neurons, p = 0.016). (C) Schematic of computational experiment (top). Fit obtained by three spline functions (black line) of results redrawn from B_3 (black dots), and integral of the fit over 300 ms (blue line) and synaptic weight change for pre_t-$post_b$ protocols redrawn from Fig 1 in Manuscript IV (blue dots), suggesting that pre_t-$post_b$ weight change result from the cumulation of plasticity over the length of $post_b$ (300 ms) from the pre_t-$post_s$ trace. *p < 0.05, ***p < 0.001. Data are shown as mean ± sem.

Textual explanation:

During our investigation, we delved into the burst dependence of BTSP and made a notable discovery, such that single synaptic stimulation induced STAPCD and BTSP if paired with a postsynaptic burst (Fig. 1). As such, we continued our investigation to test whether 5 pairings of a synaptic train with a single spike (pre_t-$post_s$), were capable of inducing potentiation at extended delays. We found that this pairing induced potentiation following a temporal profile broadly analogous to the induction rules of BTSP induced by the pairing of a synaptic train and postsynaptic bursting (pre_t-$post_b$; see Manuscript IV), but with a temporal shift (Fig. 4B). We thus hypothesized that pre_t-$post_b$ plasticity reflects the convolved accumulation of plasticity triggered by multiple postsynaptic spikes, each obeying the learning rule revealed in the pre_t-$post_s$ protocol. Using a model, we tested this idea and found that pre_t-$post_s$ predicted the timing, but not the amplitude of plasticity of pre_t-$post_b$ pairings (Fig. 4C). The finding that pre_t-$post_s$ is sufficient to induce BTSP was surprising, in that it implies that plateau potentials are not required to induce BTSP in the PFC. Importantly, pairings of single synaptic stimulation with single bAP (pre_s-$post_s$) did not induce plasticity (250 ms - 500 ms; Fig. 4A). Collectively, these results showed that strong stimulation of either presynaptic or postsynaptic neurons is essential for BTSP induction in mPFC L5 pyramidal neurons, but that confluence of both is not necessary.

Appendix B - Supplementals for Manuscript IV

Parameters	Definitions	Values
k_{syn}	Amplitude of synaptic currents	5.11
k_{AP}	Amplitude of AP currents	4.83
τ_c (ms)	Decay time constant of Ca^{2+}	23.48
k_e	Amplitude of Ca^{2+} currents in ER	1.91
τ_{ER} (ms)	Decay time constant of ER state	999.25
k_f	Amplitude of function *f*	0.29
τ_f (ms)	Decay time constant of function *f*	1618.17
k_t	Strength modulating factor	0.91
β	Sensitivity of sigmoidal function	0.0024
k_r	Coupling between cytosolic Ca^{2+} and *r*	80.81
τ_r (ms)	Decay time constant of *r*	664.91

Table S1. Fitted Parameters for Ca^{2+} Model.

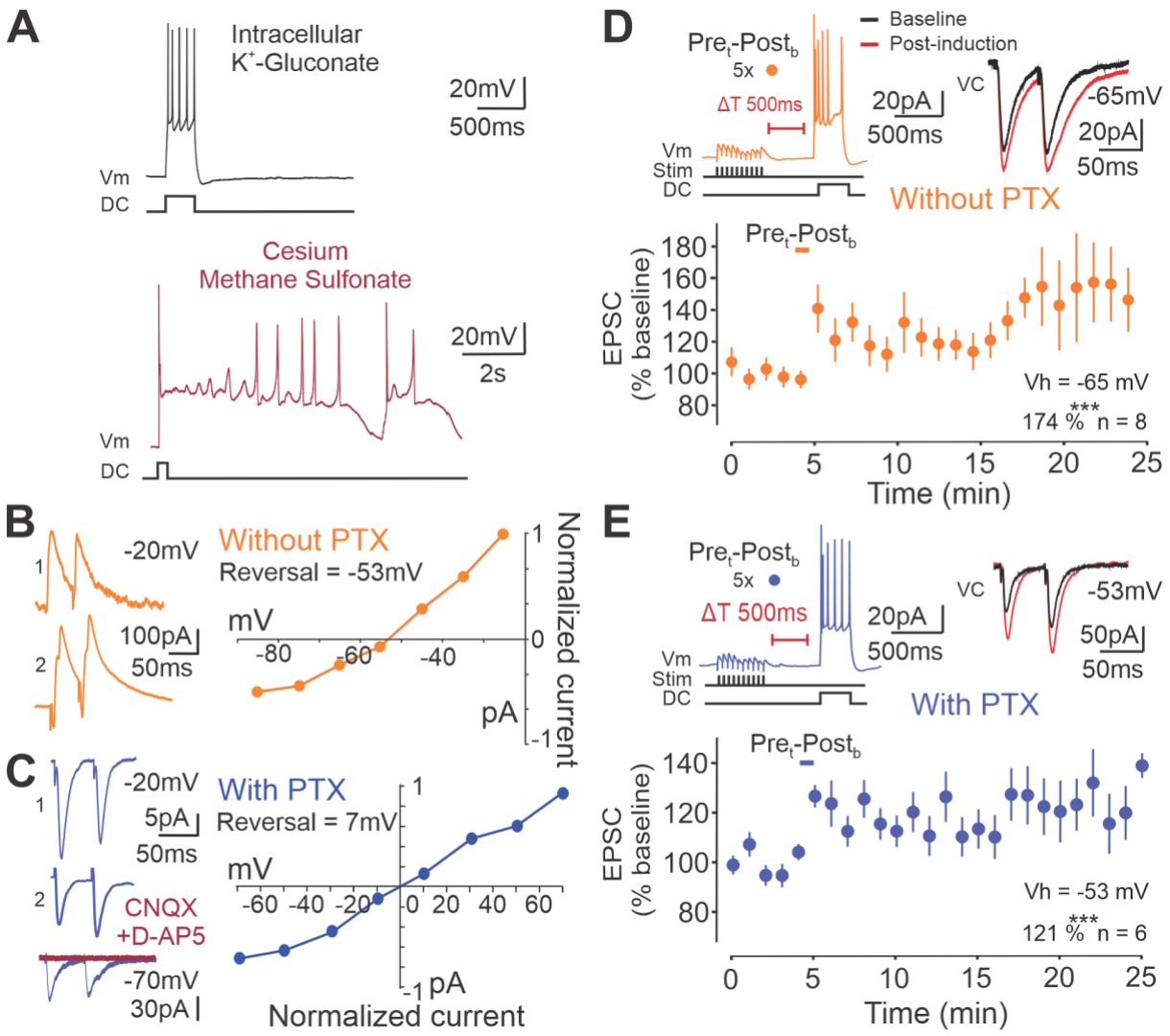

Figure S1. PTX does not affect BTSP. (A) Representative traces of membrane voltage of L5 pyramidal neurons of the mPFC during a post$_b$ with K^+-Gluconate (top) or Cesium (bottom) based intracellular solution. Due to the time for repolarization, we used K^+-Gluconate internal solution for the remaining of our recordings. (B) Two representative EPSC traces obtained by paired stimulation at 50 ms interval without PTX while holding at -20 mV using K^+-Gluconate intracellular solution (left). Amplitude of EPSCs (pA) against membrane voltage (mV). (C) Same as B except in the presence of intracellular PTX (blue), and example trace of EPSCs after 10 µM CNQX and 100 µM D-AP5 wash-in (red; lower left). (D) Representative trace of pre$_t$-post$_b$ pairings and EPSCs recorded without PTX at -65 mV (top) and resulting normalized EPSCs change over time (n = 8 neurons, p = 5.63 x 10^{-8}, bottom). (E) Same as in D except with PTX and holding at -53 mV (at reversal; n = 6 neurons, p = 0.00011). Vh: Voltage holding. Data are shown as mean ± sem.

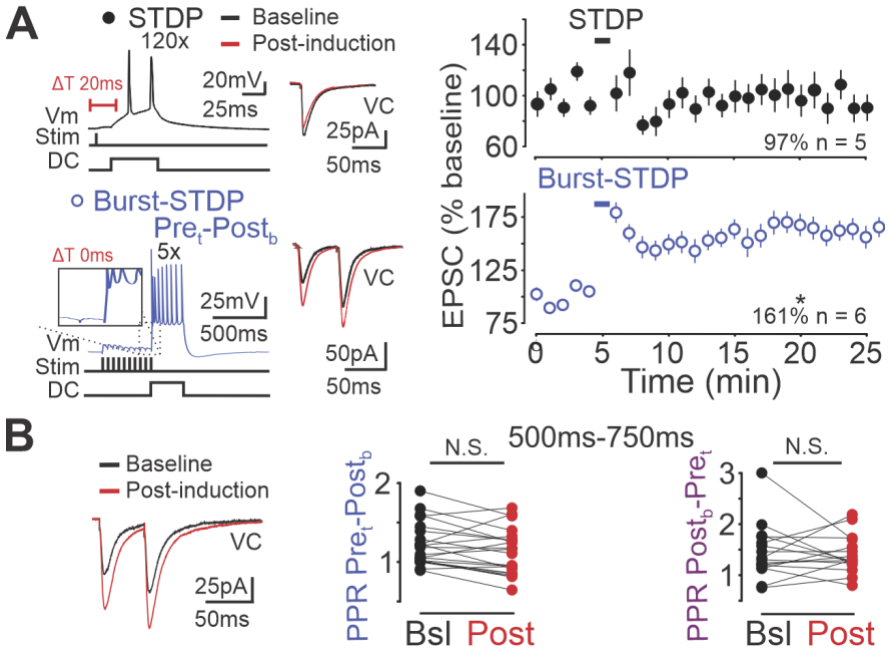

Figure S2. Effect of burst on STDP protocol and PPR of BTSP. (A) Representative trace of STDP and burst-STDP pairings in current clamp and baseline and post-pairing EPSCs in voltage clamp (VC; left). Normalized EPSC changes over 5 minutes of baseline and 20 minutes of post-induction recordings for STDP induction (top: n = 5 neurons, p = 0.71) and burst-STDP induction (bottom: same as Fig. 1D) protocols induced at the time indicated by color coded bars (right). (B) Representative trace of baseline and post-induction EPSCs (left). PPR for protocols shown in Fig 1D at time intervals between 500 ms and 750 ms (middle: post$_b$-pre$_t$, n = 16 neurons, p = 0.73, bottom: pre$_t$-post$_b$, n = 20 neurons, p = 0.054). bsl; baseline. ** p < 0.01; Data are shown as mean ± sem.

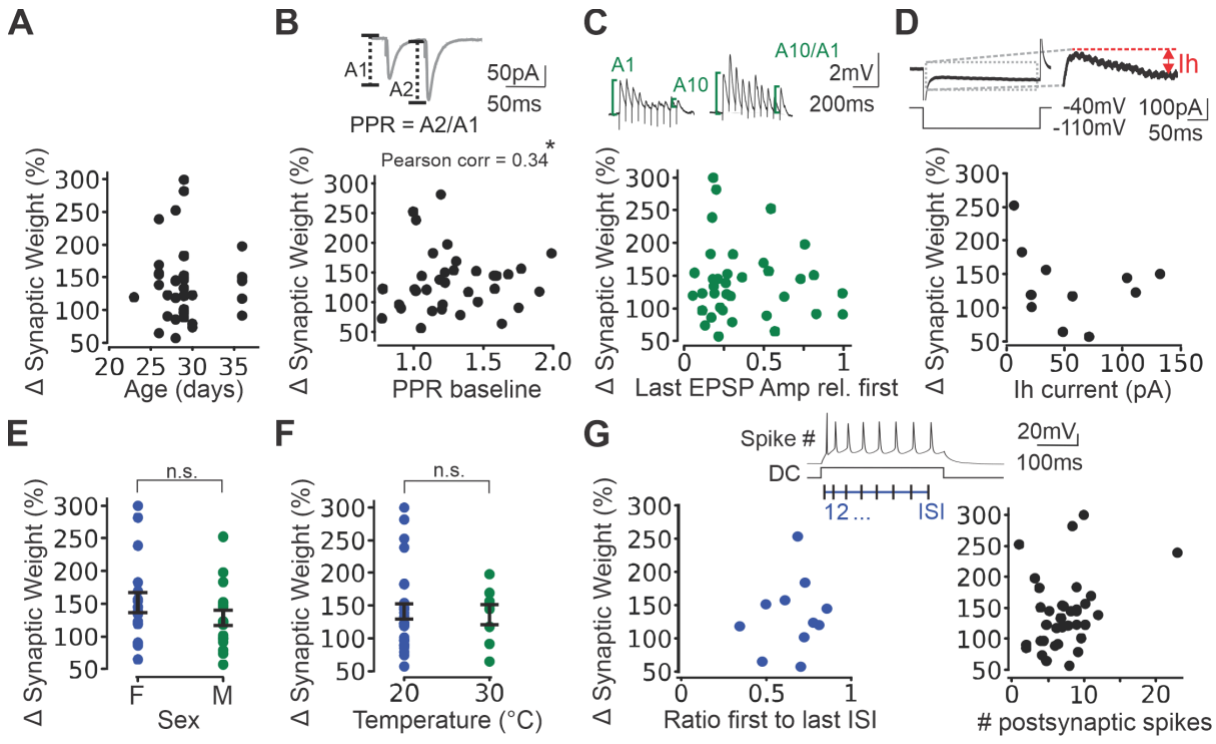

Figure S3. Generalization of synaptic rules during pre_t-$post_b$ and $post_b$-pre_t pairings (500 ms – 750 ms). (A) LTP magnitude against age in days at time of death (n = 32 neurons, p = 0.94). (B) Representative EPSC trace obtained during baseline recordings (top). LTP magnitude against PPR at baseline (n = 35 neurons, p = 0.04, coefficient = 0.34). (C) Representative trace of EPSPs during pre_t-$post_b$ pairings (top). LTP magnitude against synaptic transmission in a train calculated as the ratio of the last EPSP amplitude (A10) to the first (A1) in the train (n = 36 neurons, p = 0.63, bottom). (D) Representative trace of voltage clamp recordings of a cell depolarized from -40 mV to -110 mV, and schematic of Ih current amplitude measurement (top). LTP magnitude against Ih current (n = 11 neurons, p = 0.43, bottom). (E) LTP magnitude against sex of the animal (female (F): n = 15 neurons, male (M): n = 13 neurons, p = 0.22). (F) LTP magnitude against recording temperature (20: n = 18 neurons, 30: n = 7 neurons, p = 0.84). (G) Representative trace of a $post_b$ induced in current clamp and calculation of # of spikes and inter-spike interval (ISI; top). LTP magnitude against the duration of the last ISI to the first (n = 14 neurons, p = 0.69, bottom left). LTP magnitude against # of postsynaptic spikes during $post_b$ induced by 400 pA to 600 pA direct current injection (n = 35 neurons, p = 0.08, bottom right). Rel: relative. DC: Direct current. Data are shown as mean ± sem.

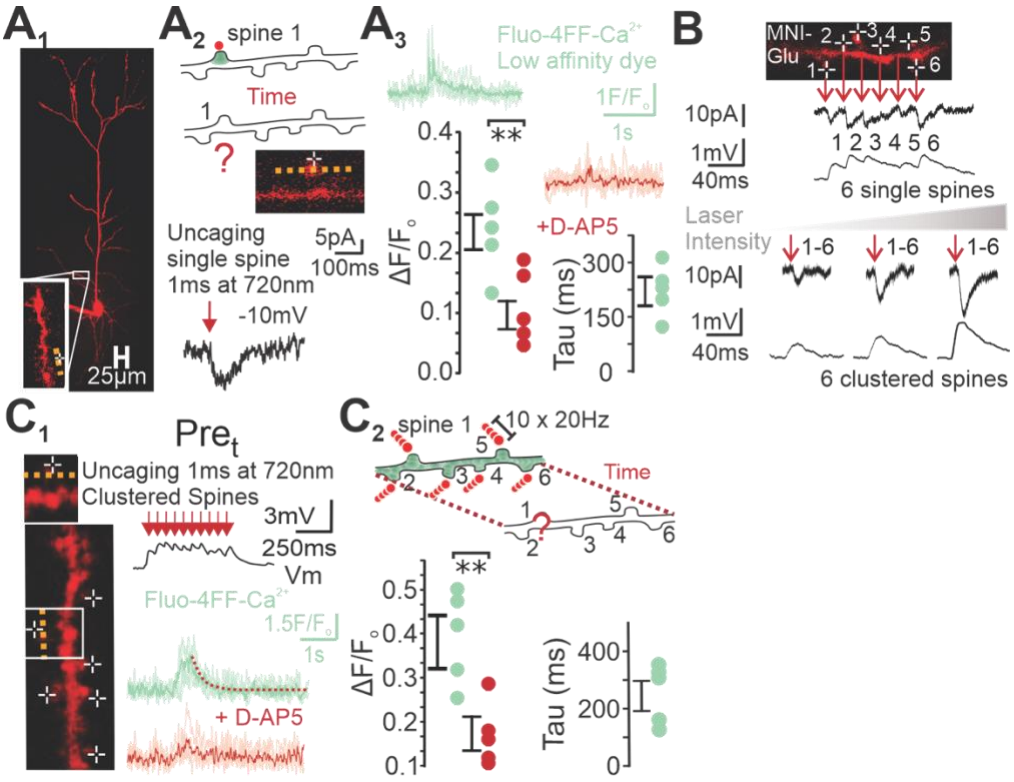

Figure S4. Ca^{2+} dynamics of $uPre_t$ induced on spines on proximal dendrites of L5 mPFC pyramidal neurons. (A) A_1 Example image of L5 pyramidal neuron and proximal apical dendrite for which glutamate uncaging and line scans were performed at the spine. A_2 Cartoon of experiment (top). Example image of proximal apical spine (middle). Representative trace of 1 EPSC induced by glutamate uncaging at -10 mV (bottom). A_3 Ca^{2+} traces obtained with Fluo-4FF dye for protocol shown in A_2 in control condition (green) and following bath-application of D-AP5 (red) (n = 5 neurons; top) and resulting ΔF/F (p = 0.0063) and Tau values (bottom). (B) Example image of proximal apical dendrite of L5 pyramidal neurons on which glutamate uncaging was performed on 6 individual spines at 40% laser power (top), and on spatially and temporally clustered spines (6 spines at the same time) at varying laser powers (20 % - 40 %), with their representative voltage and current clamp traces (bottom). (B) B_1 Representative trace of $uPre_t$ induced with glutamate uncaging on 6 clustered spines of the proximal apical dendrites of L5 pyramidal neurons (top), and resulting Ca^{2+} traces in control condition (green) and with bath-application of D-AP5 (red) (bottom). B_2 Cartoon of experiment (top) and resulting ΔF/F (p = 0.0012) and tau values (bottom). **p < 0.01; Data are shown as mean ± sem.

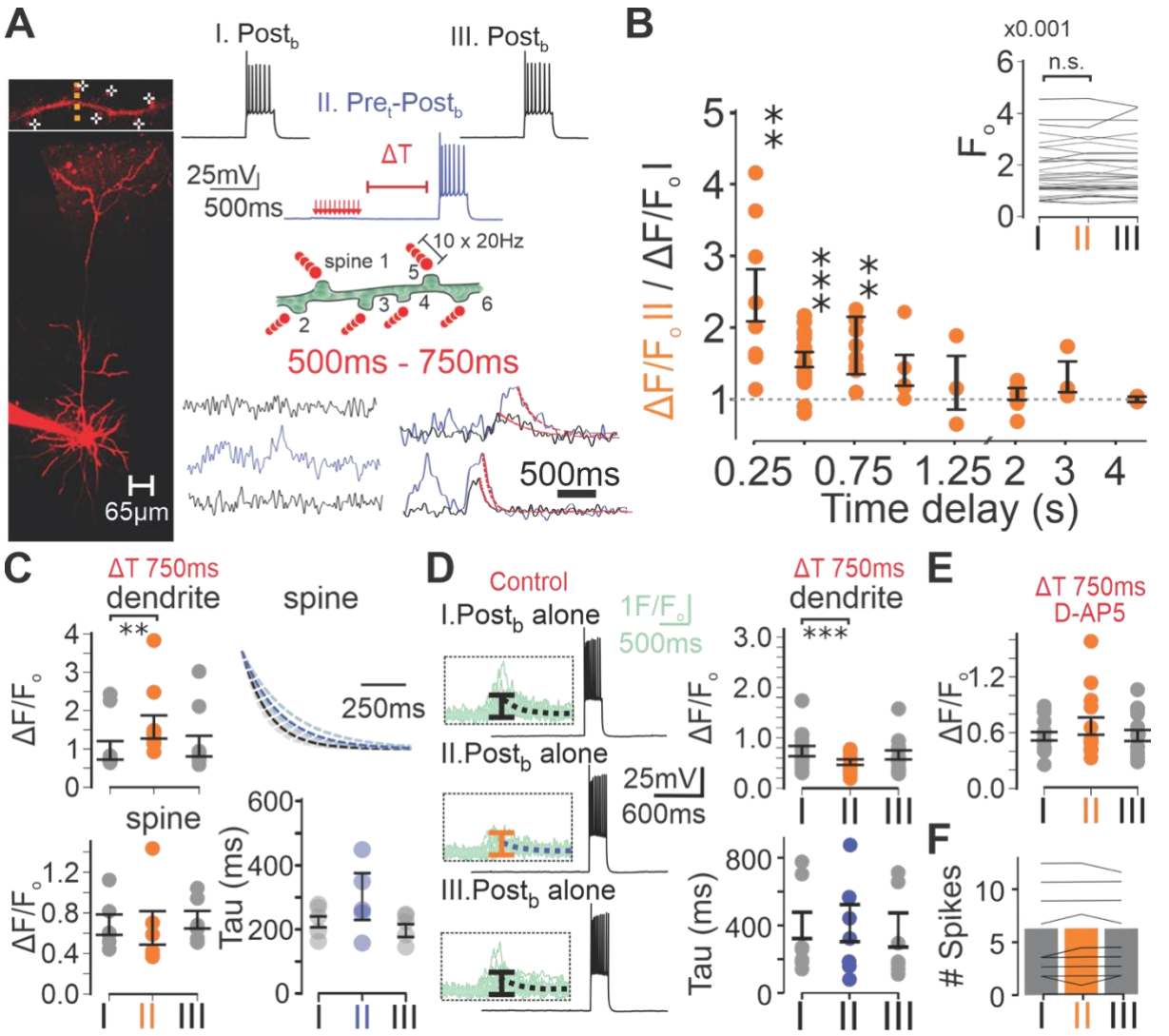

Figure S5. Ca^{2+} dynamics elicited by pre$_t$-post$_b$ pairings. (A) Example image of L5 pyramidal neuron and proximal apical dendrite on which clustered glutamate uncaging and line scans of the dendritic segment were performed (left). Representative electrophysiological trace of three post$_b$ induced at 30 s interval with the second post$_b$ preceded by pre$_t$ at varying time interval (top right). Cartoon of synaptic stimulation (middle right). Ca^{2+} fluorescence example traces with Fluo-4FF in proximal apical dendrites of L5 pyramidal neurons for 500 ms to 750 ms delay protocol (bottom right). Note that example like the Ca^{2+} trace on the left was not included in data due to their rare occurrence and difficulty with fitting decays. (B) Normalized relative ΔF/F values of post$_b$ preceded by pre$_t$ compared to the first post$_b$ given alone as shown in A (250 ms: n = 8 dendrites, p = 0.0078, 500 ms: n = 15 dendrites, p = 0.00026, 750 ms: n = 9 dendrites, p = 0.002, 1000 ms: n = 5 dendrites, p = 0.13, 1250 ms: n = 3 dendrites, p = 0.75, 2000 ms: n = 8 dendrites, p = 0.546, 3000 ms: n = 3 dendrites, p = 0.25, 4500 ms: n = 3 dendrites, p = 1.0). Baseline fluorescence (F_o) prior to each of the three post$_b$ shown in A across all time delays (inset, n = 47 dendrites, p = 0.30). (C) ΔF/F values for protocol shown in A for time delay of 750 ms in dendrite (same as in B) and spine (n = 6 spines, p = 0.84) and resulting decay traces and tau values of post$_b$ from line scans in the spines (n = 11 dendrites, p = 0.024) and at the spines (n = 5 spines, p = 0.19). (D) Representative trace of three post$_b$ given at 30 s interval without pre$_t$ and resulting Ca^{2+} trace

(left). Dendritic ΔF/F (n = 14 dendrites, p = 0.00061) and tau (n = 7 dendrites, p = 0.38) values (right). (E) ΔF/F values for $post_b$ Ca^{2+} events from protocol shown in A at 750 ms delay with the presence of D-AP5 (n = 12 dendrites, p = 0.27). (F) Number (#) of spikes for each $post_b$ for dendritic data shown in C (n = 9 dendrites, p = 0.23). **p < 0.01, *** p < 0.001. Data shown as mean ± sem.

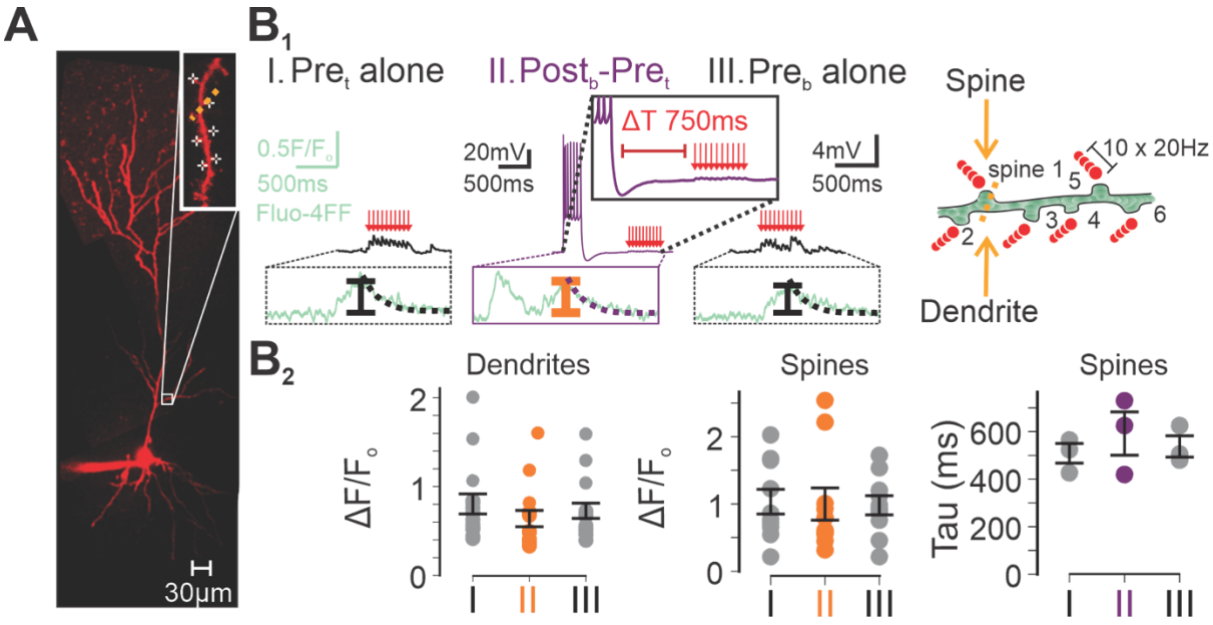

Figure S6. STAPCD is symmetrical. (A) Example image of L5 pyramidal neuron and proximal apical dendrite on which clustered glutamate uncaging and line scans of the dendritic segment were performed. (B) B_1 Representative voltage and mean Ca^{2+} traces of three pre_t induced at 30 s intervals with the second pre_t preceded by $post_b$ 750 ms prior (left). Cartoon of synaptic stimulation (right). B_2 Resulting ΔF/F values in dendrites (n = 15 dendrites, p = 0.23, left) and spines (n = 10 spines, p = 0.70, middle) and spine tau values (n = 3 spines, p = 0.5, right). Data shown as mean ± sem.

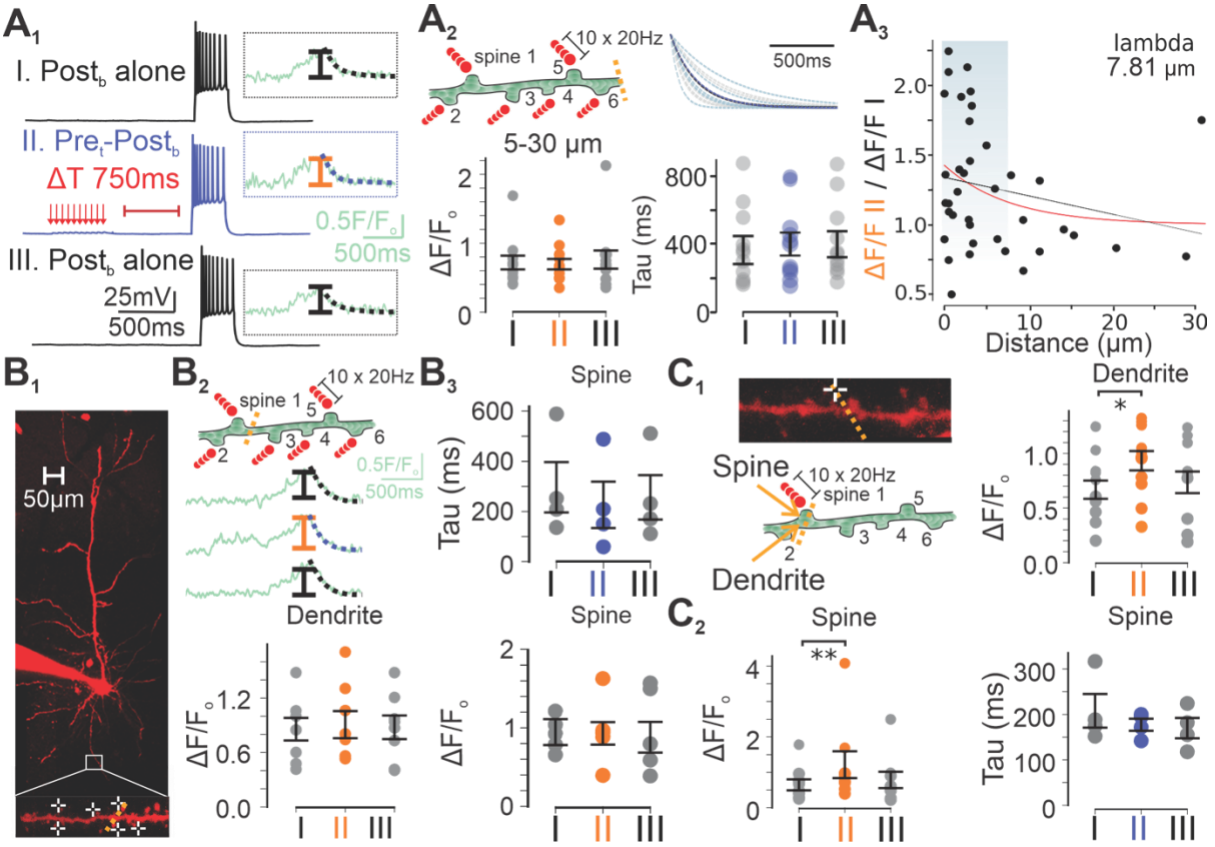

Figure S7. Properties of STAPCD during effective BTSP. (A) A_1 Representative voltage and mean Ca^{2+} traces of three $post_b$ induced at 30 s interval with the second $post_b$ preceded by pre_t 750 ms prior. A_2 Cartoon of synaptic stimulation showing line scans performed 5-30 µm away from the middle of the synaptic cluster (top left) and resulting dendritic ΔF/F values (n = 11 dendrites, p = 0.64, bottom left) and decay traces and time constants (right, n = 11 dendrites, p = 0.58). A_3 Example image of L5 pyramidal neuron's proximal apical dendrite on which clustered glutamate uncaging and line scans of the dendritic segment 5-30 µm away were performed (left). Distance dependence of relative normalized ΔF/F values (n = 20 dendrites, right). (B) B_1 Example image of L5 pyramidal neuron and proximal basal dendrite on which clustered glutamate uncaging and line scans were performed. B_2 Cartoon of synaptic stimulation (top), mean Ca^{2+} traces (middle) and resulting dendritic ΔF/F values (n = 7 dendrites, p = 0.81, bottom). B_3 Resulting spine values of tau (n = 4 spines, p = 0.13, top) and ΔF/F (n = 5 dendrites, p = 0.81, bottom). (C) C_1 Synaptic stimulation example (left) during protocol shown in A_1 but on a single spine, and resulting dendritic ΔF/F values (n = 11 dendrites, p = 0.032, right). C_2 Same as C_1 (right), except for spines ΔF/F (n = 9 spines, p = 0.0039, left) and spine tau values (n = 4 spines, p = 0.63, right). *p < 0.05, **p < 0.01. Data shown as mean ± sem.

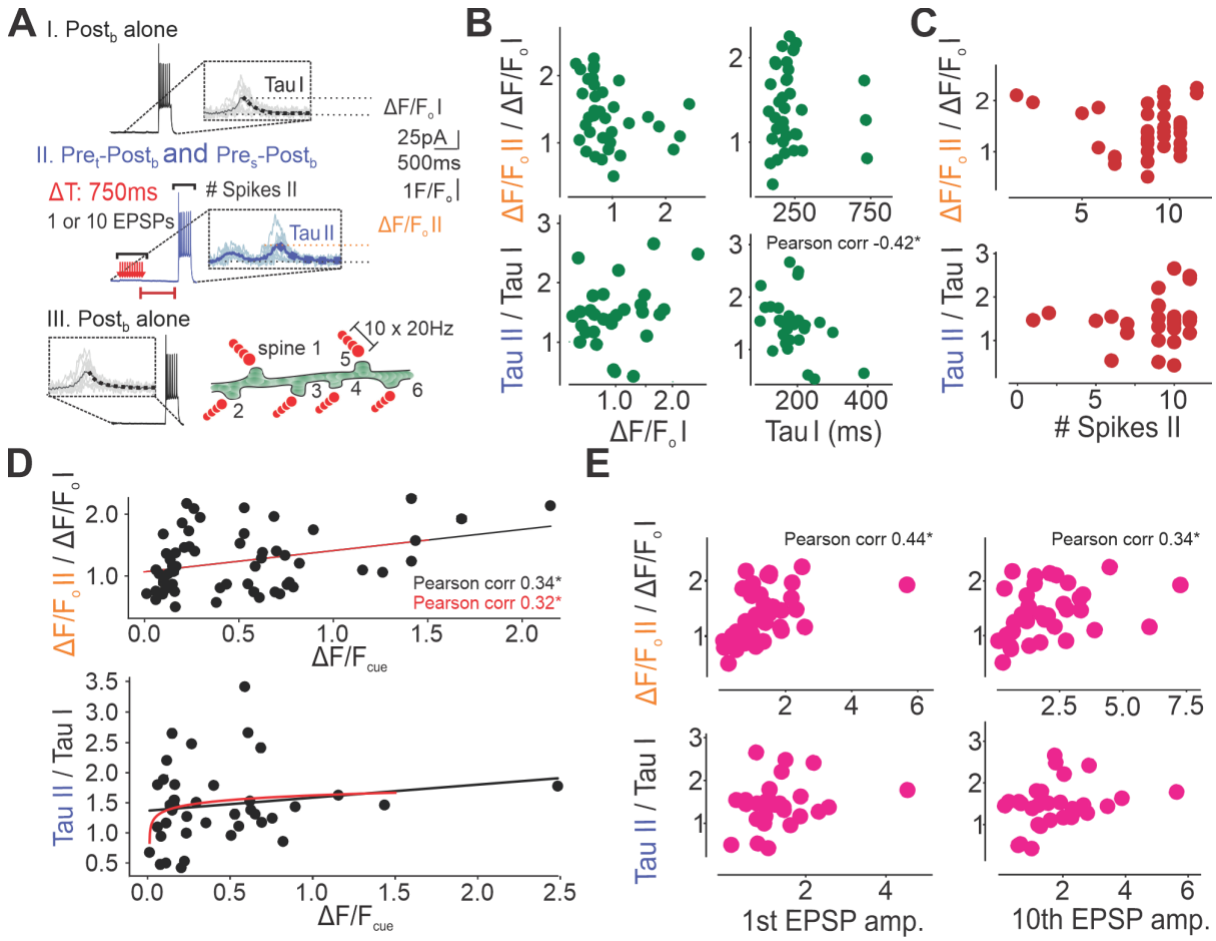

Figure S8. Relationship between STAPCD, Ca^{2+} and voltage. (A) Representative STAPCD protocol. (B) Relative ΔF/F and tau values against ΔF/F and tau value of the first post$_b$ (Relative ΔF/F against ΔF/F$_1$: n = 36 dendrites, p = 0.09; Relative ΔF/F against Tau$_1$: 36 dendrites, p = 1.0; Relative Tau against ΔF/F$_1$: n = 29 dendrites, p = 0.16; Relative Tau against Tau$_1$: n = 29 dendrites, p = 0.02, correlation coefficient = -0.42). (C) Relative ΔF/F and tau values against # spikes in the second post$_b$ (ΔF/F: n = 36 dendrites, p = 0.69; Tau: n =29 dendrites, p = 0.48). (D) Correlation between relative ΔF/F (top; n = 57 dendrites, linear black (p = 0.01, correlation coefficient = 0.34) and logarithmic red (p = 0.02, correlation coefficient = 0.32)) and tau (bottom; n = 40 dendrites, linear (black, p = 0.32) and logarithmic (red, p = 0.19)) and ΔF/F from the cue preceding the paired input (pre$_t$ during pre$_t$-post$_b$, or post$_b$ during post$_b$-pre$_t$,). (E) Relative ΔF/F and tau values against the 1st and last EPSP in the pre$_t$ (Relative ΔF/F against 1st EPSP: n = 36 dendrites, p = 0.01, correlation coefficient = 0.44; Relative ΔF/F against 10th EPSP: n = 36 dendrites, p = 0.04, correlation coefficient = 0.34; Relative tau against 1st EPSP: n = 29 dendrites, p = 0.25; Relative tau against 10th EPSP: n = 29 dendrites, p = 0.12). *p < 0.05. Data for B, C and E from protocols pre$_t$-post$_b$ 500 ms and 750 ms, Data for D same as B, C and E, with the addition of post$_b$-pre$_t$ 750 ms.

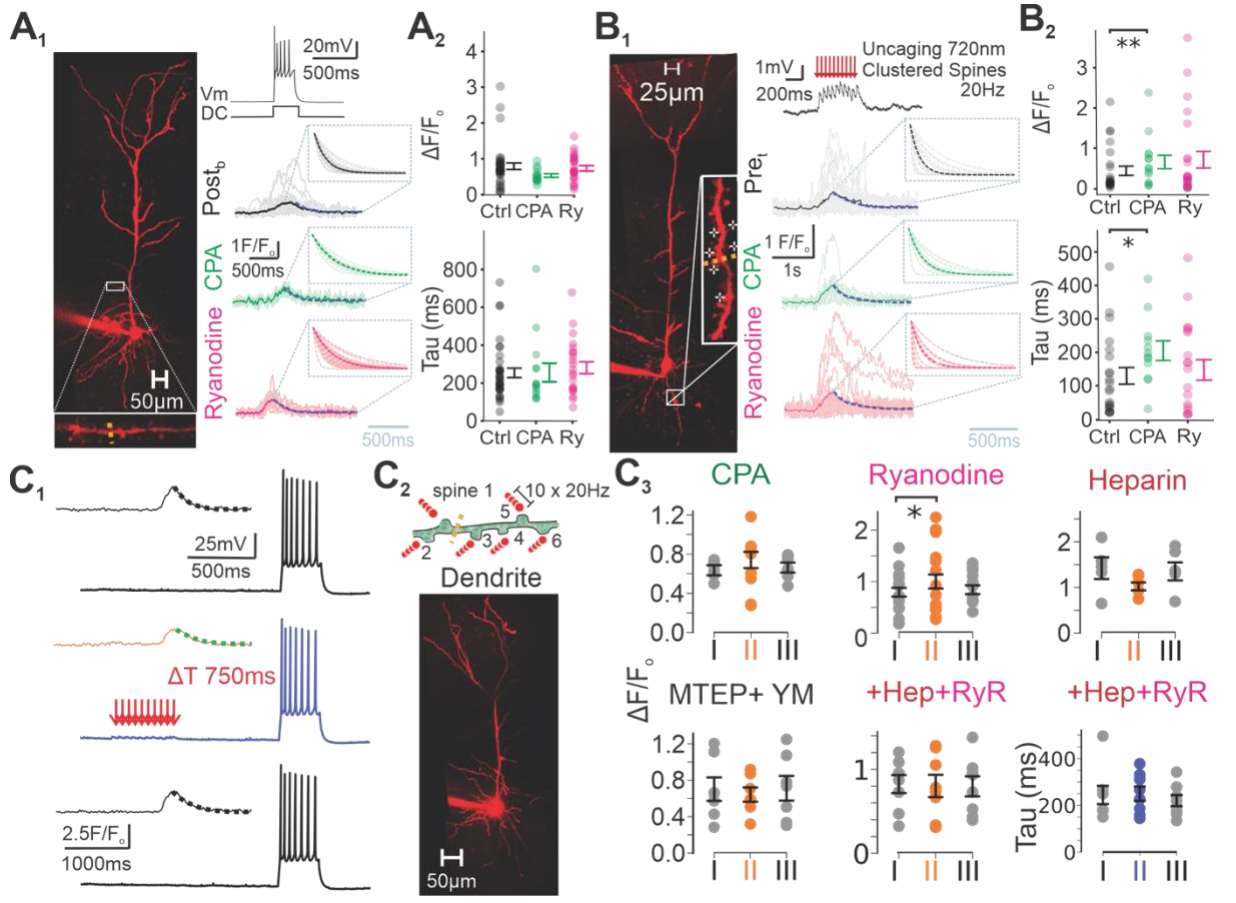

Figure S9. Dependence of STAPCD to ER. (A) A_1 Representative voltage trace, and resulting Ca^{2+} and decay traces of $post_b$ performed on L5 proximal apical dendrites in control condition (black, n = 38 dendrites), with bath-application of CPA (green), or intracellular ryanodine (pink). A_2 Resulting peak Ca^{2+} fluorescence (CPA: n = 14 dendrites, p = 0.40, ryanodine: n = 24 dendrites, p = 0.18) and decay time constant (CPA: n = 14 dendrites, p = 0.42, ryanodine: n = 22 dendrites, p = 0.19). (B) Same as A except for $uPre_t$ ΔF/F (control: n = 38 dendrites, CPA: n = 14 dendrites, p = 0.0077, ryanodine: n = 24 dendrites, p = 0.086), and decay time constant (control: n = 22 dendrites, CPA: n = 12 dendrites, p = 0.016, ryanodine: n = 20 dendrites, p = 0.49). (C) C_1 Representative voltage and mean Ca^{2+} traces of three $post_b$ induced at 30 s interval with the second $post_b$ preceded by pre_t 750 ms prior during bath-application of drugs. A_2 Cartoon of synaptic stimulation and dendritic line scans (top) and example image of L5 pyramidal neuron (bottom). C_3 ΔF/F values of protocol shown in C_1 for cells exposed to either extracellular CPA (n = 8 dendrites, p = 0.31), MTEP and YM298198 (n = 7 dendrites, p = 0.94), or intracellular ryanodine (n = 13 dendrites, p = 0.040) or heparin (n = 5 dendrites, p = 0.13) or a mix of ryanodine and heparin (ΔF/F: n = 5 dendrites, p = 0.44 ; τ: n = 6 dendrites, p = 0.84). Data shown as mean ± sem.

Appendix C – Manuscript VI

Le vaccin à ARNm, au-delà du COVID-19

Authors: Léa Caya-Bissonnette

This manuscript was published at the University of Ottawa Journal of Medicine

Caya-Bissonnette L. Le vaccin à ARNm, au-delà du COVID-19. UOJM. Published online August 26, 2021;11(S1). doi:10.18192/uojm.v11iS1.6028

Author contribution: L.C.B. wrote and edited the manuscript.

La pandémie mondiale causée par la COVID-19 a occasionné beaucoup de turbulences dans la dernière année et, chose certaine, beaucoup d'énergie et de financement ont été attribués au développement de vaccins pour inoculer la population mondiale. Cet effort collectif en quête de vaccin avancera-t-elle par inadvertance la recherche sur le cancer?

C'est en 1796 que le premier vaccin a été administré par le médecin Edward Jenner à un enfant dans le but de lutter contre la variole, un virus infectieux ayant causé la mort de centaines de milliers de personnes à travers le temps [1]. La découverte du médecin découlait de l'observation que les fermiers ayant contracté la vaccine, une forme de variole bénigne chez l'humain et affectant les vaches, semblait les protéger de la variole. C'est alors que Edward Jenner préleva du pus d'une vache infectée par la vaccine et l'inocula à l'enfant [2]. L'expérience étant un succès, le vaccin fit alors son entrée dans le monde, et chemina jusqu'à devenir l'une des meilleures protections contre les virus infectieux.

Nous voilà plus de 200 ans après cette découverte et l'utilisation des vaccins fait maintenant partie intégrale de nos vies. Bien que les vaccins soient souvent associés à la lutte contre les maladies virales, son utilisation ne s'en arrête pas là. En effet, en 2006, l'Agence américaine des produits alimentaires et médicamenteux a approuvé le tout premier vaccin utilisé dans la lutte contre le cancer [3,4]. Le cancer, qui est la première cause de décès au Canada [5], est une maladie causée par des mutations dans les gènes de cellules de tissu quelconque. Ces mutations modifient la croissance et le cycle de division cellulaire, rendant les cellules mutantes incontrôlables. Le premier vaccin contre le cancer agissait en ciblant et neutralisant l'infection au virus du papillome humain qui est responsable de 90% des cancers du col de l'utérus [6,7]. Depuis tout récemment, les avancées scientifiques ont porté une attention plus particulière aux vaccins utilisant l'ARN messager (ARNm). Ces vaccins, maintenant bien connus du public en raison de leurs utilisations contre la COVID-19 [8], ont d'abord été dans l'œil de mire des chercheurs sur le cancer [9].

Les vaccins par ARNm sont une nouvelle classe de vaccins ayant fait leurs débuts dans les laboratoires de recherche dès 1990 [10,11]. En général, ces vaccins contiennent des brins d'ARNm fournissant l'information nécessaire aux cellules pour bâtir une protéine qui activera le système immunitaire, permettant ainsi de combattre les corps néfastes ou étrangers, comme ceux provenant d'un virus ou d'un cancer. Somme toute, ce n'est qu'en 2005, grâce aux avancées des Drs. Katalin Kariko et Drew Weissman, que les vaccins à ARNm sont devenus assez stables pour qu'ils soient

délivrés en toute sécurité [12]. Depuis, la recherche a explosé et, à l'heure actuelle, plusieurs vaccins d'ARNm sont au stade de l'essai clinique pour le traitement du cancer.

Le mélanome, un cancer de la peau, est causé par une mutation des mélanocytes, un type de cellule produisant des pigments de la peau [13]. Ce cancer suscite un intérêt particulier dans la recherche sur les vaccins d'ARNm. Un candidat potentiel est présentement développé par Moderna (Moderna, Inc., Cambridge, MA) [14]. L'approche est individualisée, de telle sorte que l'ARNm est développé pour chaque patient et agît contre leur propre tumeur. Afin de créer ce vaccin personnalisé, l'ADN des cellules cancéreuses du patient est séquencé et analysé. Les chercheurs développent ensuite une séquence ARNm contenant de l'information sur les épitopes des antigènes des cellules cancéreuses [15]. Les antigènes sont de grosses protéines à la surface des pathogènes qui génèrent la production d'anticorps chez le sujet affecté, soit une réponse immunitaire. Les épitopes, quant à eux, sont la « clef » que les anticorps utilisent pour s'attacher aux antigènes. Une fois l'ARNm introduit, il est traduit dans les cellules du patient. Les épitopes sont alors bâtis et présentés à la surface des Cellules Présentatrices d'Antigènes, des cellules immunitaires. Ceci permet alors aux cellules-T cytotoxiques, un type de cellules lymphocytaires faisant partie de la famille des globules blancs, à cibler et tuer les cellules cancéreuses possédant ce néo-antigène. Encore plus important, les cellules-T de mémoire sont également générées, permettant un mécanisme de défense en cas de récurrence du cancer [15]. Ce type de traitement est donc particulièrement intéressant, puisqu'il permet d'éradiquer une fois pour toutes la tumeur cancéreuse. D'autres types de cancer, comme celui du poumon, des ovaires, de la prostate et même certains cancers sanguins et du cerveau, sont présentement ciblés par des essais cliniques du vaccin utilisant la technique à ARNm [16], ajoutant à l'intérêt de ce type de traitement.

Dans la dernière année, la recherche sur les vaccins à ARNm a été grandement accélérée, notamment en raison de la COVID-19 [17, 18, 19, 20]. En effet, les premiers vaccins contre ce virus étaient des vaccins à ARNm. Ces vaccins protègent de la COVID-19 en introduisant chez le sujet l'ARNm de *spike protein*, une protéine retrouvée à la surface du virus [8]. L'ARNm permet aux cellules du sujet de bâtir ces protéines, qui seront ensuite reconnues comme protéines étrangères et attaqués par le système immunitaire sans toutefois rendre le sujet malade. Ainsi, lors d'une infection future au COVID-19, les cellules immunitaires seront capables d'identifier rapidement cette protéine étrangère et ainsi détruire le virus [8]. L'intensification des financements sur la recherche de vaccins à ARNm occasionnée par la pandémie mondiale a donné un élan

inégalé aux grandes entreprises pionnières dans le domaine. Ces compagnies se tournent maintenant vers la course aux vaccins contre le cancer [21].

Le traitement par vaccins à ARNm est très prometteur, et deviendra bientôt un outil indispensable dans la lutte contre le cancer. Ainsi, on souligne plus que jamais l'importance de ramifier l'expertise scientifique et le financement pour la recherche des vaccins à ARNm.

Références :

1.Fenner F, Henderson DA, Arita I, Jezek Z, Ladnyi ID. Smallpox and its eradication. Geneve. WHO. 1988. 229-232 p. ISBN 92-4-156110-6

2.Moore ZS, Seward JF, Lane JM. Review Smallpox. Lancet. 2006;367(9508):425-35

3. Malagón T, Drolet M, Boily MC, Franco EL, Jit M, Brisson J, Brisson M. Cross-protective efficacy of two human papillomavirus vaccines: a systematic review and meta-analysis. Lancet Infect Dis. 2012;12:781–789.

4.Kirby T. FDA approves new upgraded Gardasil 9. Lancet Oncol. 2015;16:e56.

5.Statistic Canada. Les dix premières causes de décès [Internet]. Date des dernières modifications : 2018-05-17. Citer le 2021-03-30. Accéder à partir de https://www150.statcan.gc.ca/n1/pub/82-625-x/2014001/article/11896-fra.htm

6. Kumar V, Abbas AK, Fausto N, Mitchell RN. Robbins Basic Pathology. 8th ed. Saunders Elsevier. 2007. 718–721 p.

7. Donald K. Holland-Frei cancer medicine 8th ed. New York: McGraw-Hill Medical. 2009. p. 1299.

8. Center for disease control and prevention (CDC). Understanding mRNA COVID-19 Vaccines. Date des dernières modifications: Mar. 4, 2021. Citer le 2021-03-30. Accéder à partir de https://www.cdc.gov/coronavirus/2019-ncov/vaccines/different-vaccines/mrna.html

9. Van Lint S, Renmans D, Broos K, Dewitte H, Lentacker I, … Thielemanset K. The ReNAissanCe of mRNA-based cancer therapy. Expert Rev Vaccines. 2015;(14):235-251.

10.Wolff JA, Malone RW, Williams P, Chong W, Acsadi G, Jani A, Felgner PL. Direct gene transfer into mouse muscle in vivo. Science. 1990 Mar; 247(4949 Pt 1):1465-1468.

11.Jirikowski GF, Sanna PP, Maciejewski-Lenoir D, Bloom FE. Reversal of diabetes insipidus in Brattleboro rats: intrahypothalamic injection of vasopressin mRNA.Science. 1992 Feb; 255(5047):996-8.

12.Weissman D, Karikó K. mRNA: Fulfilling the Promise of Gene Therapy. Mol Ther. 2015 Sep;23(9):1416-1417.

13. Domingues B, Lopes J, Soares P, Populo H. Melanoma treatment in review. ImmunoTargets Ther. 2018;7:35−49

14.U.S. National Library of Medicine. An Efficacy Study of Adjuvant Treatment With the Personalized Cancer Vaccine mRNA4157 and Pembrolizumab in Patients With High-Risk Melanoma (KEYNOTE-942). Publier le 2019-04-01. Date des dernières modifications le 2021-03-24. Citer le 2021-30-03. Accéder à partir de https://www.clinicaltrials.gov/ct2/show/NCT03897881

15.National Cancer Institute Drug Dictionary. mRNA-based personalized cancer vaccine mRNA-4157. Citer le 2021-03-30. Accéder à partir de https://www.cancer.gov/publications/dictionaries/cancer-drug/def/mrna-based-personalized-cancer-vaccine-mrna-4157?redirect=true

16.Wang Y, Zhang Z, Luo J, Han X, Wei Y, and Wei X. mRNA vaccine: a potential therapeutic strategy. 2021 Feb;20(1):33. doi: 10.1186/s12943-021-01311-z.

17. Corbett KS, Flynn B, Foulds KE, Francica JR, Boyoglu-Barnum S, Werner AP et al. Evaluation of the mRNA-1273 vaccine against SARS-CoV-2 in nonhuman primates. N Engl J Med. 2020;383:1544–1555.

18.Tai W, Zhang X, Drelich A, Shi J, Hsu JC, Luchsinger L et al. A novel receptor-binding domain (RBD)-based mRNA vaccine against SARS-CoV-2. Cell Res. 2020;30:932–935.

19.Shin MD, Shukla S, Chung YH. COVID-19 vaccine development and a potential nanomaterial path forward. Nat Nanotechnol. 2020;15:646–655. doi: 10.1038/s41565-020-0737-y

20. Corbett KS, Edwards DK, Leist SR, Abiona OM, Boyoglu-Barnum S, Gillespie RA, et al. SARS-CoV-2 mRNA vaccine design enabled by prototype pathogen preparedness. Nature. 2020;586:567–571. doi: 10.1038/s41586-020-2622-0.

21. CBC News The Associated Press. Scientist behind COVID-19 mRNA vaccine says her team's next target is cancer. Publier 2021-03-19. Date des dernières modifications : 2021-03-19. Citer 2021-03-30. Accéder à partir de https://www.cbc.ca/news/health/covid-19-scientist-mrna-cancer-1.5956150

Appendix D – Simulations of Working Memory

Title: **COMPUTATIONAL EXPERIMENTS ON SPATIAL WORKING MEMORY**

REPRODUCED FROM THE ORIGINAL STUDY OF COMPTE, BRUNEL, GOLDMAN-RAKIC & WANG (2000)

Léa Caya-Bissonnette
University of Ottawa
Ottawa, Ontario, Canada
June 2018

Introduction

Working memory is fundamental to learning, adaptation and decision making (Carruthers, 2013). Working memory has been studied by experimental and computational neuroscientists; however, computational models describing neural activity recorded from experimental studies do not realistically integrate physiological properties of neural networks. For this reason, Compte et al. (2000) have computed a model that aims to close the gap between physiological studies and theoretical analyses. To grasp the concepts of working memory in a computational sense, the following paper will present the main findings of Compte et al. (2000). First, the biological and computational approaches of spatial working memory will be discussed, followed by a description of the model of Compte et al. (2000), including the assumptions, the numerical methods, the applications and implications of the model on studying spatial working memory.

Background

From a biological perspective, working memory is primarily encoded by the frontal lobe (Postle, 2006). In fact, Funahashi, Bruce and Goldman-Rakic (1989) found evidence of working memory processes in the dorsolateral prefrontal cortex (PFC). In their study, the researchers investigated spatial working memory during an oculomotor delayed-response task. Briefly, the task consisted of a monkey trained to fix a point while retaining the location of a transient peripheral cue. While the neural activity was recorded, the monkey was trained to indicate, with a saccade, the location of the visual stimulus following an assigned delayed-time period. Funahashi et al. (1989) found that the neurons responding to the cue location sustained the firing activity from visual stimulus onset throughout the delayed-response period and until response onset. Later, similar results were found in the posterior parietal cortex (PPC) (Chafee & Goldman-Rakic, 1998). Following these experimental findings, theoreticians have suggested that mnemonic activity is maintained through reverberatory loops between the PFC and the PPC (Amit, 1995; Chafee, & Goldman-Rakic, 1998).

Since, computational studies have built models, i.e. the firing rate model (Durstewitz , Kelc,& Güntürkun,1999), to fit physiological data of spatial working memory; however, as discussed by Compte et al. (2000), the models remain limited. In fact, the models do not allow for the distinction between spontaneous and persistent activity. Additionally, the models neglect

temporal precision of synaptic interactions, a core intermediate for neural communication and memory processes (Compte et al., 2000).

A handful of studies have tackled the challenging problem of closing the gap between theoretical studies and physiological properties of the brain. Three main studies based on the oculomotor delayed-response task of Funahashi et al. (1989) have inspired Compte et al. (2000) in the modelling of spatial working memory.

To begin with, Amit and Brunel (1997) addressed the issue of differentiating spontaneous activity from recurrent activity using a spiking neuron model. This model considers the structural connectivity between neurons in the network and allows to control the level of spontaneous activity arriving from external sources. By tuning the parameters defining the excitatory and inhibitory populations, such that the ratio of inhibitory inputs be higher than excitatory inputs, one can modulate of the level of spontaneous activity within the neural population (Amit & Brunel, 1997).

A second issue was partly resolved by Lisman, Fellous and Wang (1998), who suggested a role of NMDA receptors (NMDARs), located on recurrent synapses, in the generation of selective persistent activity following stimulus onset. Later, Wang (1999) supported and further this hypothesis. Wang (1999) suggested that kinetically slow synapses containing NMDARs would be primary to recurrent excitation. In the paper, Wang included both excitatory and inhibitory components to the model, such that AMPA receptors (AMPARs) and NMDARs mediate excitatory transmissions, while GABA receptors (GABARs) regulate the inhibitory transmissions.

Combining the three studies (Amit & Brunel, 1997; Lisman et al., 1998; Wang, 1999) taking into account the different synaptic inputs, receptors involved and the tuning of the inhibitory activity, Compte et al. (2000) created a model that realistically represents neural activity by (1) reaching a bistable network that maintains both spontaneous activity and persistent activity, (2) including the specific synaptic properties of the different excitatory and inhibitory receptors and (3) maintaining an activity that remains in at physiological range (20Hz-40Hz). From this, the authors aimed to perceptualize a computational task of spatial working memory inspired by Funahashi et al. (1989).

Regarding the task, Compte et al. (2000) aimed to answer three questions; (a) how persistent activity observed in working memory terminates, allowing for memory erasure after the response period, (b) how the width of the stimulus comes into relation with persistent activity, and (c) how a distractor interacts with the persistent activity maintained during working memory.

The Model

To compute the experiments, Compte and al. (2000) made a few assumptions. First, the authors assumed that recurrent connections in the PFC of the monkey possess a structural organization, both in terms of intrinsic and extrinsic connectivity, that agrees with the columnar organization observed in cortical circuitry and in the primary visual cortex (Mountcastle, 1997). Second, it is assumed that the noise in the inputs is not correlated between cells and finally, it is assumed that the NMDARs dominate the recurrent synaptic connections in the PFC. From these assumptions, Compte et al. (2000) built the model as follows;

First, the network topology was built as a ring network, which refers to a network where each node (a node here refers to neurons in neural networks) connects to two other nodes (Jalil, 2011). This network topology organizes neurons uniformly on a ring, where each neuron is labeled by its angle location within the circle. The angle location is later referred to as the neuron preferred angle. The ring topology provides a network with a uniformly spaced set of neurons each possessing a linear relationship between their position and their preferred cue angle (Compte et al., 2000).

Second, the authors defined both pyramidal cell (NE = 2048) and interneuron (NI = 512) populations based on Tuckwell (1988) leaky integrate-and-fire units (LIF), the postsynaptic currents and the spiking property of each neuronal type.

With a linear differential equation, the LIF model gives the firing event of each neuron considering the physiological property of the membrane (Gerstner, Kistler, Naud, & Paninski, 2014). The LIF model implies that any information related to the action potential itself, such as its shape, is ignored (Gerstner et al., 2014). A general equation for the LIF model is given by the following equation (1):

$$Cm\ dv/dt = -gL\ (V-EL) + I \quad (1)$$

Where Cm is the total capacitance, gL the total leak conductance, EL the leak reversal potential and I the input current. For pyramidal cells, the parameters were set to the values Cm = 0.5 nF, gL = 25 nS, EL = –70 mV and for interneurons the parameters were set to Cm = 0.2 nF, gL = 20 nS, EL = –70 mV. These values were chosen by the authors based on Troyer and Miller (1997) and Wang (1999). In Compte et al. (2000), the injected current (I) reproduced the cue stimulus onset of the Funahashi et al. (1989) experiment. The injected current was provided

through both external and recurrent inputs. Recurrent inputs were applied to both populations and defined by the Wang model (1999) described below.

Next, the authors added the postsynaptic currents to the definition of each population. Based on the Wang model (1999), the excitatory recurrent inputs are mediated by NMDARs and AMPARs, while inhibitory inputs are mediated by GABARs. The postsynaptic current (Isyn) specific to each receptor type is defined as follows;

$$Isyn = gsyn * s * (V - Vsyn) \quad (2)$$

Where V_{syn} is the synaptic reversal potential set to 0mV for excitatory synapses (NMDARs and AMPARs) and to –70 mV for inhibitory synapses. Here, gsyn is the synaptic conductance of recurrent excitatory synapses. Therefore, when NMDAR exclusively dominate the recurrent excitatory conductance, the conductance of excitatory synapses projecting onto the excitatory population is G_{EE} = 0.381 nS. For excitatory synapses projecting onto the inhibitory population, the conductance is G_{EI} = 0.292 nS. The inhibitory synaptic conductance projecting onto pyramidal cells is G_{IE} = 1.336 nS and inhibitory synaptic conductance projecting on interneurons is G_{II} = 1.024 nS. Moreover, s is the synaptic gating variable; however, no numerical values were given for s. Finally, since NMDARs are voltage dependent, the equation (2) applied to NMDARs is multiplied by $1/(1 + [Mg^{2+}]\exp(–0.062V_m)/3.57)$, with $[Mg^{2+}]$ = 1.0 mM and V_m as the membrane potential.

When defining the populations, the three sources of postsynaptic currents (NMDA, AMPA and GABA), defined by equation 2, were subtracted from the following term: $-g_L * (V - E_L)$ of the LIF model (equation 1) (for both excitatory and inhibitory populations). The subtraction of each term suggests, by convention, an inward current depolarizing the cell.

When the size of the population changes, it is important to keep the total recurrent conductance unchanged by re-scaling the total synaptic conductance inversely proportionally to the size of the population. Therefore, a weight scaling factor was implemented to modulate the conductance when the size of the population was modified.

Finally, the spiking property of the populations were modulated using three additional parameters. The threshold potential (V_{th}) gives a condition for spike generation, the reset potential (V_{res}) indicates how the network resets after a spiking event, and the refractory time period (τ_{ref}),

to give the minimum amount of time between two spiking events. For pyramidal cells, the values were set to V_{th} = –50 mV, V_{res} = –60 mV and τ_{ref} = 2 ms. For interneurons, they were set to V_{th} = –50 mV, V_{res} = –60 mV and τ_{ref} = 1 ms.

Third, once the populations are defined, a set of equations describing each channel kinetics was implemented in the model and is shown by the following equations (3,4):

$$ds/dt = -1/\tau s * s + \alpha s x(1-s) \quad (3)$$

$$dx/dt = -1/\tau x * x + i\,\delta(t - ti) \quad (4)$$

In equation 3, s is the fraction of open channel, x is an intermediate gating variable, τs is the decay time of NMDA currents (set to 100 ms) and αs is the saturation properties of NMDA channels at high presynaptic firing frequencies (set to 0.5Hz). In equation 4, x is an intermediate gating variable, ti are the presynaptic spike times and τ_x is the rise time of NMDA channels (set to 2 ms). For GABARs and AMPARs, only $ds/dt = -1/\tau s * s$ of equation 3 was implemented in both populations (excitatory and inhibitory). On the other hand, the kinetic of NMDARs is exclusively defined in the excitatory population by both equations 3 and 4.

Fourth, the external inputs received by the network was modeled using an uncorrelated Poisson spike trains from 1000 presynaptic connections at 1.8Hz (ν_{ext}). These external inputs were mediated by AMPARs. The conductance was set to a maximum of 3.1nS ($g_{ext,E}$) for pyramidal cells and 2.38nS ($g_{ext,I}$) for interneurons. This provided each neuron with strong external inputs, allowing the population to go over threshold and causing a spiking event.

Fifth, the effect of neighbouring neurons on recurrent connections, given their preferred angle, was considered through a connectivity footprint. The connectivity conductance ($g_{syn,ij}$) between the pairs of neuron i and neuron j is defined by equation 5

$$gsyn,ij = W(\theta i - \theta j) * Gsyn \quad (5)$$

Here, $W(\theta i - \theta j)$, refers to the 'connectivity footprint', normalized as

$$1/360 * 0360W(\theta i-\theta j)d\theta j = 1 \quad (6)$$

Where the constant W for the unstructured connections is summed and centered with a Gaussian function defined by equation 7:

$$\theta i - \theta j = 0: W(\theta i - \theta j) = J - + (J+ - J-)exp[-(\theta i - \theta j)2/2\sigma 2] \quad (7)$$

Distant pairs of neurons possess weak connections and are referred to as cross directional connections represented by J^-. Inversely, iso directional connections refer to neighbouring neurons

that possess stronger connections, represented by J^+. Finally, σ refers to the width of the connectivity footprint.

Generally, the excitatory-to-excitatory connectivity are structured, and the parameters are defined by J^+_{EE}, σ_{EE}, where $\sigma_{EE} = 18°$ and $J^+_{EE} = 1.62$. The structured connectivity also applies for the excitatory-to-inhibitory connections (parameters are J+EI σEI). On the other hand, the inhibitory connections are unstructured, giving an equal strength to both cross- and iso-directional components. Given both J^+ and σ parameters, J^- can be determined through the normalization condition (W).

Additionally, it is important to normalize W_{EE} to 1 (pyramid-to-pyramid footprint) to conserve a level of spontaneous activity independently of the connectivity footprint. The normalization allows the decrease in strength between neurons with dissimilar preferred cue location when an increase in synaptic strength between neurons with similar preferred cue location is applied.

Finally, a second-order Runge–Kutta algorithm is used as an integration method to solve differential equation with a time step of $\Delta t = 0.02$ms (Hansel Mato, Meunier, & Neltner, 1998). To reduce the computational time of the experiments, the time steps were modified to 0.1 ms; however, it is to be noted that the precision regarding the synchronization properties of the network could be reduced by this modification (Hansel et al., 1998).

The code - Modifications

To reproduce the experiments, the basis of the code was retrieved from http://neuronaldynamics.epfl.ch. The code provided a network of neurons built upon the LIF model, with the inclusion of AMPAR, NMDAR and GABAR synaptic inputs, external poisson inputs and internal excitatory recurrent connections. The model also provided the injected current for the cue presentation. The parameters were tuned to the corresponding values of Compte et al. (2000) experiments. The unknown values were chosen from the default parameters provided by the code itself. A copy of the code retrieved from http://neuronaldynamics.epfl.ch follows the reference list section. A few modifications were adopted for each experiment and are discussed in detail later. The modified or added parts of the original code are shown in orange. Some modifications were added to the built-in function plot.network.activity to change the plot settings; however, these modifications are not shown.

First experiment - Cue stimulus width

The first experiment was based on the general protocol of Funahashi et al. (1989) and aimed to answer how persistent activity responds to a change in the stimulus width and how persistent activity terminates after response onset. This experiment is shown in Figure 2 of the original paper of Compte et al. (2000). A copy of the original figure is provided following the code section.

To reproduce the task, Compte et al. (2000) injected a transient current to the subset of pyramidal cells activated by the stimulus cue location (current of 200 pA for a 250 ms duration). The delayed-time period was produced by selectively removing all external currents for 8750 ms. The motor response and reward period were reproduced through a nonspecific transient current injected to all excitatory neurons (500 pA injected for 250 ms, total simulation time is 9750 ms).

When reproducing this experiment, the code retrieved from http://neuronaldynamics.epfl.ch did not provide the nonspecific transient current associated with the response period. Therefore, the code was modified to inject a transient current to the totality of the network. Once parameters were tuned, the model was expected to generate a localise increase in activity which persisted around the cue location throughout the delayed-time period; however, the network seemed overly excitable. Consequently, the network did not distinguish the cue stimulus from the excitatory input generated from the network itself. To overcome this issue, a few modifications were adopted.

First, the default parameters for the conductance of recurrent connections were reduced, such that G_{EE}, G_{EI}, G_{IE}, G_{II} were reduced to 35 % of their initial value and G_{EI} was further increased by 120% of the resulting value. These modifications were suggested in the pre-establish code of Gerstner et al., 2014. This resulted in the reduction of the excitatory property of the network, allowing for the cue stimulus to properly excite the network.

Second, the firing profile of the network exceeded the physiological range (>80Hz). Therefore, the inhibitory conductances were increased by 2.5 times their initial values.

Third, the 200 pA current for the cue stimulus did not allow for recurrent activity to persist. This is a possible consequence of the modifications reducing the excitability of the network and increasing the inhibitory conductance. The injected current was modified (quadrupled) in the experiment to allow the persistent activity to persist throughout the delayed-time period (800 pA for the cue stimulus and 2000 pA for the response).

Finally, to reduce the computational time associated with the simulation, the populations of 2048 pyramidal cells and 512 interneurons were reduced to 256 and 64 neurons, respectively. To ensure an equal overall synaptic input from the presynaptic neurons, the scaling weight factor was scaled inversely proportionally to the population size, resulting in an increase of the weight factor from 1 to 8.

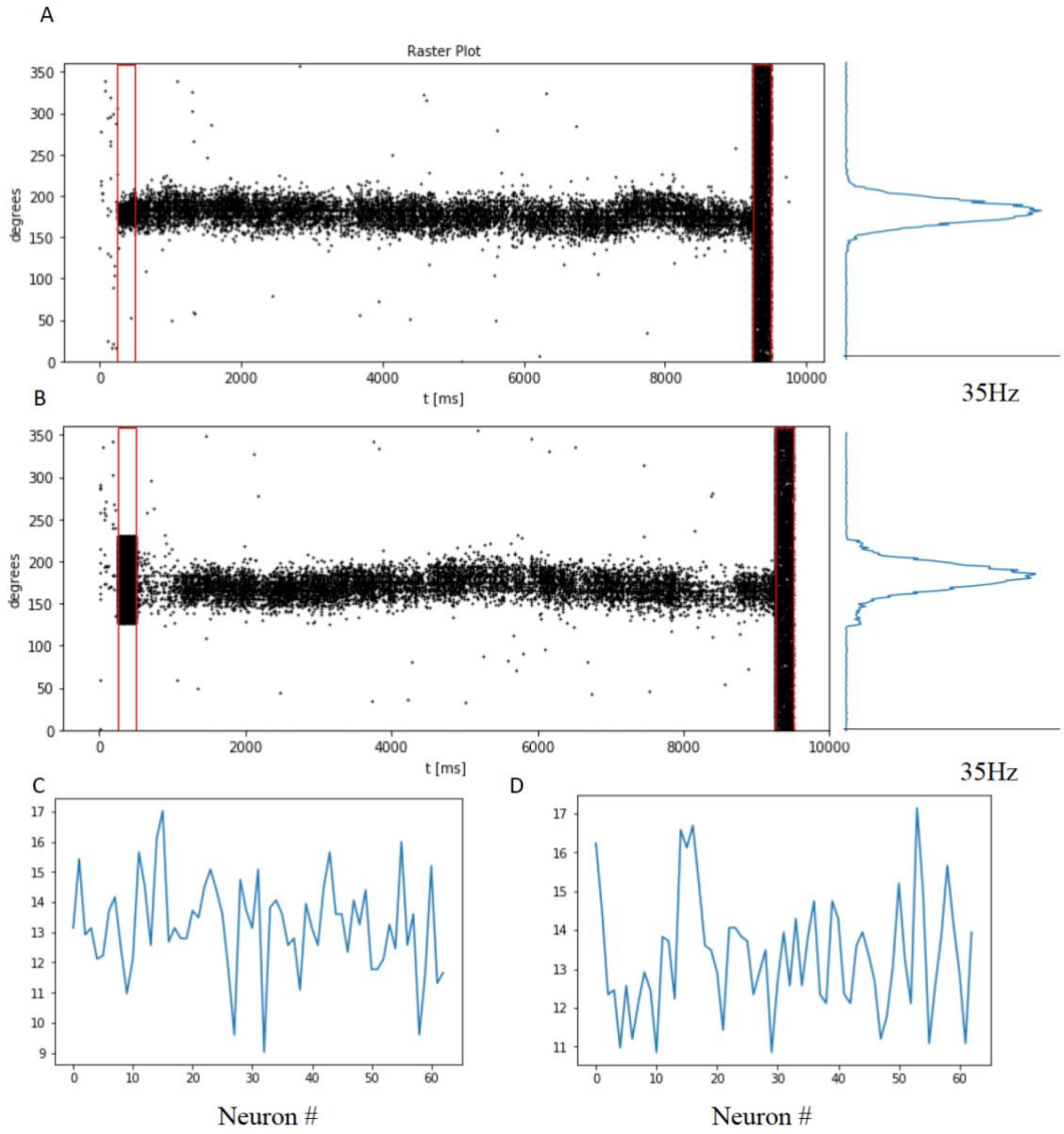

Figure 1. Spatiotemporal firing profile of the excitatory population during a spatial working memory task. A. rastergram showing neurons labeled by their preferred cue location against time. Cue stimulus presented for 250 ms duration. 800 pA current injected at 180 degrees. Stimulus width of 20 degrees. Delayed-time period of 8.75s followed by response onset for 250 ms duration generated by 2000 pA injected on the totality of the excitatory population. Both stimulus and response periods are boxed in a red rectangle. The right panel shows the firing activity profile = of the excitatory population averaged over the delayed-time period (frequency on Y axis, Neuron preferred angle on X axis) B. same as in A with a 5-fold increase (100 degrees) in stimulus width. C. Firing frequency profile of the inhibitory population shown in A (Frequency on Y axis in Hz and neuron # on X axis), averaged over the delayed-time period. D. same as in C for the population shown in B.

A ratsergram of the firing activity of the excitatory population is plotted against time in Figure 1A and B (Inspire from Figure 2 of the original paper of Compte et al. (2000)). In the rastergram, each neuron is labelled with their preferred angle location on the y axis. The cue location was set to 180 degrees. Around this area, an increase in firing activity is observed. This is due to the response of the subpopulation of neurons with a preferred cue location near the stimulus location. The cue and response period are delimited by red rectangles. Ongoing spontaneous activity is observed before cue onset and after the response period, while the delayed-time period shows a persistent activity state. This persistent activity is achieved through strong excitatory feedback within pyramidal cell subpopulation activated by the cue location (Compte et al., 2000). Finally, the injected response current increases the overall external input, consequently increasing the firing rate of the inhibitory population, resulting in strong inhibitory feedback which turns off the persistent activity (Funahashi, Bruce, & Goldman-Rakic, 1991).

Figure 1A shows a cue width of 20 degrees. In comparison, Figure 1B shows a cue width of 100 degrees (5-fold increase, as specified in Compte et al. (2000)). The width of neurons activated by the stimulus can be measured from the right panel of Figure 1A and 1B, which plots the firing frequency of the excitatory population averaged over the delayed-time response period. The panels allow to quantify the width of the persistent activity. For a stimulus width of 20 degrees (Figure 2A) and of 100 degrees (Figure 2B), the persistent activity is maintained between 135 degrees and 225 degrees. Additionally, the excitatory population shows an activity within the physiological range (approximately 35Hz, compared to 22Hz in Compte et al. (2000)). Although not shown in the original study of Compte et al. (2000), the firing frequency of the inhibitory population averaged over the delayed-time period is shown in Figure 1C and 1D derived from the population activity shown Figure 1A and 1B, respectively (Firing frequency of inhibitory population range between 9Hz and 17Hz, compared to 13Hz in Compte et al. (2000)).

The same conclusion as Compte et al. (2000) were drawn from this experiment. When changing the cue stimulus width, the width of the persistent activity that maintains the cue location remains the same, supporting the idea that the persistent activity profile is independent of the cue stimulus width. Moreover, the firing profile of both population was higher than the results presented in Compte et al. (2000); however, the idea of tuning the parameters such that the activity remains in a physiological range was achieved. Further, the original paper shows a color-coded

spatiotemporal graph to illustrate the differences in population activity profile. Here, the results are presented in a rastergram.

Second experiment - Distractor

Compte et al. (2000) explored the effect of a distractor on the persistent activity related to working memory. The distractor was simulated through a transient current specific to an angle location. The current associated with the distractor was of same strength and duration as the cue stimulus. The distractor current onset was presented 2.5 seconds after stimulus onset (total simulation time is 5 seconds). Figure 8 of Compte et al. (2000) shows the results of the experiment, a copy of the original figure is provided following the code section. The original experiment included four parts.

First, Compte et al. (2000) observed the effect of the distractor at high intensity (200 pA) when the network was tuned to the control parameters (parameters mentioned previously). The authors found that a control parameter set combined with high intensity resulted in a complete distraction of the network toward the distractor.

The second part of the experiment measured the level of distraction of a moderately intense current (100 pA) when parameters were tuned to a modulated parameter set. The modulated set of parameters was created from the control parameters and modified as follows: 20% increase in NMDAR synaptic conductance (GEE and G EI) and 40% increase in GABAR synaptic conductance (GIE and GII). These modifications aimed to increase the signal-to-noise ratio and the strength of inhibitory connections. The results showed that a moderate intensity applied to a modulated parameter set would generate a network that ignores the distractor.

The third and fourth part consisted of understanding the impact of different angular distances between the cue stimulus and the distractor on the level of distraction. Therefore, the third experiment consisted of plotting the level of distraction against the angular distances while comparing both high and low intensities (200 pA and 50 pA, respectively). The fourth experiment plotted the level of distraction against the angular distances while comparing the control set of parameters to the modulated set of parameters (current set to 120 pA).

Further, from the angular distances between the cue location and the distractor, the authors found that for a low intensity stimulus or a high signal-to-noise ratio, the level of distraction would increase linearly with distance; however, this reached a peak at 90 degrees and the level of

distraction would then decrease, reaching a low at 180 degrees. High intensity current and control parameter set, on the other hand, would reach a high level of distraction at 180 degrees.

Inspired from this original study, four experiments were conducted. The control parameters were modified as described for experiment 1. Consequently, the input currents were increased to counterbalance the reduced excitability of the network. High intensity was associated with a current of 560 pA, moderate intensity was proportionally modified to 280 pA. For the third experiment, the low intensity was ¼ of the high intensity (140 pA) and the current in the fourth experiment was set to 1.2 times the moderate intensity (336 pA).

The third and fourth experiments were not reproduced in their totality. In fact, the different angular distances were not measured. Therefore, since the optimal angle to provide the highest difference between intensities and parameter sets was found to be 180 degrees, the angular distance between the cue location and the distractor, for all reproduced experiments, was set to 180 degrees (with the cue stimulus at 225 degrees and the distractor at 45 degrees, stimulus and distractor width of 40 degrees).

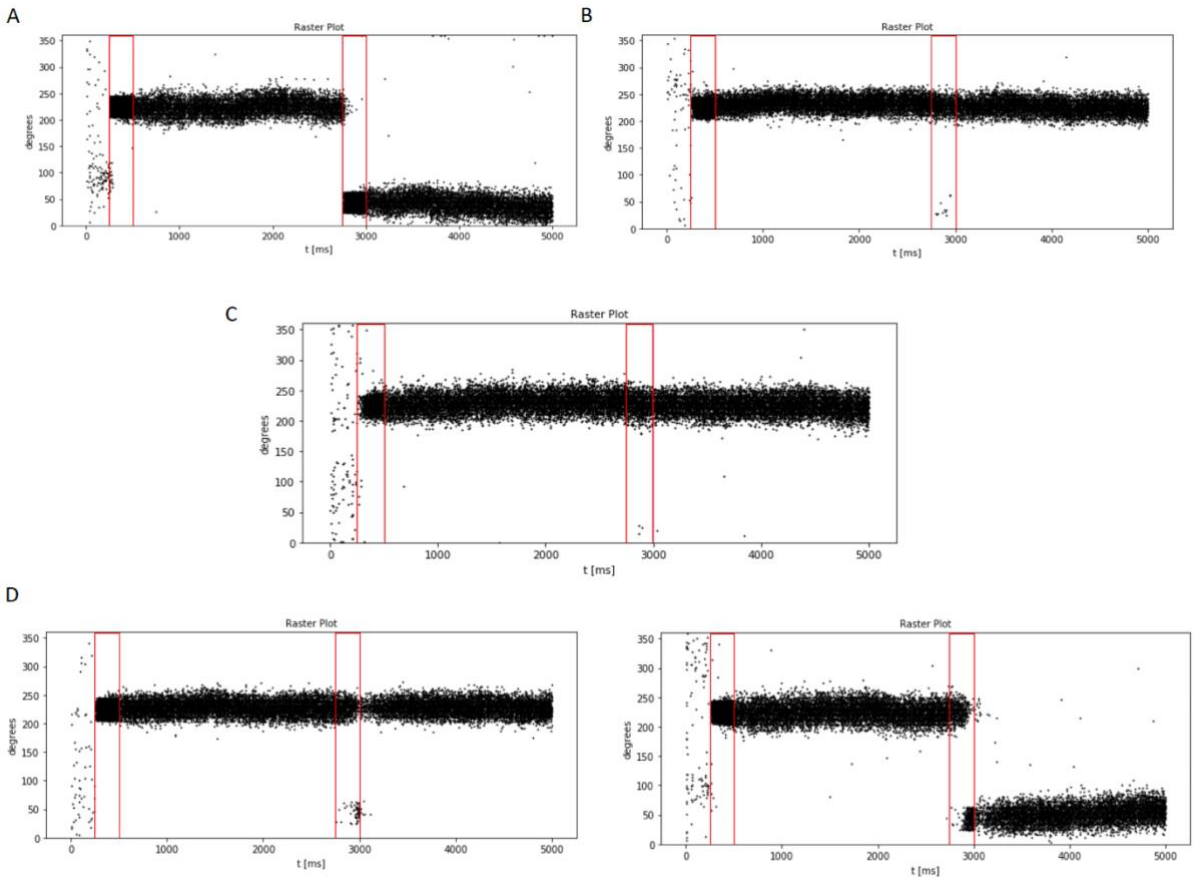

Figure 2. Influence of synaptic conductance and input currents on the level of distraction. Stimulus presented at 225 degrees and distractor presented at 45 degrees 2.5 seconds after stimulus onset with the same strength and duration (250 ms) as the cue stimulus. A. A control parameter set at high intensity (560 pA) B. Modulated parameter set at moderate intensity (280 pA) C. Control parameters at low intensity (140 pA). D. Control parameter set on the right panel and the modulated parameter set on the left panel at 1.2 times the moderate intensity (336 pA). Red rectangles delimit cue stimulus onset (start at 250 ms) and distractor onset (start at 2750 ms).

In Figure 2A, the high intensity and the control parameters were tested on the network's ability to ignore the distractor. This tuning of parameters resulted in a complete distraction of the network toward the distractor. In comparison, Figure 2B shows the modulated set of parameters with moderate intensity current. In these conditions, the distractor does not affect the working memory and the network continues to encode the location of the cue stimulus. In other words, the system ignores the distraction.

Figure 2A and C allow to visualise the differences between high intensity and low intensity currents, respectively, using a control parameter set. The high intensity shows a complete distraction of the network; however, the low intensity seemed too small to produce an activity state in the angle location associated with the distractor, resulting in only a few neurons firing and no distraction.

Figure 2D shows the difference between the level of distraction at 1.2 times the moderate input current (336 pA) between the two parameter sets. Interestingly, the network does in fact ignore the distractor for the modulated set (left panel), while the network with the control parameter set is completely distracted (right panel).

The results suggest similar conclusion as Compte et al. (2000). High currents would allow the distractor to overcome the intrinsic dynamic of the network and perturbate the recurrent state, ultimately resulting in a complete distraction of the network (Compte et al., 2000). On the other hand, at low intensity the network seems unaffected by the distractor. Similarly, the system ignores the distractor when tuned to the modulatory set and becomes distracted with the control parameter set.

Compte et al. (2000) argue that low intensity and an increase in signal-to-noise ratio (from the modulatory set) allow for a stronger ratio of inhibition generated from the persistent activity state itself, preventing the generation of a new bump specific to this state in comparison to when the network is in a spontaneous activity state. Thus, the inhibitory population is responsible for ignoring the distractor. Perhaps, if the excitatory external inputs are increased, they could overcome the inhibitory inputs and interfere with the recurrent network dynamic (Compte et al., 2000). In this case, the distractor would reset the network when the new transient stimulus is presented, refreshing the working memory as well as the persistent activity state.

Although the general conclusion follows the ones suggested by Compte et al. (2000), some of the results reproduced here differed. In fact, the graphs were not presented as color-coded graphs and the third and fourth experiments were only reproduced in parts due to time constraints. Therefore, the effect of different angles in each condition were not measured. Additionally, when presented with a distractor, the network would produce a varied set of outcomes even when tuned to the same parameters. In Figure 2, the results were chosen according to the outcomes that corresponded to the results showed in Compte et al. (2000); however, it is important to note that these results were not constant between trials. In other words, the network tuned to a certain set of

parameters could at times ignore the distractor and at times be distracted. Possibly, the random inputs generated from the uncorrelated poisson model defining the external inputs could have contributed to this variability. Nonetheless, this was not an issue discussed in Compte et al. (2000). For this reason, future computational work should include statistical analyses to better assess the significance of the results.

New experiment – Two distractors

The network response to the distractors showed a dependency on the input currents, the distances and the tuning of parameters; however, Compte et al. (2000) have not tested the effect of two distractors, presented at the same time, on persistent activity. To investigate how the network behave when presented two stimulus, the network activity was plotted in a rastergram following the same protocol as described for the distractor experiment (using a control parameter set, high intensity current (560 pA) and current width set to 30 degrees). Two experiments were conducted; a first looking at the distraction of the network when the distractors are at equal distance from the cue stimulus, and a second looking at the distraction when the two distractors were presented at different distances from the cue stimulus. The cue stimulus was presented at 180 degrees.

In Figure 3A, the two distractors were separated by an equal distance of 90 degrees from the cue stimulus angle location (distractor 1: 90 degrees; distractor 2: 270 degrees). Only one of 8 trials are shown in Figure 3A. The network was distracted in all trials, the distraction alternated between the distractors such that half of the distraction were toward the 90 degrees distractor, and the other half was toward the 270 degrees distractor. Although statistical analyses and a larger sample is needed to draw stronger conclusions, the results suggested that, when the distractors are at equal distance from the cue stimulus, the distraction will happen randomly.

Figure 3B shows a case where the two distractors are at different distances from the cue stimulus (distractor 1: 45 degrees; distractor 2:225 degrees). This resulted in a complete distraction of the persistent activity toward the distractor closest to the cue stimulus (225 degrees). These results suggested that the network favors a distractor closest to the cue stimulus.

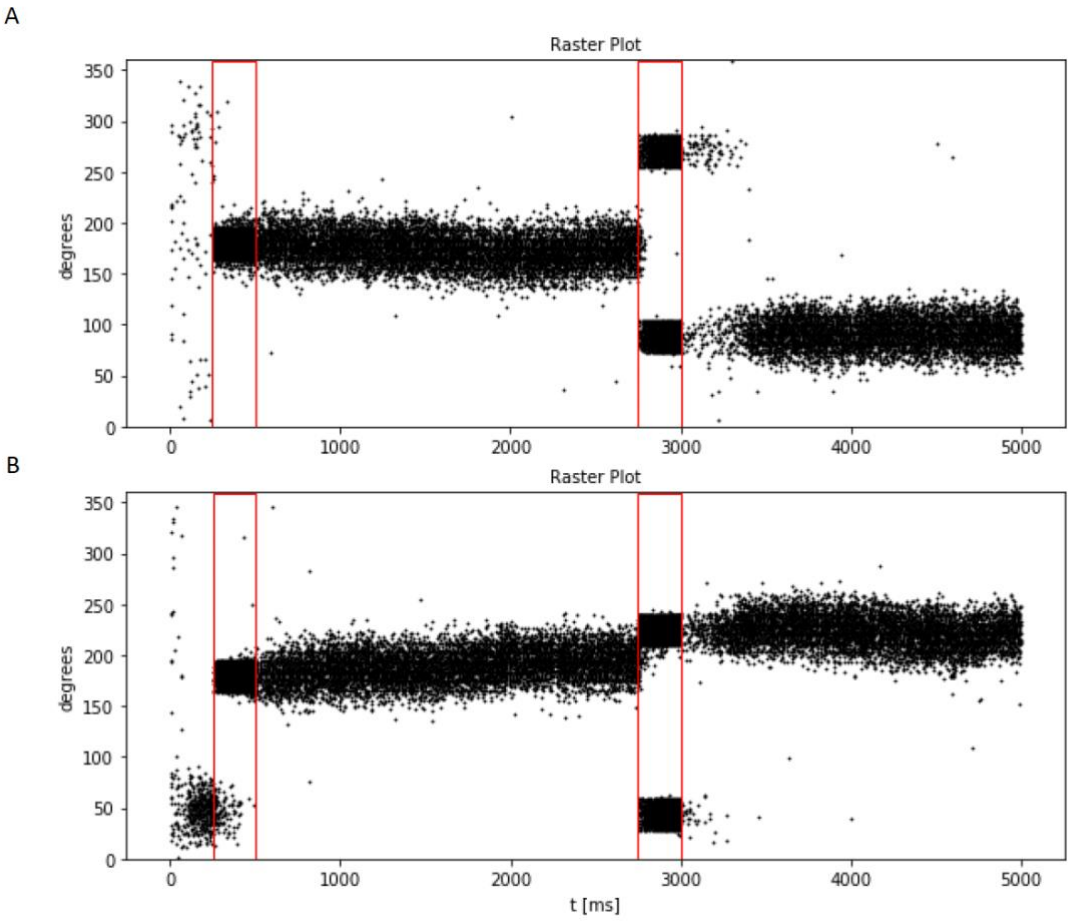

Figure 3. The network activity when presented with two distractors. Cue stimulus presented at 180 degrees. The distractors were presented 2.5 seconds after stimulus onset with the same strength and duration (250 ms) as the cue stimulus, using a control parameter set at high intensity current (560 pA) A. Two distractors presented at the same distance from the cue stimulus (90 degrees and 270 degrees) B. Two distractors presented at 225 degrees and 45 degrees. Red rectangles delimit cue stimulus onset (start at 250 ms) and distractors onset (start at 2750 ms).

Impact of the study

The model of Compte et al. (2000) for spatial working memory allows to understand the property of the PFC neural network while considering biological components previously neglected by computational models. This was achieved through; (1) a ratio between excitatory and inhibitory inputs that favors bistability in the network and that sustains both phases of spontaneous activity and of persistent recurrent excitatory activity; (2) excitatory inputs dominated by NMDARs and

strong inhibitory inputs mediated by GABAergic synaptic conductance that stabilize the network and can be tuned to overcome the persistent activity of the network; and (3) synaptic inputs producing persistent activity within a physiological range (20-40Hz).

As for understanding working memory, the study provides a possible line of answer for memory erasure. The model showed that an increase in external transient current would consequently turn off the persistent activity through the increase in inhibitory inputs. This, however, does not provide a trivial explanation regarding the origin of the external input or the processes allowing for its generation. In addition, the approach taken by the researchers to explain memory erasure in the PFC only partly accounts for the physiological observations associated with the response period. In fact, the presaccadic phase of the response shows an activity tuned toward the cue direction, which is illustrated in the model; however, the postsaccadic phase has been shown to have an activity tuned toward the opposite direction of the cue stimulus (Funahashi et al., 1991). Perhaps, computational studies aiming to understand working memory and decision making should look into modeling a physiologically-realistic model of the response period.

Moreover, the study found that enhanced inhibition facilitates the rejection of the distractor by the network. The authors proposed several future studies to better assess the network dynamic in working memory. One of the suggestions is to pharmacologically modify the synaptic transmission between neurons, such that the network would behave similarly to the network with the modulated parameter set (enhancement of inhibitory and NMDAR-mediated recurrent inputs). This would create a set of data from a network able to ignore a distractor. This could advance our understanding of the network's ability to ignore the distractor and of working memory.

In addition to the results reproduced in this paper, Compte et al. (2000) explored other properties of working memory. For example, the location of the cue stimulus, stored in the network's activity, was shown to drift as time increased. This introduced a variability that increases with time, which reduced the accuracy of the response. Another experiment found that unstructured (shown by Wang (1999)) and structured (showed in Compte et al. (2000)) recurrent activity would be abolished by high AMPARs mediated recurrent inputs. This differentiates from NMDARs. In fact, NMDARs have a longer decay time constant than AMPARs, allowing NMDARs to sustain the persistent activity (Compte et al., 2000). These results reinforce the belief that NMDARs are crucial for working memory processes.

Overall the model of Compte et al. (2000) advances the field of computational neurosciences as it allows to better predict experimental results. Nonetheless, the study is somewhat limited, leaving room for improvement.

While hypothesis regarding the PPC and the PFC acting as reverberatory loops to encode spatial working memory was proposed by Chafee and Goldman-Rakic (1998), the model only focuses on the neural activity observed in the PFC. Recently, Murray Jaramillo, and Wang (2017) have computed a model that investigate the relation between the PPC and the PFC in spatial working memory. One of their main findings was that both areas sustained persistent activity when computing a task inspired by Funahashi et al. (1989), and that the areas would differentiate in their response to distractors. The authors found that the PPC was responsible for encoding the distractor inputs, while the PFC would filter the distractor. These results show the importance of multi regional studies in computational neurosciences to differentiate between the roles of different areas in encoding a stimulus.

Moreover, future studies should assess how the network retains the different information related to visual cue stimulus. The code in Compte et al. (2000) assessed the activity of neurons associated with the angle location of the stimulus. Perhaps, a more realistic model for encoding visual cue would integrate other aspects of visual stimulus such as depth, colors, etc. Studies have already investigated how neural network encodes and memorizes different features of a visual stimulus; however, these studies investigated features and working memory separately (Mendoza-Halliday & Martinez-Trujillo, 2017). By combining the idea of multi regional studies to visual features, one could further optimize the original model of Compte et al. (2000) to better fit the complexity of experimental data associated with working memory.

Although pieces of the bridge separating biology and computer sciences in neurosciences research have slowly come together since Compte et al. (2000) paper, the study remains a turning point in the integration of physiological properties in neural modelling.

References

Amit DJ (1995) The Hebbian paradigm reintegrated: local reverberations as internal representations. Behav Brain Sci 18:617

.Amit DJ, Brunel N (1997) Model of global spontaneous activity and local structured activity during delay periods in the cerebral cortex. Cereb Cortex 7:237–252.

Carruthers, P (2013). Evolution of working memory. Proceedings of the National Academy of Sciences of the United States of America, 110(Suppl 2), 10371–10378. http://doi.org/10.1073/pnas.1301195110

Chafee MV, Goldman-Rakic PS (1998) Neuronal activity in macaque prefrontal area 8a and posterior parietal area 7ip related to memory guided saccades. J Neurophysiol 79:2919–2940.

Compte A, Brunel N, Goldman-Rakic PS, Wang XJ (2000) Synaptic Mechanisms and Network Dynamics Underlying Spatial Working Memory in a Cortical Network Model, Cerebral Cortex, Volume 10, Issue 9, pp 910–923, https://doi.org/10.1093/cercor/10.9.910

Durstewitz D, Kelc M, Güntürkun O (1999) A neurocomputational theory of the dopaminergic modulation of working memory functions. J Neurosci19:2807–2822.

Funahashi S, Bruce CJ, Goldman-Rakic PS (1989) Mnemonic coding of visual space in the monkey's dorsolateral prefrontal cortex. J Neurophysiol 61:331–349.

Funahashi S, Bruce CJ, Goldman-Rakic PS (1991) Neuronal activity related to saccadic eye movements in the monkey's dorsolateral prefrontal cortex. J Neurophysiol 65:1464–1483.

Gerstner W, Kistler WM, Naud R, Paninski L. (2014) Neuronal Dynamics: From Single Neurons to Networks and Models of Cognition. Cambridge University Press

Hansel D, Mato G, Meunier C, Neltner (1998) On numerical simulations of integrate-and-fire neural networks. Neural Comput 10:467–483.

Jalil M, Moongfangklang N, Innate K, Mitatha S, Ali J, Yupapin P. (2011). Molecular network topology and reliability for multipurpose diagnosis. International Journal of Nanomedicine, 6, 2385–2392. http://doi.org/10.2147/IJN.S24935

Lisman JE, Fellous J-M, Wang X-J (1998) A role for NMDA-receptor channels in working memory. Nature Neurosci 1:273–275.

Mendoza-Halliday, D., & Martinez-Trujillo, J. C. (2017). Neuronal population coding of perceived and memorized visual features in the lateral prefrontal cortex. Nature Communications, 8, 15471. http://doi.org/10.1038/ncomms15471

Mountcastle VB (1997) The cortical organization of the neocortex. Brain 120:701–722.

Murray, J. D., Jaramillo, J., & Wang, X.-J. (2017). Working Memory and Decision-Making in a Frontoparietal Circuit Model. The Journal of Neuroscience, 37(50), 12167–12186. http://doi.org/10.1523/JNEUROSCI.0343-17.2017

Postle BR. (2006) Working memory as an emergent property of the mind and brain. Neuroscience. 139(1):23–38.

Troyer TW, Miller KD (1997) Physiological gain leads to high ISI variability in a simple model of a cortical regular spiking cell. Neural Comput 9:971–983.

Tuckwell HC (1988) Introduction to theoretical neurobiology. Cambridge: Cambridge University Press.

Wang X-J (1999) Synaptic basis of cortical persistent activity: the importance of NMDA receptors to working memory. J Neurosci 19:9587–9603. 28

The Code

```
import brian2 as b2
from brian2 import NeuronGroup, Synapses, PoissonInput, network_operation
from brian2.monitors import StateMonitor, SpikeMonitor, PopulationRateMonitor
from random import sample
from collections import deque
from neurodynex.tools import plot_tools
import numpy
import matplotlib.pyplot as plt
import math
from scipy.special import erf
from numpy.fft import rfft, irfft
b2.defaultclock.dt = 0.1 * b2.ms


def simulate_wm( N_excitatory=2048, N_inhibitory=512, N_extern_poisson=1000, poisson_firing_rate=1.8 * b2.Hz, weight_scaling_factor=1., sigma_weight_profile=18., Jpos_excit2excit=1.62, stimulus_center_deg=225, stimulus_width_deg=40, stimulus_strength=0.56 * b2.namp, stimulus_strengthR=2* b2.namp, t_response_start= 9250* b2.ms, t_response_duration=250 * b2.ms, distractor_center_deg=45, distractor_width_deg=40, distractor_strength=.56 * b2.namp, t_distractor_start= 2750 * b2.ms, t_distractor_duration=250 * b2.ms)

    G_inhib2inhib=.35 * 1.024 * b2.nS,
    G_inhib2excit=.35 * 1.336* b2.nS,
    G_excit2excit=.35 * 0.381 * b2.nS,
    G_excit2inhib=.35 *1.2 * 0.292 * b2.nS,
    monitored_subset_size=2048, sim_time=9750. * b2.ms):
```

"""

Args:
N_excitatory (int): Size of the excitatory population
N_inhibitory (int): Size of the inhibitory population
weight_scaling_factor (float): weight prefactor. When increasing the size of the populations, the synaptic weights have to be decreased. Using the default values, we have N_excitatory*weight_scaling_factor = 2048 and N_inhibitory*weight_scaling_factor=512
N_extern_poisson (int): Size of the external input population (Poisson input)
poisson_firing_rate (Quantity): Firing rate of the external population
sigma_weight_profile (float): standard deviation of the gaussian input profile in the excitatory population.
Jpos_excit2excit (float): Strength of the recurrent input within the excitatory population.
Jneg_excit2excit is computed from sigma_weight_profile, Jpos_excit2excit and the normalization condition.
stimulus_center_deg (float): Center of the stimulus in [0, 360]
stimulus_width_deg (float): width of the stimulus. All neurons in
stimulus_center_deg +\- (stimulus_width_deg/2) receive the same input current
stimulus_strength (Quantity): Input current to the neurons at stimulus_center_deg +\- (stimulus_width_deg/2)
t_stimulus_start (Quantity): time when the input stimulus is turned on
t_stimulus_duration (Quantity): duration of the stimulus.
distractor_center_deg (float): Center of the distractor in [0, 360]
distractor_width_deg (float): width of the distractor. All neurons in
distractor_center_deg +\- (distractor_width_deg/2) receive the same input current
distractor_strength (Quantity): Input current to the neurons at
distractor_center_deg +\- (distractor_width_deg/2)
t_distractor_start (Quantity): time when the distractor is turned on
t_distractor_duration (Quantity): duration of the distractor.
G_inhib2inhib (Quantity): projections from inhibitory to inhibitory population (later rescaled by weight_scaling_factor)
G_inhib2excit (Quantity): projections from inhibitory to excitatory population (later rescaled by weight_scaling_factor)
G_excit2excit (Quantity): projections from excitatory to excitatory population (later rescaled by weight_scaling_factor)
G_excit2inhib (Quantity): projections from excitatory to inhibitory population (later rescaled by weight_scaling_factor)
monitored_subset_size (int): nr of neurons for which a Spike- and Voltage monitor is registered.
sim_time (Quantity): simulation time

Returns:
results (tuple):
rate_monitor_excit (Brian2 PopulationRateMonitor for the excitatory population),
spike_monitor_excit, voltage_monitor_excit, idx_monitored_neurons_excit, rate_monitor_inhib, spike_monitor_inhib, voltage_monitor_inhib,

idx_monitored_neurons_inhib,weight_profile_45 (The weights profile for the neuron with preferred direction = 45deg).

"""

# specify the excitatory pyramidal cells:
Cm_excit = 0.5 * b2.nF # membrane capacitance of excitatory neurons
G_leak_excit = 25.0 * b2.nS # leak conductance
E_leak_excit = -70.0 * b2.mV # reversal potential
v_firing_threshold_excit = -50.0 * b2.mV # spike condition
v_reset_excit = -60.0 * b2.mV # reset voltage after spike
t_abs_refract_excit = 2.0 * b2.ms # absolute refractory period
# specify the inhibitory interneurons:
Cm_inhib = 0.2 * b2.nF
G_leak_inhib = 20.0 * b2.nS
E_leak_inhib = -70.0 * b2.mV
v_firing_threshold_inhib = -50.0 * b2.mV
v_reset_inhib = -60.0 * b2.mV
t_abs_refract_inhib = 1.0 * b2.ms 30

# specify the AMPA synapses
E_AMPA = 0.0 * b2.mV
tau_AMPA = 2.0 * b2.ms
# specify the GABA synapses
E_GABA = -70.0 * b2.mV
tau_GABA = 10.0 * b2.ms
# specify the NMDA synapses
E_NMDA = 0.0 * b2.mV
tau_NMDA_s = 100.0 * b2.ms # orig: 100
tau_NMDA_x = 2.0 * b2.ms
alpha_NMDA = 0.5 * b2.kHz
# projections from the external population
G_extern2inhib = 2.38 * b2.nS
G_extern2excit = 3.1 * b2.nS

re_scaled

G_inhib2inhib *= weight_scaling_factor *2.5
G_inhib2excit *= weight_scaling_factor *2.5
G_excit2excit *= weight_scaling_factor
G_excit2inhib *= weight_scaling_factor

t_response_end = t_response_start + t_response_duration
t_stimulus_end = t_stimulus_start + t_stimulus_duration
t_distractor_end = t_distractor_start + t_distractor_duration

compute the simulus index

```
stim_center_idx = int(round(N_excitatory / 360. * stimulus_center_deg))
stim_width_idx = int(round(N_excitatory / 360. * stimulus_width_deg / 2))
stim_target_idx = [idx % N_excitatory for idx in range(stim_center_idx - stim_width_idx,
stim_center_idx + stim_width_idx + 1)]
# compute the distractor index
distr_center_idx = int(round(N_excitatory / 360. * distractor_center_deg))
distr_width_idx = int(round(N_excitatory / 360. * distractor_width_deg / 2))
distr_target_idx = [idx % N_excitatory for idx in range(distr_center_idx - distr_width_idx,
distr_center_idx + distr_width_idx + 1)]
# precompute the weight profile for the recurrent population
tmp = math.sqrt(2. * math.pi) * sigma_weight_profile * erf(180. / math.sqrt(2.) /
sigma_weight_profile) / 360.
Jneg_excit2excit = (1. - Jpos_excit2excit * tmp) / (1. - tmp)
presyn_weight_kernel = \
[(Jneg_excit2excit +
(Jpos_excit2excit - Jneg_excit2excit) * 31


math.exp(-.5 * (360. * min(j, N_excitatory - j) / N_excitatory) ** 2 / sigma_weight_profile
** 2))
for j in range(N_excitatory)]
# validate the normalization condition:
(360./N_excitatory)*sum(presyn_weight_kernel)/360.
fft_presyn_weight_kernel = rfft(presyn_weight_kernel)
weight_profile_45 = deque(presyn_weight_kernel)
rot_dist = int(round(len(weight_profile_45) / 8))
weight_profile_45.rotate(rot_dist)
# define the inhibitory population
inhib_lif_dynamics = """
s_NMDA_total : 1 # the post synaptic sum of s. compare with s_NMDA_presyn
dv/dt = (
- G_leak_inhib * (v-E_leak_inhib)
- G_extern2inhib * s_AMPA * (v-E_AMPA)
- G_inhib2inhib * s_GABA * (v-E_GABA)
- G_excit2inhib * s_NMDA_total * (v-E_NMDA)/(1.0+1.0*exp(-0.062*v/volt)/3.57)
)/Cm_inhib : volt (unless refractory)
ds_AMPA/dt = -s_AMPA/tau_AMPA : 1
```

```
    ds_GABA/dt = -s_GABA/tau_GABA : 1
    """
    inhib_pop = NeuronGroup(N_inhibitory, model=inhib_lif_dynamics, threshold="v>v_firing_threshold_inhib", reset="v=v_reset_inhib", refractory=t_abs_refract_inhib, method="rk2")
    # initialize with random voltages:
    inhib_pop.v = numpy.random.uniform(v_reset_inhib / b2.mV, high=v_firing_threshold_inhib / b2.mV, size=N_inhibitory) * b2.mV
    # set the connections: inhib2inhib
    syn_inhib2inhib = Synapses(inhib_pop, target=inhib_pop, on_pre="s_GABA += 1.0", delay=0.0 * b2.ms)
    syn_inhib2inhib.connect(condition="i!=j", p=1.0)
    # set the connections: extern2inhib
    input_ext2inhib = PoissonInput(target=inhib_pop, target_var="s_AMPA", N=N_extern_poisson, rate=poisson_firing_rate, weight=1.0)
    # specify the excitatory population:
    excit_lif_dynamics = """
    I_stim : amp
    s_NMDA_total : 1 # the post synaptic sum of s. compare with s_NMDA_presyn
    dv/dt = (
    - G_leak_excit * (v-E_leak_excit)
    - G_extern2excit * s_AMPA * (v-E_AMPA)
    - G_inhib2excit * s_GABA * (v-E_GABA)
    - G_excit2excit * s_NMDA_total * (v-E_NMDA)/(1.0+1.0*exp(-0.062*v/volt)/3.57)
    + I_stim
    )/Cm_excit : volt (unless refractory)
    ds_AMPA/dt = -s_AMPA/tau_AMPA : 1
    ds_GABA/dt = -s_GABA/tau_GABA : 1
    ds_NMDA/dt = -s_NMDA/tau_NMDA_s + alpha_NMDA * x * (1-s_NMDA) : 1
    dx/dt = -x/tau_NMDA_x : 1
    """
```

```
excit_pop = NeuronGroup(N_excitatory, model=excit_lif_dynamics, threshold= "v>v_firing_threshold_excit", reset="v=v_reset_excit; x+=1.0", refractory=t_abs_refract_excit, method="rk2")
# initialize with random voltages:
excit_pop.v = numpy.random.uniform(v_reset_excit / b2.mV, high=v_firing_threshold_excit / b2.mV, size=N_excitatory) * b2.mV
excit_pop.I_stim = 0. * b2.namp
# set the connections: extern2excit
Input_ext2excit = PoissonInput(target=excit_pop, target_var="s_AMPA", N=N_extern_poisson, rate=poisson_firing_rate, weight=1.0)
# set the connections: inhibitory to excitatory
syn_inhib2excit = Synapses(inhib_pop, target=excit_pop, on_pre="s_GABA += 1.0")
syn_inhib2excit.connect(p=1.0)
# set the connections: excitatory to inhibitory NMDA connections
syn_excit2inhib = Synapses(excit_pop, inhib_pop, model="s_NMDA_total_post = s_NMDA_pre : 1 (summed)", method="rk2")
syn_excit2inhib.connect(p=1.0)
# set the STRUCTURED recurrent input. use a network_operation
@network_operation()
def update_nmda_sum():
fft_s_NMDA = rfft(excit_pop.s_NMDA)
fft_s_NMDA_total = numpy.multiply(fft_presyn_weight_kernel, fft_s_NMDA)
s_NMDA_tot = irfft(fft_s_NMDA_total)
excit_pop.s_NMDA_total_ = s_NMDA_tot
@network_operation(dt=1 * b2.ms)
def stimulate_network(t):
if t >= t_stimulus_start and t < t_stimulus_end:
#excit_pop[stim_start_i - 15:stim_start_i + 15].I_stim = 0.25 * b2.namp
#Todo: review indexing
#print("stim on")
excit_pop.I_stim[stim_target_idx] = stimulus_strength
```

```
        # add distractor
        elif t >= t_distractor_start and t < t_distractor_end:
        excit_pop.I_stim[distr_target_idx] = distractor_strength 33

        # elif t >= t_response_start and t < t_response_end:
        # #excit_pop[stim_start_i - 15:stim_start_i + 15].I_stim = 0.25 * b2.namp
        # #Todo: review indexing
        # #print("stim on")
        # excit_pop.I_stim[:] = stimulus_strengthR
        else:
        #print("stim off")
        excit_pop.I_stim = 0. * b2.namp
        def get_monitors(pop, nr_monitored, N):
        nr_monitored = min(nr_monitored, (N))
        idx_monitored_neurons = \
        [int(math.ceil(k))
        for k in numpy.linspace(0, N - 1, nr_monitored + 2)][1:-1] # sample(range(N), nr_monitored)
        rate_monitor = PopulationRateMonitor(pop)
        spike_monitor = SpikeMonitor(pop, record=idx_monitored_neurons)
        voltage_monitor = StateMonitor(pop, "v", record=idx_monitored_neurons)
        return rate_monitor, spike_monitor, voltage_monitor, idx_monitored_neurons
        return get_monitors
        # collect data of a subset of neurons:
        rate_monitor_inhib, spike_monitor_inhib, voltage_monitor_inhib, idx_monitored_neurons_inhib = get_monitors(inhib_pop, monitored_subset_size, N_inhibitory)
        rate_monitor_excit, spike_monitor_excit, voltage_monitor_excit, idx_monitored_neurons_excit = get_monitors(excit_pop, monitored_subset_size, N_excitatory)
        b2.run(sim_time)
```

Return rate_monitor_excit, spike_monitor_excit, voltage_monitor_excit, idx_monitored_neurons_excit, rate_monitor_inhib, spike_monitor_inhib, voltage_monitor_inhib, idx_monitored_neurons_inhib, weight_profil

def getting_started():

b2.defaultclock.dt = 0.1 * b2.ms

rate_monitor_excit, spike_monitor_excit, voltage_monitor_excit, idx_monitored_neurons_excit, rate_monitor_inhib, spike_monitor_inhib, voltage_monitor_inhib, idx_monitored_neurons_inhib,weight_profile= simulate_wm (N_excitatory=256, N_inhibitory=64, weight_scaling_factor=8., sim_time=5000. * b2.ms, stimulus_center_deg=225, t_stimulus_start=250 * b2.ms, t_stimulus_duration=250 * b2.ms, stimulus_strength=0.560 * b2.namp, distractor_center_deg=45, distractor_strength=0.560* b2.namp, t_distractor_start=2750 * b2.ms, t_distractor_duration=250 * b2.ms, t_response_start=9250 * b2.ms, t_response_duration=250 * b2.ms, stimulus_strengthR=2* b2.namp)

plt.plot.plot_network_activity(rate_monitor_excit, spike_monitor_excit, voltage_monitor_excit, t_min=0. * b2.ms)

plt.show()

```
# spike_trains_inhib =spike_monitor_inhib.spike_trains()
# spike_trains_excit =spike_monitor_excit.spike_trains()
#

# for c in range(0,63):
# to_remove_low_i = np.where(spike_trains_inhib[c] < 0.5* b2.second)
# to_remove_high_i = np.where(spike_trains_inhib[c] > 9.25* b2.second)
# spike_trains_inhib[c] = np.delete(spike_trains_inhib[c], to_remove_low_i)
# spike_trains_inhib[c] = np.delete(spike_trains_inhib[c], to_remove_high_i)

# for c in range(0,255):
# to_remove_low_e = np.where(spike_trains_excit[c] < 0.5* b2.second)
# to_remove_high_e = np.where(spike_trains_excit[c] > 9.25* b2.second)
# spike_trains_excit[c] = np.delete(spike_trains_excit[c], to_remove_low_e)
# spike_trains_excit[c] = np.delete(spike_trains_excit[c], to_remove_high_e)
#

# firing_numb_inhib =np.zeros(63)

# for i in range(0,63):

# firing_numb_inhib[i]= len(spike_trains_inhib[i])
```

```
#
# firing_numb_excit =np.zeros(255)
# for i in range(0,255):
# firing_numb_excit[i]= len(spike_trains_excit[i])
#
# delay_period = 8.75
# firing_rate_excit=(firing_numb_excit/delay_period)
# firing_rate_inhib=(firing_numb_inhib/delay_period)
# plt.plot(firing_rate_inhib)
# plt.show()
# plt.plot(firing_rate_excit)
# plt.show()
if __name__ == "__main__":
getting_started() 35
```